THE EVOLUTION OF THE INTRA-CARPATHIAN BASINS

AND

THEIR RELATIONSHIP TO THE CARPATHIAN MOUNTAIN SYSTEM

by

LEIGH HANDY ROYDEN

A.B., Harvard University
(1977)

SUBMITTED TO THE DEPARTMENT OF
EARTH AND PLANETARY SCIENCES
IN PARTIAL FULFILLMENT OF
THE REQUIREMENTS FOR THE
DEGREE OF

DOCTOR OF PHILOSOPHY
IN GEOLOGY AND GEOPHYSICS

at the

MASSACHUSETTS INSTITUTE OF TECHNOLOGY

March 1982

Signature of Author_____
Department of Earth and Planetary Sciences
March 15, 1982

Certified by_____
John G. Sclater
Thesis Supervisor

Accepted by_____
Theodore R. Madden
Chairman, Departmental Graduate Committee

MASSACHUSETTS INSTITUTE
OF TECHNOLOGY

JUL 1 1982

TABLE OF CONTENTS

(cont.)

Leigh Handy Royden

Personal Vitae

Leigh Handy Royden
Department of Earth and Planetary Sciences
Massachusetts Institute of Technology
Cambridge, Massachusetts 02139
     (617) 253-5735

Social Security Number: 549-94-4763

Date and Place of Birth: 10/15/55   Palo Alto, California

Family: Tajer (dog)

Subjects of Special Interest: Regional Geology and Geophysics, Plate Tectonics,
        Thermal Effects and Consequences of Continental Deformation.

Educational Background:

        1977 A.B. Harvard (cum laude, physics)
        1982 Ph.D. M.I.T. (expected, January 1982, geophysics)
              (thesis advisor, John G. Sclater)

Employment and Teaching History:

        1974 June-August, Teaching Assistant, Harvard, Introductory Physics
        1976 June-August, Research Assistant, Woods Hole Oceanographic Inst.
        1977-78 June-June, Research Assistant, Woods Hole Oceanographic Inst.
        1978 January-July, Consultant, Dobex International
        1981 February-May, Teaching Assistant, M.I.T., Introduction to
              Marine Geophysics
        1981 April, Consultant, Exxon Production Research

Geologic Experience:

        1976 Summer, Data analysis and computer work, etc., Age vs Area of
              the Oceans and Continents.
        1976 Seagoing experience, Site Survey in Central Atlantic
        1977 Seagoing experience, Heatflow determinations and Piston Coring,
              Southeast of Iceland
        1977-78 Research on thermal effect of sedimentary basin formation,
              and subsidence.
        1979 January, Field Mapping, Southern California (near Baker)
        1981 December (1980)-February, March, Field Mapping Southern
              California (Kingston Range, and Mountain Springs Pass).
        1979-present Thesis work, Eastern Europe

My general research interests lie in the application of both geologic and geophysical techniques to understanding zones of continental deformation. My approach is to use the results of detailed geologic mapping together with quantitative analyses of thermal structure, subsidence and uplift histories to reconstruct the tectonic and sedimentological evolution of specific regions. My past work includes thermal analyses of extensional sedimentary basins and rifted continental margins determined from subsidence histories.

Present work:

1) Carpathian region (thesis): I have applied my work on the evolution of sedimentary basins to my thesis work in the Carpathian region, where the development of Miocene basins is intimately connected with synchronous shortening and Alpine deformation along the Carpathian mountain chain. In addition to examining the extensional and thermal histories of individual basins, it was my plan to investigate the timing and kinematics of basin formation within a regional tectonic framework. Using detailed isopach maps, seismic profiles, drill hole data, structural and facies information, etc., these basins can be shown to be the result of local extension associated with a conjugate system of strike-slip faults, and appear to be directly controlled by the magnitude and location of thrusting in the Eastern Carpathians. A simple mechanical picture can relate basin extension to crustal shortening in the mountains, and explain the apparent inconsistence of an actively extending terrain existing immediately adjacent to one of active shortening.

2) Uplift and thermal history of orogenic belts: I have devised an approach whereby uplift rates and thermal structure of orogenic belts can be determined from geobarometry and geothermometry data. The major difference between my approach and previous work on this topic is that my approach does not rely on assumptions about the initial thermal conditions or initial thickness of the nappe pile. This approach can be used in conjunction with geochronologic data to gain further information about changes in uplift and erosion rates through time. I have applied this technique to geobarometry and geochronology data from the Norwegian Caledonides. This work is nearly complete and should result in a manuscript by late summer or early fall.

Intended research:

1) Carpathian region: Although much of my work in the Carpathian region will have been completed by the time I leave graduate school (December, 1981), the scope of this project is beyond that of a Ph.D. thesis, and I expect to continue with this work for at least a year beyond graduation. We (John Sclater, Clark Burchfiel, several Hungarian scientists, and myself) plan to publish a summary of our work in monograph form. The outline for this will be my Ph.D. thesis, and I expect that I will do all the editing and much of the writing for this volume. We hope to have a preprint by the summer of 1982, when we plan a Penrose-type conference in Hungary. At present I have a proposal in to NSF to fund myself as a post-doctoral fellow for a year and a half beginning in March, 1982, and hope to provide full, or at least partial, support for myself over that period.

2) Northern Adriatic and Po basins: I hope to set up a joint project with the Italians to study loading and thermal problems in the Northern Adriatic in a regional tectonic and geologic framework. I have been invited to Pisa for a short time this summer and hope that a cooperative project similar to that with the Hungarians will evolve out of this meeting. The Adriatic, separated from the Carpathians by a large continental transform, represents an adjacent piece of the same tectonic picture (late Cenozoic deformation along the Alpine chain) and also resulted in mountainous and subsided regions. However in the northern Adriatic the subsided regions are loaded foredeeps rather than extended regions. To my knowledge, little work has been done on the thermal evolution of compressional basins, and one of the aims of this research would be to produce a thermal history of the northern Adriatic and contrast it with those of extensional-type basins. A second aim of this research would be to examine the loading and subsidence of the basin area in light of the timing and magnitude of deformation in the adjacent mountain belts, and in light of present day seismic activity beneath the Po basin.

3) I plan to apply the quantitative method which I have developed to examine the uplift and temperature history of the Norwegian Caledonides to several young orogenic belts. In particular, I would like to look at the Western Alps, since in addition to geobarometry data, cooling ages are known for a variety of different minerals. Furthermore, because the Alps are still experiencing rapid uplift and erosion, present day surface heatflow provides an additional constraint. The Canadian Rockies may be another region where this type of analysis would be informative. A more long range goal is to apply some of these techniques to Proterozoic orogenic belts. I hope that this may result in some insight into the thermal structure of the lithosphere during an earlier period of the earth's history, and into the evolution of the lithosphere through time.

Leigh Royden

A.B. Harvard, 1977

PhD. (expected date) January 1982, M.I.T.

Bibliography of Leigh Royden

1980   L. Royden, J.G. Sclater, and R.P. Von Herzen, Continental Margin
Subsidence and Heat Flow: Important Parameters in Formation of
Petroleum hydrocarbons, Amer. Assoc. Petrol. Geol. Bull., 64,
p. 173-187.

1980   J.G. Sclater, L. Royden, F. Horvath, C. Burchfiel, S. Semken, and
L. Stegena, Neogene to Quaternary Subsidence and Thermal History of
the intra-Carpathian Basins, Earth Planet. Sci. Lett., 51, p. 139-162.

1980   L. Royden and C.E. Keen, Rifting Process and Thermal Evolution of
the Continental Margin of Eastern Canada Determined from Subsidence
Curves, Earth Planet. Sci. Lett., 51, p. 343-361.

1981   L. Royden and J.G. Sclater, The Neogene intra-Carpathian Basins,
Phil. Trans. R. Soc. Lond., A300, p. 373-381.

in press

L. Royden, F. Horvath, and B.C. Burchfiel, Transform Faulting, Extension
and Subduction in the Carpathian-Pannonian Region, (Geol. Soc. Amer.).

B.C. Burchfiel, L. Royden, and J.G. Sclater, The Foreland Fold and
Thrust Belt of the Carpathians and its Relations to the Pannonian
and Related Basins, (Amer. Assoc. Petrol. Geol. Memoir).

L. Royden and B. Parsons, A Comparison of Discrete and Continuous
Intrusion Models for the Thermal Structure of the Plates, (Geophys.
Jour. R. Astr. Soc.).

in preparation

L. Royden and K. Hodges, Quantitative Constraints on Cooling and
Uplift Rates in Orogenic Terrains: a Norwegian Example.

ACKNOWLEDGEMENTS

support (given to John Sclater) which sometimes paid my summer tuition and helped greatly with European travel expenses. I would also like to thank Charlotte Keen for a productive but exhausting two months at the Bedford Institute of Oceanography in Halifax, Nova Scotia.

Many of my friends and collegues at MIT have contributed directly and indirectly to my research. I am grateful to Clark Burchfiel for my introduction to geology and field mapping, and to both Clark and Bill Brace for a seemingly endless supply of moral support. Lastly and most importantly I am endebted to my advisor, John Sclater, who is single-handedly responsible for my introduction to the earth sciences during two summers spent as a research assistant in Woods Hole. Five hour working days and long lunch hours spent at the beach added greatly to my enthusiasm. More than any one else, John has shaped my philosophy of scientific research, which is perhaps best illustrated by the following quote:

"You don't have to be right as long as you're interesting."
                                        - J.G. Sclater, 1976

Completion of this thesis has certainly not been dull.

THE EVOLUTION OF THE INTRA-CARPATHIAN BASINS AND

THEIR RELATIONAHIP TO THE CARPATHIAN MOUNTAIN SYSTEM

by

Leigh Handy Royden

ABSTRACT

The Carpathian arc formed during the Cretaceous to Miocene
continental collision of Europe with smaller continental fragments
following southward and westward subduction of an oceanic terrane.
During the last stages of thrusting in the outer Carpathians, a set of
discrete basins formed behind the Carpathian loop in a back-arc position.
These basins, which in places contain up to 7 km of Neogene and
Quaternary sedimentary rocks, appear to be regions of late Miocene
extension They are connected to each other and to areas of coeval
shortening in the outer Carpathian thrust belt by a system of strike-slip
faults. Sinistral northeast trending and dextral northwest trending sets
of conjugate shears reflect overall east-west extension of the
intra-Carpathian region during the late Miocene.

Qualitative geological data and regional tectonic considerations
were combined with quantitative sedimentation, subsidence and thermal
data for individual wells in several of the intra-Carpathian basins to
determine the timing, magnitude and distribution of extension within the
different intra-Carpathian basins. This analysis indicates that the
Pannonian basin is 50% to 100% hotter than would be expected if the basin
were the result of late Miocene uniform extension. A second mode of
extension whereby lithospheric extension is accompanied by introduction
of large amounts of additional heat into the upper mantle predicted:
1) temperatures and heat flow in good agreement with observation, 2)
rates of thermal subsidence (due to conductive cooling and thermal
contraction of lithospheric rocks after extension) in good agreement with
observation, 3) rates of heat loss not strongly dependent on present
basement depth, also in good agreement with observation, and 4) that
uplift could occur during extension - such syn-extensional uplifts have
been observed in both the Pannonian and Danube basins. Crustal extension
beneath most parts of the Pannonian basin was calculated to have been
about 85% to 170% (β = 1.85 to 2.70).
The Vienna basin, which is superimposed partly on the flysch nappes
of the outer West Carpathians, is interpreted as the result of
thin-skinned extensional tectonics above a shallow detachment surface
within the upper crust. Extension of upper crustal rocks above this
detachment was probably compensated by thrusting of the outermost nappes
of the West Carpathians over the European platform. Subsidence and
thermal data from the Vienna basin support this interpretation.

Extension within the Danube and Zala basins seems to have involved the entire lithosphere, possibly with the introduction of extra heat into the upper mantle. The Transylvanian basin does not appear to be extensional in origin and may be the result of temporary loading from below during subduction. Heat flow data from the Transylvanian basin are consistent with this interpretation.

Extension within the intra-Carpathian basins was not synchronous and may be divided into three principle periods: Karpatian (17.5-16.5 Ma), Badenian (16.5-13 Ma) and Sarmatian (13-10.5 Ma), probably extending into early Pannonian time. Karpatian extension affected the north Vienna and north Transcarpathian basins, and the locus of extension migrated generally southward and eastward with time. Badenian extension was dominant in the south Vienna and Transcarpathian basins, and affected the Danube basin, and parts of the Zala, Sava, Drava and Pannonian basins. Sarmatian and Pannonian age extension was responsible for most of the subsidence of the east Danube and Pannonian basins.

Palinspastic reconstruction of the basins prior to each of these periods of extension predicts eastward migration of the zone of thrusting and shortening within the Carpathian mountains to accomodate eastward and southward migration of areas of extension. This is consistent with the eastward and southward migration of the last major thrusting event as determined directly from rocks within the thrust belt. From these reconstructions we estimate about 120 (±60) km of east-west shortening across the outer East Carpathians from the beginning of Karpatian time until the present. This figure is consistent with estimates of shortening based on direct reconstruction of nappes in the thrust belt. From this I infer a source-sink relationship for late Miocene extension of the intra-Carpathian region and late Miocene crustal shortening within the outer Carpathians.

I conclude that during late Micene time, deformation of the Pannonian fragment was dominated by extensional tectonics, except along a narrow zone in the outer Carpathian thrust belt. Late Miocene thrusting in the Carpathians is interpreted as the result of simple shear caused by relative motion between Europe and the overriding Pannonian fragment at the subduction boundary, rather than of regional compression of lithospheric rocks at depth. In this way, buoyant sedimentary rocks originally deposited on the European plate could have been stripped from the downgoing European basement and stacked into a series of imbricate slices without widespread compression and crustal shortening extending far beyond the fragment boundaries. Overall compression of lithospheric rocks at depth would not have been necessary to cause imbrication of sedimentary cover, and thus the proximity of an active thrust belt to areas of coeval extension can be easily explained. The initation of extensional tectonics within the intra-Carpathian region was probably the direct result of reorganization of major fragment boundaries of the Eastern European Alpine system in late Oligocene-early Miocene time.

Thesis supervisor: John G. Sclater
Title: Professor

INTRODUCTION

The main body of this thesis consists of three papers which examine the extension and subsequent evolution of the intra-Carpathian basins. An earlier paper (Royden et al., 1980) which treats the general problem of extended and subsided regions is included as an appendix. Most of the work presented in this paper was completed before I began my graduate work at MIT, but it is included here because it lays the fundamental groundwork for the interpretation of passive continental margins and other subsided regions as extensional terranes. This paper develops a quantitative relationship between lithospheric extension, basin subsidence and surface heat flow and outlines a procedure for reconstructing the thermal history of basin sediments.

The other three papers are an application of the approach used by Royden et al. (1980) to the intra-Carpathian area and an attempt to synthesize subsidence and thermal data with other geologic information to construct a comprehensive regional tectonic history. In the first paper, a preliminary analysis of subsidence and heat flow data was used to determine the magnitude and timing of lithospheric extension beneath the intra-Carpathian basins. Two fundamental results from this paper are relevant to studies of other sedimentary basins and subsided continental margins. First, lithospheric deformation need not be distributed uniformly with depth, and there seems to be a difference between the behavior of upper crustal and lower lithospheric rocks. A separate study of the eastern Canadian continental margin conducted at about the same time by Charlotte Keen and myself suggests similar results (Royden and Keen, 1980; see bibliography, paper three), but

has not been included as part of this thesis. Second, accurate
subsidence and thermal data is necesssary for the reconstruction of
realistic extension histories, particularly for young basins. When
accurate data are not available, it is impossible to distinguish from
among a wide range of mechanisms for basin subsidence.

The second paper examinines the structural and kinematic framework
within which extension of the intra-Carpathian basins occurred. The
location, magnitude, direction and timing of basin extension appears to
be connected directly to the location, magnitude and timing of
shortening within the outer Carpathian thrust belt. In map view,
extension was inhomogeneous and occurred within localized areas
connected by strike-slip or transform boundaries. Thus, when these
results are coupled with those from the first paper, deformation
appears to have been distributed inhomogeneously in three dimensions.
This study further suggests that one of the intra-Carpathian basins,
the Transylvanian basin, is not of extensional origin, even though its
age, size, and depth are comparable to those of the other basins.

The third and final paper synthesizes the quantitative techniques
of the first paper and the more qualitative geologic interpretations of
the second paper. The result is a more detailed and comprehensive
analysis of the intra-Carpathian basins, although the fundamental
conclusions from the previous papers remain largely unchanged. Three
general conclusions emerge from this paper. First, there may not be a
direct correspondence between the magnitude, style and spatial
distribution of crustal and sub-crustal deformation. Second,
sedimentary basins may be created by a variety of mechanisms. Even
within the small intra-Carpathian area there appear to be at least

three distinctly different types of basins, with similar ages and depths. Thus, an understanding of the mechanisms of basin formation is critical to the incorporation of any basin within its regional tectonic setting. Third, Miocene shortening in the outer Carpathians and development of several different types of basins can probably be tied together within a simple mechanical framework. It seems likely that this type of analysis may provide insights into our understanding of the evolution and mechanical development of other similar young tectonic systems.

Each of the papers which constitute this thesis is built upon the ideas developed in the previous papers. Therefore this dissertation is intended to record the progression of my understanding of extensional processes within the continental lithosphere. Some of the information within papers two and three is a review of sections in the preceding papers. Most readers should find it sufficient to confine their attention the third paper; little is contained in the preceeding papers which is not elaborated here in greater detail. However, this paper could not have been written without the fundamental groundwork laid previously, and for this reason I have included the first and second papers as part of this thesis.

CHAPTER ONE

THE FORMATION OF THE INTRA-CARPATHIAN BASINS

DETERMINED FROM SUBSIDENCE HISTORY

PREFACE

S. Semken plotted most of the subsidence data used in this paper and compiled a file of relevant literature.

L. Royden devised all theoretical calculations (see appendix) and plotted several of the figures.

J. Sclater did the decompaction, etc. of the observed subsidence.

J. Sclater, L. Royden, F. Horvath and C. Burchfiel all contributed to the ideas and basic organization of this paper. J. Sclater wrote the first draft, which was revised and re-organized by L. Royden.

C. Burchfiel and L. Stegena contributed their expertise on the geology, tectonic setting and thermal environment of the region.

THE FORMATION OF THE INTRA-CARPATHIAN BASINS AS DETERMINED FROM SUBSIDENCE DATA

J.G. SCLATER [1], L. ROYDEN [1], F. HORVÁTH [2], B.C. BURCHFIEL [1], S. SEMKEN [1] and L. STEGENA [3]

[1] *Department of Earth and Planetary Sciences, Massachusetts Institute of Technology, Cambridge, MA 02139 (U.S.A.)*
[2] *Department of Geophysics, Lorand Eötvös University, Kun Bela t. 2, Budapest (Hungary)*
[3] *Department of Cartography, Lorand Eötvös University, Kun Bela t. 2, Budapest (Hungary)*

The Carpathian arc is the result of continental collision during subduction of the European plate beneath a Pannonian continental block. In the Early/Middle Miocene, during and after the last stages of thrusting in the Outer Carpathians, several "back-arc" basins started to form within the Carpathian loop. These basins are of two types: (1) those lying in the peripheral regions of the intra-Carpathian lowlands (Vienna, West Danube, Transcarpathian and Transylvanian), and (2) those lying in the central intra-Carpathian region (East Danube, Little Hungarian and Great Hungarian (Pannonian)).

Though both groups of basins have thin crust, the subsidence history and the present heat flow are different. The peripheral basins exhibit a rapid initial subsidence followed by a much slower general increase in depth. Their heat flow is close to the average for continental areas. In contrast the central basins have no initial subsidence but do show a fast linear increase in depth which has continued until the present. The heat flow is nearly twice the average for continents.

We believe that the basins are thermal in origin and are the direct result of the continental collision which formed the Carpathian arc. The peripheral basins appear to be the result of uniform stretching of the lithosphere by about a factor of two. The rapid initial subsidence is an immediate isostatic adjustment to the stretching, the slower linear subsidence is due to conductive cooling of the thinned lithosphere. In the central basins, uniform stretching by about a factor of 3 could explain the thermal subsidence and the high heat flow. Unfortunately such a simple explanation is not supported by either the geology or the absence of a clearly defined initial subsidence. Alternative explanation involve crustal stretching with additional subcrustal thinning or, alternatively, attenuation of the whole subcrustal lithosphere and part of the crust by melting and erosion. Both explanations create a very thin lithosphere, reduce the initial subsidence to a minimum but still give a rapid thermal subsidence and high heat flow.

The subsidence history gives quantitative information concerning the evolution of the inter-Carpathian basins. In other areas, it may place equally important constraints on the development of intercontinental basins and continental shelves.

1. Introduction

One of the fundamental concepts of plate tectonics is that sea floor is created by the intrusion of hot molten material along mid-ocean ridges. As this material moves away from the spreading centers, it cools and contracts. This intrusion process creates an initial thermal anomaly in the lithosphere, and the subsequent cooling of the lithosphere toward thermal equilibrium can explain the observed increase in depth of the ocean floor and the decrease in heat flow with age [1]. Continental shelves and intra-continental basins also appear to subside with age in an analogous fashion. Like the oceans gravity anomalies are small and hence the subsidence is compensated. Although the early subsidence of these regions

may be complex, 20–30 m.y. after formation the increase in depth is observed to be exponential and to have a time constant of 50–60 m.y. [2–4]. Because this is similar to the sbusidence observed for normal ocean floor, it is strong evidence that the long-term subsidence of continental shelves and basins also results from the decay of a thermal anomaly in the lithosphere. Except for a study of the Gulf of Lyon [5] little effort has been devoted to analyzing the early subsidence of these regions. Hence here is little quantitative data on which to base a reasonable reconstruction of the specific thermal and mechanical. processes which are associated with the creation of continental shelves and inland basins.

A variety of models have been suggested to account for these regions. However, most early explanations involved only crustal processes [6–8] and are unable to account for long-term subsidence. Other models have suggested that these regions have been created by a thermal plume which causes the lithosphere to expand and results in uplift and erosion of the crust [2]. As the lithosphere cools a basin is formed because the upper surface returns to a depth below its original position. However, the amount of sediment deposited will correspond roughly to the amount of crust removed by erosion. Thus thick sedimentary deposits on continental shelves and in inland basins present a major space problem for this model. Based on work in the Aegean, McKenzie [9,10] has recently suggested simple extension as an explanation for basin formation. Royden et al. [11] have suggested similar extensional explanations of these areas based on an analysis of Atlantic-type continental margins. In this paper three simple mechanical models will be dealt with in detail. Two of these mechanisms, stretching and dike intrusion, involve significant extension of both crust and lithosphere. Since these processes have been discussed in detail in previous publications [9,11,12], they will only be briefly described. The third involves attenuation of the subcrustal lithosphere and can leave the crust relatively undeformed. Each of these mechanisms result in two distinct phases of subsidence or uplift. The first is an immediate isostatic response to density changes associated with changes in the structure of the lithosphere and can result in either subsidence or uplift. The second is a long-term subsidence controlled by decay of the thermal anomaly associated with that change in structure. As will be

seen this is an important distinction.

Subsidence and sedimentation began in the intra-Carpathian basins in the early Miocene, during and after the last stages of compression and thrusting in the Outer Carpathians. Subsidence has continued until the present. We show that in these basins both an initial, isostatic subsidence, and the long-term thermal subsidence are observed. Our objective in this paper is to examine the subsidence of these basins in a regional geologic and tectonic framework and to show that calculations of sedimentation rate and total sediment thickness give valuable insight into the mechanical processes which formed these basins.

We start by analyzing the data within the framework of the crustal stretching model that has been successful in simple extensional settings [10,12]. However, we are forced by the observations in the Pannonian Basin to consider a modified version of the original model.

2. Three thermal models

2.1. Stretching

Rapid extension of the entire lithosphere results in pronounced attenuation in both the crust and the underlying material (Fig. 1a). When extension occurs, the upper portion of the lithosphere exhibits brittle failure, whereas the lower lithosphere extends and attenuates by ductile flow and is replaced by passive upwelling of hot asthenosphere. Graben formation, block and listric faulting are manifestations of brittle failure in the crust. This attenuation of lighter crustal rocks results in an initial isostatic subsidence when crustal thickness is originally greater than about 20 km (Fig. 2a). After the initial isostatic subsidence, the early ($t \leqslant 20$ m.y.) thermal subsidence is approximately linear (Fig. 2b). In this model it is not necessary that the extension be uniform, i.e. that the crustal thinning exactly match the attenuation of the lithosphere. Flow in the ductile layer can attenuate the lithosphere over a broader area than that observed in the crust (Fig. 1c).

2.2. Dike intrusion

Rapid extension leads to cracking of the lithosphere and large-scale intrusion of vertical dikes (Fig. 1b)
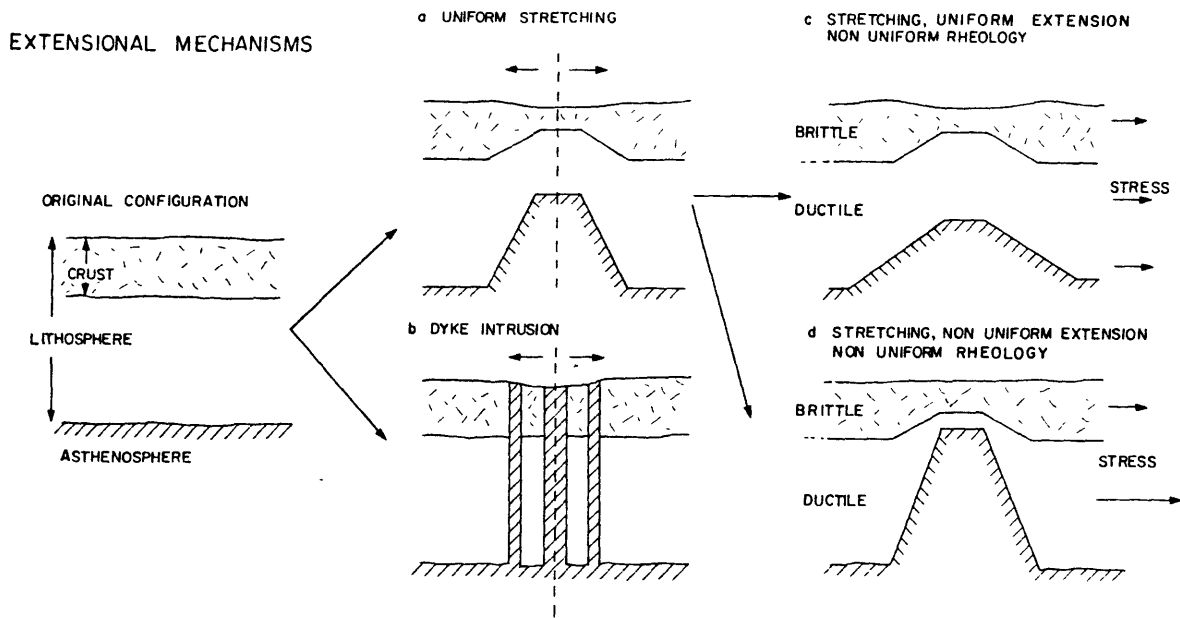
Fig. 1. Various extensional models for the creation of the initial thermal anomaly which can account for the subsidence and heat flow of intracontinental basins. (a) and (b) are uniform stretching [10] and dike intrusion [11]. (c) and (d) are modifications of the stretching model for a non-uniform rheology. In model (c), the ductile lithosphere thins over a wider zone than the rigid crust, although net extension is the same. In model (d), net extension is greater in the lithosphere than in the crust.

[11,13]. Replacement of light crustal rocks by denser ultrabasic or basaltic material also results in initial isostatic subsidence for crustal thickness greater than 20 km (Fig. 2a). It is unlikely that this mechanism can operate at depth where the lithosphere is thought to deform by ductile flow and we do not believe that this model has widespread geological applicability [12]. On the other hand, dyke intrusion is observed in some of the smaller basins within the Carpathians. As we believe these dikes have a significant effect on the local heat flow and subsidence, we included the model in this section and work out the simple theory in the Appendix.

2.3. Subcrustal attenuation

Attenuation of subcrustal lithosphere without significant extension or deformation of the crust results in initial isostatic uplift. If a sufficient thickness of the crust is involved in the attenuation process, initial isostatic subsidence rather than uplift may occur (Fig. 2a). This attenuation could be the result

of either subcrustal extension (Fig. 1d) or of subcrustal erosion and melting of the lithosphere. Such a mechanism may be supported by observations in the Basin and Range in the Western United States where 30 km crust is underlain by a thin subcrustal lithosphere [14,15]. Further evidence comes from drill holes and seismic refraction information across the Labrador Shelf. Royden and Keen [16] have shown that the thermal subsidence can only be explained by stretching significantly greater than that consistent with the observed decrease in crustal thickness.

The general equations governing initial subsidence or uplift, and the thermal subsidence and heat flow after the initial deformation are presented in the Appendix. In each model the extension or thermal event is assumed to occur instantaneously. Jarvis and McKenzie [17] have shown that only extensional events of long duration are likely to have a significant effect on these simple calculations. In the region of this study the extensional and other events are of short duration ($\leqslant 5$ m.y.). For each of the three models we have examined the initial and thermal
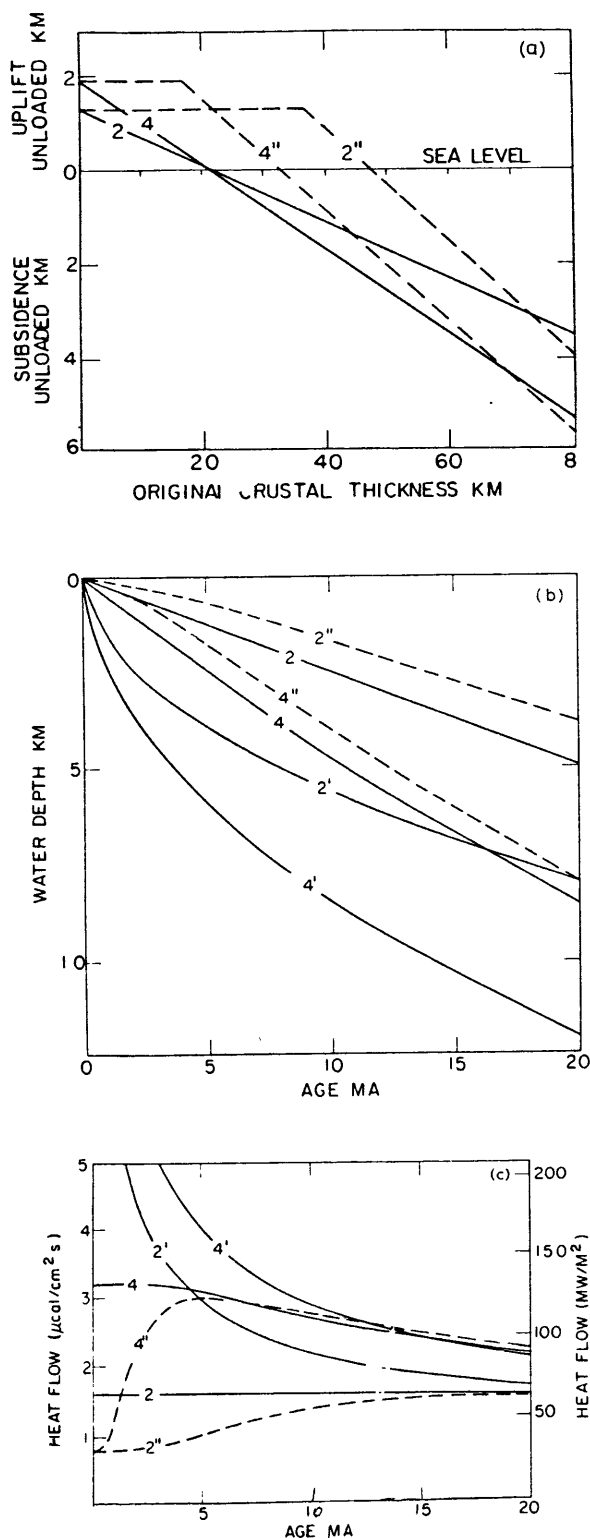
subsidence and the heat flow as a function of time for two different amounts of heat input (Fig. 2a, b and c). Note that the initial subsidence in the cases of uniform stretching and dike intrusion is the same for equivalent heat input. However, except when a large volume of crustal material is involved in the deformation, the subcrustal extension (or erosion) model (2″ and 4″, Fig. 2c) more often results in an initial uplift rather than in an initial subsidence. Uniform stretching and subcrustal thinning give roughly the same thermal subsidence curves for the same amount of heat input. The dike intrusion model yields a much faster early subsidence because heat is preferentially distributed near the surface. These differences are clearly illustrated by the early heat flow decay: the dike intrusion model shows a very high initial heat flow followed by a rapid decay, the uniform stretching model shows a lower initial heat flow followed by a less rapid decay, and the subcrustal thinning shows an early increase, a point of maximum heat flow, and then a decay which closely parallels the uniform stretching model. About 15 Ma after the extensional or thermal events have ceased all three models show approximately the same heat flow. Thus, for basins older than 10 Ma, it is not possible to use heat flow to distinguish among these models for basin formation.

Fig. 2. (a) Initial isostatic subsidence (unloaded) as a function of crustal thickness for various models of extension. The solid lines represent both the stretching and dike instrusion models, the dashed lines represent the subcrustal attenuation model. For the uniform stretching and dike intrusion models the subsidence curves represent extension by a factor of 2 and 4, respectively. For the subcrustal attenuation, the subsidence curves correspond to the same initial heat input as simple stretching by a factor of 2 or 4. For the purposes of calculation we have assumed that subcrustal attenuation is the result of eroding the base of the lithosphere. β = 2″ and 4″ correspond to eroding to depth of 36 and 17 km, respectively. (b) Calculated thermal subsidence/water loaded as a function of time corresponding to the models considered in (a). The solid curves are uniform stretching (2 and 4) and dike intrusion (2′ and 4′) and the dashed curves are subcrustal attenuation (2″ and 4″). (c) Calculated heat flow as a function of time, corresponding to the models in (a) and (b). The solid lines are simple stretching and dike intrusion, the dashed lines in subcrustal attenuation.
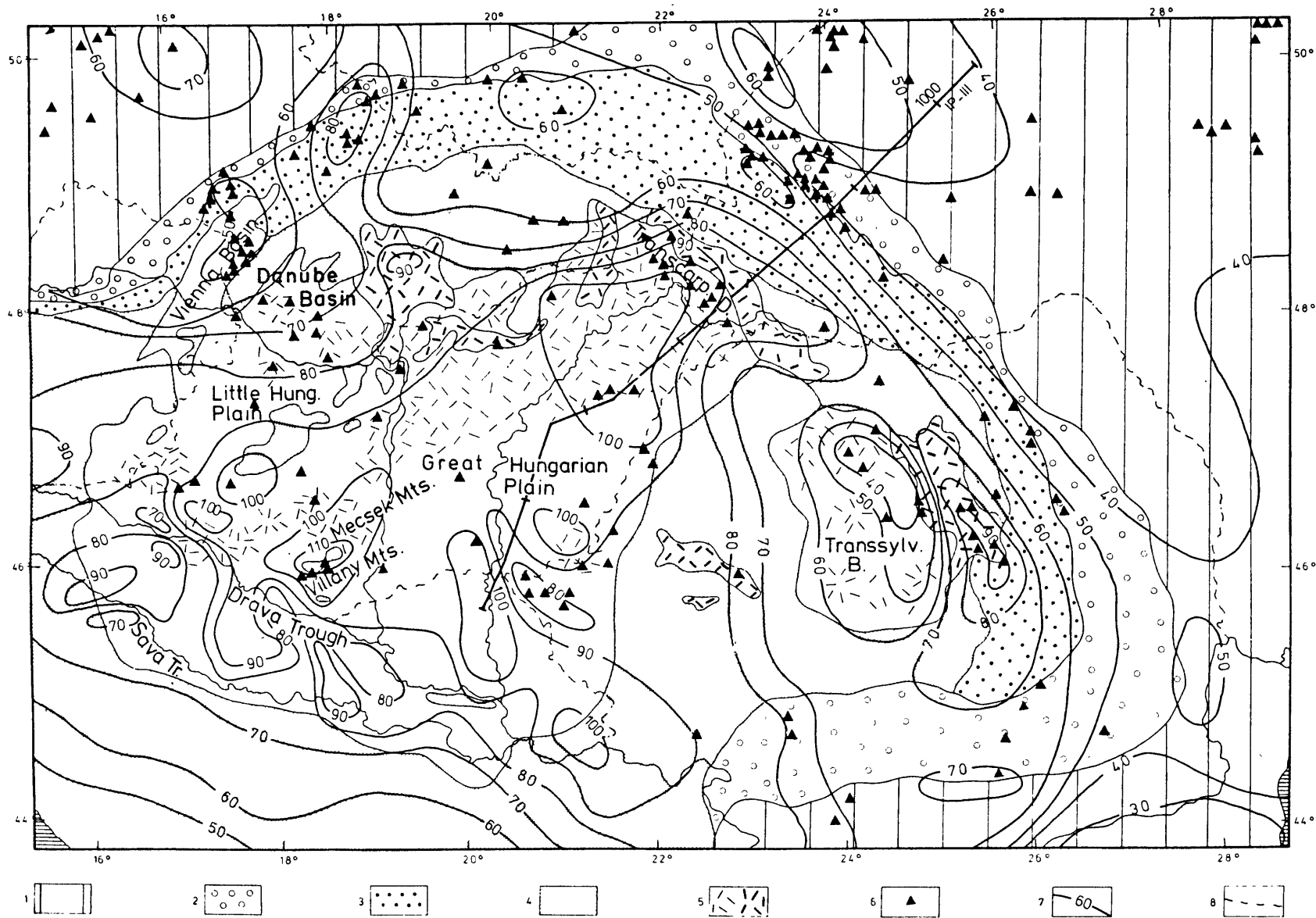
Fig. 3. Tectonic sketch and heat flow map of the Pannonian Basin and the surrounding Carpathian arc. The position of the heat flow stations and the seismic refraction profile discussed in the text are shown. Key: 1 = European foreland; 2 = Oligocene to Pliocene molasse foredeep; 3 = Upper Cretaceous, and Paleogene Flysch Nappes; 4 = Late Mesozoic (mainly Upper Cretaceous) nappe system of the eastern Alps, inner Carpathians, Apuseni Mountains and Dinarides; 5 = Mio-Pliocene calc-alkaline volcanics (covered and outcropping respectively); 6 = Neogene through Quaternary basins with heat flow stations; 7 = heat flow isolines, in mW/m^2; 8 = political boundaries. The heavy continuous line is a seismic refraction profile.

3. Geology, tectonic setting and basin development

The Carpathian arc can be divided into three units
of different origin: the Western, Eastern and Southern
Carpathians. The Western and Eastern Carpathians
can be further subdivided into two major belts: an
outer and inner belt. The outer, morphologically con-
tinuous belt is a pile of large thrust sheets composed
of Cretaceous/Paleogene flysch which overrode the
foredeep molasse during the Early and Middle Mio-
cene (Fig. 3). The inner belt of the Carpathian arc,
comprised mainly of Mesozoic and older rocks, is
discontinuous: large areas are subsided, others are
covered by Neogene volcanics. The Inner Western
Carpathians are composed of north vergent nappes
which came into existence during mid-Cretaceous

tectonic events. The Inner East Carpathians were
deformed into northeast and east vergent nappes
during the mid-Cretaceous and latest Cretaceous/
Paleocene tectonic phases. The sourth vergent nappe
structure of the Southern Carpathians was com-
pleted during the latest Cretaceous/Paleocene events.
The basin surrounded by the folded arc is not uni-
form. The Neogene/Quaternary subsidence only
affected certain areas, leaving some ranges emergent
and/or uplifted. These ranges divide the back-arc
area into several sub-basins (Fig. 4). Of these basins,
we shall call the Vienna Basin, Transcarpathian
Depression, West Danube Basin and the Transylvanian
Basin *peripheral* basins as they are situated at the
margin of the *central* Pannonian Basin.

The basement of the peripheral basins, Danube
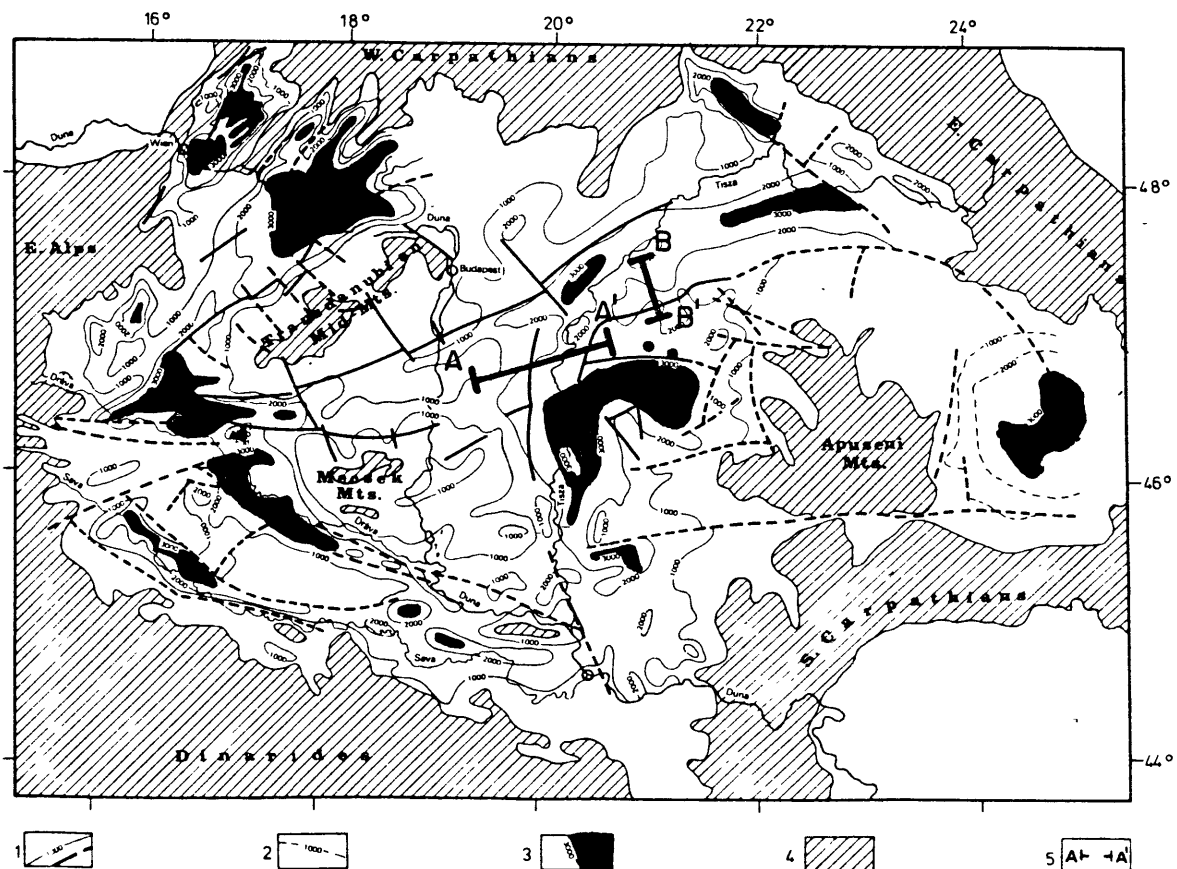
Fig. 4. Neogene-Quaternary sedimentary thickness of the intra-Carpathian basins (modified after Mahel [43]). Key: 1 = isoline of
the thickness of Neogene and Quaternary deposits and main faults; 2 = isoline of the thickness of the post early Miocene deposits
in the Transylvanian Basin; 3 = deep depressions; 4 = outcropping pre-Neogene rocks; 5 = profiles of wells discussed in Fig. 6a, b.
Solid dots show location of magnetic dating of sediments in boreholes.

Lowland and Little Hungarian Plain, is made up from the subsided blocks of the mountain arc, and their nappe structure is confirmed by deep borings and geophysical data [18—21]. The structure of the pre-Neogene bedrock of the Great Hungarian Plain is still under discussion. Though no extensive thrust sheets have been demonstrated by drilling, the pre-Neogene basement is known to be composed of belts which can be correlated with nappe units of the Apuseni Mountains and Inner Eastern Carpathians [22,23]. Thus we believe that much of the pre-Neogene basement of the intra-Carpathian depressions was part of a Late Cretaceous/Paleogene orogenic belt before it became involved in general extension and subsidence during the Neogene. The present block-like structure is the result of this neotectonic development.

The existence and significance of tectonic boundaries within the intra-Carpathian region is not generally agreed upon. Facies and faunal data, and structural connections suggest that the Inner West Carpathians and the western part of the Pannonian basement are continuous with the Austroalpine and South Alpine units to the west. While it has been suggested that the Inner East Carpathians, Apuseni Mountains and the southeastern part of the Pannonian basin have European affinities [24—26], the derivation of these regions and their relation to western terranes is controversial and uncertain. Anyway, the supposed large-scale movements of these regions occurred during the Late Cretaceous/Paleogene, and the beginning of Miocene saw a single, but certainly not immobile, Pannonian unit.

Sedimentological analysis has shown that the Carpathian flysch was deposited on continental rise and partly on deep-sea plains [27], and the deepest parts of the flysch basin were probably floored by oceanic crust [28—30]. The subduction of the oceanic crust went on, possibly with intermission, during the latest Cretaceous/Paleogene and was directed toward the Pannonian center [26,29]. Thrusting of the flysch nappes onto each other and their transport, on the foredeep molasse during the Early and Middle Miocene, indicate continental collision. The European foreland was overriden at least 35—60 km by the Outer Carpathian nappes [31] and the onset of extension and subsidence of the intra-Carpathian basins are synchronous with the continental-continen-
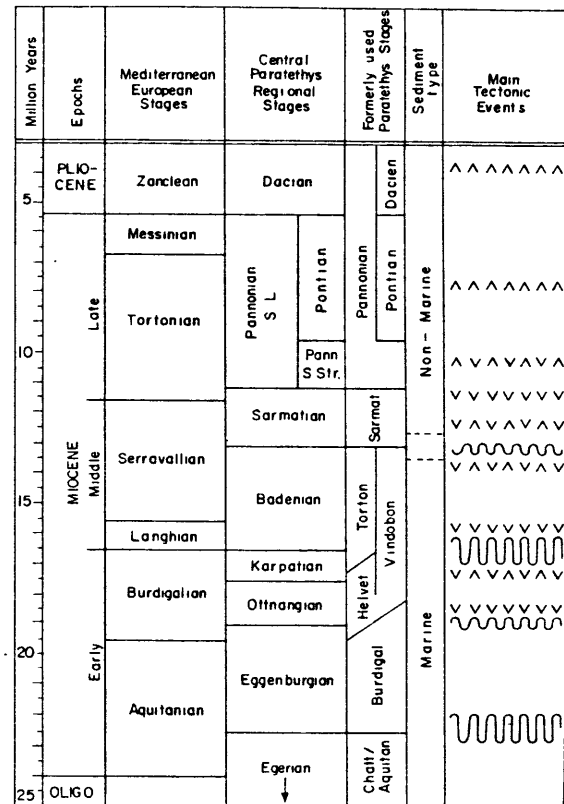
Fig. 5. Comparison of world-wide and regional biostratigraphical time scales. Also shown are the sediment type and the major episodes of compression (~~~~) and rhyolitic (V) and andesitic (Λ) volcanism within the Carpathian system.

tal collision in the arc.

Because of the isolation of the Paratethys from the Mediterranean during the late Middle Miocene, there is some difficulty in correlating the dating on regional stages in the Carpathians with that of the better known Mediterranean stages. For simplicity and consistency in our analysis we have adjusted all ages and dates to the time scale developed by Rögl et al. [32], as modified by F.F. Steininger (personal communication) (Fig. 5).

During the Late Oligocene, the central Paratethys covered southeastern Europe and parts of the slightly deformed flysch basin. At this time a large part of the central Pannonian region was emergent and subject to erosion, while the surrounding areas remained below sea level [33]. Beginning in the Eggenburgian folding and thrusting of the flysch complex was associated with intense vertical movements. Initiation

of rapid subsidence in the periphery of the Pannonian region led to marine sedimentation in the Vienna Basin and Transcarpathian Depression [20,34], while a large part of the central Pannonian region remained uplifted until the Badenian. The Neogene calc-alkaline volcanism began in this central region during the Ottnangian and continued sporadically until the Pannonian (s.s.) [35–37]. Here block faulting, graben formation and marine sedimentation began in the Karpatian, and rhyolites were erupted at several places including the Danube Basin and Transcarpathian Depression (Fig. 5). The tectonic activity reached its climax during the Badenian. Continuing compression gave rise to the overthrusting of the flysch nappes onto the foredeep molasse. The fill of the Vienna Basin was also deformed. In the early Badenian subsidence started which affected nearly the whole Carpatho-Pannonian area. Synsedimentary faulting was very active in the Vienna Basin, Danube Basin and Transcarpathian Depression. Andesitic lavas were erupted in northern Hungary, central Slovakia, and in the Apuseni Mountains. Rhyolites and their pyroclastics constitute beds of regional extent in the Badenian sediments of the Danube Basin, Transcarpathian Depression and Transylvanian Basin. This general period of extension in the back-arc area was interrupted by periods of slight compression, shown locally by gentle folding of the basin fill [38]. Reverse faulting of this age is evidenced to the south of the Transdanubian Mid-Mountains [39].

During the Sarmatian the whole Carpathian "firebelt" except the easternmost range, was active [40]. Andesites, dacites and rhyolites were erupted. At this time, the very fast subsidence of the peripheral basin finished. The central, Pannonian area was characterized by rapid subsidence which was accompanied by the eruption of rhyolites on the northeastern part of the basin. The Transdanubian Mid-Mountains and Mecsek Mountains started to emerge and elsewhere new areas subsided below sea level.

In the central region the transgression became general during the Pannonian. At about the same time the rate of subsidence in the peripheral depression drastically decreased and the uplift of the present-day Carpathian arc began.

Subsidence and lacustrine-fluvial sedimentation has continued during the Pliocene and Quaternary in the central part of the Little Hungarian Plain and over a large part of the Great Hungarian Plain [41]. The Carpathian arc, Apuseni Mountains and the Hungarian Mid-Mountains have remained emergent.

4. Basin subsidence

In this preliminary analysis of the Carpathian region we concentrate on the subsidence of the Neogene basins (Fig. 4). We begin with a discussion of subsidence in the peripheral basins, whose development is in marked contrast to that of the central basins. Although we shall only discuss the subsidence history of three of these, the Vienna and West Danube Basins and the Transcarpathian Depression, the general pattern of subsidence in the Transylvania Basin is similar.

From the Egerian to Ottnangian increased tectonic mobility, subsidence and uplift can be observed in the three basins. After this the subsidence in these basins may be divided into two distinct phases. The first of these begins in the Ottnangian (Vienna Basin) or the Karpatian (West Danube Basin and Transcarpathian Depression) and continues until the end of the Sarmatian. This phase is characterized by rapid subsidence. Initially deep-water deposits dominated but by the end of the Sarmatian the whole depositional environment became shallow water with a total sediment accumulation of more than 4 km. During the second phase of subsidence, from the end of the Sarmatian to present, the subsidence rate is considerably reduced and the sedimentary environment is generally shallow water. This second phase of subsidence appears to be linear and remarkably uniform from basin to basin (Fig. 6a).

In contrast, the subsidence of the Little and Great Hungarian Basins consists of a single phase after an early period of tectonic unrest (Ottnangian/Karpatian). In these basins, the major onset of sedimentation did not begin until the late Badenian or early Sarmatian. This single phase has continued until the present, and the sedimentary environment has been generally shallow water (Fig. 6b). Although the amount of subsidence varies across the basin, the rate of subsidence is remarkably consistent. The mean subsidence for the Great Hungarian Basin since the Sarmatian is approximately 1700 m. This is almost double that in the peripheral basins during the same time period.

AGE MA

(a)

25 20 15 10 5 0

DEPTH KM

W.D

V

T

Eg | E | O | K | B | S | Pa | Pont. | D | Q
                      | L. Pa | U Pa |
| Early | Middle | Late
         Miocene | Plio. | Q |

25 20 15 10 5 0

(b)

AGE
5   0

DEPTH

Cooke et al, (in prep.)

1

2

3

4

DEPTH KM

Eg | E | O | K | B | S | Pa | Pont | D | Q
                      | L. Pa | U. Pa |
| Early | Middle | Late
         Miocene | Plio. | Q |
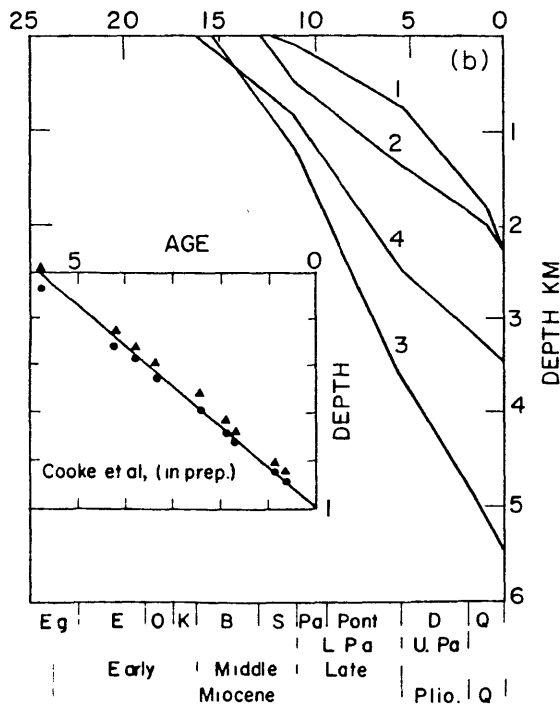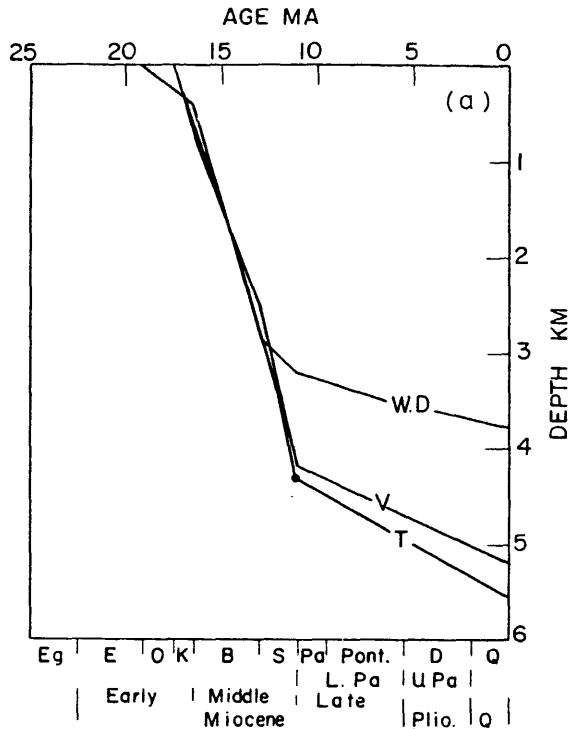
Recent paleomagnetic analysis of sediments recovered from two wells in the center of the Great Hungarian Plain, show a linear sedimentation/subsidence history for the last 6 Ma (Fig. 6b) (H.B.S. Cooke, personal communication). These data consist of approximately six hundred measurements for each well. The calculated subsidence rates are in good agreement with subsidence rates determined from paleontological dating and those estimated from fluvial terraces [41]. Furthermore, these data suggest that the cyclic nature of sedimentation is primarily the result of climatic variations and/or paleocurrents, rather than major changes in overall subsidence rate. Recent geodetic leveling measurements in Hungary also yield comparable subsidence rates.

The rate and amplitude of basement subsidence is easily measured and is directly related to the manner in which the basin was created. It is possible to use these observations to distinguish between the various explanations of basin formation. For this purpose we examined in detail the three wells from the peripheral basins discussed in the previous section (Fig. 6a) and twelve wells from the Great Hungarian Plain, the largest of the central Carpathian basins.

Our choice of wells in the peripheral basins is restricted since, apart from the Vienna Basin, there are few lithologic logs or complete cross sections available. Fortunately there are many drill holes in the central Carpathian basins from which subsidence data can be gathered and maps showing the sites and the overall thickness of sediments have been published in the Hungarian literature [44]. However, few profiles of wells with sufficient detail have been presented. Thus even in these basins, our choice of wells is limited. We have selected two profiles presented by Körössy [45] from the center of the Great Hungarian

Fig. 6. (a) Subsidence of basement as inferred from a well in the center of the Vienna Basin (V) [42], the Transcarpathian Depression (T) [34] and West Danube Basin (W.D.) [43]. The symbols represent the regional biostratigraphic zonation. (b) Subsidence as inferred from three wells in the great Hungarian Basin (1–3) and one bore hole in the Little Hungarian Plain (4). The symbols are the same as for (a). The inset shows on a proportionally exaggerated scale ages from paleomagnetic dating plotted against depth in the bore holes at Devavanya and Vesztö from H.B.S. Cooke (personal communication).

Plain for our analysis. These holes have been selected because all the stratigraphic boundaries, except the Quaternary on the lower profile, are documented. The position of the holes is known and it is possible to determine the thickness of the Quaternary from another map [46]. We selected twelve wells, six from the eastern profile and six from the north-south profile in Fig. 4.

In order to compute the depth of the basement through time it is necessary to allow for compaction, remove the sediment load, adjust for water depth at the time of deposition and add eustatic sea level changes [3]. All the wells were corrected for compaction using an exponential porosity/depth relation:

$$f = f_0 e^{-cz}$$

where f_0 and c were 0.42 and 0.31 $\times$ 10^{-5} cm, respectively. These figures were calculated from the density versus depth plots of Stegena [47] assuming a sediment grain density of 2.85 g/cm^3. The basic principles and the method used are discussed at length in Sclater and Christie [12]. For this analysis we ignored the effect of eustatic sea level and have

assumed that the depth of burial is close to sea level. Apart from the early Badenian in the Vienna Basin where deep-water marine fauna have been reported this is a reasonable assumption. Endemic molluscs are found from the Sarmatian onwards in the Carpathian basins and are a good indicator of a shallow-water environment. Except for the Transylvanian Basin where there has been Quaternary uplift, all the basins are currently within 200 m of sea level.

When corrected for sediment load (Table 1) the three peripheral basins still retain the remarkably sharp initial drop in basement depth followed by a slow linear increase shown by the uncorrected plots of sediment thickness versus time (compare Figs. 6a and 7). The large amount of early subsidence in the Transcarpathian Depression may not be significant. For this basin we followed the cross section given in Mahel [43, p. 123] and assumed basement as base Karpatian. This could well be in error as below the Karpatian there is an absence of sediment (Ottnangian uplift) followed by several hundred meters of Eggenburgian strata [34]. If the compaction of this were considered the initial subsidence would be much

TABLE 1

Subsidence analysis of three peripheral basins

Basin	Horizon	Age (Ma)	Depth (m)	Sediment thickness above basement (m)		ρ (g/cm^3)	Unloaded depth (m)	
				observed	corrected		1	2
Vienna	surface	0	0	7200	7200	2.53	2482	1302
	Pannonian	11	1000	6200	6544	2.52	2319	1139
	Badenian	16.5	4800	2400	3107	2.34	1333	153
	Ottnangian	19	5200	2000	2667	2.31	1180	—
	basement	—	7200	—	—	—	—	—
Transcarpathian	Upper Pannonian	6	0	5514	5514	2.47	2052	
	Pannonian	11	1103	4411	4755	2.44	1843	
	Sarmatian	13	2014	2500	3071	2.34	1321	
	Badenian	16.5	4749	765	1111	2.18	557	
	Karpatian	17.5	5514	0	0	—	—	
West Danube	surface	0	0	3782	3782	2.39	1553	
	Pontian	6	232	3550	3627	2.38	1504	
	Pannonian	11	582	3200	3377	2.36	1423	
	Sarmatian	13	873	2909	3152	2.34	1349	
	Badenian	16.5	3782	—	—	—	—	

1 = basement subsidence, 2 = basement subsidence since Ottnangian.
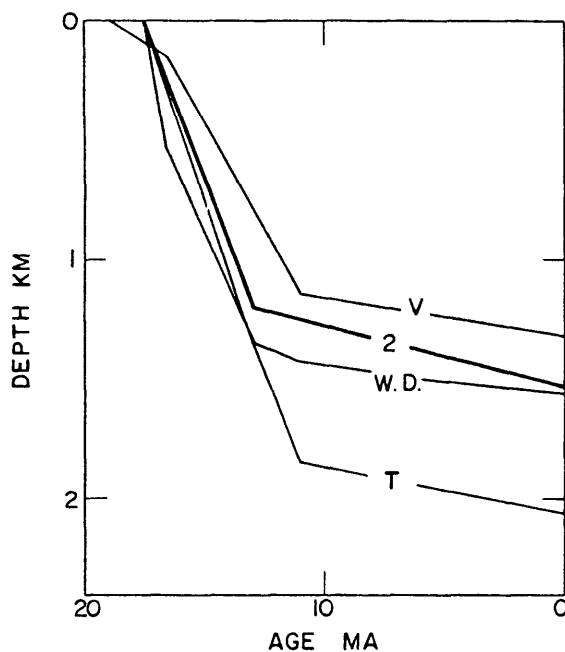
Fig. 7. Comparison of the inferred water loaded basement subsidence for the three peripheral basins from Table 1 with stretching by a factor of 2 (β = 2) of 40 km thick continental crust. The stretching was assumed to occur in the Badenian (16.5–13 Ma).

subsidence from compaction of the underlying sediments. When we recomputed each profile with the basement at this depth, we found the overall basement subsidence to be reduced to between 300 and 600 m.

To simplify the data anlysis and to permit easy comparison with theoretical models we averaged the subsidence data and calculated basement depth as a function of age assuming, first, no sediment, and then, 2 km of sediment below the base Sarmatian (Table 3). The resulting profiles cover the likely range of the mean subsidence of the twelve wells. To generalize these results we compared these two profiles with the averages depths to the base Quater-

reduced. Even given these differences the structure of the profiles from each of the three basins show exactly the same initial sharp drop of about 1.5 km followed by a much slower linear subsidence totaling 200–300 m from the Sarmatian to present (Fig. 7).

The subsidence information for the 12 wells on the Great Hungarian Plain is presented in Table 2. Though the total depth to base Sarmatian (13 Ma) of the wells varies from about 1100 to 2400 m the subsidence is fairly linear. When corrected for compaction and loading the basement subsidence remains linear but reduces to between 600 and 1050 m. Because of the porosity of the sediments changes only slowly with depth, compaction has little effect on the thickness of the sedimentary layers when basement is assumed to be base Neogene. However, there is sediment below the base Neogene in parts of the basin and as it also compacts on burial the effect must be considered. To estimate the range of this effect we chose basement at 2 km below the base Neogene as the maximum realistic contributon to the

Fig. 8. (a) The inferred basement subsidence for the mean of twelve holes in the Great Hungarian Plain (Table 3) assuming a basement 2 km below base of base Neogene (a) and basement at base Neogene (b) compared with the thermal subsidence expected after uniform stretching by a factory of 2 and 4. (b) The inferred basement subsidence for the mean depths of various horizons in the Great Hungarian Plain from Horvàth and Stegena [44] (Table 4) compared with the thermal subsidence expected after uniform stretching. The symbols are the same as in (a).

TABLE 2

Subsidence data from wells along profiles AA' and BB' (Fig. 4)

Well	Horizon	Age (Ma)	Depth (m)	Sediment thickness above basement (m) observed		corrected		ρ (g/cm^3)		Unloaded depth (m)		
				1	2	1	2	1	2	1	2	3

Subsidence data from six wells along profile AA'

Well	Horizon	Age (Ma)	Depth (m)	obs 1	obs 2	corr 1	corr 2	ρ1	ρ2	U1	U2	U3
Kecskemét W.1	sediment surface	0	–	2316	4316	2316	4316	2.29	2.43	1052	1715	618
	Pleistocene	2	263	2053	4053	2122	4144	2.26	2.41	980	1664	547
	Upper Pannonian	6	972	1344	3344	1522	3626	2.21	2.37	738	1504	407
	Lower Pannonian	11	1916	400	2400	522	2819	2.11	2.32	276	1234	137
	Sarmatian	13	2316	–	2000	–	2434	–	2.29	–	1097	–
	basement	–	4316	–	–	–	–	–	–	–	–	–
Kecskemét 1	surface	0	–	1156	3156	1156	3156	2.18	2.35	578	1352	321
	Pleistocene	2	270	886	2886	927	2925	2.16	2.33	472	1286	255
	Upper Pannonian	6	815	341	2341	395	2550	2.11	2.30	211	1139	108
	Lower Pannonian	11	1116	40	2040	49	2294	2.05	2.28	27	1043	12
	Sarmatian	13	1156	–	2000	–	2259	–	2.28	–	1031	–
	basement	–	3156	–	–	–	–	–	–	–	–	–
Kecskemét 3	surface	0	0	1291	3291	1291	3291	2.19	2.35	637	1395	355
	Pleistocene	2	272	1019	3019	1066	3104	2.17	2.34	537	1333	293
	Upper Pannonian	6	842	449	2449	519	2668	2.11	2.31	275	1182	142
	Lower Pannonian	11	1091	200	2200	243	2459	2.08	2.29	132	1106	66
	Sarmatian	13	1291	–	2000	–	2282	–	2.28	–	1040	–
	basement	–	3291	–	–	–	–	–	–	–	–	–
Jászkarajenö-1	surface	0	0	1496	3496	1496	3496	2.21	2.36	726	1462	409
	Pleistocene	2	360	1136	3136	1201	3248	2.19	2.35	547	1381	328
	Upper Pannonian	6	1110	386	2386	464	2659	2.11	2.31	247	1179	126
	Lower Pannonian	11	1420	76	2076	97	2387	2.06	2.29	54	1079	26
	Sarmatian	13	1496	–	2000	–	2317	–	2.28	–	1053	–
	basement	–	3496	–	–	–	–	–	–	–	–	–
Rakoczifalva-1	surface	–	–	1483	3483	1483	3483	2.21	2.37	720	1458	406
	Pleistocene	2	250	1233	3233	1282	3314	2.19	2.36	633	1403	351
	Upper Pannonian	6	920	563	2563	654	2804	2.13	2.32	341	1230	178
	Lower Pannonian	11	1425	58	2058	74	2368	2.06	2.28	41	1072	20
	Sarmatian	13	1483	–	2000	–	2315	–	2.28	–	1052	–
	basement	–	3483	–	–	–	–	–	–	–	–	–
Turkeve-1	surface	–	–	2218	4218	2218	4218	2.27	2.41	1016	1686	594
	Pleistocene	2	300	1918	3918	1994	4021	2.26	2.39	929	1627	535
	Upper Pannonian	6	1349	869	2869	1041	3215	2.17	2.35	525	1369	277
	Lower Pannonian	11	2142	76	2076	105	2496	2.06	2.30	57	1120	28
	Sarmatian	13	2218	–	2000	–	2422	–	2.29	–	1092	–
	basement	–	4218	–	–	–	–	–	–	–	–	–

29

TABLE 2

Subsidence data from wells along profiles AA' and BB' (Fig. 4)

Well	Horizon	Age (Ma)	Depth (m)	Sediment thickness above basement (m) observed 1	observed 2	corrected 1	corrected 2	ρ (g/cm³) 1	2	Unloaded depth (m) 1	2	3
Subsidence data from six wells along BB'												
Biharnagybajom-27	surface	–	0	1100	3100	1100	3100	2.18	2.34	552	1331	304
	Pleistocene	2	200	900	2900	931	2962	2.16	2.33	474	1284	257
	Upper Pannonian	6	650	450	2450	505	2623	2.11	2.31	268	1165	122
	Lower Pannonian	11	1050	50	2050	61	2292	2.06	2.28	34	1043	16
	Sarmatian	13	1100	–	2000	–	2248	–	2.28	–	1027	–
	basement	–	3100	–	–	–	–	–	–	–	–	–
Püspökladány-1	surface	0	0	1939	3939	1939	3939	2.25	2.39	910	1602	524
	Pleistocene	2	300	1639	3639	1708	3739	2.23	2.38	815	1539	461
	Upper Pannonian	6	1030	909	2909	1053	3190	2.17	2.35	531	1362	284
	Lower Pannonian	11	1839	100	2100	134	2480	2.07	2.30	·73	1114	36
	Sarmatian	13	1939	–	2000	–	2388	–	2.29	–	1078	–
	basement	–	3939	–	–	–	–	–	–	–	–	–
Nádudvar-6	surface	0	0	1715	3715	1715	3715	2.23	2.38	·817	1532	466
	Pleistocene	2	200	1515	3515	1560	3582	2.22	2.37	754	1490	424
	Upper Pannonian	6	985	730	2730	847	2992	2.15	2.34	435	1294	228
	Lower Pannonian	11	1688	27	2027	36	2377	2.05	2.29	20	1076	10
	Sarmatian	13	1715	–	2000	–	2352	–	2.29	–	1066	–
	basement	–	3715	–	–	–	–	–	–	–	–	–
Nádudvar-11	surface	0	0	1696	3696	1696	3696	2.23	2.38	809	1526	461
	Pleistocene	2	200	1496	3496	1541	3563	2.22	2.37	745	1484	419
	Upper Pannonian	6	912	784	2784	890	3024	2.16	2.34	460	1296	231
	Lower Pannonian	11	1609	87	2087	114	2430	2.06	2.29	63	1096	31
	Sarmatian	13	1696	–	2000	–	2349	–	2.28	–	1065	–
	basement	–	3696	–	–	–	–	–	–	–	–	–
Nádudvar-7	surface	0	0	1931	3931	1931	3931	2.25	2.39	904	1599	521
	Pleistocene	2	200	1731	3731	1780	3780	2.24	2.39	844	1559	481
	Upper Pannonian	6	985	946	2946	1088	3217	2.17	2.35	547	1370	292
	Lower Pannonian	11	1778	153	2153	202	2528	2.07	2.30	110	1131	53
	Sarmatian	13	1931	–	2000	–	2383	–	2.29	–	1078	–
	basement	–	3931	–	–	–	–	–	–	–	–	–
Nagyiván 1	surface	–	0	1812	3812	1812	3812	2.24	2.39	857	1562	490
	Pleistocene	2	300	1512	3512	1579	3612	2.22	2.37	762	1500	428
	Upper Pannonian	6	1247	565	2565	682	2876	2.13	2.33	356	1255	148
	Lower Pannonian	11	1712	100	2100	132	2460	2.07	2.30	72	1107	35
	Sarmatian	13	1812	–	2000	–	2366	–	2.29	–	1072	–
	basement	–	3812	–	–	–	–	–	–	–	–	–

TABLE 3

Mean subsidence data for twelve wells in the Great Hungarian Plain

Horizon	Age (Ma)	Depth (m)	Sediment thickness above Sarmatian (m)	Unloaded depth (m) 1	2
Surface	0	0	1679 (1100−2316)	798 (552−1052)	456 (304−618)
Pleistocene	2	259 (200− 360)	1426 (900−2053)	712 (472− 980)	400 (255−567)
Upper Pannonian	6	960 (650−1149)	695 (341−1344)	410 (211− 238)	212 (108−407)
Lower Pannonian	11	1566 (1050−2142)	114 (27− 400)	80 (20− 276)	39 (10−157)
Sarmatian	13	1679 (1100−2316)	−	−	−

Numbers between brackets indicate range of values. 1 = depth computed assuming basement at base Sarmatian, 2 = depth computed assuming basement 2 km below base Sarmatian.

nary, Pannonian and Sarmatian from Horváth and Stegena [44] when corrected for compaction and sediment load (Table 4). The mean of the twelve wells and the average data from all wells in the central basins are remarkably similar showing a steady basement subsidence of between 400 and 700 m since the Sarmatian (Fig. 8a, b). This steady subsidence of the central basins contrasts strongly with the very rapid initial and then slow later subsidence of the peripheral basins (Fig. 7).

5. Other geophysical data

Any viable thermal model for the formation and evolution of the intra-Carpathian basins must be con-

sistent with the geophysical observations. In this region these consist of heat flow, electrical conductivity, crustal seismics, magnetics, and gravity. Horváth et al. [48] have recently completed a re-analysis of the heat flow measurements in Hungary, and these have been added to the heat flow data for the surrounding regions (Fig. 3). There is a significant contrast between the heat flow through the peripheral basins, excluding the Transcarpathian Depression, and that through the central Great Hungarian Plain. The former is low, 1.2 $\mu cal/cm^2$ s (50 mW/m^2) while the latter is high, about 2.4 $\mu cal/cm^2$ s (100 mW/m^2). The Danube Basin and Little Hungarian Plain are transitional and are characterized by nearly normal values of 1.7 $\mu cal/cm^2$ s (70 mW/m^2). Based on the most reliable heat flow measurements in the Great

TABLE 4

Mean subsidence data for the Great Hungarian Plain from Horváth et al. [26]

Horizon	Age (Ma)	Depth (m)	Sediment thickness above basement (m) observed 1	2	corrected 1	2	$\rho(g/cm^3)$ 1	2	Unloaded depth (m) 1	2	3
Surface	0	0	1617	3617	1617	3617	2.23	2.38	756	1500	439
Quaternary	2	183	1434	3434	1473	3494	2.12	2.37	716	1461	400
Lower Pannonian	11	1423	194	2194	245	2513	2.07	2.30	133	1126	65
Sarmatian	13	1617	−	200	−	2336	−	2.29	−	1061	−
Basement	−	3617	−	−	−	−	−	−	−	−	−

1 = assuming basement at base Sarmatian, 2 = assuming basement 2 km below base Sarmatian, 3 = unloaded depth in the case of 2.

Hungarian Plain, we have computed a mean heat flow of 2.5 μcal/cm^2 s (110 mW/m^2), considerably higher than the average heat flow for the continents of 1.5 μcal/cm^2 s (63 mW/cm^2). We think it likely that the slightly high heat flow observed in the Carpathians and other areas not affected by subsidence, 1.7—2.0 μcal/cm^2 s (70—80 mW/m^2), is due to erosion. This value is average for recent orogenic belts. In contrast, the heat flow in the basins, which have clearly not been subjected to erosion, must be due to increased temperatures within the lithosphere.

Many seismic refraction lines have been shot in the vicinity of the Carpathians. These include individual profiles in localized areas such as the Vienna and Danube Basins and long composite lines crossing both basins, mountains and shields. The individual refraction profiles in the Vienna, West Danube and Transcarpathian Basins have revealed Moho depths of 26—32 km [49]. The most extensive of the composite profiles is the IP-III line which has been combined with the geological observations to produce a cross section of the crust from the Ukrainian Platform to the Great Hungarian Plain (Fig. 9). Note that while the depth of the crust under the Ukrainian Platform is normal, 40 km, that under the Outer Carpathians is deeper than normal, 50—65 km. Under

the Great Hungarian Plain the Moho is quite shallow, 25—30 km. Other seismic data from the Great Hungarian Plain clearly show the same shallow Moho, and demonstrate that the IP-III profile is representative for the basin. Density estimates for the subcrustal lithosphere, obtained from inversion of gravity data along this profile [44] indicate that the upper mantle under the Plain is less dense than that under the Ukrainian Shield. This discrepancy may reflect temperature differences in the two regions.

Adam et al. [51] have made a comparison of seismic velocities and electrical conductivity measurements from beneath the Great Hungarian Plain. They have shown that both the P-wave velocity and the specific resistivity decreases markedly at a depth of 60 km. Extending the present high heat flow to depth, they interpret these decreases as the onset of partial melting at the base of the lithosphere. The depth of this feature lies between 50 and 70 km. This is very much shallower than elsewhere under the continents, except for areas like the Basin and Range (Fig. 9). Positive travel time residuals in this region (0.7—2.6 seconds [52]) also suggest that lithosphere under the Pannonian Basin is hot compared to normal continental lithosphere.

The geophysical measurements from the central
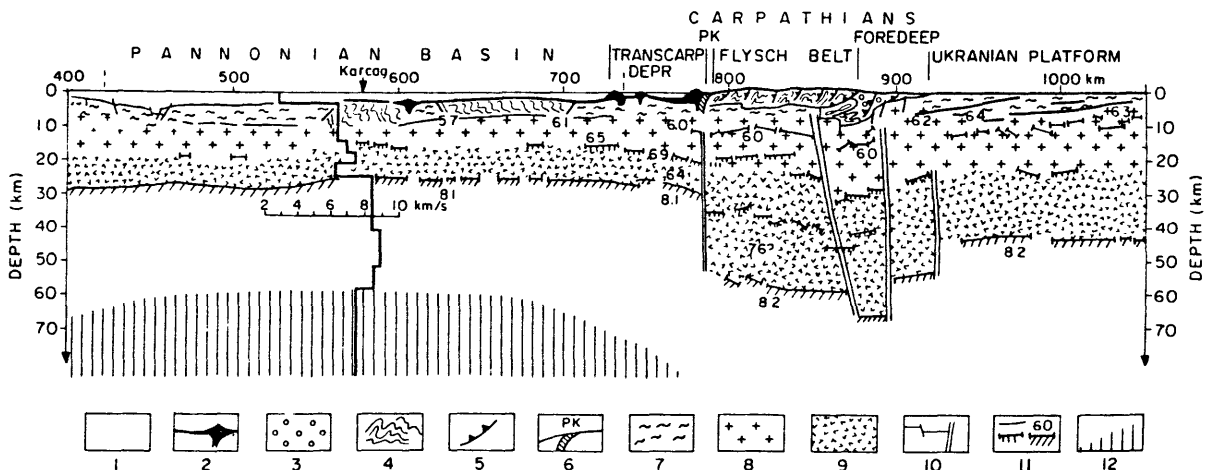
Fig. 9. Crustal structure of the Pannonian basin, Carpathians, and Ukrainian platform along the IP-III seismic line (see Fig. 3) (modified after Sollogub et al. [49]. The velocity vs. depth function was determined by Posgay [50] in the vicinity of Karcag. Key: 1 = Neogene-Quaternary sediments; 2 = Mio-Pliocene calc-alkaline volcanoes and volcanoclastics; 3 = molasse of the Carpathian foredeep; 4 = Upper Cretaceous Paleogene flysch; 5 = major thrust plane; 6 = Pieniny Klippen belt; 7 = Paleozoic and earlier basement, locally including Mesozoic rocks; 8 = upper crust; 9 = lower crust; 10 = local and major faults, respectively; 11 = seismic reflector, Conrad and Moho discontinuity, respectively, and seismic velocity, in km/s; 12 = subcrustal lithosphere and asthenosphere, respectively.

TABLE 5

Comparison of observations and predictions

	Observations	Predictions	
Peripheral basins			
Basement subsidence (water filled)		$\beta = 2$	
initial (km)	1.4	1.2	
thermal (m)	200	300	
Crustal thickness (km)	25	20 *	
Heat flow (μcal/cm^2 s)	1.4	1.7 **	
Pannonian Basin			
Basement subsidence (water filled)		$\beta = 4$,	β *** $= 4$
initial (km)	0	1.6,	0
thermal (m)	500–800	600,	500
Crustal thickness (km)	20–25	10 *,	20 *
Heat flow (μcal/cm^2 s)	2.5	2.8 **,	2.8 **

* Assuming 40 km thickness for pre-stretched crust.
** Assuming 0.6 μcal/cm^2 s heat flow from pre-stretched crust.
*** In this model the lithosphere was attenuated to 40 km and then stretched by a factor of 2.

basins are remarkably consistent. They imply a high heat flow, shallow lithosphere, and an attenuated crust.

6. Simple extensional explanations

Three idealized thermal models have been proposed to account for the geological development of continental shelves and intracontinental basins. These mechanisms are not exclusive and combinations of some or all could be operational in any basin. In this section we examine the compatibility of these proposed thermal models with the Neogene subsidence of the intra-Carpathian basins and the regional geological and geophysical information.

The development of the peripheral basins and that of the central basins are quite distinct. The peripheral basins are characterized by a subsidence history with two phases; the first with rapid sedimentation and a precipitous drop in basement depth, the second with slower, linear subsidence which continues to the Present (Fig. 6a). We propose that this first phase is an initial isostatic adjustment to deformation or alteration of the lithosphere, and that the second results from conductive decay of a thermal anomaly. In the central basins, there is only a linear subsidence phase which we propose is thermally controlled. For

reasons which we shall discuss later, the initial, isostatic subsidence is not observed.

In considering mechanisms which are compatible with observations for the peripheral basins, we can rule out both dike intrusion and subcrustal attenuation as the dominant mechanism. The strikingly linear subsidence during the second (thermal) phase is not in good agreement with the $\sqrt{t}$ relationship predicted by the dike intrusion model. Furthermore, in the Vienna Basin there is little or no evidence of igneous activity. Although both the stretching model and subcrustal attenuation predict linear subsidence compatible with the observed subsidence, only one of these, stretching, can satisfactorily explain the initial isostatic subsidence. In order for the subcrustal attenuation model to produce initial isostatic subsidence, a considerable fraction of the lower crust would have to be melted, presumably resulting in huge amounts of calc-alkaline volcanism. This is not observed in the Vienna Basin. There is considerable volcanism in the other peripheral basins. Moreover, the heat flow average of the Transcarpathian Depression is nearly the double that of the Vienna Basin, 95 mW/m^2, as opposed to 50 mW/m^2 (Fig. 3). It shows that stretching alone cannot explain the formation of the depression. However, the observed features can be explained in terms of stretching by a factor of two combined with 30% dike intrusion

which occurred some time later (cf. Appendix for computational procedure).

The present depth of Moho under the Vienna Basin and Transcarpathian Depression is 27–32 km and 26–28 km, respectively. By subtracting the 4- to 6-km sedimentary thickness 20–26 km is obtained, which is the end-product of the suggested stretching by a factor of two. This is reasonable since the crust under the Outer Carpathians is now about 50–55 km thick. Initial isostatic adjustment to stretching by a factor of two results in 2 km of unloaded subsidence. If 1 km of subsidence occurred above sea level, this would result in the observed 4 km of sediment fill. Thereafter, the water-filled subsidence would be about 300 m in 15 Ma (Fig. 2a, b and Appendix). This simple history is remarkably close to what is observed in the center of the Vienna Basin and Transcarpathian Depression. By reducing the amount of stretching it can be made to explain the West Danube Basin (Fig. 7).

The timining of these subsidence events is consistent with the geological history of the region. Extensional tectonics associated with compressional events started in the Eggenburgian, and continued until the earliest Badenian when the last major phase of compression terminated. It is during the latter part of this period that the rapid, isostatic subsidence occurred. Heat flow predicted for stretching by a factor of two gives 1.56 $\mu cal/cm^2$ s (65 mW/m^2) for the heat flow at present, i.e. after 15 Ma of conductive cooling. If the cooling effect of fast sedimentation is taken into consideration a slightly lower value is obtained (1.3–1.4 $\mu cal/cm^2$ s).Stretching by a factor of two and 30% dike intrusion at 10 Ma ago gives 2.4 $\mu cal/cm^2$ s for the heat flow at present, which is decreased by the sedimentation to 2.1–2.2 $\mu cal/cm^2$ s in good agreement with the observed values in the Transcarpathian Depression.

Although application of the stretching model gives good results in the peripheral basins, there are difficulties when this model is applied to the central basins. If we assume that the Pannonian was initially high, and subsided to sea level during the isostatic adjustment phase, then stretching by a factor of between 3 and 4 could account for the rapid basement subsidence since the Sarmatian. The present crustal thickness is 20–25 km. Stretching by the amount suggested implies an original crustal thickness

of at least 60–80 km and an initial unloaded isostatic subsidence of between 3 and 5 km (Fig. 2a). Though not totally unreasonable it is excessive. Furthermore, three- to four-fold stretching requires about 250–300 km of extension, a figure which is considered extreme by all geologists working in the area. It is these geological constraints coupled with the absence of any observed initial subsidence that imply that simple uniform stretching is not the total explanation of the observed subsidence.

The crust under the Pannonian Basin appears to have been attenuated by about a factor of two. If we assume a stretching by a factor of two it gives a total extension of 150–200 km. This amount of extension cannot be excluded because extreme estimates of overthrusting of the Western Carpathian flysch complex onto the foredeep molasse are of this magnitude [54]. However, stretching by this amount cannot explain the observed subsidence and high heat flow and therefore we have to consider the thermal role of some other mechanisms.

We have calculated subsidence for a model where extension occurs by 50% stretching and 50% dike intrusion. This gives a good fit to the observed subsidence, but is not entirely consistent with other observations. First, an intrusional event of this magnitude would result in variable Moho depth which is not seen in these basins. Second, in the deeper portions of the basins, where maximum dike intrusion would be expected, a $\sqrt{t}$ contribution to the depth-age relation should be observable. On the contrary, the subsidence in these regions is still linear, as shown by the deepest profile in the basin (Fig. 6b).

As a consequence of these problems it is clear that there is no simple explanation of the peripheral basins that will also account for the central basins. In essence the subsidence and heat flow observations from the central basins require the rapid shallowing of the isotherms in the Middle Miocene without any initial subsidence or stretching by more than a factor of two.

7. Modified stretching model

In order to explain the observations it is necessary to introduce extra heat into the lithosphere during the initial phase of basin formation. The simplest way of doing this is to assume that the initial conditions

were wrong and that the lithosphere was hotter than the linear equilibrium condition assumed before stretching. This is not unreasonable as the Pannonian basin was part of the Pannonian plate that lay over the downgoing European plate in the Early to Mid-Miocene [53]. Though it is unlikely that this extra heat was carried upwards by conduction because of the time constants involved there are other mechanisms by which the subcrustal lithosphere could be heated above equilibrium conditions. One possibility is that this entire heat results from tectonic interaction of smaller units within the Pannonian continental fragment which coincided chronologically with the termination of subduction along the arc. An alternative possibility is that the extra heat resulted directly from the termination of subduction. For example, assuming that the lithosphere consists of a brittle layer possibly as thick as the crust, overlying a more ductile layer then during subduction drag from the downgoing plate could remove some of the ductile layer from the bottom of the overlying plate. In this model the subcrustal attenuation could raise the depth of the lithosphere from 120 to roughly 40 km, without affecting the crust. This could have been followed by uniform stretching of the thinned lithosphere by a factor of two. If the initial crustal thickness were 40 km then the crust would be thinned to 20 km, and the asthenosphere raised to 20 km. These processes did not necessarily happen in the order given, and may have been synchronous. As a result of combining the two effects there is little or no initial isostatic subsidence and the temperature profile is close to that of simple stretching by a factor of 4. The consequent subsidence due to cooling is linear and matches that which is observed. In addition, the calculated heat flow is close to the average heat flow 2.5 $\mu cal/cm^2$ s (110 mW/m^2) in the basin. A simple schematic representation of how the initial temperature structure would be changed by this model is presented as Fig. 10.

There are spatial problems with this explanation. Extension of the lower lithosphere in the overriding plate cannot be greater or more rapid than the length or rate of subduction of the downgoing slab. It is unclear whether or not the amount of Miocene subduction is sufficient to produce the requisite thinning under the Great Hungarian Plain. On the other hand, we know little about the behavior of subducted plates
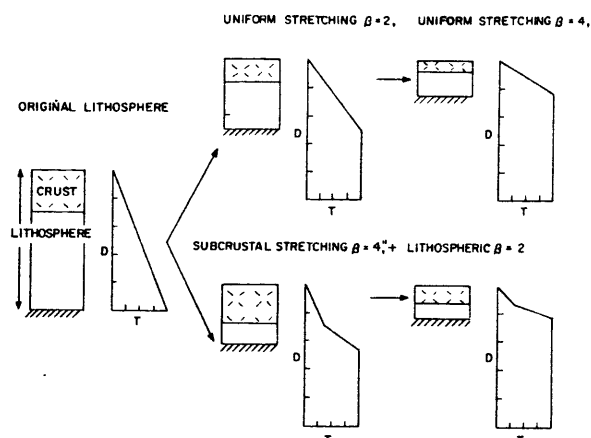
Fig. 10. A schematic diagram outlining how subcrustal stretching followed by whole lithosphere stretching can result in close to the same temperature profile as extensive uniform stretching. This enables high-temperature material to be brought close to the surface without excessive crustal thinning thus removing or reducing the initial subsidence. The same effect could also be created by lithospheric erosion.

at the time subduction ceases. Thus, it may be possible to create additional extension in the overriding plate by some sort of downward rotation or hinging of the subducted plate (Fig. 11b). In Roumania, where there is still some folding and crustal shortening in a small region in the outer portion of the arc, focal mechanisms for deep seismic activity suggests that the subducted plate is now descending vertically [55].

8. Erosional model

An alternative explanation for the extra heat necessary to produce the observed thermal subsidence not involving significant extension is subcrustal thinning and crustal erosion. If the downgoing plate drags with it aesthenospheric or even lithospheric material there would necessarily be flow in the aesthenosphere. Andrews and Sleep [56] have suggested that under these conditions erosion and melting of the lithosphere is rapid and results in the replacement of part of the lithosphere by asthenosphere. In this model the lithosphere under the central basin is fully attenuated by melting, erosion and downward

a) EARLY MIOCENE

EUROPE   PANNONIAN PLATE

MOLASSE   FLYSCH SUTURE ZONE INNER WEST CARPATHIANS   APUSENI

CRUST   BRITTLE

LITHOSPHERE   DUCTILE

ASTHENOSPHERE

b) EARLY MIDDLE MIOCENE

VIENNA B.   W DANUBE B.   APUSENI

SUBCRUSTAL EROSION OR STRETCHING THINS LITHOSPHERE

? ?   ?

c) LATE MIOCENE

BUDAPEST

VIENNA BASIN   DANUBE BASIN   GREAT HUNGARIAN BASIN   APUSENI

1 Molasse   2 Flysch   3 Suture   4 Calc-alkaline volcanism   5 Basin fill   6 Cont/Cont collision   7 Extension   8 Crust

Fig. 11. (a) Early Miocene position of the European and Pannonian plates showing the development of the molasse and flysch deposits, rhyolitic volcanism and oceanic subduction. (b) Early Middle Miocene collision of the two continental portions of the plates. The Outer Carpathians are formed by the collision. Stresses, associated with the subduction of the ductile portion of the Pannonian plate and asthenospheric processes, thin the lithosphere. (c) At the end of Middle Miocene collision terminates and the Vienna and West Danube Basins are formed by the uniform stretching of a cold thick crust and lithosphere. In contrast the Little and the Great Hungarian Basin are formed by the cooling of a thin hot lithosphere. Key: 1 = molasse; 2 = flysch; 3 = suture zone; 4 = calc-alkaline volcanism; 5 = basin fill; 6 = continent-continent collision; 7 = extension; 8 = continental crust.

drag caused by the undergoing slab. Further about 10 km from the originally 35 km thick crust is also melted and replaced by hot asthenosphere. This process also does not necessarily happen in the order given, and may be synchronous. After these combined events there is a slight initial isostatic subsidence (0.1 km) and temperature profile is also close to that of a simple stretching by a factor of 4. The subsequent subsidence history and heat flow matches that which is observed. This model is similar to that presented by Haxby et al. [57] for the Michigan Basin.

The melting and erosion mechanism has the advantage of requiring only one process to account for the elevated temperatures. As a consequence for this case the amount of extension of the Pannonian Basin was most probably about 50 km and certainly not more than 100 km. The subcrustal melting model is compatible with the geographic distribution of regional volcanism. The largest volume of the calc-alkaline volcanics in the Carpatho-Pannonian system can be found in the Pannonian Basin, where they are mostly rhyolite ignimbrites. It is widely accepted that ignimbrites originate by widespread crustal fusion [37,58,59]. However, this model has a major space problem: if 10 km of the lower crust has been melted then where has all this igneous material gone? There is no evidence for 30–40% dyke intrusion in the crust or for a 10-km igneous layer at the base of the sedimentary layer.

Four of the authors (J.G.S., L.R., B.C.B. and S.S.) prefer the modified stretching and the other two the erosional explanation. The differences of interpretation are based on different approaches to the physics of the problem. The four who prefer to modify the stretching model view thermal anomalies as the passive reaction of the lithosphere to extensional or mechanical forces. The two who favor lithospheric erosion are satisfied with this concept and prefer it because it is the simplest mechanically.

Though we disagree on the interpretation of the high heat flow and subsidence of the central basins it is important to note that we agree on the observations and the interpretation of the peripheral basins. Furthermore, all of us are convinced that the uniform subsidence in the central basins results from the cooling of a very thin lithosphere created some time in the Badenian (13 Ma).

9. Tectonic model for Carpathian basin development

By correlating the timing of events in the Carpathian arc with the onset and rates of subsidence in the intra-arc basins, we can suggest a tentative outline for the Neogene development of the Carpatho/Pannonian region. We will use a profile from the Vienna Basin, extending through Budapest, and terminating against the Apuseni Mountains. During the latest Oligocene and earliest Miocene the European foreland was underthrusting the "Pannonian plate" along a zone where the crust of the Carpathian flysch basin had largely been consumed. There was molassic sediment deposited on the European foreland while more towards the inner West Carpathians (leading edge of the Pannonian plate) the piling up of the flysch nappes commenced (Fig. 11a). The Pannonian plate is under both compression and tension. Compression in the crust is due to the beginning of the collision with the European plate and tension at depth resulting from the subduction of part of the ductile lower lithosphere of the Pannonian plate (Fig. 11a). Sometime in the early Middle Miocene the paroxysm of the continental collision occurred. The flysch sequence is compressed against and overrides the European plate. There is some extension at depth under the Pannonian Plate and the lithosphere starts to thin by either subcrustal erosion and melting or by simple extension (Fig. 11b). The considerable Middle Miocene andesitic and rhyolitic volcanism on the Pannonian plate is related to this process. This is the last stage of compression and thrusting in the Carpathians, the Vienna Basin, West Danube Basin, and the other peripheral basins are formed by simple stretching within the nappe type structures. At this time the lithosphere under the Pannonian Basin is further thinned by continued subcrustal erosion or by stretching. Such stretching may be associated with the downward rotation of the subducted portion of the European plate (Fig. 11b). By the end of Middle Miocene the active extension in peripheral basins has terminated leaving the lithosphere boundary close to the base of the crust, at a depth of some 50–60 km under the Vienna and West Danube Basins (Fig. 11c). The uniform stretching by a factor of two and the subsequent cooling of the thin lithosphere explains the rapid early subsidence and slow post-Sarmatian subsidence of the peripheral basins. In the central

basins, either twofold crustal stretching accompanied by extra thinning of the lithosphere or subcrustal erosion and lower crustal melting accounts for the absence of initial subsidence in these basins. The more rapid post-Sarmatian subsidence is a result of the cooling of an extremely shallow (20–30 km) lithosphere. Between the Late Miocene and the present there is no major tectonic activity and, except for the slight Quaternary uplift in the Transdanubian Mid-Mountains and Transylvanian Basins, the basins have subsided quiescently to their present depths.

The model we have presented above is necessarily much simpler than the actual development of the Carpathians and Pannonian. However, if it is in essence correct, it may have major implications for creation of black-arc basins and for extension behind continental collision zones and Andean type margins. If subcrustal attenuation of the overriding plate occurs continuously during subduction of oceanic material, and if the rate of subduction is so great that cracks form in the rigid part of the overriding plate, then passive penetration of basaltic material may result in formation of back-arc basins.

Careful reconstruction of thermal histories from subsidence data has great importance for the maturation of hydrocarbons in these basins. Although the total thickness of sediment in the peripheral and central intra-Carpathian basins is roughly equivalent, their temperature histories are radically different. For example, the Vienna Basin started cold and has never been very hot. In contrast, the Pannonian Basin started hot and has cooled down very little. This may explain why source material for hydrocarbons in the Vienna Basin is Mesozoic while that in the Pannonian Basin is probably Neogene. Our analysis explains how adjacent basins which are tectonically related can have very different thermal histories. Such ideas could be very important in the search for hydrocarbons and geothermal reservoirs in similar tectonic areas.

10. Conclusions

(1) We have shown that the intra-Carpathian basins are thermal in origin and are separated into two distinct categories. The first type of basin lies in the peripheral regions of the intra-Carpathian lowlands and has very fast initial subsidence followed by a period of slower, linear subsidence. These basins were formed by about two-fold stretching of the lithosphere with some contribution from dike intrusion in the Trans-Carpathian Depression. The rapid initial subsidence is an isostatic response to stretching which occurred during the Early/Middle Miocene (Eggenburgian to Sarmatian). The slower linear subsidence from the Sarmatian onward is thermally controlled.

(2) The second type of basin lies in the central intra-Carpathian region, has high heat flow and a reasonably fast linear subsidence since the late Middle Miocene (Sarmatian). This type of basin may be formed by either (a) two-fold stretching accompanied by subcrustal attenuation of the lithosphere, or (b) attenuation of the whole subcrustal lithosphere and part of the crust by subcrustal melting and erosion. These may be the result of lithospheric drag and/or secondary convection induced by subduction along the Carpathian arc.

(3) Careful analysis of sedimentation and subsidence rates enables us to reconstruct the thermal history of these complex intermountain basins. When detailed records of subsidence history are not available, models for the genesis of intracontinental sedimentary basins are unconstrained and open to debate. The subsidence history gives quantitative, rather than qualitative, constraints on basin evolution and should prove to be a valuable tool in sorting out how and why intracontinental basins and continental margins are formed.

Acknowledgements

Appendix

In general we may consider the lithosphere as a slab whose upper surface, $z = a$, is maintained at

temperature $T = 0$ and lower surface, $z = 0$, at $T = T_1$. If the slab is thermally perturbed at time $t = 0$, and subsequently cools through vertical conduction, the temperature distribution may be given by:

$$T = T_1 \left(1 - \frac{z}{a}\right) + T_1 \sum_{n=1}^{\infty} \left(\frac{2}{n\pi}(-1)^{n+1}\right) x_n$$

$$\times \sin\frac{n\pi z}{a} \exp\left(\frac{-n^2\pi^2 kt}{a^2}\right) \tag{A-1}$$

where $[(2/n\pi)(-1)^{n+1}]x_n$ is the nth Fourier coefficient of the initial temperature distribution. Likewise, surface heat flux, Q, and elevation above final equilibrium elevation, U, may be written:

$$Q = \frac{KT_1}{a}\left[1 + \sum_{n=1}^{\infty} 2x_n \exp\left(\frac{-n^2\pi^2 kt}{a^2}\right)\right] \tag{A-2}$$

and:

$$U = \alpha a T_1 \frac{4}{\pi^2} \sum_{m=0}^{\infty} \frac{x_{(2m+1)}}{(2m+1)^2}$$

$$\exp\left[-(2m+1)^2 \frac{\pi^2 kt}{a^2}\right] \tag{A-3}$$

We can calculate the x_n's which correspond to the three thermal processes described in the text; uniform stretching, dike intrusion, and subcrustal attenuation. If the lithosphere stretches by a factor δ from the surface to a depth y, and stretches by a factor β from y to the base of the lithosphere and is finally intruded by dikes, comprising a fraction γ of the lithosphere, the initial temperature distribution is:

$$T = T_1 \delta\left(1 - \frac{z}{a}\right)(1-\gamma) + \gamma T_1 \text{ for } \left(a - \frac{y}{\delta}\right) \leqslant z \leqslant a$$

$$T_1 \beta\left(1 - \frac{z}{a}\right) + \frac{y}{a}\left(1 - \frac{\beta}{\delta}\right)(1 - \gamma) + \gamma T_1$$

$$\text{for } a - \frac{y}{\delta} - \frac{(a - y)}{\beta} \leqslant z \leqslant \left(a - \frac{y}{\delta}\right)$$

$$T = T_1 \quad \text{for } 0 \leqslant z \leqslant a - \frac{y}{\delta} - \frac{(a-y)}{\beta}$$

and x_n is:

$$x_n = \gamma + \left\{(1 - y)[(\delta - \beta)\sin n\pi H + \beta \sin n\pi G]\right.$$

$$\left. \times \frac{(-1)^{n+1}}{n\pi}\right\} \tag{A-4}$$

where:

$$H = 1 - \frac{y}{a\delta}$$

$$G = 1 - \frac{y}{a\delta} - \left[\left(1 - \frac{y}{a}\right)\middle/\beta\right]$$

The total amount of heat (dimensionless) added to the lithosphere is:

$$\Delta H = \left[\left(1 - \frac{1}{\beta}\right) + \left(\frac{y^2}{a^2} - \frac{2y}{a}\right)\left(\frac{1}{\delta} - \frac{1}{\beta}\right)\right](1 - \gamma) + \gamma \tag{A-5}$$

where $\Delta H = 1$ is "total oceanization", or non-equilibrium heat input at a mid-ocean ridge. $\Delta H = 0$ represents a stable thermal equilibrium in the lithosphere (cold continent).

In addition to the thermal subsidence caused by conductive cooling of the lithosphere there is an immediate isostatic elevation change at $t = 0$ in response to deformation of the lithosphere. There are two contributing factors: (1) density changes due to elevated temperatures in the lithosphere and thermal expansion, and (2) density changes due to crustal thinning and replacement of light crustal rocks by. denser ultrabasic material. Elevation changes associated with thermal expansion are proportional to the total amount of heat added' to the lithosphere (equation A-5) and may be written:

$$E = \frac{T_1 \alpha a \, \Delta H}{2(1 - \alpha T_1)} \tag{A-6}$$

Elevation changes due to crustal thinning or replacement can be written:

$$-\left(\frac{\rho_m - \rho_c}{\rho_m(1 - \alpha T_1)}\right) t_c \left(1 - \frac{1}{\delta} + \frac{\gamma}{\delta}\right)\left(1 - \frac{T_1 \alpha t_c}{2a}\right)$$

$$(y \geqslant t_c)$$

$$\frac{-(\rho_m - \rho_c)}{\rho_m(1 - \alpha T_1)}\left\{y\left(1 - \frac{1}{\delta} + \frac{\gamma}{\delta}\right)\left(1 - \frac{\alpha T_1 y}{2a}\right)\right.$$

$$\left. + (t_c - y)\left(1 - \frac{1}{\beta} + \frac{\gamma}{\beta}\right)\left[1 - \frac{\alpha T_1}{2a}(y + t_c)\right]\right\}$$

$$(y \leqslant t_c) \tag{A-7}$$

where t_c is the original crustal thickness. Positive values indicate uplift, negative values indicate subsidence. The parameters used in the calculations are

ρ_m, the density of the mantle = 3.3 g/cm^3; ρ_c, the mean density of the crust = 2.9 g/cm^3; α, the thermal expansion coefficient = 3.2 X 10^{-5} °C^{-1}; a, the thickness of the lithosphere = 125 km; T_1, the temperature at the bottom of the plate = 1350°C; KT_1/a, the equilibrium heat flux = 0.8 X 10^{-6} cal/cm^2 s; and k, the thermal diffusivity = 0.0075 cm^2/s; and all are taken from Parsons and Sclater [1].

References

1 B. Parsons and J.G. Sclater, An analysis of the variation of ocean floor bathymetry and heat flow with age, J. Geophys. Res. 82 (1977) 803–827.

2 N.H. Sleep, Thermal effects of the formation of Atlantic continental margins by continental breakup, Geophys. J. R. Astron. Soc. 24 (1971) 325–350.

3 M.S. Steckler and A.B. Watts, Subsidence of the Atlantic-type continental margin off New York, Earth Planet. Sci. Lett. 41 (1978) 1–13.

4 C.E. Keen, Thermal history and subsidence of rifted continental margins — evidence from wells on the Nova Scotian and Labrador shelves, Can. J. Earth Sci. 16 (1979).

5 A.B. Watts and W.B.F. Ryan, Flexure of the lithosphere and continental margin basins, Tectonophysics 36 (1976) 25–44.

6 B.J. Collette, On the subsidence of the North Sea Area, in: Geology of Shelf Seas, D.T. Donovan, ed. (Oliver and Boyd, Edinburgh, 1968) 15–30.

7 R.J. O'Connell and G.J. Wasserburg, Dynamics of the motion of a phase boundary to change in pressure, Rev. Geophys. 5 (1967) 329.

8 M.H.P. Bott, Formation of sedimentary basins of graben type by extension of the continental crust, Tectonophysics 36 (1976) 77–86.

9 D. McKenzie, Active tectonics of the Alpide-Himalayan belt: the Aegean Sea and surrounding regions, Geophys. J. R. Astron. Soc. 55 (1978) 217–254.

10 D. McKenzie, Some remarks on the development of sedimentary basins, Earth Planet. Sci. Lett. 40 (1978) 25–32.

11 L. Royden, J.G. Sclater and R.P. Von Herzen, Continental margin subsidence and heat flow: important parameters in formation of petroleum hydrocarbons, Am. Assoc. Pet. Geol. Bull. 64 (1980) 173–187.

12 J.G. Sclater and P. Christie, Continental stretching — an explanation of the post-mid-Cretaceous subsidence of the central North Sea basin, J. Geophys. Res. (in press).

13 K. Burke, Hot spots and aulacogens of the European margin: Leicester/Shropshire; Oslo/Fen; Geol. Soc. Am. Abstr. 7 (1975) 34–35.

14 C.H. Scholz, U. Barazangi and M.L. Sbar, Late Cenozoic evolution of the Great Basin, Western United States, as an ensialic inter-arc basin, Geol. Soc. Am. Bull. 82 (1971) 2979–2990.

15 A.H. Lachenbruch, Heat flow in the Basin and Range Province and thermal effects of tectonic extension, Pageoph 117 (1978) 34–50.

16 L. Royden and C. Keen, Rifting process and thermal evolution of the continental margin of eastern Canada determined from subsidence curves, Earth Planet. Sci. Lett. 51 (1980) in press.

17 G.T. Jarvis and D. McKenzie, Sedimentary basin formation with finite extension rates, Earth Planet Sci. Lett. 48 (1980) 42–52.

18 O. Fusan, F. Ibrmajer, F. Plancar, F. Slavik and M. Smisek, Geological structure of the basement of the covered southern part of the inner west Carpathians, Zb. Geol. Vied, Zapadne Karpaty 15 (1971) 115–173.

19 Gy. Wein, Eine strukturgeologische Skizze des vorneogenen Untergrund des klienen Tiefebene, Proc. 10th Congr. Carpatho-Balkan, Geol. Assoc., Geol. Ust., Bratislava 3 (1975) 36–345.

20 F. Steininger, A. Papp, I. Cicha and J. Senes, Marine neogene in Austria and Czechoslovakia, in: Excursion "A", Reg. Comm. Med. Neog. Stratigr., 6th Congr. (Veda Publ. House, Slov. Akad. Sci., Bratislava, 1975) 1–96.

21 D. Ciupagea, M. Pauca and Tr. Ichim, Geologica Depresiunii Transilvanici, Bucuresti, Ed. Acad. (1970) 1–256.

22 Gy. Wein, Tectonic review of the Neogene-covered areas of Hungary, Acta Geol. Acad. Sci. Hung. 13 (1969) 399–436.

23 K. Szepesházy, Structural and stratigraphical connection between the basement of the Great Hungarian Plain east of the river Tisza and the Apusei Mts. in western Transylvania, Alt. Földt. Szemle, Budapest, 12 (1979) 178–198.

24 B. Géczy, Plate tectonics and paleogeography of the East-Mediterranean Mesozoic, Acta Geol. Acad. Sci. Hung. 17 (1973) 421–428.

25 J. Channel and F. Horváth, The African/Adriatic promontory as a paleogeographical premise for Alpine orogeny and plate movements in the Carpatho-Balkan region, Tectonophysics 35 (1976) 71–101.

26 F. Horváth, A. Vörös and K.M. Onuoha, Plate tectonics of the Western Carpatho-Pannonian region, a working hypothesis, Acta Geol. Acad. Sci. Hung. 21 (1977) 207–221.

27 R. Marschalko and T. Korab, The position of the east Slovakian flysch in the Carpathians, Mineral. Slovaca 7 (1975) 53–80.

28 D.P. Radulescu and M. Sandulescu, The plate tectonics concept and the geological structure of the Carpathians, Tectonophysics 16 (1973) 155–161.

29 M. Mahel, Development model of the West Carpathians, Geol. Zb., Geol. Carpath. 28 (1977) 203–218.

30 M. Mahel, Some particularities of development of the European Alpides and West Carpathians, mainly from the viewpoint of new global tectonics, Geol. Zb., Geol. Carpath. 21 (1978) 1–18.

31 Z. Roth and B. Lesko, The Outer Carpathian flysch belt in Czechoslovakia, in: Tectonics of the Carpathian-Balkan Regions, M. Mahel, ed. (Geol. Inst. D. Stur, Bratislava, 1974) 158–163.

32 F. Rögl, F.F. Steininger and C. Müller, Middle Miocene

salinity crisis and paleogeography of the Paratethys (Middle and Eastern Europe), in: K. Hsü, L. Montadert et al., Initial Reports of the Deep Sea Drilling Project, 42, part 1 (1978) 985–990.

33 F. Senes and I. Cicha, Neogene of the West Carpathian Mts. in: Guide to Excursion F, 10th Congr. Carpatho-Balkan, Geol. Assoc. (Geol. Inst. D. Stur, Bratislava, 1973) 1–46.

34 R. Rudinec, Paleogeographical, lithofacial and tectogenetic development of the Neogene in eastern Slovakia and its relation to volcanism and deep tectonics, Geol. Zb., Geol. Carpath. 29 (1978) 225–240.

35 G. Pantó, Cenozoic volcanism in Hungary, in: Guide to Excursion 40C, 23rd Sess. Int. Geol. Congr., Prague (1968) 1–106.

36 G. Hámor and A. Jámbor, A magyarországi közepsömiocén (The middle Miocene in Hungary), Föld. Közl. 101 (1971) 91–102.

37 L. Szádeczky-Kardoss, Gy. Pantó, T. Poka, G. Pantó, V. Szckyne-Fux, F. Kiss and I. Kubovics, Die neovulkanite Ungarns, Acta Geol. Acad. Sci. Hung. 11 (1967) 161–180.

38 K. Balogh and L. Körössy, Hungarian mid-Mountains and adjacent areas, in: Tectonics of the Carpathian-Balkan Regions, M. Mahel, ed. (Geol. Inst. D. Stur, Bratislava, 1974) 391–403.

39 F. Kokay, Geomechanical investigation of the southeastern margin of the Bakony Mts. and the age of the Liter fault line, Acta Geol. Acad. Sci. Hung. 20 (1976) 245–257.

40 D. Radulescu and M. Borcos, Spätsubsequenter alpiner Magmatismus in Rumanien, Acta Geol. Acad. Sci. Hung. 11 (1967) 139–152.

41 A. Ronai, Size of Quaternary movements in Hungary's area, Acta Geol. Acad. Sci. Hung. 18 (1974) 39–44.

42 R. Grill, J. Kapounek, H. Kupper, A. Papp, B. Plochinger, S. Prey and A. Tollmann, Guide to Excursion 33C Austria, Neogene Basins and Sedimentary Units of the Eastern Alps near Vienna, International Geological Congress XXIII Session (Geological Survey of Austria, Vienna, 1968) 1–75.

43 M. Mahel, Tectonics of the Carpathian-Balkan Regions (Geol. Inst. D. Stur, Bratislava, 1974),

44 F. Horváth and L. Stegena, The Pannonian Basin: a Mediterranean interarc basin, in: International Symposium on the Structural History of the Mediterranean Basins, Split(Yugoslavia), B. Biji-Duval and L. Montadert, eds. (Editions Technip, Paris, 1977) 333–340.

45 L. Körössy, Tectonics of the Basin Areas of Hungary, Acta Geol. Acad. Sci. Hung. 8 (1964) 377–394.

46 L. Stegena, B. Geczy and F. Horváth, Late Cenozoic evolution of the Pannonian Basin, Tectonophysics 26 (1975) 71–90.

47 L. Stegena, The structure of the earth's crust in Hungary, Acta Geol. Acad. Sci. Hung. 8 (1964) 413–431.

48 F. Horváth, L. Bodri and P. Ottlik, Geothermics of Hungary and the tectonophysics of the Pannonian basin "red spot", in: Terrestrial Heat Flow in Europe, V. Cermak and L. Rybach, eds. (Springer, Berlin/Heidelberg/New York, N.Y., 1979) 206–217.

49 V.B. Sollogub, D. Prosen and co-workers, Crustal structure of Central and Southeastern Europe by data of explosion seismology, in: The Structure of the Earth's Crust Based on Seismic Data, S. Mueller, Tectonophysics 20 (1973) 1–33.

50 K. Posgay, Mit Reflexionsmessungen bestimmte Horizonte und Geschwindigkeitsverteilung in der Erdkruste und in Erdmantel. Geophys. Trans., Budapest 23 (1975) 13–17.

51 A. Adam, F. Horváth and L. Stegena, Geodynamics of the Pannonian basin: geothermal and electromagnetic aspects, Acta Geol. Acad. Sci. Hung. 21 (1977) 251–260.

52 C. Morelli, S. Belleno and G. De Visintini, Non-directional travel-time anomalies for European stations, Bull. Geofis. Teor. Appl. 10 (1968) 164–180.

53 B.C. Burchfield, Eastern European Alpine systems and the Carpathian Orocline as an example of collision tectonics, Tectonophysics 63 (1980) 31–62.

54 C. Tomek, F. Svancara and L. Budik, The depth and origin of the West Carpathian gravity low, Earth Planet. Sci. Lett. 44 (1979) 39–42.

55 C. Roman, Seismicity in Romania – evidence for the sinking lithosphere, Nature 228 (1970) 1176–1178.

56 D.F. Andrews and N.H. Sleep, Numerical modeling of tectonic flow behind island arc, Geophys. J. R. Astron. Soc. 38 (1974) 237–251.

57 W.F. Haxby, D.L. Turcotte and J.M. Bird, Thermal and mechanical evolution of the Michigan Basin, Tectonophysics 36 (1976) 57–75.

58 H. Pichler and W. Ziel, The Cenozoic rhyolite-andesite associations of the Chilean Andes, Bull. Volcanol. 35 (1972) 424–452.

59 J. Klerkx, S. Deutsch, H. Pichler and W. Ziel, Strontium isotope composition and trace element data bearing on the origin of Cenozoic volcanic rocks of the central and southern Andes, J. Volcanol. Geotherm. Res. 2 (1977) 48–71.

CHAPTER TWO

TRANSFORM FAULTING, EXTENSION AND SUBDUCTION

IN THE CARPATHIAN-PANNONIAN REGION

PREFACE

L. Royden developed most of the ideas in this paper and wrote all versions of the text, with helpful suggestions from C. Burchfiel and F. Horvath.

F. Horvath made the isopach map, based on both published and unpublished data. L. Royden constructed the remaining figures and L. Royden and C. Burchfiel drafted the figures.

TRANSFORM FAULTING, EXTENSION, AND

SUBDUCTION IN THE CARPATHIAN PANNONIAN REGION

Leigh H. Royden
Department of Earth and Planetary Sciences
Massachusetts Institute of Technology
Cambridge, Massachusetts 02139, USA

Ferenc Horvath
Department of Geophysics
Lorand Eotvos University
Kun Bela ter 2
1083 Budapest, Hungary

B. C. Burchfiel
Department of Earth and Planetary Sciences
Massachusetts Institute of Technology
Cambridge, Massachusetts 02139, USA

ABSTRACT

The Carpathian arc formed during the Cretaceous to Miocene continental collision of Europe with a smaller continental fragment following southward and westward subduction of an oceanic terrane. During and after the last stages of thrusting in the outer Carpathians, a set of discrete basins opened up inside the Carpathian loop. These basins are regions of local extension, which appear to be associated with strike-slip faults. In general, northeast and northwest trending sets of conjugate shears reflect east-west extension of the intra-Carpathian region during the Middle and Late Miocene. Palinspastic reconstruction of the basins indicates roughly 75 to 100 km of extension, comparable to the magnitude of synchronous crustal shortening in the East Carpathians. Extension may have occurred to accommodate continued westward (A-type) subduction after plate convergence was prohibited by geometrical constraints and suggests that in this region Miocene subduction is driven by forces acting on the downgoing plate.

INTRODUCTION

The Carpathians form an eastward convex loop in the Alpine-Himalayan
mountain chain. Their internal structure can be traced westward into
the Eastern Alps and southward into the Balkanides. The Carpathians
consist of externally or radially directed thrust and fold nappes which
were emplaced during Cretaceous to Miocene time and may be divided into
two major belts: an outer, morphologically continuous belt, and an
inner, morphologically and structurally discontinuous belt. The inner
belt may be further subdivided into the West, East and South
Carpathians (Fig. 1). Thrusting, which occurred first in the internal
units and progressed outward, emplaced the nappes of the inner belt
during the Cretaceous and early Paleocene (Mahel, 1974; Burchfiel,
1980). In the East and West Carpathians, tectonic activity ceased by
the early Paleocene, and, except for Eocene deformation in the West
Carpathians, flysch deposition was continuous throughout the Paleogene
until the emplacement of the outer nappes during late Oligocene and
Miocene time. In the South Carpathians, major tectonic activity was
completed by the Late Cretaceous, although the entire region was later
subjected to minor folding and warping (Burchfiel, 1980).

The Carpathian loop surrounds a partially subsided
intra-Carpathian region whose pre-Tertiary basement is composed of
several continental fragments juxtaposed by Cretaceous to Eocene
tectonic events (Channell and others, 1979; Sandulescu, 1980). Since
Eocene time these fragments have behaved as a single unit, although
some internal deformation has occurred. This unit is now separated
from the Adria plate to the southwest by the continuation of the

peri-Adriatic line which extends southeast through the Vardar zone in Yugoslavia (Fig. 1). Part of the intra-Carpathian basement probably belonged to Adria during the Mesozoic and Early Tertiary. In the north, a narrow Eocene-Oligocene basin trends east northeast (Fig. 1). Eocene andesitic magmas were intruded and erupted along the axis of the basin, and lherzolite inclusions in these rocks suggest that they have a mantle source (Gy. Panto, 1980, pers. comm.). Traces of similar igneous rocks are found in the inner West Carpathians (Central Slovakia). Paleocurrent and sediment transport directions suggest a topographic elevation within the rest of the intra-Carpathian region of a few hundred meters, or less, during the Paleogene (T. Baldi, 1980, pers. comm.).

The Cretaceous-Paleogene evolution of the Carpathian system can be best described by the convergence and collision of two major continental units: (1) Europe and a rigid Moesian plate already welded together and (2) a smaller, non-rigid and highly deformed unit consisting of a complex assemblage of small continental fragments, which now forms most of the pre-Cenozoic basement for the intra-Carpathian region (Channel and others, 1979; Sandulescu, 1980). Convergence was probably the result of southward- and westward-directed subduction of a Jurassic-Cretaceous oceanic terrane of unknown extent. The polarity of subduction can be determined from the northward and eastward vergence of thrusting throughout the arc and from the internal position of Early Tertiary acidic magmatism. In the South Carpathians, continental collision was completed by Late Cretaceous time (Burchfiel, 1980). In the West and East Carpathians, convergence was interrupted during the Late Cretaceous and Paleocene, and, except for Eocene

deformation and convergence in the West Carpathians, most of the Paleogene was a period tectonic tranquility (Mahel, 1974).

NEOGENE EVOLUTION

Thrusting was reactivated along the outer Carpathian belt in latest Oligocene-early Miocene time (Mahel, 1974; Burchfiel, 1980). Outward of thrusting resulted in the emplacement of external flysch nappes and overriding of the foreland molasse. This late compressional event also affected the external units of the Eastern Alps. The age of major thrusting appears to become younger eastward around the arc (Fig. 2), but it is certain only that the end of thrusting is younger to the east (Jiricek, 1979). The thrust belt terminates near the juncture of the East and South Carpathians, although minor folding of the South Carpathian molasse occurred at this time (Sandulescu, 1975; Burchfiel, 1976).

Miocene and recent shortening has been estimated from palinspastic reconstruction as 60 km in the West Carpathians (Ksiazkiewicz and others, 1972) and about 100 km in the East Carpathians (Burchfiel, 1976), both minimum estimates.

Reactivation of thrusting in the outer belt was accompanied by a magmatic arc which extended from the Graz basin eastward to the Transylvanian basin (Sandulescu 1980; Boccaletti and others, 1973). The igneous rocks are primarily rhyolite, rhyolite tuff, andesite and dacite. Lherzolite inclusions within the andesitic rocks suggest a deep magmatic source. On the basis of major and trace element chemistry, these andesites are indistinguishable from Eocene volcanics erupted in northern Hungary (Panto, Gy., 1980, personal communication).

Eruption of magma was episodic (Fig. 3), and there is a clear eastward migration of volcanic activity along the arc consistent with eastward migration of thrusting (Lexa and Konecny, 1974). In addition, the internal position of the magmatic arc suggests south- and west-dipping subduction (Fig. 3).

During and after the last stages of thrusting in the outer Carpathians, a series of discrete basins opened up within the intra-Carpathian region. The basins are characterized by high heat flow and thin crust, and exhibit a two-phase subsidence history (Sclater and others, 1980). The first phase is a (usually) rapid Badenian (16.5-13.0 ma) subsidence which corresponds to a maximum sediment thickness of 4 km (Vienna and Transcarpathian basin). These mostly shallow-water sediments are well localized within distinct fault-bounded basins, are typically cut by syn-sedimentary normal faults, and exhibit rotated bedding. The second phase is a slow, long-term subsidence which began at the end of the Badenian and has continued to the present. Sedimentary rocks deposited during this phase are generally flat-lying and unfaulted. Their horizontal extent is much greater than that of first-phase sediments, and the sediments onlap onto the pre-Neogene basement. Onset of both phases is approximately the same for all basins, although subsidence began slightly earlier in the Transcarpathian basin, and the first phase is poorly developed in the Pannonian basin. This pattern of development does not seem to fit the Transylvanian basin, which shows normal crustal thickness, low heat flow, and little or no signs of extension or faulting during the Miocene (Ciupagea and others, 1970, Veliciu and Demetrescu, 1979). Furthermore, this basin has undergone recent uplift

and erosion, although there has been little or no folding and deformation of the basin fill. Surface elevation of the Transylvanian basin is approximately 500-600 m, whereas the other basins have elevations of ~100 m above sea level. Basin development was accompanied by folding in the southwest (Sava fold belt). These folds are arranged en echelon, and the fold axes trend approximately east-west (Fig. 3).

The generalized development of an extensional basin may be divided into two stages (McKenzie, 1978; Royden and Keen, 1980). During and immediately after extension there is a rapid change in elevation (usually subsidence). This occurs in isostatic response to net density changes resulting from crustal thinning and from heating and thermal expansion. The second stage of subsidence is a relatively long-term process caused by cooling and contraction of the lithosphere following the extension phase. Overall subsidence is generally amplified by effects of sediment loading. If original crustal thickness, elevation, and temperature structure are known, a detailed analysis of subsidence history can be used to determine the magnitude of extension. Subsidence of the intra-Carpathian basins may be interpreted as the result of Badenian extension, which affected the entire intra-Carpathian region but was inhomogeneous and left some blocks emergent and relatively undeformed (Sclater and others, 1980). The two types or phases of subsidence can be summarized as follows: the first phase is rapid, fault-bounded and extremely localized and is due to crustal extension. The second phase is a long-term subsidence of greater areal extent and is thermally controlled by decay of a thermal anomaly produced by extension of the crust and underlyuing lithosphere.

It should be noted that the first phase is a response to active processes in the crust and lithosphere which are reflected by syn-sedimentary faulting and rotation of bedding. The second is the result of the passive cooling of the lithosphere towards thermal equilibrium, and sediments are correspondingly flat-lying and undisturbed.

Sclater and others (1980) give a detailed analysis of subsidence, heat flow and crustal thickness of the intra-Carpathian basins which will not be repeated here. They conclude that these basins formed by 100% extension of the crust and underlying lithosphere (although the Pannonian and east Danube basins seem to require and additional heat source which may be related to subduction along the arc (?)). On the average, these estimates of extension are probably too high, since they were generally determined from subsidence of the deepest part of the basins.

Although the major phase of tectonic activity and extension was completed in the Middle to Late Miocene, minor tectonic activity continues throughout much of the Carpathian region. Strike-slip and normal faults of small displacement cut Pliocene sediments in the Pannonian basin, and along the arc, folding and deep earthquakes in Romania suggest continued seismic activity (Roman, 1970; Fuchs and other, 1979). Weak seismic events have also been detected in the intra-Carpathian area (magnitude <5.5), and while it is not clear thar present seismic activity is a direct reflection or continuation of earlier events, the sense of motion and local stress pattern inferred from fault plane solutions is compatible with that inferred for Miocene events (Gutdeutsch and Aric, 1976).

A MECHANICAL MODEL FOR MIOCENE BASIN FORMATION

Although Sclater and others (1980) demonstrate that the intra-Carpathian basins formed by lithospheric and crustal extension, the exact relationship of these extensional processes to the geometry and structural evolution of the basins is unclear. The small size, limited areal extent and apparent isolation of the intra-Carpathian basins presents certain conceptual difficulties when viewed in light of a consistent pattern of regional extension and deformation. Small, isolated basins of similar character occur along the San Andreas fault (Crowell, 1974) and in other regions where they appear to be associated with major strike-slip faults (Quennell, 1959). In map view these "pull-apart" basins are typically rhombohedral and are bounded by steep normal faults. This phenomenon has been demonstrated theoretically by finite difference calculations (Segall and Pollard, 1980).

In map view, the Vienna basin, which was superimposed on Early Miocene and older thrust nappes, has a rhombohedral shape, suggesting that it may have formed as a pull-appart basin along strike-slip fault segments (Fig. 4). Large normal faults which cut the basement and older sediments indicate that the major phase of extension was lower and middle Badenian, and that strike-slip faulting may have been most active at this time. The orientation of the rhombohedron-shaped sedimentary basin fill and the location of known faults suggest that the sense of lateral displacement was left shear. Minor seismic activity along a northeast-trending fault at the southeastern end of the basin exhibits fault plane solutions which indicate east-west extension and steeply dipping or vertical nodal planes (Gutdentsch and Aric, 1976). These data are also consistent with left shear. The strike-slip components of

motion along this and other faults which strike northeast is difficult
to show directly by surface and subsurface mapping because these faults
strike parallel to the thrust fronts. However, north of the Vienna
basin, large sinistral displacements have been proposed along
north-northeast trending faults within the external flysch Carpathians
(see, for example, Krs and Roth, 1977, 1979). Since the deepest part of
the Vienna basin appears to be the result of 50 to 100% extension of the
crust, probably a few tens of kilometers of strike-slip displacement are
sufficient to produce the Vienna basin. This general style of basin
formation can be extended to other intra-Carpathian basins.

Figure 5 shows one system of strike-slip faults which can explain
the extension of the intra-Carpathian basins, their individual
geometries, and their relationship to one another. Some faults are
known from geologic and subsurface mapping. Other faults were
identified by steep isopach gradients in the sediments or from air
photos, and some of these may have large components of lateral motion.
Direct geologic corroboration is somewhat difficult to obtain for many
of these faults. Much of the intra-Carpathian region is covered by
post-extensional (Pliocene and Quaternary) sediments. Drill hole data
and reflection seismic profiles show normal and growth faults bounding
many of these basins, but horizontal displacements cannot be detected
from these subsurface data. Some faults in the emergent blocks and in
the Carpathians have surface traces which disappear under the Neogene
basins. Many of these have been interpreted as thrust and normal
faults, as in the Vienna basin, but because they strike parallel to
thrust fronts, they may have a significant component of lateral offset.
The age of many of these faults is also uncertain, although some are

known to be late Miocene. Up to 30 km of Badenian (16.5-13.0 ma) displacement can be shown on some of these faults (Z. Balla, 1980, pers. comm.)

There is some latitude in connecting the various faults in Fig. 5, but the variations appear to be of only minor importance. Regional extension occurred along mostly northeast- and northwest-trending sets of conjugate shears, and the sense of motion is consistent with east-west extension (northeast sinistral shear, northwest dextral shear). Not all the basins are directly analogous to simple rhombic pull aparts like the Vienna basin, and some formed at the intersection of conjugate faults (for example the Zala basin). However, all (with the probable exception of the Transylvanian basin) are regions of local extension related to motion along strike-slip faults, and the extended regions form a series of eastward-opening arcs. This style of extensional faulting is similar to recent extension in the Basin and Range, where areas of significant extension are separated from relatively undeformed regions by a complex system of shear zones (Davis and Burchfiel, 1973).

The synchronous development of en echelon folds in the western part of the intra-Carpathian region (Sava fold belt) is probably related to this extension and, locally, to dextral shear along west-northwest-trending strike-slip faults. The east-west trend of the fold axes suggests relative north-south compression and is consistent with the stress field inferred from strike-slip faults. Similar en echelon folding associated with large shears has been demonstrated experimentally in clays (Wilcox and others, 1973). Regional seismic activity is quite weak, but the few shocks large enough to produce

reliable fault plane solutions are also consistent with east-west extension and north-south compression. Most Miocene faults appear to be reactivated parts of older Mesozoic tectonic lines. In the northwest, left-slip faults parallel the northeast strike of the thrust fronts in that portion of the West Carpathians (Brix and Schultz, 1980). Similarly, in the Transcarpathian depression, dextral shear occurred along a northwest-trending fault system parallel to the thrust fronts. The large shear zone north of the Pannonian basin appears to have been a major Mesozoic and early Cenozoic tectonic line of uncertain significance.

DISCUSSION

The eastward migration of thrusting around the Carpathian loop and extension of the intra-Carpathian basins, which occurred mostly during the Badenian (16.5-13 ma), can be correlated within a simple regional tectonic framework. In late Oligocene and early Miocene time, Adria (and Africa) moved north relative to stable Europe, causing compression and thrusting across the Eastern Alps and dextral shear along a major intra-continental transform parallel to the Dinaric Alps (Fig. 6a). As a direct result of this north-south convergence between Adria and Europe, the intra-Carpathian region was displaced eastward, (or northeastward?) initiating late Cenozoic thrusting in the West and East Carpathians. This is analogous to the present situation in Turkey where a continental fragment in western Turkey is moving westward due to the collision of Arabia and Asia (McKenzie, 1972).

By Badenian time (16.5-13 ma), north-directed thrusting was essentially completed in the Eastern Alps and West Carpathians, but major crustal shortening continued until about 12 ma in the northern part of the East Carpathians and through the Pliocene in the southeastern part (Fig. 6b). Convergent motion between Adria and Europe occurred primarily by dextral shear along the peri-Adriatic-Vardar fault system (Burchfiel, 1980) although far to the west thrusting continued in the Western Alps (Laubsher, 1971). This large transform boundary essentially isolated the Carpathian region structually from the rest of the Mediterranean. Miocene splays off of the peri-Adriatic fault system extend into the Carpathian area and indicate that isolation was not total, but it is our opinion that the Carpathian region was not strongly coupled to Adria during the Middle

and Late Miocene. Hence, it appears that east-west crustal shortening in the East Carpathians was compensated by east-west extension of the intra-Carpathian region. We cannot exclude the possibility that some north-south extension also occurred. The migration of thrusting around the Carpathian belt probably corresponds to the migration of (A-type) subduction also suggested by the eastward migration of calc-alkaline volcanics. Back-arc-type extension of the upper plate seems to have occurred when continued subduction along the plate boundary in the East Carpathians was not matched by the rate of rigid plate convergence. A similar relation was proposed by Molnar and Atwater (1978) for oceanic back-arc basins.

If extension of the intra-Carpathian basins did occur to accomodate crustal shortening in the East-Carpathians, the net east-west extension across the entire intra-Carpathian region should be roughly equal to the total Badenian and post-Badenian shortening in the East Carpathians. Palinspastic reconstruction assumes that the crust may be treated as a system of more-or-less rigid blocks which are bounded by zones of deformation. These zones may be grouped as extensional (basins), transform boundaries (strike-slip faults and more diffuse shear zones), and compressional (overthrusting and folding—along the Carpathian arc only). This system is very roughly analogous to the large-scale tectonics of ridges, subduction zones, and transform faults. The major difficulties in attempting to make "tectonic reconstructions" at this scale are: (1) The division between a "rigid block" and a zone of deformation is somewhat ambiguous, and all the blocks may be subject to some internal deformation, (2) the magnitude and direction of crustal extension are not always clear. Hence, rigorous reconstruction of

pre-Miocene geometries is not feasible for the intra-Carpathian region.

However, this approach may be useful as a first-order approximation in determining the relative motions and style of deformation within the Carpathian system. Additional information is supplied by estimates of crustal shortening in the Carpathians. This constraint is lacking for large-scale tectonic reconstructions, where the rates of subduction of oceanic plates must be inferred from the plate motions. By further analogy with the consistency condition for relative motion of large-scale plates, the motions of all the blocks within the system should be internally consistent. This also applies to the zone of shortening along the Carpathian loop and to the European foreland.

Assuming 50% to 100% extension in the basins, total east-west extension is estimated as 75 to 100 km. Comparing this to about 100 km of Miocene shortening estimated for the East Carpathians by Burchfiel (1976), the magnitudes are seen to be in fair agreement. However, it should be remembered that palinspastic restoration of thrusts and folds within orogenic belts always provides only a minimum estimate of crustal shortening.

The temporal and spatial connection between thrusting, volcanism, and basin extension is not unique in the history of the Carpathian region. A similar situation seems to have prevailed during Eocene time, when northwest crustal shortening in the West Carpathians and to the south (Zagreb line) was accompanied by basin formation and eruption of andesitic magmas, apparently from a deep source (Fig. 1). Because the orientation of the regional stress field for this Eocene event must have been totally different from that for later Miocene extension, it is not surprising that the orientation and location of the Paleogene basin

appears totally unrelated to that of the Neogene basins.

The development of extensional basins adjacent to a zone of subduction and apparent compression suggests that this subduction cannot be driven by rigid plate convergence, since it is difficult to understand how compressional stress can be transmitted across an extending terrane. Furthermore, motion between Europe and Adria appears to be taken up along a transform boundary parallel to the strike of the Dinaric Alps, and to be unrelated to Miocene shortening in the East Carpathians. Hence, in the East Carpathians, subduction must be driven from the subduction zone itself and might be accomplished by gravitational forces acting on the downgoing slab. One possibility is that shortening in the East Carpathians and corresponding basin extension is the result of bending of an initially shallow-dipping subducted plate into a vertical position and retrograde motion of the position of the trench (Fig. 7). This mechanism is supported by intermediate depth earthquakes in Romania which indicate the existence of a vertical slab to depths of 150 km, with down dip component of extension (Fuchs and others, 1979). Furthermore, this mechanism can explain the migration of the andesitic volcanic arc toward the suture (Szadeczky-Kardoss, 1976). In the East Carpathians some of these volcanic rocks are very near to and almost superimposed on the suture zone. This mechanism may be a common process following the termination of true subduction and may help to explain the spatial and temporal distribution of volcanism in some Mediterranean back-arc basins.

This downbending of the subducted plate may also help to explain the existence of the Transylvanian basin. As mentioned above, this basin shows little or no evidence of extension and heating, and its 3 to

4 km of Miocene sediment fill a regular, saucer-like depression which is not cut by major faults. In addition, the basin has experienced recent uplift and erosion, although little compression or folding has occurred. The mean surface elevation of the Transylvanian basin is 600-700 m, significantly higher than the other intra-Carpathian basins, which are approximately 100 m above sea level. If erosion continues until the surface of the basins is reduced to sea level, isostasy predicts that 3 km of sediment will have been eroded and that less than one km of Miocene sediment will remain in the basin. This suggests that whatever active forces produced the Miocene subsidence of the Transylvanian basin (amplified by the effect of sediment loading) were transient and are no longer active in this region. One explanation may be that this downwarping of the basement was produced by downward pull or suction from the downbending plate. When this action was "turned off", the basement would have rebounded to its original elevation if the weight of the accumulated sediments could have been removed instantly by erosion. Since erosion proceeds slowly, the surface of the basins has been uplifted and is being gradually reduced to sea level. A similar situation may exist at present in the Vrancea region of southeast Romania, where extremely rapid subsidence of the area, which is not in isostatic equilibrium, seems to be related to the occurrence of intermediate depth earthquake on the downgoing plate (Fuchs and others, 1979).

We suggest that in this region subduction or downbending of the subducted slab results in an extensional stress field and that thrusting and apparent compression along the mountain belt are only thin-skinned, superficial effects due to the inability to subduct light, upper crustal

material, and to detachment of the crust from the underlying lithosphere. This may explain the focal mechanisms for both crustal (thrusting) and mantle (down-dip extension) earthquakes in the Eastern Carpathians. Extension of the intra-Carpathian basins may have occurred because of lithospheric flow to fill the space left by the retreating or downbending plate. In this region, the dominant forces seem to be those acting on the downgoing slab, which produce shortening along the plate boundary, and plate geometry which inhibits rigid plate convergence.

There does not seem to be any reason to believe that the processes which produced the Carpathian loop and subsided intra-Carpathian region were fundamentally different from those operating elsewhere in the Alpine belt. The opening of the intra-Carpathian basins can be explained purely as the result of local geometrical and structural constraints.

REFERENCES

Boccaletti, M., Manetti, P., and Peltz, S., 1973, Evolution of the Upper Cretaceous and Cenozoic Magmatism in the Carpathian Arc: Geodynamic Significance, Memoir of the Geological Society of Italy, v. 12, p. 252-276.

Brix, F. and Schultz, O. (eds.), 1980, Erdol und Erdgas in Osterreich: Verlag: Naturhistorisches Museum Wien und F. Berger, Horn, Wien, 312 p.

Burchfiel, B.C., 1976, Geology of Romania: Geological Society of America Special Paper 158, 82 p. Burchfiel, B.C., 1980, Eastern Alpine System and the Carpathian Orocline as an Example of Collision Tectonics: Tectonophysics, v. 63, p. 31-62.

Channell, J.E.T., D'Argenio, B., and Horvath, F., 1979, Adria, the African Promontory, in Mesozoic Mediterranean Paleogeography: Earth Science Reviews, v. 15, p. 213-292.

Ciupagea, D., Panca, M., and Ichem, Tr., 1970, Geologia Depresiunii Transilvaniei: Editura Academiei Republicii Socialiste Romania, Bucuresti, 256 p.

Crowell, J.C., 1974, Origin of Late Cenozoic Basins in Southern California: in Dickenson, W.R., (ed.), Tectonics and Sedimentation, Society of Economic Paleontologists and Mineralogists, Special Publication 22, p. 190-204.

Davis, G.A. and Burchfiel, B.C., 1973, Garlock Fault: An Intracontinental Transform Structure, Southern California: Geological Society of America Bulletin, v. 84, p. 1407-1422.

Fuchs, K., Bonjer, P., Bock, G., Cornea, D., Radu, C., Enescu, D., Jiame, D., Nouescu, G., Merkler, G., Moldoveanu, T. and Tudorache, G., 1979, The Romanian Earthquake of March 4, 1977: Aftershocks and Migration of Seismic Activity: Tectonophysics, v. 53, p. 225-247.

Gutdeutsch, R. and Aric, K., 1976, Erdbeben im Ostalpinen Raum: Arbeiten aus der Zentralanstalt fur Meteorologie und Geodynamic, v. 19, no. 210, 23 p.

Krs, M. and Roth, Z., 1977, A Hypothesis of the Development of the Insubric-Carpathian Tertiary block System: Acta Geolgica Academia Scientiarum Hungaricae, v. 21, no. 4, p. 237-249.

Krs, M. and Roth, Z., 1979, The Insubric-Carpathian Tertiary Block System: Its Origin and Disintegration: Geology Zbornik Geologica Carpathica, v. 30, no. 1, p. 3-17.

Horvath, F. and Royden, L., in press, Mechanism for the Formation of the Intra-Carpathian Basins: A Review: Earth Evolution Sciences, v. 1, no. 3.

Jiricek, R., 1979, Tectonic Development of the Carpathian Arc in the Oligocene and Neogene: in Mahel, M. (ed.), Tectonic Profiles through the West Carpathians: Geologicky Ustav Dionyza Stura, Bratislava, p. 205-214.

Ksiazkiewicz, M., Oberc, J. and Pozaryski, W., 1972, Geology of Poland v. IV, Tectonics: Geological Institute, Warsaw, 718 p.

Laubscher, H., 1971, Das Alpen-Dinariden problem und die Palinspastik der Sudlichen Tethys: Geologie Rundschau, v. 60, p. 813-833.

Lexa, J. and Konecny, v., 1974, The Carpathian Volcanic Arc: A Discussion: Acta Geologica Academial Scientiarum Hungaricae, v. 18(3-4), p. 279-293.

Mahel, M. (ed.), 1974, Tectonics of the Carpathian-Balkan Regions: Geological Institute of Dionyz Stur, Bratislava, 453 p.

McKenzie, D., 1972, Active Tectonics of the Mediterranean Region: Geophysical Journal of the Royal Astronomical Society, v. 30, p. 109-185.

McKenzie, D., 1978, Some Remarks on the Development of Sedimentary Basins: Earth and Planetary Science Letters, v. 40, p. 25-32.

Molnar, P. and Atwater, T., 1978, Interarc Spreading and Cordilleran Tectonics as Alternates Related to the Age of Subducted Oceanic Lithosphere: Earth and Planetary Science Letters, v. 41, p. 330-340.

Quennell, A.M., 1959, Tectonics of the Dead Sea Rift: 20th Session, International Geological Congress, African Section, p. 385-403.

Roman, C., 1970, Seismicity in Romania-Evidence for the Sinking Lithosphere: Nature, v. 228, p. 1176-1178.

Royden, L. and Keen, C.E., 1980, Rifting Process and Thermal Evolution of the Continental Margin of Eastern Canada Determined from Subsidence Curves, Earth and Planetary Science Letters, v. 51, p. 343-361.

Sandulescu, M., 1975, Essai de Synthese Structurale des Carpathes: Bulletin of the Geological Society of France, v. XVII, p. 299-358.

Sandulescu, M., 1980, Analyse Geotectonique des Chaines Alpines Situees au tour de las Mer Moire Occidentale: Annuaire de l'Institut de Geolgie et de Geophysique, v. LVI, p. 5-54.

Sclater, J.G., Royden, L., Horvath, F., Burchfiel, B.C., Semken, S., and Stegena, L., 1980, The Formation of the Intra-Carpathian Basins as Determined from Subsidence Data: Earth and Planetary Science Letters, v. 51, p. 139-162.

Segall, P. and Pollard, D.D., 1980, Mechanics of Discontinuous Faulting: Journal of Geophysical Research, v. 85, p. 4337-4350.

Steininger, F., Papp A., Chicha, I., Senes, J., and Vass, D., 1975, Excursion "A", Marine Neogene in Austria and Czechoslovakia: VIth Congress of the Regional Committee on Mediterranean Neogene Stratigraphy, 96 p.

Szadeczky-Kardoss, E., 1976, Plattentektonik im Pannonich-Karpatischen Raum: Geologische Rundschau, v. 65, p. 143-151.

Veliciu, S. and Demetrescu, C., 1979, Heat Flow in Romania and Some Relations to Geological and Geophysical Features: in Cermak, C. and Rybach, L. (eds.), Terrestrial Heat Flow in Europe, Springer-Verlag, Berlin, p. 253-260.

Wilcox, R.E., Harding, T.P., and Seely, D.R., 1973, Basic Wrench Tectonics: American Association of Petroleum Geologists Bulletin, v. 51, p. 74-96.

ACKNOWLEDGMENTS

FIGURE CAPTIONS

Fig. 1.   Major structural divisions of the Carpathians into inner and
          outer units. EA, Eastern Alps; SA, Southern Alps, pA,
          peri-Adriatic line; WC, West Carpathians; E, Europe; EC, East
          Carpathians; SC, South Carpathians; A, Apuseni Mountains; M,
          Moesia; V, Vardar Zone; DA, Dinaric Alps; Ad, Adria.

Fig. 2.   Age of last major thrusting and folding event versus horizontal
          distance along the Carpathian chain. Vertical bars show upper and
          lower time limits for this final event. Where a minimum age could
          not be determined, the vertical bars were extended downward with
          arrows. Dashed arrows indicate probable, but not certain,
          determination of the last thrusting or folding event. Shaded
          region represents the Badenian stage, when basin extension is
          assumed to have occurred. See Fig. 3 for location of cities.
          Data from Steininger and others, 1975, Ksiazkiewicz, 1977 and
          Mahel and others, 1968.

Fig. 3.   Isopach map showing depth to base Miocene. Approximate ages of
          igneous rocks are also shown (T. Poka, personal communication).
          Fold axis symbols show location and trend of some of the Sava
          folds. Basins: S-Sava, Dr-Drava, Z-Zala, G-Graz, D-Danube,
          V-Vienna, P.-Pannonian, Tc-Transcarpathian, Ts-Transylvanian.
          Dashed lines show regions of pre-Neogene outcrop. (Modified after
          Horvath and Royden, in press.)

Fig. 4a. Isopach map to base of Miocene for the Vienna Basin. Heavy lines
          show locations of major faults (modified from Horvath and Royden,
          in press, Brix and Schultz, 1980). Fault plane solutions
          (compressional quadrant shaded) from Gutdeutsch and Aric, 1976.

Fig. 4b. Cross section through northeast corner of Vienna basin (after
          Mahel and others, 1968).

Fig. 5.   Generalized map of Neogene faults in the intra-Carpathian region.
          Shaded pattern covers areas that have undergone significant
          extension. Arrows indicate sense of shear on proposed zones of
          strike-slip displacement. Some basins are interpreted as
          "pull-apart" basins, whereas others are regions of extension
          bounded by zones of differential shear.

Fig. 6.   Plate tectonic sketch showing boundaries between continental
          fragments before the opening of the intra-Carpathian basins in
          pre-Badenian time and during opening of the basins in Badenian
          time. The boundaries between the continental fragments are shown
          in single heavy lines, but in reality are broad zones of
          differential motion.

Fig. 7. Diagram showing proposed downbending of the subducted plate under
the East Carpathians. Flow is induced in the overriding plate to
fill space formerly occupied by the downbending plate resulting
in extension of the Pannonian basin and temporary suction on the
Transylvania basin. P, Pannonian basin; A, Apuseni Mountains;
Ts, Transylvania basin; EC, East Carpathians; Vr, Vrancea zone;
E, Europe. Dip of plate at 0 ma constrained by epicenter
locations of recent seismic events (Fuchs and others, 1979).

Figure 1

Figure 2

69
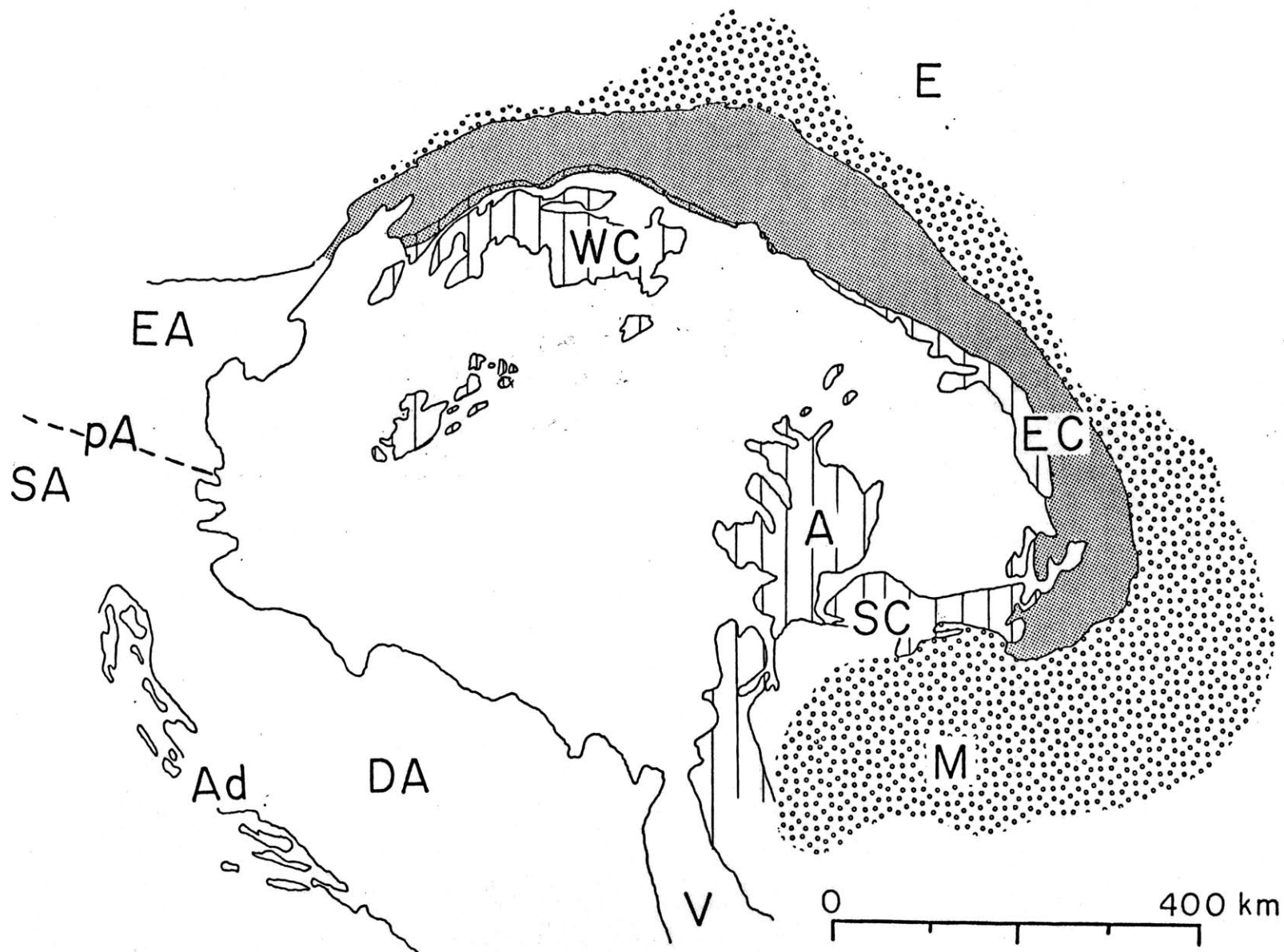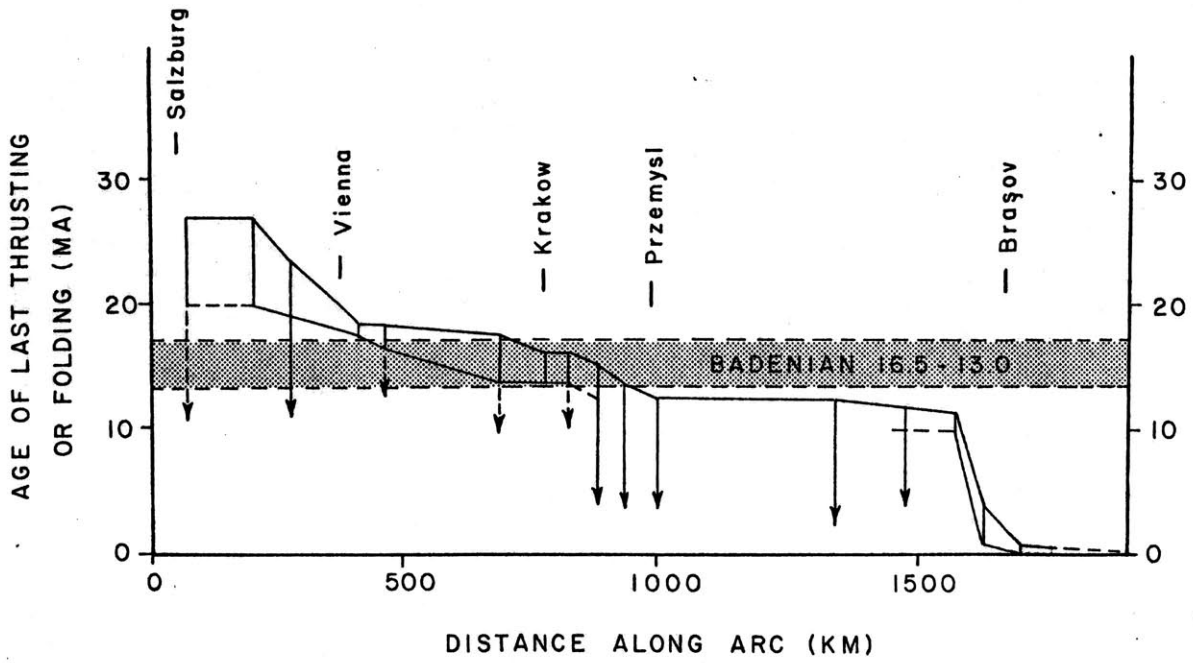
Figure 3

Late Cenozoic volcanic rocks

ISOPACH INTERVAL

1-2 km
2-3 km
> 3 km

Krakow

Przemysl

10.5-5.5

15-10.5

10.5-3

V

16-10.5

Tc

Vienna

17.5-15

13-3

D

G

10.5-0

Z

Ts

13-10.5

Dr

S

Braşov

0   400 km

70

Figure 4a

ISOPACH INTERVAL

1 - 2 km

3 - 4 km

> 5 km

0   50 km

Figure 4b

NW   SE

0

km

4

10.5 - 0 ma (Pannonian - Present)

13 - 10.5 ma (Sarmatian)

16.5 - 13 ma (Badenian)

22 - 16.5 ma (Eggenburgian - Karptian)

Pre - Neogene basement

Figure 5

0   400 km

72

PRE-BADENIAN (>16.5 Ma)

BADENIAN (16.5-13 Ma)

Figure 6

73

16 Ma

P A Ts EC E

O Ma

P A Ts EC Vr E

0   400 km
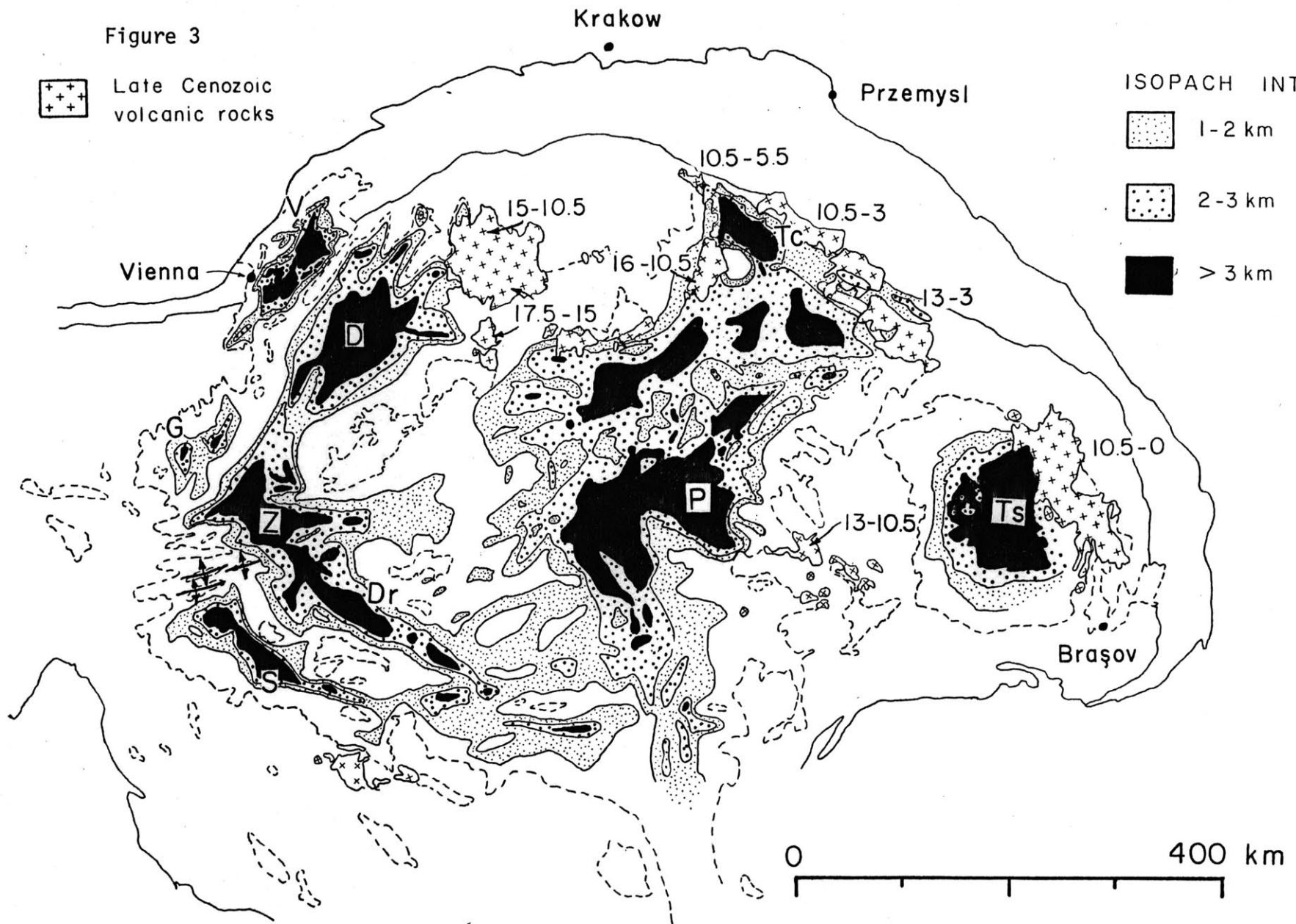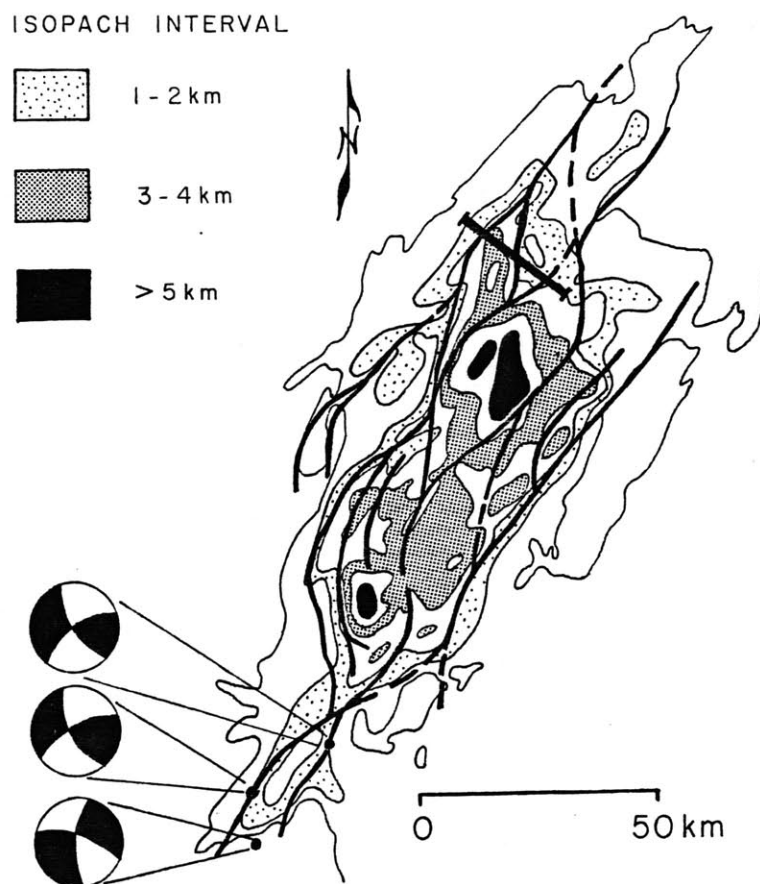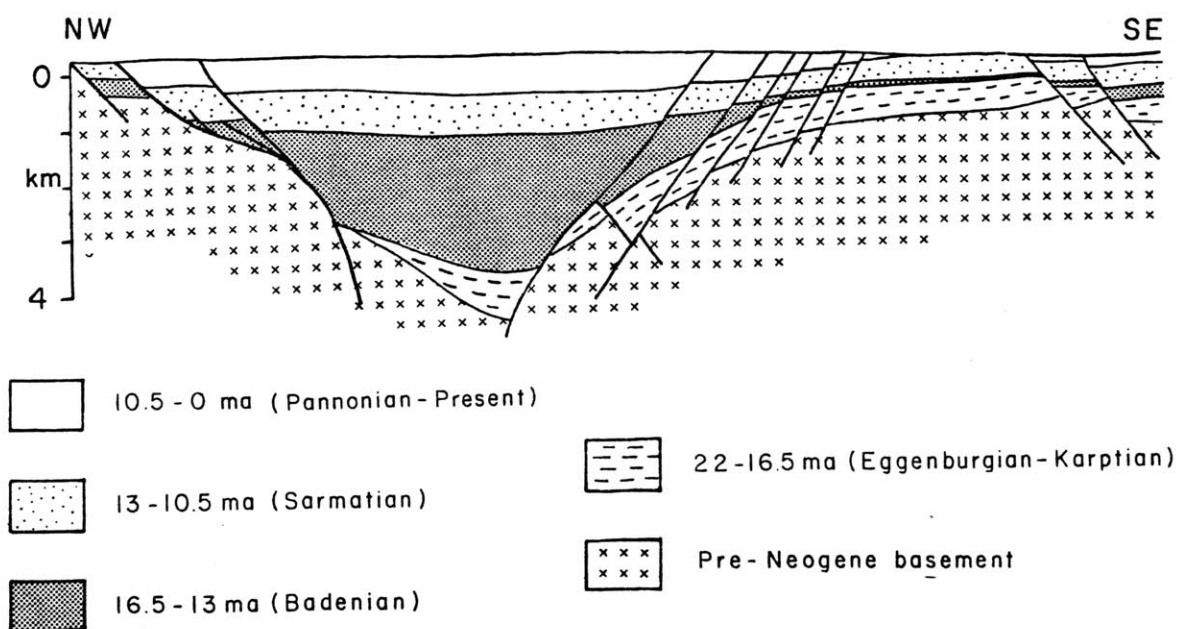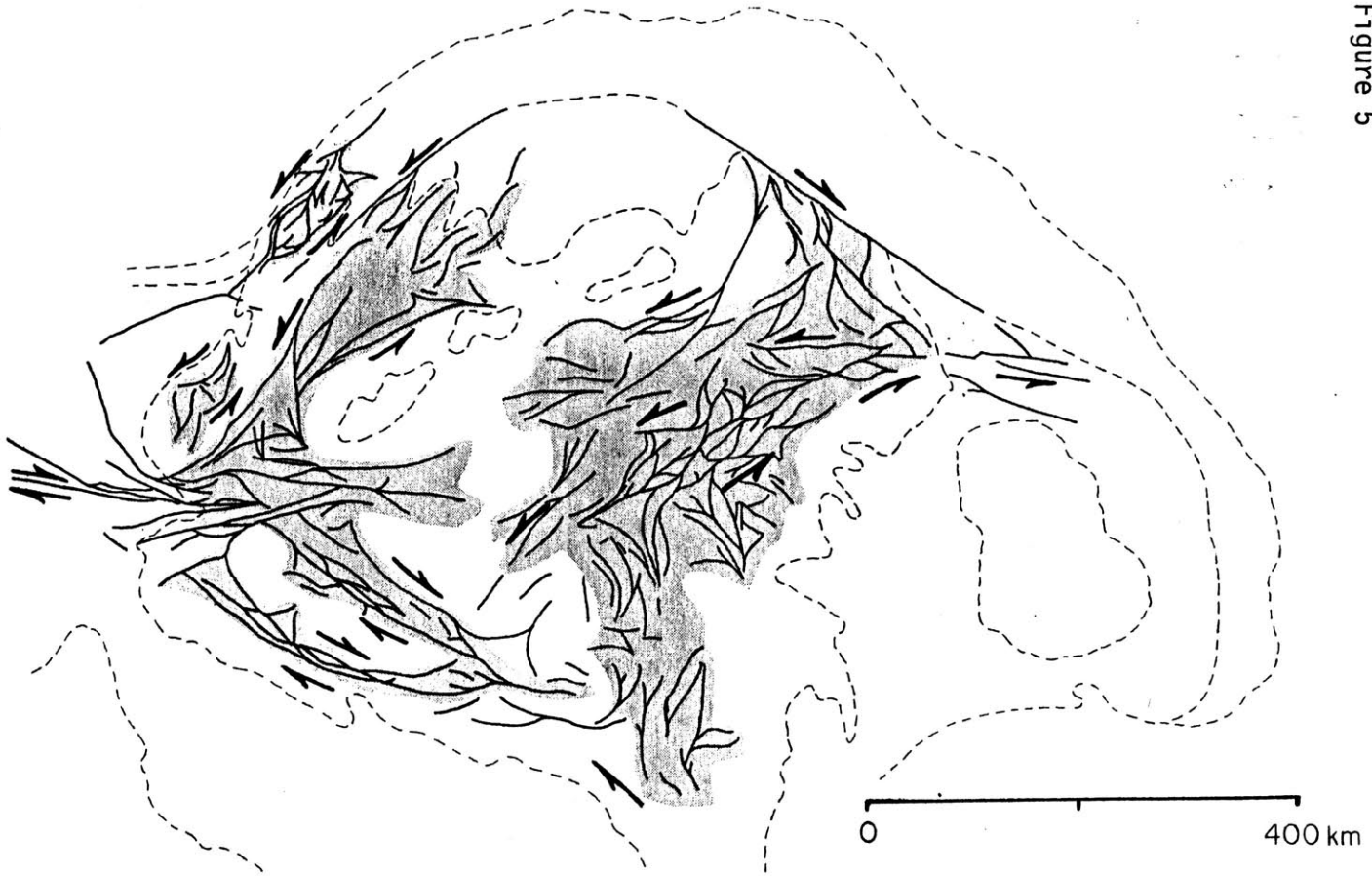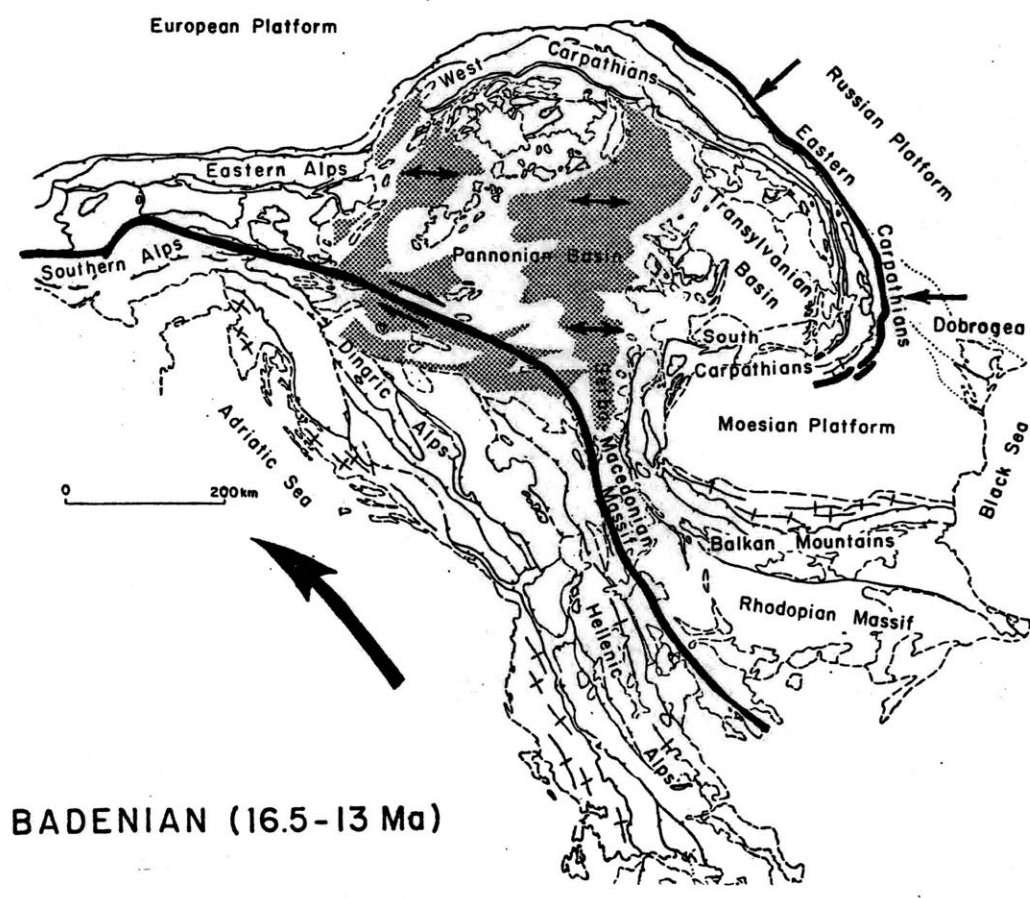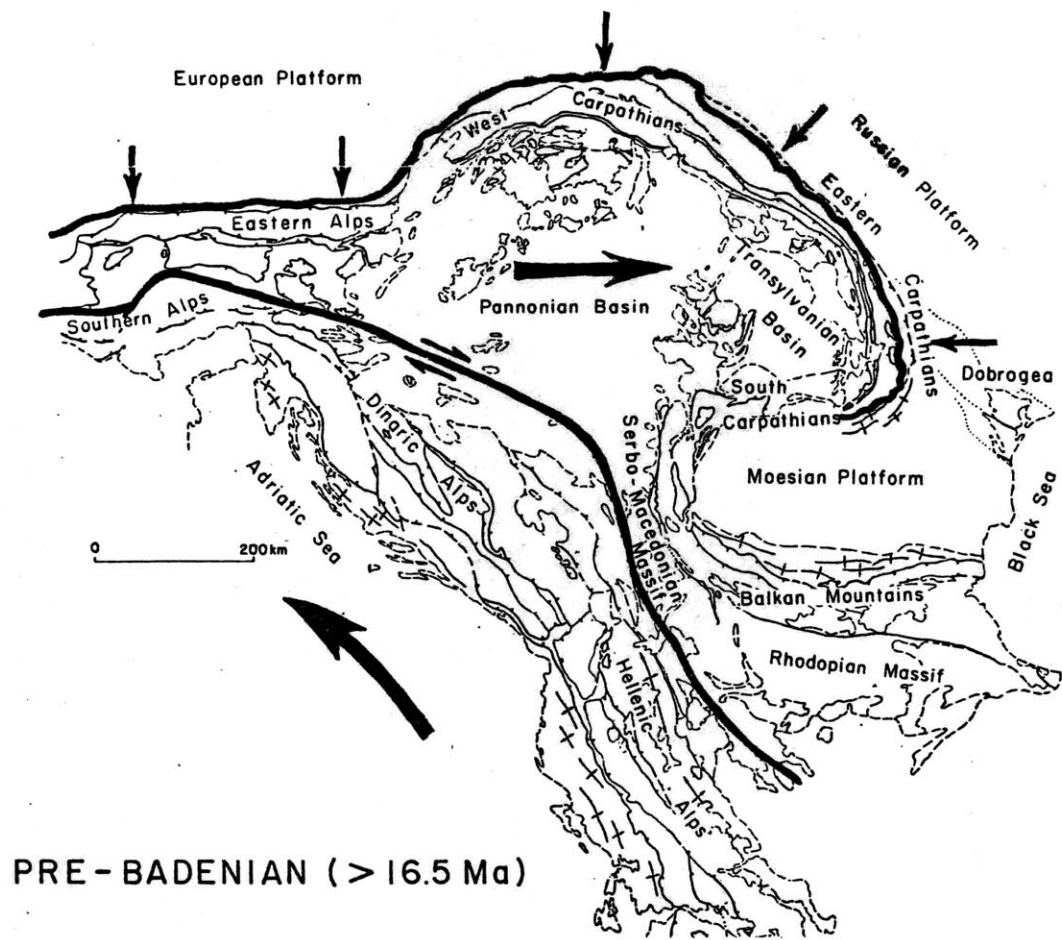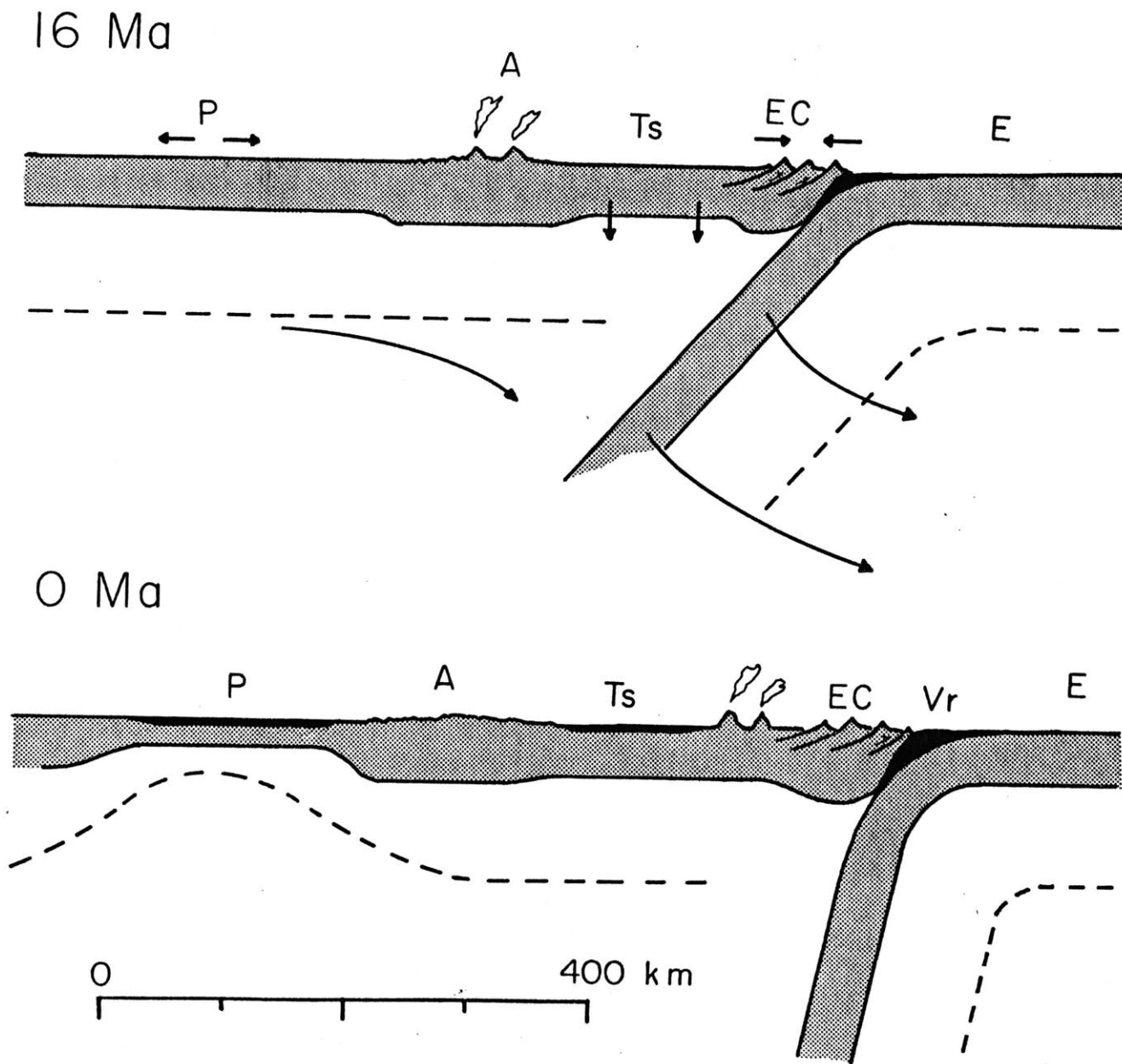
Figure 7

CHAPTER THREE

THE EVOLUTION OF THE INTRA-CARPATHIAN BASINS

AND

THEIR RELATIONSHIP

TO THE CARPATHIAN MOUNTAIN SYSTEM

PREFACE

A revised version of this paper will be submitted for publication in an as yet undetermined journal. The authorship will probably be follows:

L. Royden

F. Horvath

A. Nagymarosy

L. Stegena

The work presented in the current version is entirely my own.

ABSTRACT

The Carpathian arc formed during the Cretaceous to Miocene
continental collision of Europe with smaller continental fragments
following southward and westward subduction of an oceanic terrane.
During the last stages of thrusting in the outer Carpathians, a set of
discrete basins formed behind the Carpathian loop in a back-arc
position. These basins, which in places contain up to 7 km of Neogene
and Quaternary sedimentary rocks, appear to be regions of late Miocene
extension They are connected to each other and to areas of coeval
shortening in the outer Carpathian thrust belt by a system of
strike-slip faults. Sinistral northeast trending and dextral northwest
trending sets of conjugate shears reflect overall east-west extension
of the intra-Carpathian region during the late Miocene.

Qualitative geological data and regional tectonic considerations
were combined with quantitative sedimentation, subsidence and thermal
data for individual wells in several of the intra-Carpathian basins to
determine the timing, magnitude and distribution of extension within
the different intra-Carpathian basins. This analysis indicates that
thermal gradients within the Pannonian basin are 50% to 100% higher
than would be expected if the basin were the result of late Miocene
uniform extension of a plate of normal thickness. A second mode of
extension whereby lithospheric extension is accompanied by introduction
of large amounts of additional heat into the upper mantle predicted:
1) temperatures and heat flow in good agreement with observation, 2)
rates of thermal subsidence (due to conductive cooling and thermal

contraction of lithospheric rocks after extension) in good agreement
with observation, 3) rates of heat loss not strongly dependent on
present basement depth, also in good agreement with observation, and
4) that uplift could occur during extension -such syn-extensional
uplifts have been observed in both the Pannonian and Danube basins.
Crustal extension beneath most parts of the Pannonian basin was
calculated to have been about 85% to 170% (β = 1.85 to 2.70).

We interpret the Vienna basin, which is superimposed partly on the
flysch nappes of the outer West Carpathians, as the result of
thin-skinned extensional tectonics above a shallow detachment surface
within the upper crust. Extension of upper crustal rocks above this
detachment was probably compensated by thrusting of the outermost
nappes of the West Carpathians over the European platform. Subsidence
and thermal data from the Vienna basin support this interpretation.

Extension within the Danube and Zala basins seems to have involved
the entire lithosphere, possibly with the introduction of extra heat
into the upper mantle. The Transylvanian basin does not appear to be
extensional in origin and may be the result of temporary loading from
below during subduction. Heat flow data from the Transylvanian basin
are consistent with this interpretation.

Extension within the intra-Carpathian basins was not synchronous
and may be divided into three principle periods: Karpatian (17.5-16.5
Ma), Badenian (16.5-13 Ma) and Sarmatian (13-10.5 Ma), probably
extending into early Pannonian time. Karpatian extension affected the
north Vienna and north Transcarpathian basins, and the locus of
extension migrated generally southward and eastward with time.

Badenian extension was dominant in the south Vienna and Transcarpathian basins, and affected the Danube basin, and parts of the Zala, Sava, Drava and Pannonian basins. Sarmatian and Pannonian age extension was responsible for most of the subsidence of the east Danube and Pannonian basins.

Palinspastic reconstruction of the basins prior to each of these periods of extension predicts eastward migration of the zone of thrusting and shortening within the Carpathian mountains to accomodate eastward and southward migration of areas of extension. This is consistent with the eastward and southward migration of the last major thrusting event as determined directly from rocks within the thrust belt. From these reconstructions we estimate about 120 ($\pm$60) km of east-west shortening across the outer East Carpathians from the beginning of Karpatian time until the present. This figure is consistent with estimates of shortening based on direct reconstruction of nappes in the thrust belt. From this we infer a source-sink relationship for late Miocene extension of the intra-Carpathian region and late Miocene crustal shortening within the outer Carpathians.

We conclude that during late Micene time, deformation of the Pannonian fragment was dominated by extensional tectonics, except along a narrow zone in the outer Carpathian thrust belt. Late Miocene thrusting in the Carpathians is interpreted as the result of simple shear caused by relative motion between Europe and the overriding Pannonian fragment at the subduction boundary, rather than of regional compression of lithospheric rocks at depth. In this way, buoyant sedimentary rocks originally deposited on the European plate could have

been stripped from the downgoing European basement and stacked into a series of imbricate slices without widespread compression and crustal shortening extending far beyond the fragment boundaries. Overall compression of lithospheric rocks at depth would not have been necessary to cause imbrication of sedimentary cover, and thus the proximity of an active thrust belt to areas of coeval extension can be easily explained. The initation of extensional tectonics within the intra-Carpathian region was probably the direct result of reorganization of major fragment boundaries of the Eastern European Alpine system in late Oligocene-early Miocene time.

INTRODUCTION

East of the Eastern Alps, the Alpine chain separates into two divergent belts, the Carpathian mountains and the Dinaric Alps (Fig. 1). Between these two mountain belts, the low-lying intra-Carpathian region is underlain by Neogene and Quaternary sedimentary rocks which locally reach a thickness of 7 km. This region consists of small deep basins formed by rapid subsidence of pre-Neogene basement (Fig. 2). These basins are underlain partly by Mesozoic nappes of the inner Carpathian and Dinaric orogenic belts. Initial subsidence of the basins was synchronous with the Middle and Upper Miocene thrusting of flysch nappes of the outer Carpathians towards the European foreland.

The intra-Carpathian region was classified by Kober (1912) as a type "zwischen gebirge", a relatively undeformed region characterized by block faulting and situated between externally vergent thrust belts. After plate tectonics became generally accepted in Europe, the Pannonian region was reclassified as a Mediterranean back-arc type basin that formed as the European plate was subducted southward and westward beneath the inner Carpathians (see, for example, Boccaletti et al., 1976). Late Miocene volcanism and elevated heatflow in the intra-Carpathian region (up to 110 mW/m^2) were interpreted as the result of a mantle diapir beneath the basin area (Stegena et al., 1975). A more recent analysis suggests that these basins are the result of lithospheric extension which occurred during the last stages of thrusting in the outer Carpathians (Sclater et al., 1980). The elevated thermal gradients can be explained by the passive upwelling of hot asthenosphere during extension. The basin subsidence can be

explained by the combined effects of isostatic compensation for crustal

thinning and the subsequent cooling and thermal contraction of the

crust and upper mantle (for a general discussion see, for example,

McKenzie, 1978; Steckler and Watts, 1978 or Royden et al., 1980).

From their analysis of subsidence in the intra-Carpathian basins,

Sclater et al. (1980) concluded that these basins formed as the result

of a single phase of extension during Badenian time (16.5-13 Ma; for

biostratigraphic time scale see Fig. 3). They divided the basins into

two groups (Fig. 2): the peripheral basins adjacent to or superimposed

on the mountain belts (Vienna, Transcarpathian, Sava, Drava and west

Danube basins); and the central basins that lie in the central part of

the intra-Carpathian region (the east Danube and Pannonian basins which

occupy areas sometimes called the Little and Great Hungarian plains,

respectively). (The term "Pannonian basin" generally refers also to

parts of the Danube and Drava basins, but in this paper we shall use it

to designate only the deeply subsided area indicated by Fig. 2.)

Sclater et al. (1980) proposed that two-fold lithospheric extension

could explain the observed subsidence and heatflow within the

peripheral basins, while two-fold extension plus additional heat from

the uppermost mantle could account for those of the central basins.

In this paper we attempt to synthesize qualitative geological data

with a quantitative analysis of extension, subsidence and thermal

structure within the intra-Carpathian basins. Because several

different types of data and analysis are used, we have broken the text

into discrete sections which present ideas in the following order: 1)

regional tectonic setting, 2) qualitative geological data, 3)

quantitative geological and geophysical data 4) quantitative analysis

of extension within the intra-Carpathian basins, 5) palinspastic reconstruction of the Carpathian/ intra-Carpathian area, and 6) speculations on the nature of the dynamic processes operating at depth beneath the intra-Carpathian basins and Carpathian mountains. The aim of this paper is to present a rigorous analysis of extension within the basins in light of more general regional tectonic features of the Eastern European Alpine system. In particular, we wish to explore the spatial and temporal relationship between basin extension and coeval crustal shortening in the adjacent Carpathian mountains.

Basic data to support the overview of the tectonic evolution of the Eastern European Alpine system cannot be presented or adequately referenced in this paper. Unless otherwise indicated, most of the regional tectonic information presented below can be found in the following works: Eastern Alps - Tollman (1963,1966), Oxburgh (1968,1974) and Oberhauser (1980); Carpathians - Andrusov (1965,1968), Mahel et al. (1968), Sàndulescu (1975,1980) and Burchfiel (1976); Dinarides - Aubouin (1973) and Aubouin et al. (1970); Hellenides - Aubouin (1973) and Smith and Moores (1974). A succinct overview of the Mesozoic to present evolution of the Eastern European Alpine system is given by Burchfiel (1980). Proper referencing is also diffucult to provide for some stratigraphic and paleontologic studies in this region because much of the relevant work on Paratethyan faunas was begun more than a century ago. In these cases, we have tried to give references to recent publications, because proper referencing of original work would be a lengthy study in itself.

TECTONIC SETTING

The Carpathian mountains form an eastward convex loop which consists of externally or radially directed thrust and fold nappes. They may be divided into two major belts: An outer morphologically and structurally continuous belt, and an inner, morphologically and structurally discontinuous belt. The inner belt may be further subdivided into the West, East and South Carpathians (Fig. 1). Thrusting, which occurred first in the internal units and progressed outward, emplaced the nappes of the inner belt during the Cretaceous and early Paleocene. In the East and West Carpathians, tectonic activity ceased by the early Paleocene, and, except for Eocene deformation in the West Carpathians, flysch deposition was continuous throughout the Paleogene until the emplacement of the outer nappes during late Oligocene and Miocene time. In the South Carpathians, major tectonic activity ceased by the Late Cretaceous, although the entire region was later subjected to minor folding and warping.

The Dinaric Alps form a relatively straight belt of externally (southwest) directed nappes. Thrusting occurred first in the most internal units beginning in latest Jurassic-Early Cretaceous time, and progressed outward until the external units were emplaced in Eocene and Oligocene time.

The present structure and morphology of the Eastern European Alpine system are the result of Jurassic to recent suturing of Europe and several smaller continental fragments. Most of these fragments cannot be called micro-plates because they have been subject to considerable internal deformation and it is doubtful that discrete plate boundaries can be defined. For practical purposes, fragment

boundaries can be defined as broad zones of deformation that contain

the most prominent faults in a continuously deforming continental

crust. Convergence between fragments seems to have taken place by

diachronous subduction of oceanic crust along fragment boundaries until

collision occurred between continental parts of the fragments. During

collision, new fragment boundaries were formed that often cut

across former boundaries. This style of suturing and fragmentation

continued through Mesozoic and Cenozoic time. The rearrangement of

fragment boundaries in late Oligocene-early Miocene time led to the

development of the intra-Carpathian basins.

Early Cenozoic Time

The latest Cretaceous to Oligocene evolution of the Eastern

European orogenic system can be adequately understood as the

interaction of two major continental units (Fig. 4a and Fig. 5a):

(1) Europe and the Moesian fragment already sutured and, (2) the

Apulian fragment. During Eocene and Oligocene time, prior to the

development of the intra-Carpathian basins, tectonic activity was

concentrated in the Dinaric Alps and along the northern boundary of the

Apulian fragment.

Intra-fragment shortening of Apulia resulted in Eocene-Oligocene

emplacement of southwest vergent nappes in the outer Dinarides (Fig.

5a). The proven magnitude of shortening is only a few tens of kms in

the north near the Eastern Alps and increases southward towards

southern Greece where it may reach more than 200 or 300 km. A belt of

Eocene-Early Miocene volcanic and plutonic rocks to the northeast of

the belt trends parallel to and partly overlaps it. Evidence for the

direction of Cenozoic subduction is inconclusive, but an east dip is

suggested by the southwest vergence of Cenozoic nappes, the general
northeast location of volcanic rocks, and by the probable development
of this Cenozoic subduction system from an earlier east-dipping
subduction zone known at least in the southern part of the Dinarides.

At the same time as major intra-fragment shortening occurred in
the Dinarides, north-south convergent activity took place between
Europe and Apulia along the northern margin of the Apulian fragment
from the Western Alps to the West Carpathians during Eocene time.
Continental collision along the Eastern Alps probably resulted in
Eocene-Oligocene shortening of continental crust by about 100 to 200
km. Eocene convergent activity did not result in continental collision
in the West Carpathians, as indicated by the presence of a wide flysch
basin of Oligocene age floored in part by oceanic crust (Fig. 4b).

Structural evidence for the magnitude of Eocene convergence in the
West Carpathians is inconclusive. The presence of a poorly developed
Eocene magmatic arc along the southern part of the Eastern Alps and
south of the West Carpathians suggests that Early Cenozoic convergence
was more than 100 to 200 km (Fig. 1). This magmatic arc consists of a
few small calcalkaline plutons with lherzolite inclusions and is
probably related to southward subduction of the European plate. The
eastward limit of this Eocene convergent activity is not known, but
convergence does not appear to have involved the East Carpathians where
flysch deposition was continuous from Paleocene until latest Oligocene
time. There is little evidence for convergent activity anywhere in the
Carpathians from latest Eocene until latest Oligocene time.

Late Cenozoic Time

By the end of the Oligocene, the two-fragment system which had characterized the Early Cenozoic Eastern European Alpine system became disrupted into a new system consisting of three fragments (Fig. 5b): (1) Europe and Moesia welded together, (2) that part of Apulia southwest of the Dinaric Alps, referred to below as Apulia and (3) that part of Apulia to the northeast of the Dinaric Alps, referred to below as the Pannonian fragment. Reorganization of fragment boundaries was a gradual process, so that the time at which this new system developed is to some extent a subjective interpretation, as are the number of fragments and the definition of fragment boundaries. The shifting nature of these fragment boundaries means that unique and distinct fragments cannot be permanently defined. For example, during Eocene time rocks of the West Carpathians may be considered as part of the Apulian fragment, whereas by Miocene time they moved separately from the rest of Apulia. This introduces some ambiguity in the use of fragment names because the areas included within each fragment change with time.

During Early Miocene time, tectonic activity was concentrated along fragment boundaries in the Dinaric Alps, and from the Western Alps to the East Carpathians. In addition to the formation of new fragment boundaries in late Oligocene time, the sense of displacement changed along pre-existing boundaries, but displacement was not necessarily localized along the same faults. The previously convergent zones along the Eastern and Dinaric Alps were replaced by zones associated primarily with large dextral strike-slip displacements. Strike-slip displacement occurred along a broad zone of high angle

faults which disrupted earlier compressive structures in the Eastern

Alps and Dinarides. The most prominent of these faults is the

peri-Adriatic line, but the boundary is best defined as system of

faults which includes the peri-Adriatic line and continues southeast

through the Sava and Drava troughs into the Vardar zone (Figs. 1, 2 and

5). The net Miocene dextral displacement across this zone is

uncertain, but is probably several hundred km (Laubscher, 1971;

Schönlaub, 1980; Grubić, 1980). Some north-south convergence between

Apulia and Europe continued throughout Miocene time, probably

accommodated mainly by south-vergent backthrusting south of the

peri-Adriatic line. Folding of the Dinaric foreland (and possible

thrusting in the most external units) is partly of Miocene age and

probably represents the final stage of early Tertiary intra-cratonic

convergence.

At about the same time, externally vergent thrusting was

reactivated along the outer East and West Carpathians with latest

Oligocene emplacement of nappes consisting of Cretaceous and early

Tertiary flysch (Figs. 4b and 5b). At this time no oceanic crust

remained in the region of the Eastern Alps. Between the Pannonian

fragment and the European plate was a broad sea of flysch, possibly

several hundred km wide and probably floored in part by oceanic crust

(Fig. 4b). Outward migration of thrusting involved progressively

younger rocks and eventually resulted in overriding of the European

foreland by the flysch nappes.

Major convergence across the Carpathians probably occurred first

in the westernmost part and migrated eastward along the Carpathian belt

(Jiříček, 1979). The end of thrusting and convergence becomes

continuously younger to the east (Fig. 6). By Badenian time
(16.5-13 ma), north-directed thrusting was essentially completed in the
Eastern Alps and West Carpathians, but major crustal shortening
continued until about 12 ma in the northern part of the East
Carpathians and through Pliocene time in the southeastern part of the
East Carpathians (Fig. 6). The thrust belt terminates near the
junction between the East and South Carpathians, but minor Pliocene and
Quaternary folding occurred in the South Carpathian molasse
(Săndulescu, 1975; Burchfiel, 1976). Miocene and recent shortening
estimated from palinspastic reconstruction is 60 km in the West
Carpathians (Książiewicz et al., 1972) and about 100 km in the East
Carpathians (Burchfiel, 1976). Both are minimum estimates.

Reactivation of externally vergent thrusting in the outer
Carpathian belt was accompanied by the formation of a calcalkaline
magmatic arc which extended from the Graz basin eastward to the
Transylvanian basin (Fig. 2) (Săndulescu, 1980; Boccaletti et al.,
1973). These rocks contain lherzolite inclusions and are probably
related to south-and west-dipping subduction of the European plate (Gy.
Panto, 1981, pers. comm.). Eruption of magma was episodic and there is
a clear eastward migration of volcanic activity along the arc (Fig. 2)
(Lexa and Konečný, 1974). This is consistent with eastward migration
of thrusting and subduction along the Carpathian mountain belt.

During the last stages of thrusting in the outer Carpathians, the
intra-Carpathian basins formed within the Pannonian fragment (Figs. 2
and 5c). These basins have been interpreted as regions of local
extension separated from relatively undeformed blocks by strike-slip
faults or fault zones (Royden et al., 1982), similar in style to

recently extended areas of the Basin and Range Province (Davis and Burchfiel, 1973) and coastal California (Crowell, 1974). In general, sinistral northeast trending and dextral northwest trending sets of conjugate shears reflect east-west extension and possibly north-south compression of the intra-Carpathian region (Fig. 7). Some of these strike-slip faults appear to be splays of the peri-Adriatic-Vardar fault system. Estimates of about 100% extension within the deep basins suggest that total east-west extension across the intra-Carpathian region was approximately 100 km during the late Miocene (Royden et al., 1982).

North-south compression within the intra-Carpathian region is suggested by the presence of Badenian-age east-west trending folds which crop out in the southwest part of the intra-Carpathian region and continue eastward in the subsurface (Dank, 1962). Folding, imbrication and south-directed thrusting also severely shortened Eocene flysch in the area of the Szolnok "graben" (Fig. 1) as late as Karpatian and possibly early Badenian time, (I. Varga, 1981, pers. comm.). This north-south compression appears to precede slightly the initiation of major extension (I. Varga, 1981, pers. comm.; this paper).

Although the major phase of tectonic activity was completed in the Carpathian region in the Late Miocene, minor tectonic activity continues throughout much of the Carpathian region. Strike-slip and normal faults of small displacement cut Pliocene and Quaternary sedimentary rocks in the basins. Folding in the southeastern part of the Carpathian foredeep and intermediate depth earthquakes in Romania suggest continued shortening and subduction (Roman, 1970; Fuchs et al., 1979). Weak seismic events have also been detected in the

intra-Carpathian area (magnitude <5.5), and while it is not clear that present seismic activity is a direct reflection or continuation of earlier events, the sense of motion and local stress pattern inferred from fault plane solutions is compatible with that inferred for Miocene events (Gutdeutsch and Aric, 1976).

Interpretation

Throughout the early Cenozoic, Apulia moved generally north relative to stable Europe, resulting in Eocene (?) continental collision in the Eastern Alps and subsequent shortening and imbrication of continental crust (Fig. 5). This motion was probably accomodated partly by Eocene consumption of oceanic lithosphere in the region of the West Carpathians, and partly by early Tertiary intra-cratonic shortening within the Dinaric Alps. A zone of dextral shear may have begun to develop parallel to the Dinarides at this time.

By late Oligocene time, major shortening had ceased in the Eastern Alps. Continued motion between Europe and Apulia seems to have been accomodated during the Early and Middle Miocene partly by eastward and northeastward displacement of the Pannonian fragment relative to Europe, thus initiating late Cenozoic thrusting in the West and East Carpathians (Fig. 5b) (Royden et al., 1982). This may be analogous to the present situation in Turkey where a continental fragment in western Turkey is moving westward with respect to Asia due to the collision of Arabia and Asia (McKenzie, 1972). Continued motion between Apulia and Europe was also accomodated by dextral shear along the peri-Adriatic-Vardar fault system (Burchfiel, 1980). This broad strike-slip boundary appears to have separated the Pannonian fragment tectonically from

Apulia, so that during the Miocene these fragments moved independently from one another.

Royden et al. (1982) have suggested that east-west shortening within the East Carpathian mountains continued even after eastward translation of the entire Pannonian fragment became incompatible with motion of the Apulian block in the Late Miocene. They further suggested that the Late Miocene east-west extension of the intra-Carpathian region occurred to accomodate this continued shortening (Fig. 5c). Comparable magnitudes of synchronous east-west shortening and extension tend to support this hypothesis (see above). Thus, the extension of the intra-Carpathian basins and the shortening and thrusting within the Carpathian mountains seem to be inter-related phenomena which developed from earlier events within the Eastern Alps and Dinarides. An understanding of extensional processes within the intra-Carpathian region depends partly on the reconciliation of these different tectonic elements within a dynamic framework.

The objective of this section has been to provide a simplified tectonic framework within which the extension of the intra-Carpathian basins may be viewed. In the next sections, the timing, direction, magnitude and style of extension within the individual basins are examined in detail. The results of this quantitative analysis may be correlated with constraints on the timing, direction and magnitude of crustal shortening within the Carpathians to provide a better understanding of the regional tectonic system as well as a better understanding of local extensional processes within each basin.

GEOLOGY OF THE INTRA-CARPATHIAN AREA

Pre-Miocene Rocks

The pre-Cenozoic basement of the intra-Carpathian basins consists of a complex assemblage of small continental fragments juxtaposed mostly during Mesozoic time (Channell et al., 1979; Burchfiel, 1980; Săndulescu, 1980). These rocks are the continuation in the sub-surface of the internal structural units of the West, East and South Carpathians, the Dinaric Alps, and north vergent thrust sheets in the Apuseni Mountains. Seismic reflection profiles indicate that imbricate structures may be traced from the inner-Carpathians and Dinarides beneath the Neogene sedimentary cover of the intra-Carpathian basins (Brix and Schultz, 1980; Ciupagea et al., 1970; Rudinec et al., 1981; I. Varga, 1981, pers. comm.; and others). The central part of the intra-Carpathian region does not appear to have imbricate slices within the basement (I. Varga, 1981, pers. comm.), and probably acted as a hinterland for the Carpathians and Dinarides in the Mesozoic. Beneath the Pannonian basin the Mesozoic and Paleozoic section is separated in a series of tilted fault blocks bounded by normal faults (Körössy, 1981), probably of late Miocene age.

Paleozoic and Mesozoic rocks are partly overlain by early Cenozoic marine sedimentary rocks (Fig. 8). Eocene flysch (the intra-Carpathian flysch) was deposited unconformably on older units of the inner West Carpathians and in parts of the intra-Carpathian region (Transcarpathian flysch)(Szepesházy, 1973; Mahel et al., 1968; Bleahu et al., 1968; Varga and Pogácsás, 1981). Eocene through upper Oligocene or lower Miocene shallow marine and brackish water sedimentary rocks covered much of the intra-Carpathian region (T. Báldi, 1982). The

thickness of early Cenozoic flysch beneath the Pannonian basin has not

been determined by deep drilling, but extrapolation of the

Transcarpathian flysch westward beneath the Pannonian basin suggests a

total depositional thickness of less than 1000 to 1500 m (Szepesházy,

1973). The maximum thickness of other early Cenozoic rocks within the

intra-Carpathian region is about 1500m, but early Cenozoic rocks may be

more than 2 km thick in a few small depressions superimposed on the

innermost belt of the West Carpathians (Báldi, 1982). Thus from

Eocene through late Oligocene time, much of the region was covered by a

shallow sea. This provides important constraints on the crustal and

thermal structure beneath the intra-Carpathian basins prior to the

initiation of late Miocene subsidence, and will be discussed in a later

section of this paper.

The areas around the southern Pannonian and Danube basins appear

to have remained emergent throughout the early Cenozoic (Fig. 8).

However, paleocurrent directions suggest that, except for the northwest

part of the Danube basin in late Oligocene-early Miocene time, these

areas were not major sources of sediment supply, and there is no

evidence for significant erosion of these areas during Eocene and

Oligocene time (Körössy, 1977). It is thought that the entire

intra-Carpathian region remained near sea-level during this time

(Báldi, 1982), but definite evidence for this does not exist in the

sedimentary record.

Note on Miocene Timescale

From Oligocene to Pliocene time, much of the intra-Carpathian

region and the foredeep of the Eastern Alps was covered by the Central

Paratethys sea (Laskarev, 1924). At times the Central Paratethys was

connected to the Mediterranean by marine seaways, but the specific

faunas within the Paratethys are distinct from those of the

Mediterranean. This makes direct correlation between Central

Paratethyan and Mediterranean stages difficult, particularly after the

last marine transgression into the Central Paratethys at the end of

Badenian time (13.0 Ma). (For a succinct English summary, see

Nagymarosy, 1981. For more detail, see Papp, 1968; Báldi, 1969; and

Steininger and Rögl, 1979.)

Independent radiometric dating is available for some of the

Central Paratethyan stratigraphic boundaries (for example, Vass et al..

1975; Vass, 1978; and Vass and Bagdasarian, 1978). However, absolute

ages for some of the Central and Eastern Paratethyan stage boundaries

cannot be well determined by radiometric dating or by stratigraphic

correlation. Most of the absolute age determinations shown in Fig. 3

have an uncertainty of about ±1 m.y. or less, but estimates of the

Pannonian-Pontian boundary vary between 9.5 and 5.5 Ma (see Nagymarosy,

1981). In this paper we use 8 Ma suggested by the data of Vass and

Bagdasarian (1978), and by magnetostratigraphic dating of sediments in

the Pannonian basin (Rónai, 1981; Gy. Pogácsás, unpublished data).

Intra-Carpathian Basin Sediments

Neogene and Quaternary rocks within the intra-Carpathian basins

reach a maximum thickness of 7 km in the Pannonian basin. They consist

primarily of sandstone, shale and claystone with some marl and

limestone in the lower part of the sequence. These sedimentary rocks

are generally fine-grained with occasional coarser grained units that

contain rare Pannonian age turbidites. Molluscan faunal evidence

indicates deposition in a shallow water environment, probably less than

100-200 m, although deeper water could have present locally during
Badenian time (Báldi, 1982, pers. comm.).

1) Karpatian (17.5-16.5 Ma) and Badenian (16.5-13.0 Ma)

The oldest Miocene sedimentary rocks within the Pannonian, Danube,
Drava and Zala basins are mostly of Karpatian and Badenian age. These
rocks were generally deposited in shallow marine conditions, interupted
by short periods of uplift. After Badenian time, brackish, lacustrine,
and finally fluvial conditions prevailed as the Central Paratethys Sea,
which had formerly covered the region, gradually disappeared (see, for
example, Steininger and Rögl, 1979). The final isolation of the
Central Paratethys from the Mediterranean occurred at the end of the
Badenian when elevation (and compression?) of the Eastern and Southern
Alps and Dinarides permanently closed the temporary seaways to the west
(Hörnes, 1856).

Within most of the peripheral basins (Vienna, Transcarpathian,
northwest Danube, Sava and Drava) Badenian and Karpatian sedimentary
rocks lie within well defined fault-bounded grabens and may be up to
4 km thick. These grabens are typically asymmetric, bounded along one
side by large normal faults (up to 4 km vertical throw) which may also
have tens of km of horizontal displacement (Fig. 9a) (for example, Brix
and Schultz, 1980; Jiříček and Tomek, 1981; Varga and Pogácsás, 1981;
Royden et al., 1982; and others). Bedding planes may be rotated along
the boundary faults, which suggests that the Badenian and Karpatian
sediments were deposited during active faulting. Smaller
syn-sedimentary normal faults within the Badenian sediments also
suggest that extension and sedimentation were synchronous.

Badenian sedimentary rocks originally covered most of the central intra-Carpathian region, including those areas which now underlie the Pannonian and Danube basins. The extent of Karpatian sediments was less but they also covered a large part of the central area (Nagymarosy, 1981). In the central basin area, the Karpatian-Badenian sequence reaches a maximum thickness of 1.5 km in the deepest part of the Pannonian basin. In other parts of the Pannonian basin these rocks are thin (~100 m) or missing, which may in part reflect subsequent erosion (see below). In the southern part of the Pannonian basin, Badenian-Karpatian rocks dip 45° (Körössy, 1981), suggesting tectonic activity during or after Badenian time.

2) Sarmatian (13.0-10.5)

The thickness of Sarmatian rocks is generally less than about 100 m, even in the deepest parts of the basins, but in a few places it reaches 500 m (Tokaj Mountains, northeast Danube basin). Sarmatian rocks, mostly deposited in brackish water, rest unconformably on older rocks in some parts of the Danube and Pannonian basins and are often missing (Nagymarosy, 1981; Metwalli, 1971). This suggests an erosional event or depositional hiatus over the central basin area at about the Badenian-Sarmatian boundary. Sedimentation appears to have been continuous only within the deepest parts of the Pannonian basin and in a few other restricted areas.

The Sarmatian appears to have been a period of tectonic activity within the central part of the intra-Carpathian region. Normal faulting was active in the Apuseni Mountains from middle Badenian to earliest Pannonian time (Săndulescu, pers. comm., 1981). Intra-Sarmatian dextral shear occurred along a northwest trending fault

system within the Bakony Mountains, with about 20 km of proven

cumulative displacement (Meszaros, 1981, pers. comm.).

3) Pannonian to Recent (10.5-0)

Pannonian age and younger rocks within the Vienna, east Danube,

and Transcarpathian basins are mostly flat-lying and may be cut by a

few normal faults with small displacements (Fig. 9b) (Brix and Schultz,

1980; Rudinec et al., 1981). These rocks are not usually restricted to

fault bounded troughs as are the underlying Badenian and Karpatian

rocks, and often onlap onto the pre-Miocene basement adjacent to the

Badenian age grabens. This suggests that there has been little

tectonic activity within these basins since Sarmatian time.

Over almost the entire central basin area a significant

unconformity occurs between Sarmatian and Pannonian rocks (Körössy,

1968; Nagymarosy; 1981). The lowermost part of the Pannonian age

sequence is missing over most of the central area, even in the deep

basins. Sarmatian-Pannonian age sedimentation was uninterrupted only

in a few small areas (southwest Zala and southern Pannonian basins)

(Nagymarosy, 1981). Where Pannonian age rocks lie directly on the

older crystalline or carbonate basement of the central area, the lower

part of the Pannonian sequence is represented by a transgressive

sequence, with a basal conglomerate typically 5-30 m thick (Körössy,

1968). The conglomeratic unit contains carbonate and crystalline

clasts from the local basement, with occasional claystone boulders.

This unit indicates a widespread erosional event of upper Sarmatian to

lower Pannonian age, which probably cut into older Miocene and early

Cenozoic sedimentary rocks as well as the crystalline and carbonate

basement. The lack of significant transport of the cobbles and the

fact that coarse rocks were not shed into the deepest basin areas suggests low topographic relief (Körössy, 1968). This is consistent with the shallow water depositional environment inferred for basin sediments.

Pannonian age to recent sedimentation has been mostly continuous. These sedimentary rocks were deposited in a brackish-lacustrine-fluvial environment (Steininger and Rögl, 1979), and reach a maximum thickness of about 5.5 km in the deepest part of the Pannonian basin (well 6, Fig. 10).

These sedimentary data suggest widespread tectonic activity during Karpatian and Badenian time, which, in the central region, was probably sustained through Sarmatian and even earliest Pannonian time. In the central basin area, a pervasive erosional event at the Sarmatian Pannonian stage boundary suggests probable uplift at this time. The style of sediment deposition suggests very gentle topographic relief. Pannonian to recent sedimentation has been mostly continuous. These are key points in our reconstruction of basin evolution, and will be returned to in a later section of this paper.

QUANTITATIVE GEOLOGICAL AND GEOPHYSICAL DATA

In earlier sections we have given a qualitative overview of the geology and tectonic setting of the intra-Carpathian basins. In this section we present specific quantitative data from drill holes, heat flow measurements, etc., to be used in determination of extension histories for some of the intra-Carpathian basins.

Sediment accumulation

Sedimentation histories for 23 boreholes, mostly within Hungary, were obtained using faunal and lithologic data collected from the

explanatory text volumes of the Geological map series of Hungary, 1:200,000 (1965-1975) and Radócz (1968) (Fig. 10). These well data were selected from more than 5,000 well logs obtained by the Hungarian Oil Company, and were re-evaluated using detailed descriptions of coring samples in the files of the Hungarian Oil Company and the Hungarian State Geological Survey. The major uncertainties in constructing these curves were:

1) Coring was discontinuous and the distance between cores sometimes exceeded 200m. Moroever, the upper 1000 to 2000m were occasionally not sampled, although this interval usually contains the Mio-Pliocene and Pliocene-Quaternary boundaries. In these cases, lithologic features were used to infer the chronostratigraphic boundaries based on information from neighboring wells. Identification of unconformities within the sedimentary rocks was impaired by the distance between cores.

2) Diagnostic macroscopic faunas were rarely sampled because the length of the cores was small and thus the probability of finding diagnostic species within the sampled material was also small.

3) In western Hungary (wells 13-23), Dacian, Romanian and Quaternary diagnostic faunas were not found, although sedimentation appears to have been continuous until the present.

4) Correlation of Pannonian and post-Pannonian rocks within the Paratethys is controversial and an accurate radiometric time scale for the uppermost Miocene is lacking (see above).

Because of difficulties in dating, we have combined the Dacian and Romanian stages, which we considered to be the equivalent of the "Levantinian" or "Upper Pliocene" in Hungary.

In this study we chose only wells with sedimentary rocks that which could be dated reliably (considering the difficulties in dating sediments deposited between 10.5 and 2 Ma), and in only those basins where the thermal structure seemed to be unperturbed by late Miocene and Pliocene volcanism. Water-depths in the intra-Carpathian region have been uniformly shallow throughout late Cenozoic and Recent times so that sedimentation histories from these basins give a reasonable representation of basement subsidence. Corrections for compaction of sediments during burial are made in a later section.

The sedimentation curves have been grouped by location, and in general the sedimentation patterns for wells that are within the same part of each basin are similar (Figs. 10 and 11). The most notable exceptions occur in wells 1 and 6, which were located in deep troughs. Well 1 appears to have subsided more rapidly during Pannonian-Pontian time than did wells 2-5. However, the basal Pannonian age unit may be older in well 1 than in the other four wells (I. Varga, 1981, pers. comm.), and the apparent difference in sedimentation rate may partly reflect different ages for the initiation of Pannonian age sedimentation following Sarmatian age denudation. Well 6 shows a large thickness of sediment deposited in Badenian time (2.15 km), whereas the other wells shown for this part of the southern Pannonian basin (7-9) show little or no Badenian age sedimentary rocks. Total accumulation of Pannonian and younger rocks (3 to 5 km) is more uniform than that of older rocks. This sedimentation history probably reflects a Badenian

age for formation of this deep trough, followed by a fairly uniform

Pannonian age subsidence of the trough and surrounding areas.

Wells 1-23 show a very different subsidence history from those in

the Vienna basin, which experienced a rapid phase of subsidence during

Ottnangian through Badenian time, followed by a slow, much reduced

subsidence that has continued until present (Fig. 11). The

Transcarpathian basin (not used in this study because of the large

volume of young igneous rocks that surround and intrude the basin) has

had a subsidence history similar to that of the Vienna basin (Rudinec,

1978 and Rudinec et al., 1981). Other areas that show significant

thicknesses of Karpatian-Badenian sedimentary rocks are the western

Drava trough and parts of the Zala basin (Fig. 2) (Körössy, 1970; Gy.

Pogácsás, 1979, unpublished map). Locally in the Zala basin, several

km of Badenian rocks form large anticlines, which are the result of

Badenian folding (Budafa area) (Dank, 1962). Because of folding,

the present thickness of these rocks does not reflect the original

depositional thickness, so that wells drilled in these areas were not

used in this study. Pannonian age initiation of major subsidence in

the Zala basin, indicated by wells 20-23, is only representative of

part of the basin. Other parts of the Zala basin probably subsided at

least 1 km during Badenian time.

Karpatian-Badenian sediment accumulation and subsidence seem to

be best developed in the northern intra-Carpathian basins (Vienna and

Transcarpathian basins), and decrease southward into the central part

of the intra-Carpathian region. Sarmatian age sedimentary rocks are

best developed in the Danube basin area and southern Transcarpathian

depression (not shown), while Pannonian-age rocks are thickest in the

Pannonian basin. Thus the locus of major subsidence seems to have migrated southward from the Vienna and Transcarpathian basins towards the Pannonian basin. There is some indication that it moved from west to east as well.

Paleomagnetic dating of sediments was also used to provide subsidence histories for two drill holes in the Pannonian basin. Nearly 1000 measurements were made in the upper 1 km of sedimentary rocks near Vésztő and Dévaványa (Fig. 10), and the inclination of remanant magnitization was correlated with the major geomagnetic epochs determined from deep ocean sediments (Table II and later sections) (Cooke et al., 1979; Rónai, 1981). The resulting depth-age relationship shows a remarkably linear rate of sediment accumulation, with average sedimentation rates of 160 m/m.y. and 175 m/m.y. for Dévaványa and Vésztő respectively. The ten absolute age horizons determined for these wells have relatively small uncertainties, so that the subsidence of these two wells is accurately constrained over the last 6 m.y.

Data from nearby wells that reached basement and from seismic reflection profiles indicate that the oldest basin sediments beneath Devavanya and Vestzo are probably of Pannonian age, and that the depth to basement is roughly 2.5 to 3.0 km (Gy. Pogácsás, unpublished data).

Thermal Data

In addition to heat flow data obtained from temperature and conductivity measurements in deep boreholes in the intra-Carpathian region, hundreds of downhole temperature measurements are available from wells which have attained near-equilibrium thermal conditions. A few of these are shown in Fig. 12. The Pannonian basin is

characterized by high heat flow (up to about 110 mW/m^2) (see, for example, Čermák and Rybach (eds.) 1979 and Horváth et al., 1981). Because of rapid deposition of cold sediments (up to 7.5 km thick), thermal gradients and heat flow within the sediments are 10% to 30% lower than they would be had little sediment deposition occurred. We shall refer to this as the "thermal blanketing effect".

The area of high heat flow extends northwestwards from the Pannonian basin, across the Hungarian mid Mountains, and possibly into the southern part of the Danube basin (see below). Heatflow within the northern Danube basin is lower than that in the Pannonian basin (about 70 mW/m^2). Further northwest, heat flow within the Vienna basin is even lower, about 50 mW/m^2. Measured heat flow also decreases east of the Pannonian basin, with average heat flow around 50 mW/m^2 in the Transylvanian basin.

A major hydrothermal system exists in the Hungarian mid-Mountains and southern part of the Danube lowland where water circulation within the karstic basement reaches depths of 4 km. The apparent surface heat flow is 52±20 mW/m^2, but Horváth et al. (1981) state that the sum of convective plus conductive heat loss for the area is 112±20 mW/m^2, and that this is in good agreement with heat flow measurements in neighboring wells not affected by hydrothermal circulation.

A second hydrothermal system exists in parts of the Pannonian basin where meteoric water circulates within the upper few hundred meters. Horváth et al. (1981) estimate that in places this convective circulation may change the surface heat flow by 10 to 20 mW/m^2, but that the effect on temperatures at 1 km depth is less than 5%. For

this reason we use mostly temperature and heat flow data based on measurements at depths greater than 1 km.

Other lines of evidence also suggest high temperatures beneath the Pannonian basin: 1) electrical resistivity and conductivity measurements suggest that the base of the lithosphere is in an elevated position, about 70 km depth as compared to normal values of 125 km (Ádám et al., 1977; Ádám and Wallner, 1981); 2) gravity model calculations suggest that the upper mantle beneath the Pannonian basin has anomalously low density (Horváth and Stegena, 1977); 3) the top of the low velocity zone is in an elevated position (60-70 km) (Posgay, 1975); 4) Seismic travel time residuals are positive (Morelli et al., 1968 and Roman, 1973). These data are consistent with the heat flow determinations in deep boreholes, indicating that the Pannonian basin is an area of anomalously high temperatures, both at the surface and at depth.

Other Geophysical Data

The intra-Carpathian region is characterized by thin continental crust (25 to 30 km including Neogene sedimentary rocks), particularly in comparison with the thick crust (40 to 60 km) under the surrounding mountains (Fig. 13). However, because many of the deepest parts of the basins are less than about 50 km wide, significant thinning of the crust in these areas would not normally be detected on seismic refraction profiles. Beneath the Pannonian basin, crustal thickness is 24-28 km.

Earthquakes at depths of 70-140 km beneath the southern East Carpathians yield focal mechanisms which indicate down dip extension on steeply dipping nodal planes (Roman, 1970; Fuchs et al., 1979).

Shallow earthquakes (up to 30 km) yield focal mechanisms which suggest eastward overthrusting along a surface dipping about 30° to the west. These earthquakes may represent the final stages of subduction and crustal shortening in the East Carpathians. Fuchs et al. (1979) have interpreted the intermediate depth earthquakes as the result of a detached slab of lithospheric rocks sinking into lighter asthenospheric material.

ANALYSIS OF EXTENSION

From the data presented above, we conclude that the intra-Carpathian basins are primarily extensional in origin. In this section we present a physical and mathematical framework to describe the development of extensional basins. We will use this framework to make a quantitative analysis of the sedimentation, thermal and geophysical data given above, and to draw some conclusions about the nature of the extensional processes in the intra-Carpathian area.

Salient Features of Extensional Basins

In this paper we consider two different modes of extension to explain the subsidence and thermal structure of the intra-Carpathian basins. First, uniform extension, discussed in detail by McKenzie (1978), requires that the amount of extension be constant throughout the lithosphere and independent of depth. Second, a modified or non-uniform extension model, discussed in detail by Royden and Keen (1980), allows for decoupling between upper and lower lithosphere at some arbitrary depth. Clearly, uniform extension is a special case of the modified extension model.

The reason for using a modified extension model is that it may provide an explanation for the subsidence and thermal structure of some

apparently extensional basins that are not compatible with uniform extension. The justification for using this model is that, because rheological properties vary continuously with pressure and temperature, it seems reasonable that the lithosphere may not deform homogeneously under stress. It should be noted that extension of the upper and lower lithosphere by different amounts causes space problems. This question will be considered in a later section of this paper.

The general development and subsidence of an extensional basin may be divided into two main stages. During extension, the crust and mantle lithosphere become attenuated and are replaced from below by passive upwelling of hot asthenosphere (Fig. 14). This attenuation and upwelling results in elevated thermal gradients. At the same time, there is an initial change in elevation (usually subsidence) (Figs. 14 and 15). This occurs in isostatic response to net density changes resulting from crustal thinning, which is partially, or sometimes entirely, compensated by replacement of thinned mantle lithosphere by asthenosphere. This phase is a response to <u>active</u> extensional processes in the lithosphere and the area of subsidence is usually well localized and fault bounded. Sediments deposited during this phase usually contain syn-sedimentary faults and may have rotated bedding. Most of the pre-Pannonian age sediments within the intra-Carpathian basins are probably in this category.

Following extension, the subsequent cooling of the crust and upper mantle towards thermal equilibrium results in long-term subsidence which we will refer to as thermal subsidence. This second stage of subsidence is a <u>passive</u> process. Thermal subsidence is usually of greater areal extent than that of the first phase and not usually confined to fault

bounded grabens. Sediments are relatively flatlying and undisturbed, often onlapping onto basement rocks adjacent to the initial grabens. Most of the Pannonian age and younger sediments in the intra-Carpathian basins were probably deposited during passive thermal subsidence of the basement. During both phases, subsidence is amplified by isostatic compensation for sediment loading.

If the original crustal thickness, elevation and temperature structure are known, and the effects of sediment loading are removed, the amount of extension can be determined from subsidence data alone, or from subsidence data in combination with heat flow, geologic and other geothermal measurements. Equations which relate extension, subsidence, heat flow and hydrocarbon potential have been published in recent literature and will not be reiterated in this paper (see, for example, Lachenbruch and Sass, 1978; McKenzie, 1978; Steckler and Watts, 1978; Royden et al., 1980, Sclater et al., 1980; Sclater and Christie, 1980; Royden and Keen, 1980; Steckler and Watts, 1980; McKenzie, 1981; and others). Unless otherwise stated, most of the equations used in this paper can be found in Royden and Keen (1980).

Correction of Subsidence Data

The first step in the analysis of subsidence data is the correction for sediment loading and compaction. We assumed that porosity decayed exponentially with depth:

$$\phi = \phi_0 \, e^{-ax}$$

where ϕ is porosity, ϕ_0 is surface porosity, and a is a decay parameter that must be determined experimentally for each lithologic type. The sedimentary rocks within the intra-Carpathian basins comprise a sequence

of interbedded sandstone, shale, and claystone, so porosity variations

with depth were determined separately for claystone and for sandstone.

We assumed that these two curves provided outer bounds for average

porosity at depth (Fig. 16). (Physical parameters used in this study are

summarized in Table III.) Surface porosity was constrained by surface

densities of 2.05 g/cm^3 (Stegena, 1964). An intermediate porosity-depth

relationship was chosen by eye as a best estimate of average porosity

versus depth.

Using the equation given above, sediment density as a function of

depth may be written:

$$\rho_{sed} = \phi\rho_w + (1-\phi)\rho_{matrix}$$

or

$$\rho_{sed} = \rho_{matrix} + \phi_0 e^{-ax}(\rho_w - \rho_{matrix})$$

where ρ_{matrix} is the density of the sediment matrix at zero porosity and

ρ_w is the density of water. When the median values of ϕ_0, a, and ρ_{matrix}

(Table III) are substituted into this expression, the resulting

depth-density relationship differs by less than .05 g/cm^3 from that

derived by Stegena (1964) from analysis of Bouguer anomalies within the

Pannonian and Danube basins.

We assumed that the sedimentary rocks in the basins could be treated

as a single lithologic unit, and that the porosity-depth and

density-depth relationships given above were also valid for past times.

Sedimentary rocks could then be decompacted or "backstripped" to

determine depth to basement at any time by removing the effects of

subsequent compaction within the sediments. For example, corrected

basement depth at the beginning of the Quaternary was calculated by: (1)

Determining the thickness of the pre-Quaternary basin fill, (2) Assuming

that the porosity within the sedimentary rocks is given by the
porosity-depth relationship in Fig. 16, (3) Reconstructing the thickness
of pre-Quaternary rocks at the beginning of the Quaternary by placing the
Quaternary boundary at the surface and using the assumed porosity-depth
relationship. (For details of calculation, see Sclater and Christie,
1980.) This reconstructed sediment thickness gives the corrected depth
(below the surface) to basement at the beginning of the Quaternary, and
will be referred to as "decompacted sediment thickness". Because
compaction of sedimentary rocks during burial decreases the thickness of
lithologic units, corrected depth to basement is greater than the present
thickness of the corresponding sedimentary rocks.

Following decompaction, the effects of sediment loading were removed
by assuming pointwise isostasy to calculate the depth to basement that
would result if the sedimentary rocks were replaced by water. The
purpose of this was to separate the amount of subsidence due to sediment
loading from that due to extension and crustal thinning. Thus:

$$\text{equivalent water loaded depth} = (\text{loaded depth}) \left(\frac{\rho_a - \overline{\rho}_{sed}}{\rho_a - \rho_w} \right)$$

where ρ_a is the density of the asthenosphere and $\overline{\rho}_{sed}$ is the average
density of the sedimentary column.

A useful rule of thumb for correcting the effects of sediment
loading is that about 2 to 3 km of sediment fill is equivalent to about
1 km of water fill, but this varies somewhat with lithologic type,
sediment thickness, and other factors.

Equivalent water loaded depths for wells 1-23 are shown in Fig. 17. Sedimentation data for wells within the same area and with the same general sedimentation history were averaged prior to decompaction, so that some of the curves in Fig. 17 are composites. This was done to minimize non-systematic errors in dating for individual wells.

Three different sets of parameters were used to calculate the equivalent water loaded basement depths (which we shall refer to as corrected depths or corrected subsidence) in Fig. 17. One set corresponds to the intermediate value or best estimate for each parameter (Table III). The other two sets correspond to the extreme values of sediment matrix density, mantle density and porosity that would combine to give the greatest and the least corrected depths. Thus Fig. 17 shows both our best estimate the for the corrected subsidence for each well (or composite well group), as well as maximum and minimum estimates. It should be noted that the latter cases correspond to a coincidence of end members. Even for a random probability distribution for each parameter within the allowed range, it is more likely that the equivalent water loaded subsidence curves lie near the best estimate for water loaded subsidence than near the extreme limits.

Thermal Analysis:

Most previous reconstructions of thermal and extensional histories from subsidence curves deal with subsided areas considerably older than the intra-Carpathian basins (see authors sited previously). After extension, surface heat flow decays quickly toward equilibrium values and uncertainties in determining representative surface heat flow are large relative to the size of the anomalies that one wishes to observe. Therefore, surface heat flow does not provide strong constraints on the

magnitude of extension and details of the extension process in basins older than about 50 m.y. Within younger basins, particularly those less than about 20 m.y. old, surface heat flow measurements can be a useful constraint in determining the magnitude and style of extension. In these sections on thermal analysis we match the water-loaded subsidence curves for wells in the intra-Carpathian basins to theoretical subsidence curves assuming first, uniform extension, and second, modified extension. The theoretical heat flow and thermal gradients predicted in this way may then be compared with those actually observed.

Most of the parameters used in this study are from Parsons and Sclater (1977) (Table III). Density of continental crust was chosen so that continental crust 35 km thick would have a surface elevation at sea level when the lithosphere was at thermal equilibrium. As long as the physical parameters chosen are close to generally accepted values, are self-consistent, and are consistent with the depth-age and heat flow-age relationships in the oceans, the exact values of these parameters are not very important. For example, we could have chosen density values such that an area underlain by 40 km thick continental crust at equilibrium conditions was at sea level. The only noticeable result would be that, after extension of an area initially at sea level, the predicted values of crustal thickness would be proportionately greater.

A simple linear relationship was used to characterize the thermal conductivity within the sedimentary rocks (Fig. 18 and Table III), and thermal conductivity as a function of depth was assumed to remain unchanged through time:

$$K_{sed} = K_o + bx$$

We chose two envelope curves to characterize the range of conductivity values with depth as well as a best fit or intermediate curve to characterize the average conductivity depth relationship. Only a one dimensional thermal analysis was used because horizontal conduction of heat is probably significant only near steep faults which juxtapose basement and sedimentary rocks (for example, the Steinberg fault in the southwest Vienna basin).

For simplicity of calculation, radiogenic heat sources within the crust were assumed to be concentrated at a single depth (point source in a one-dimensional model). At equilibrium conditions we assumed that 16 mW/m^2 was generated by radiogenic elements at 8 km depth. During stretching, the depth below the surface and the magnitude of the radiogenic heat source were assumed to vary linearly with crustal thickness. For example, after stretching by a factor of 2, 8 mW/m^2 would be generated 4 km below the surface. This was done to simulate the effects of crustal thinning on heat sources distributed arbitrarily within the upper crust. The errors introduced by this approximation are small (see Appendix). Heat sources within the sediments were ignored because their contribution to the surface heat flow has been negligible over the 15 m.y. or less since deposition.

A semi-numerical computational method was used to accomodate an arbitrary number of extension phases. During each phase, extension was assumed to proceed at a constant rate. Each extension phase was divided into time increments of 0.5 m.y. The total amounts of extension and sedimentation that occurred during each 0.5 m.y. increment were assumed to have occurred instantaneously at the beginning of that increment (sediments deposited at 5°C, the assumed

surface temperature). Following each episode of instantaneous stretching and sedimentation, the temperature structure was Fourier transformed by numerical integration, so that the temperature structure at the end of each time increment could be calculated analytically from the Fourier coefficients (Carslaw and Jaeger, 1959, p. 93-94). Further details are given in the appendix.

THERMAL ANALYSIS: PANNONIAN BASIN

Initial Conditions

From early Eocene to early Miocene time, most of the area beneath the Pannonian basin (wells 1-5) was a slowly subsiding, but relatively stable, region covered by shallow marine to non-marine sediments (see above and Fig. 8). This suggests:

(1) the thickness of the crust beneath the northern Pannonian basin should have been about 35-40 km, similar to that of other stable continental regions that have a low surface elevation. In this study we used an initial crustal thickness of 35 km.

(2) the thermal structure of the underlying lithosphere should have been near equilibrium conditions by the beginning of late Miocene extension. If a major thermal anomaly had existed beneath this area during Eocene time, subsequent cooling of the upper mantle would have resulted in considerably greater subsidence than is observed. An alternative possibility might be that throughout the early Cenozoic a thermal anomaly was maintained at depth by tectonic processes so that cooling and subsidence did not occur. However, there is little evidence for much tectonic activity at this time. Therefore we assumed that the lithosphere beneath the northern part of the Pannonian basin (under wells 1-5) was at thermal equilibrium conditions.

Although early Cenozoic rocks do not occur beneath wells 6-12 (Fig. 8), this area was probably near sea level by early Miocene time because: 1) Apparent lack of early Cenozoic sediment transport from this area into adjacent marine basins or anywhere else, and 2) Distribution and structure of Badenian, Sarmatian, and earliest Pannonian age sedimentary rocks suggests low topographic relief at this time. Therefore we assumed that at the beginning of late Miocene extension this area was also near sea level, and the lithosphere at thermal equilibrium conditions.

Uniform extension: wells 1-12

Conceptually and mathematically, uniform extemsion is the simplest way in which to extend lithospheric rocks to form subsided basins. Furthermore, extension distributed non-uniformly with depth implies serious space problems for adjacent unstretched, which, if possible, would be best avoided. For these reasons we chose to begin our analysis of extension within the Pannonian basin by assuming that extension was uniformly distributed with depth.

In order to analyze the subsidence, thermal structures and extension histories of wells 1-12 in light of uniform extension, we matched the corrected subsidence history of each well or composite well group (Fig. 17) to a predicted subsidence history corresponding to appropriate extension parameters. (For simplicity, subsidence and thermal values calculated from extension parameters will be referred to as predicted values, while those calculated or estimated directly from observations will be referred to as observed values.) Three phases of extension were considered: Badenian (16.5-13.0 Ma), Sarmatian (13.0-10.5 Ma) and Pannonian (10.5-8.0 Ma). We assumed that the basement

was at sea level prior to the initiation of Badenian extension. In so far as possible, the predicted subsidence histories were constrained to be within about 20 m of the corrected subsidence histories calculated from observations at 13.0 Ma, 10.5 Ma and the present. For wells 1-6, theoretical extension histories were constructed to fit the maximum and minimum determinations of corrected subsidence histories calculated from observations (Fig. 17), as well as the intermediate corrected subsidence history, in order to provide an estimate of the uncertainties involved (Fig. 19 and Tables IV and V).

The total extension determined for the well groups varied from β = 1.26-1.35 for wells 2-4 to β = 2.61-5.88 for well 6 (Fig. 19). Uncertainties in total extension for any well group increased with increasing depth to basement because: (1) absolute magnitude of uncertainties in corrected basement depth increased with total depth, and (2) present corrected depth is roughly proportional to $(1-1/\beta)$. Therefore, a fixed uncertainty in corrected depth, Δd, will correspond to larger uncertainties in β as the total corrected depth, d, increases.

Because there has been no significant tectonic activity in the Pannonian basin area during the last 8 m.y., basement subsidence and sediment accumulation during this time have been controlled by the cooling and thermal contraction of underlying crust and upper mantle. Thus, the rate of subsidence and sediment accumulation during this time is a measure of heat loss from the crust and upper mantle, mostly through the surface. Except for wells 1 and 6, predicted subsidence over the last 8 m.y. (thermal subsidence) was 2 to 3 times slower than the observed subsidence. For well 6, predicted subsidence was only

somewhat slower than that observed. In fact, the observed rates of thermal subsidence for all wells (except well 1) were reasonably close to rates predicted for well 6 (roughly equivalent to β=2.5 to 6.0). For well 1, the 2.0 and 5.0 my age dates suggest that the rate of (observed) thermal subsidence was much slower than for the other wells, but it seems likely that the apparently slow rates of subsidence observed for well 1 may be due to errors in determining biostratigraphic horizons within the sediments.

Predicted heat flow values calculated from the theoretical extension histories include a correction for the thermal blanketing effect of sediment deposition (Tables IV and V). This was done by calculating the predicted temperatures within the sediments and underlying lithosphere using the conductivity depth relationship in Fig. 18 (see Appendix), and then converting temperatures back to heat flow. Three values of predicted heat flow were computed from extension parameters: an intermediate value (intermediate values of extension parameters and intermediate conductivity-depth relationship) and two end-member values (largest extension values plus highest conductivity and smallest extension values plus lowest conductivities). The calculated decrease in heat flow because of thermal blanketing was 25%-33% of the uncorrected heat flow for well 1, 18%-23% for well 5, and 32%-37% for well 6, depending on the conductivity-depth relationship assumed for the sedimentary rocks: greater decreases were calculated for lower conductivities. The decrease in heat flow due to thermal blanketing for wells 2-4 was about 10%. Uncertainties in theoretical temperature gradients and heatflow increased with increasing depth to basement, because heat flow is roughly proportional to β (see above).

Most of the heat flow measurements in the Pannonian basin were made in sedimentary rocks with total thickness less than 3 km, so that it is most appropriate to compare them to the predicted heat flow values for wells 2-5 and 8-12. Predicted values for these wells (46-63 mW/m^2) are lower than observed values (102±11 mw/m^2) by nearly a factor of two. Observed values are somewhat higher than, but consistent with, predicted values (59-99 mW/m^2) for well 6 (basement at 7.5 km).

Predicted temperature values were plotted against temperatures determined by formation tests near the bottom of wells 1 and 6, and bottom hole measurements for wells 7,8,10 and 12. In addition, bottom hole temperatures from other wells in the Pannonian basin were also used for comparison (Fig. 12b); each of these wells penetrated to within a few hundred meters of basement, and temperatures were extrapolated to the nearest 500 m interval (Juhász, 1977).

Predicted temperatures at a given depth show a systematic increase with increasing depth to basement (Fig. 20). In contrast, temperatures observed in wells 1,6,7,8,10,12 and other wells in the Pannonian basin show little correlation with present basement depths. For all wells, observed temperatures were in good agreement with temperatures predicted for well 6. However, except for well 6, observed temperatures in each well were higher than predicted temperatures by as much as a factor of two.

It should be noted that maximum and minimum values of predicted temperatures and heat flow result from exteme values of assumed conductivities and extension parameters. Predicted temperatures and heat flow are more likely to fall near the intermediate values than near the extreme values.

Except under the deepest troughs (wells 1, 6 and 7), predicted

crustal thicknesses calculated from extension parameters (including

basin sediments) are 25-30 km. This is in good agreement with seismic

refraction data (Fig. 13).

Uniform extension: Dévaványa and Vésztő

A similar analysis of the extension history of these two wells was

carried out by assuming uniform extension. Because the oldest basin

sediments beneath these wells are probably Pannonian age, we assumed

that extension occurred during Pannonian time (10.5-8.0 Ma), and that

the basement was at sea level prior to extension. The present basement

depth beneath these wells is between 2.5 and 3.0 km, so we assumed that

the Pannonian age extension resulted in a present depth of 3.0 km.

This corresponds to a corrected basement depth of 950 to 1230 m, or β =

1.45 to 1.69.

Instead of plotting theoretical subsidence and corrected basement

depth as done for wells 1-5, we calculated the present theoretical depth

to various age horizons with the sediment column from the theoretical

subsidence curves. This was done by assuming that, instead of being

filled with water, the theoretical basin was always filled to sea level

by sediments with the same porosity, density, etc. as those in the

Pannonian basin. As before, three curves were constructed,

corresponding to maximum, intermediate and minimum depths to each time

horizon within the sediments (Fig. 21). For sediments deposited at

Dévaványa and Vésztő, the depth to each paleomagnetically determined age

horizon within the sedimentary column is roughly twice that predicted by

uniform extension. Observed values are, however, in good agreement with

results predicted by uniform extension for a present depth of 7.5 km, or

β = 2.5–6. Therefore, thermal subsidence, and thus the rate of heat loss from the crust and upper mantle beneath Dévaványa and Vésztő, is nearly twice that which would be predicted by assuming uniform extension. This is consistent with observed values of surface heat flow and temperature, which are also about twice those predicted by uniform extension.

Comparison of observed and predicted thicknesses is more definative than comparison of observed and predicted temperatures and heat flow in wells 1–12. This is partly because large uncertainties are associated with estimates of thermal conductivity within the sedimentary rocks (compare Figs. 20 and 21). Unfortunately, magnetostratigraphic dating of sedimentary rocks has not been done for other wells in the intra-Carpathian basins. Errors associated with biostratigraphic dating of intra-Carpathian basin sediments younger than about 10.5 m.y. make the determination of thermal phase subsidence rates on the basis of biostratigraphy somewhat unreliable. Nevertheless, all the wells examined so far reveal a consistent pattern: thermal subsidence rates, heat flow, and temperatures observed for wells 1–12 are in reasonable agreement with predicted values for well 6, now at a depth of 7.5 km (β=2.5 to 6). Except for well 6, these observations are not consistent with the magnitudes of uniform extension determined from analysis of the subsidence histories of wells 1–12. Uniform extension may just account for observations in the deepest part of the Pannonian basin (7.5 km depth), but it does not work elsewhere in this basin.

Modified extension: wells 1–12

The Pannonian basin appears significantly hotter than is compatible with a uniform extension history. Therefore, we were forced to investigate alternative methods of introducing heat into the crust and

upper mantle. A few small Miocene volcanic centers, probably erupted

around 18 Ma, underlie the Pannonian basin sediments (Balla, 1981;

Körössy, 1981), but most of the Miocene volcanic activity in the

intra-Carpathian region occurred adjacent to the Carpathian mountains

(Fig. 2). Heat associated with eruption of magma in the Pannonian basin

area probably had a negligible effect on present surface heat flow

because: (1) the fraction of the basement covered by these extrusive

rocks is small (less than 5%), (2) surface heat flow and near surface

temperatures do not seem to be influenced by proximity to a volcanic

center, (3) in the shallower parts of the Pannonian basin ($<$3 km), the

amount of volcanism required to match the observed subsidence is

insufficient to produce the observed temperatures, heat flow, etc., and

(4) volcanism pre-dates subsidence by about 8 m.y. It is difficult to

assess the possible contribution of magmatic intrusions that do not reach

the surface, but it seems unlikely that a large fraction of the crust

could be comprised of magma without extensive surface volcanism.

In order to account for the high temperatures within the Pannonian

basin, we analyzed the corrected subsidence of wells 1-12 in light of a

modified extension history where crustal extension was accompanied by

almost complete replacement of the mantle lithosphere by hot

asthenospheric material. For purposes of calculation, we assumed a

detachment horizon at the base of the crust (see Appendix). Removal of

subcrustal lithosphere could then be simulated by requiring arbitrarily

large values for lithospheric extension below the detachment horizon.

This is not to imply that additional extension of sub-crustal

lithosphere is the only way to introduce extra heat into the upper

mantle. Erosion of subcrustal lithosphere from below, mechanical

removal of the lower lithosphere, or upward migration of magma are all mechanisms that might result in apparent attenuation of sub-crustal lithosphere. The mechanism of non-uniform extension used in calculation is merely a convenient way of representing the thermal effects of lithospheric extension coupled with the introduction of extra heat into the upper mantle.

During uniform lithospheric extension of areas with an initial crustal thickness greater than about 20 km, the initial isostatic change in surface elevation is almost always subsidence. During non-uniform extension, the initial change in elevation depends upon the relative importance of density increases, due to crustal thinning, and density decreases, due to partial replacement of lithospheric material by hot asthenosphere. Depending upon the initial crustal thickness, the depth to the detachment horizon, and the magnitudes of upper and lower lithospheric extension, non-uniform extension can result in either initial uplift or subsidence. For initial crustal thickness of 35 km, complete attenuation of the sub-crustal lithosphere results in initial uplift when crustal extension is less than about $\beta = 1.7$, and in initial subsidence when $\beta > 1.7$ (Fig. 15).

This phenomenon provides a possible explanation for regional erosion, and probable uplift, during Sarmatian time (Fig. 22). Therefore we specified that the addition of extra heat into the lower lithosphere occur during Sarmatian time. As before, three extensional phases were considered: Badenian (16.5-13.0), Sarmatian (13.0-10.5), and Pannonian (10.5-8.0 Ma), and predicted subsidence was constrained to match the corrected subsidence calculated from observations at 13.0 Ma, 10.5 Ma and the present. During Badenian and Pannonian time, extension was assumed

to be uniform throughout the lithosphere, but during Sarmatian time attenuation of subcrustal lithosphere was assumed to be 10 times greater than crustal attenuation during extension (Fig. 22). It is probable that the addition of extra heat into the upper mantle was not confined exclusively to the Sarmatian, but errors introduced by this assumption are probably undetectable. Theoretical subsidence curves, initial conditions, uncertainty ranges, etc. were constrained in the same fashion as before.

The total magnitude of crustal extension ranged from β = 1.86-1.98 for wells 2-4 to β = 3.63-7.10 for well 6 (Fig. 23 and Tables IV and V). The magnitude of Sarmatian age crustal extension was roughly β = 1.6 for all wells. The amount of predicted uplift during Sarmatian extension was very sensitive to the relative rates of crustal and subcrustal extension. Since it is difficult to constrain the rate of attenuation of mantle lithosphere, we arbitrarily specified a maximum uplift of 200 m during Sarmatian time.

Except for the 2.0 and 5.0 Ma horizons in well 1 and the 8.0 Ma horizon in wells 8-9, predicted subsidence histories provide a reasonably good fit to corrected basement depths calculated from observations (Fig. 23 and Tables IV and V). Predicted thermal subsidence rates (8.0-0 Ma) determined by assuming a modified extension model were 2 to 3 times faster than those determined by assuming a uniform extension model, and reflect a proportionately greater heat loss from the crust and upper mantle. Predicted rates of thermal subsidence are not strongly dependent on present basement depth for the modified extension model (Tables IV and V), so that heat loss from the crust and upper mantle also appears not to be strongly dependent on present basement depth.

Predicted heat flow values, calculated as before, range from 95-103 mW/m^2 for wells 2-4 to 102-122 mW/m^2 for well 6. These values are in reasonably good agreement with observed heat flow values of 102 ± 11 mW/m^2. Predicted temperature gradients assuming a modified extension model are 50% to 100% higher than those predicted by assuming a uniform extension model, and are in fairly good agreement with observations (Fig. 24). Note that neither predicted temperature profiles, heat flow, nor rates of thermal subsidence determined by a modified extension model are strongly dependent on present basement depths. This is consistent with observation (Horváth et al., 1981; Pogácsás, Gy., 1980, unpublished data).

Predicted values of crustal thickness (including sedimentary rocks) are about 20-21 km (except for wells 1,6, and 7). These values are less than the 25-30 km determined by seismic refraction. However, this is probably within the uncertainty range of the refraction profiles.

Modified extension: Dévaványa and Vésztő

The subsidence history of wells at Dévaványa and Vésztő was analyzed in the same manner as before, except that Sarmatian age crustal extension was assumed to be equivalent to β = 1.66, coupled with severe attenuation of the lower lithosphere. Pannonian age extension was found to be equivalent to β = 1.28-1.48, so that total extension was β = 2.05-2.37, depending on density and compaction parameters used. Predicted depth-age relationships within the sedimentary column are in excellent agreement with observation (Fig. 25).

Discussion and Implications

From the analysis presented above, we conclude that the subsidence, temperatures and heat flow within the Pannonian basin are compatible with an extensional origin. However, many features of the evolution and thermal state of the Pannonian basin are not compatible with the assumption that extension occurred uniformly throughout the underlying lithosphere. A modified extension model, where additional heat is supplied to the upper mantle during extension, seems to provide a reasonable alternative. Matching of subsidence histories for all but the deepest well (well 6) in the Pannonian basin to theoretical extension histories gave the following results:

I) Uniform extension

1) Outside of deep troughs, predicted crustal thicknesses are 25-30 km, in good agreement with observation.

2) Predicted thermal subsidence rates, heat flow, and temperatures are lower than observed values by as much as a factor of two.

3) Predicted thermal subsidence rates, heat flow and temperatures vary systematically with present basement depths. Observations suggest little correlation.

4) No mechanism is provided to account for regional erosion and probable basement uplift between Sarmatian and Pannonian time.

II) Modified extension

1) Outside of deep troughs, predicted crustal thicknesses are 20-21 km, somewhat less than observed values of 24-28 km.

2) Predicted thermal subsidence rates and heatflow are in excellent agreement with observed values. Predicted temperatures are sometimes in excellent agreement with observation, but occasionally give values somewhat higher than observed.

3) Predicted thermal subsidence rates, heat flow, and temperatures are not strongly dependent on present basement depths. This is consistent with observation.

4) A mechanism is provided to account for regional erosion and probable basement uplift between Sarmatian and Pannonian time.

For highly extended (and deep) areas, the difference between the two types of extension is small because in either case the subcrustal lithosphere is highly attenuated. For moderately extended areas, the difference between the two is larger because in one case the lower lithosphere is severely attenuated, while in the other it is only moderately attenuated. This explains why the analysis of the shallowest wells was most useful in distinguishing between these two types of extension, while analysis of the deepest well (6) was not.

If the elevation of the Pannonian basin area is not assumed to be near sea level prior to extension, it would be possible to explain the thermal subsidence rates, temperatures and heat flow calculated from observations as the result of uniform extension by about β=3 to 4. However, the initial elevations required by the approach are: 3 to 4 km for wells 2-4 and 10-12, 2 to 3 km for wells 5 and 8-9, 1 to 2 km for wells 1 and 7, and near sea level for well 6. This implies an average regional elevation of more than 2 to 3 km for the Pannonian basin area prior to extension (see also Fig. 2), which is not compatible with sedimentological studies of Paleogene sediments within the Pannonian area (Báldi, 1982).

The uniform and modified extension models examined above are designed to simulate special cases of a broad spectrum of possibilities. By admitting a zone of decoupling at some arbitrary depth within the lithosphere we have introduced extra degrees of freedom into our system, and thus made it more difficult to constrain the magnitude of crustal extension within the Pannonian or other young basins. This means that it is not possible to determine the magnitudes of crustal extension within young basins from the age and total depth of these basins alone. Thermal

gradients and heat flow, rates of thermal subsidence, and regional geology all need to be examined in reasonable detail before the magnitude of crustal extension can be estimated in very young basins. This point will be reiterated in a later discussion of the Vienna basin.

The introduction of extra heat into the upper mantle beneath the Pannonian basin probably occurred at about the same time as basin extension. We believe that it occurred during and is related to basin extension, and suggest that it can account for periods of uplift observed during extension. The processes by which this was accomplished are unknown; heating could be related to the presence of an active subduction zone several hundred km distant, or it might be a more general feature of some extended areas. However, because heating (and attendant uplift) probably occurred within an interval of less than 10 m.y., heating was probably not accomplished by passive conduction of heat, which would be a slower, more gradual process. Therefore, heating probably involved active processes within the lower lithosphere, for example: erosion of the lithosphere from below, injection of magma from deep levels, non-uniform extension, or wholesale removal of lower lithospheric material.

Some of these proposed mechanisms involve obvious space problems. For example, extension of lower lithospheric material by a greater amount than upper lithospheric material has serious consequences for adjacent unstretched regions. Similar difficulties would be encountered during large-scale injection of magmatic material into the upper mantle or mechanical stripping of the lower lithosphere. In order to conserve mass, all of the processes listed above require active mass transfer, that is, removal of a part of the lower lithosphere and replacement by

asthenospheric material. Whether this is done via the coeval subduction zone in the Carpathians or in some other way is not apparent from our study of the intra-Carpathian basins. If, as we suspect, similar heating phenomena can be documented in other extensional basins which are not immediately adjacent to zones of coeval subduction, then: 1) heating is not related to subduction and may be a more general feature of extended terranes and 2) conservation of mass during heating must be maintained in some way other than by a subduction zone.

Heating seems to have occurred irrespective of the amount of local crustal extension. In fact, west of wells 10-12, heat flow measurements in areas with little or no Miocene to recent sedimentary cover yield values greater than 110 mW/m^2 (Horváth et al., 1981). Thus, although heating appears to be spatially related to extension within the Pannonian basin in a gross way, there is certainly not a one-to-one correspondence between crustal extension and the behavior of lithospheric rocks at depth. This suggests that beneath the Pannonian basin there is a transitional zone within the lithosphere which separates it into two parts: 1) an upper part characterized by extensional processes which can be observed at the surface, and 2) a lower part characterized by some unknown processes which are roughly coincident in space and time with surface extension.

At least one fundamental aspect of the evolution of the Pannonian basin has not been explained by the modified extension model proposed above. Although extensional features are evident in many of the other intra-Carpathian basins, and there is clear evidence for Karpatian-Badenian extension in some parts of the Pannonian basin, Pannonian age sedimentary rocks within the Pannonian basin are mostly

unfaulted, and show little evidence for Pannonian age extension. This suggests that extension was essentially completed prior to initiation of Pannonian age sedimentation. If so, then immediately after extension, water depths would have been around 400 to 800 m (difference between water loaded basement depths before and after Pannonian age extension). However, water depths of Pannonian age sediments were probably less than 100-200 m, and the transgressive nature of lower Pannonian age rocks suggests that these rocks were deposited near sea level. Thus, the rapid subsidence observed during Pannonian time does not appear to be accompanied by synchronous extension within the sedimentary rocks.

We have no satisfactory explanation for this phenomenon, but note that something similar has been observed in recently extended areas in the Basin and Range Province. Major extension is thought to have occurred along low-angle normal faults which may produce little topographic relief (see, for example, Anderson, 1971; Wernicke, 1981; and Zoback et al., 1981). Topographic relief probably developed subsequently by normal faulting along high-angle faults that cut the earlier low-angle faults. In some places, where faulting can be dated reliably, the time interval between low-angle and high-angle faulting seems to be a few million years (Zoback et al., 1981). A similar sequence of events may have occurred in the Pannonian basin, but this has not yet been documented.

DANUBE AND ZALA BASINS

Subsidence data for wells 13-23 were analyzed in light of both uniform and modified extension models as described above (Table VI and Fig. 26). Unfortunately, for many of these wells time horizons

between 0 and 8.0 Ma could not be determined. Therefore, comparison between observed and predicted rates of thermal subsidence is not very useful. Thermal phase subsidence rates obtained from dating of sediments at 8.0 Ma and the present are in better agreement with subsidence rates predicted by the modified extension model, but this is not conclusive evidence. The thermal phase subsidence rate for wells 18 and 19 determined from dating of sediments at 2.0 Ma and the present is probably not very useful either, because the thicknesses of Quaternary sediments in these two wells were very different (Fig. 11).

Observed heat flow in the Danube and Zala basins (73 ± 8 mW/m^2 and 88 ± 8 mW/m^2, respectively) is intermediate between that predicted by either model. Thus, until better subsidence data can be obtained, we tentatively conclude that during extension some additional heat may have been added to the lithosphere beyond that associated with uniform extension.

VIENNA BASIN

1) Tectonics

The Vienna basin is the most external of the intra-Carpathian basins and is superimposed partly on the flysch nappes of the outer Carpathians (Fig. 2). Extension began in the northwestern part of the basin with Ottnangian-Karpatian (19.0-16.5 Ma) faulting and subsidence. At about the end of Karpatian time extension ended in the northwestern Vienna basin and began in its southeastern part (Jiříček and Tomek, 1981). Major extension of the Vienna basin probably ended at about the Badenian-Sarmatian boundary (13.0 Ma). Its obvious rhombohedral shape and left-stepping en echelon pattern of faults suggest that it is a pull-apart feature associated with left-slip along a northeast trending

fault system (for example, Crowell, 1974). The migration of extension and subsidence observed in the Vienna basin is also characteristic of pull apart basins (see examples from Crowell, 1974).

The pull apart interpretation is consistent with geologic mapping by Z. Roth (1981, pers. comm.), which indicates roughly 50-100 km of sinistral displacement along a fault that trends northeast from the northern end of the Vienna basin (see also Krs and Roth, 1977, 1979). Fault plane solutions indicate left-slip along another high-angle fault which trends southwest from southern end of the basin (Gutdeutsch and Aric, 1976), but the relationship between recent seismic activity and Late Miocene tectonics is not entirely clear. Miocene strike-slip displacement on this fault has not been documented.

In the vicinity of the Vienna basin, as in the rest of the Eastern Alps-Carpathian chain, the end of thrusting migrated continuously from west to east. In the easternmost Eastern Alps thrusting ended during the Ottnangian. In the westernmost Carpathians (west of the Vienna basin) thrusting ended in Karpatian time, and far to the northeast (west of Krakow) thrusting ended during Badenian time (compare Figs. 2 and 6). This geometry implies that, during Karpatian and Badenian time, that part of the Carpathians that was northeast and east of the Vienna basin was translated generally northward relative to both the European plate and the inactive nappes in the external part of the Alps west of the Vienna basin. Relative motion may have occurred partly by left-slip along the northeast-trending fault zone described above. The timing and direction of displacement along this fault are in good agreement with those required to accomodate continued thrusting to the northeast. Thus extension of the Vienna basin, which resulted from

strike-slip motion along this boundary fault, is probably a consequence of diachronous crustal shortening in the outer Carpathians.

Because of the arcurate shape of the Carpathian mountain belt and the radial and diachronous nature of thrusting, shortening across the outer Carpathians requires considerable internal deformation of either the European foreland or the Pannonian hinterland. Crustal shortening in the Carpathians seems to have been accomodated mostly by transcurrent faulting and extension within the Pannonian fragment while the European plate has remained relatively undeformed (except for block faulting associated with downward bending beneath the Carpathian thrust belt and molasse). None of the Miocene high-angle (strike-slip?) faults observed in the Carpathians extend into the European foreland, and it is likely that many of these faults end against or merge into thrust faults. Because thrust faulting and high-angle faulting were synchronous, they were probably related. Thus it seems likely that many of these high-angle faults, especially those in the outer Carpathians, function partly as tear faults and merge into gently dipping detachment surfaces at depth, which are sub-parallel to the decollement surfaces for the overriding nappes (Fig. 27).

Because extension of the Vienna basin was probably related to synchronous left-slip along one of these faults systems, the nature of these strike-slip faults has important consequences for the crustal structure beneath the basin. If the northeast trending faults that extend through the Vienna basin merge into a gently dipping detachment horizon at depth, then it is likely that extension of the basin was restricted to shallow crustal levels above that detachment horizon. Thus extension of the Vienna basin may reflect thin-skinned tectonics within

the upper crust rather than significant extension of the entire lithosphere. We interpret the large faults that bound the Vienna basin to be listric faults that flatten towards the southeast and have both normal and left-slip components of displacement.

Drilling and reflection seismic data from the area of the Vienna basin are equivocal. The largest deep faults that bound the basin dip about 45° toward the southeast, and appear to flatten slightly with depth (Grill et al., 1968; Kröll et al., 1981; Wachtel and Wessely, 1981). It is not clear whether these faults involve autochthonous rocks of the European basement or flatten into a decollement surface at shallower depth. Block faulting of both Mesozoic and Miocene age has affected rocks of the European plate beneath the outer Carpathians, and in places it is difficult to tell if these faults are the same as extensional faults within and below the Vienna basin.

Thermal Analysis

The nature of Miocene extension within the Vienna basin and the structure of the crust beneath the basin should be reflected by the heat flow through the basin. If basin subsidence resulted from uniform extension of the entire lithosphere, then observed heat flow values should coincide roughly with predicted values determined by the methods outlined previously. If, on the other hand, the Vienna basin is the result of upper crustal extension only, then we might expect measured heat flow to be lower than values predicted by assuming uniform extension and roughly comparable to measured heat flow in the adjacent foredeep. Because standard heat flow determinations were available only from the northern part of the Vienna basin (Fig. 12c), and because standard heat flow determinations were also available for the

Carpathian flysch belt adjacent to the northern Vienna basin, we used a representative subsidence curve from the northern part of the basin (Jiříček and Tomek, 1981) to predict theoretical amounts of extension and theoretical heat flow values (Fig. 17).

We assumed that prior to extension and emplacement of flysch nappes, the European platform, which in part now underlies the Vienna basin, had crust 35 km thick and was near thermal equilibrium conditions (see above). Using values from Table III, we calculate that the heat flow through the European platform prior to extension was abour 50 mW/m^2. This is in reasonable agreement with measured heat flow values of 58±8 mW/m^2 and measured crustal thickness of 30-40 km in the European platform near the Vienna basin (Čermák, 1979).

In early Miocene time, the European basement beneath the Vienna basin was overridden by about 8 km of flysch and carbonate rocks of the outer West Carpathians and Eastern Alps (see cross sections in Kröll et al., 1981; Wachtel and Wessely, 1981; and others). About 2 to 5 m.y. after nappe implacement, extension and subsidence began in the northern Vienna basin. Therefore we assumed that 8 km of rocks at 0°C was instantaneously thrust over the European basement at 22 Ma, 3 m.y. prior to the beginning of extension. Neither the assumed temperature of the nappes nor the exact time of nappe emplacement had significant effect on subsequent calculations.

Three sets of calculations were made:

1) A predicted value for present heat flow in the flysch nappes and foredeep of the outer Carpathians was calculated using the assumptions above and assuming no subsequent extension occurred. The resulting value was 44 mW/m^2, slightly lower than observed values of

53 ± 7 mW/m^2 (average of 11 measurements, Fig. 12c).

2) Sedimentation data from the north Vienna basin was corrected for the effects of sediment loading and compaction (Table VII). Maximum, minimum and intermediate corrected subsidence histories were constructed from sedimentation data as before. These histories were then matched to extension parameters assuming uniform extension (Fig. 28 and Table VII) (β = 1.98-2.40), and assuming that extension occured at a constant rate during Ottnangian-Karpatian time (19.0-16.5 Ma). Predicted heat flow values determined from these extension parameters were about 64 mW/m^2 with an uncertainty range 56-67 mW/m^2, as compared to observed values of 50 ± 7 mW/m^2 (average of 9 measurements, Fig. 12c).

3) Corrected subsidence curves were used to determine amounts of Ottnangian-Karpatian subsidence using a modified extension model to approximate the effects of upper crustal extension above a detachment surface. We arbitrarily assumed that the detachment surface coincided with the base of the crust (at 43 km depth), and that no extension occurred below the crust. We calculated that the present corrected basement depth beneath the northern Vienna basin required crustal extension by β = 1.60-1.75 (Fig. 28 and Table VII). The predicted heat flow was 46 (44-47) mW/m^2, as compared to observed values of 50 ± 7 mW/m^2. If the detachment surface were placed at a higher level within the crust, larger values of β would be required, but the predicted heat flow would not be significantly different.

The predicted surface heat flow was depressed about 10-12% by the presence of the cold nappes on the European basement, and about 13% by deposition of cold sediments into the basin.

The observed heat flow values are intermediate between those predicted by the uniform and modified extension models. However, the differences between predicted and observed values are small enough that they could easily be the result of small errors in some of our assumptions (for example, radiogenic heat production within the crust). Perhaps more significant is the ratio of heat flow within the basin to that of the foredeep area and Bohemian massif. Observed heat flow within the basin (50 ± 7 mW/m^2) is roughly the same as observed heat flow in the unextended nappe-foredeep area (53 ± 7 mW/m^2), and slightly lower than observed values in the adjacent part of the Bohemian massif (58 ± 8 mW/m^2. Assuming crustal extension only, we predict heat flow within the basin, 46 (44-57) mW/m^2, to be roughly the same as that in the foredeep, 44 mW/m^2, and also roughly the same as, but lower than, that in the adjacent European plate, 50 mW/m^2. In contrast, predicted heat flow within the basin, assuming uniform extension, is 64 (56-67) mW/m^2. This is 25% to 50% higher than that predicted for adjacent foredeep and nappes, and about 15% to 30% higher than that predicted for the Bohemian massif. This is not compelling evidence in favor of upper crustal extension only beneath the Vienna basin. It does, however, indicate that heat flow within the Vienna basin is not elevated above that of the surrounding area. This is not consistent with uniform lithospheric extension beneath the Vienna basin, but is consistent with thin-skinned extension of upper crustal rocks only.

It should also be noted that the (observed) thermal subsidence (16.5-0 Ma) in the northern part of the Vienna basin has been rather slow (about 100 m, Figs. 17 and 28). In fact, if a correction is added for the present elevation of the basin surface above sea level (~200 m), the

corrected basement depths indicate uplift by about 100–200 m since the end of the Karpatian time. This is not really consistent with the hypothesis that the Vienna basin is the result of uniform lithospheric extension, and therefore associated with initially elevated temperatures at depth. It is, however, consistent with the interpretation that the Vienna basin is the result of thin-skinned extension in the upper crust, possibly superimposed on a region that is being uplifted slowly. It should be remembered that neither flexural effects nor horizontal conduction of heat have been considered in these calculations.

On the basis of the data presented above, we interpret the Vienna basin to be the result of surficial extension within the upper crust. No space problem is implicit in this interpretation, because upper crustal extension can be accommodated by northeastward transport of nappes in the outer Carpathians. Thus, in the Vienna basin, as well as in the Pannonian basin, upper crustal processes may not directly reflect deformation occurring at depth. In most other respects, however, these basins are dissimilar.

One of the special aspects of the Vienna basin and other intra-Carpathian basins is that they preserve many features of Miocene extensional and translational events in an early stage of development. For example, pull apart basins along the San Andreas fault have had complicated histories, with many superimposed phases of extension and compression (for example, Crowell, 1974). In contrast, the Vienna basin formed during a short phase of extensional faulting, after which tectonic activity ceased almost completely. In this respect the Vienna basin and some of the other intra-Carpathian basins may represent ideal areas in which to study the evolution of simple pull apart structures.

THE TRANSCARPATHIAN BASIN

We interpret the Transcarpathian basin, in the northeastern part of the intra-Carpathian region (Fig. 2) to be the result of processes similar to those within the Vienna basin. Its rhombohedral shape, the north to south migration of areas of subsidence within the basin, and the orientation of high-angle (strike-slip?) faults adjacent to the basin suggest a pull apart origin for this basin as well. Because this basin is superimposed on a more internal part of the thrust belt than is the Vienna basin, it is probable that extension of this basin affected rocks to much greater depths than that of the Vienna basin. We did not make a thermal analysis of extension within Transcarpathian basin because thermal gradients are probably perturbed by large amounts of arc volcanism beneath and adjacent to the basin.

THE TRANSYLVANIAN BASIN

Although its age, size and depth are superficially similar to those of the other intra-Carpathian basins, the Transylvanian basin is unusual in several respects. It is underlain by crust of approximately normal thickness (30-37 km) and its 3 to 4 km of mostly marine to brackish water Miocene sedimentary rocks fill a regular, saucer-like depression that is not cut by major faults (Ciupagea et al., 1970) (Fig. 2). Therefore, it seems unlikely that this basin is extensional in origin. Because of Quaternary uplift, surface elevation of the Transylvanian basin is now approximately 400-500 m, whereas the other basins have surface elevations ~100 m above sea level. Uplift and erosion is not confined to the Transylvanian basin, but also affects the surrounding areas including the southern East Carpathians and the adjacent part of the South Carpathians (M. Săndulescu, 1981, pers.

comm.). If erosion continues until the surface of this basin is reduced to sea level, the principle of isostasy predicts that 2 km of sediment will be eroded and that about one km of Miocene sediment will remain in the basin. This suggests that whatever forces produced the Miocene subsidence of the Transylvanian basin (amplified by loading effects of the sedimentary rocks), they were transient dynamic forces and no longer active.

Observed heat flow within the Transylvanian basin is 42 ± 10 mW/m^2 (Demetrescu, 1978, average of 5 standard heat flow measurements). One additional measurement of 74 mW/m^2 (Veliciu et al., 1977) was not used in this study because thermal conductivities were determined by the needle probe transient method and no corrections were applied. In contrast, 38 conductivity measurements used for the other 5 heat flow determinations were made using a divided bar apparatus, and conducted on samples saturated with water, oil, and air (Demetrescu, 1977). Furthermore, temperature measurements by Veliciu et al. (1977) were make over a 300 m interval, while those of Demetrescu (1977) were made over depth intervals from 900 to 3000 m. We therefore regarded the heat flow determination of Veliciu et al., (1977) as less reliable, and did not include it in calculating average heat flow through the basin.

In order to test whether the observed heat flow through the Transylvanian basin is compatible with a non-extensional origin for the basin, we calculated the heat flow which would result if the sediments of the Transylvanian basin had been deposited onto unextended lithosphere at equilibrium thermal conditions (Table VII). Predicted heat flow was 42-43 mW/m^2, in good agreement with observed values. For the sake of comparison, we calculated the predicted heat flow through the basin

assuming that basin subsidence were the result of uniform lithospheric extension (see previous sections and Table VII for details). The resulting values (51-60 mW/m^2) were somewhat higher than those observed. Thus, while heat flow measurements and predicted heat flow values are probably not accurate enough to be diagnostic of a non-extensional origin for the Transylvanian basin, they are consistent with this interpretation.

TECTONIC INTERPRETATION AND PALINSPASTIC RECONSTRUCTION

Because of the arcuate shape of the Carpathian mountain belt, the radial and diachronous nature of thrusting, and the relative rigidity of the European plate, shortening across the outer Carpathians requires considerable deformation of the Pannonian fragment. Deformation seems to have occurred by extensional and strike-slip faulting (Fig. 7 and preceding sections). Many of these strike-slip faults can be thought of as transform boundaries which connect areas of extension within one basin to areas of extension within other basins (Fig. 7). Other faults connect areas of extension to areas of compression and shortening in the outer Carpathians, such as the fault system north of the Vienna basin (Fig. 26). In the most external parts of the Carpathians, deformation may be confined to shallow crustal levels, and may not significantly involve autochthonous rocks of the European plate. In more internal areas it seems likely that these zones of deformation extend through the lithosphere of the Pannonian fragment; thermal and subsidence data from the Pannonian basin suggests considerable heating and attenuation of subcrustal rocks.

The style of deformation within the Pannonian fragment could be thought of as a system of semi-rigid and poorly defined microfragments

separated by zones of more intense deformation (Fig. 7). This is analogous, on a smaller scale, to the overall tectonic style of Cenozoic deformation in the Eastern European Alpine system. At both scales, fragment boundaries can be defined as the most prominent faults in continuously deforming crust. Definition of fragment boundaries is largely subjective and partly a matter of convenience. Another basic similarity between these larger scale and smaller scale tectonic systems is the style of repeated suturing and disruption of fragments, as well as the replacement of one type of tectonic boundary by another. For example, in Oligocene time, the previously convergent boundary along the Eastern Alps was replaced by a zone of horizontal dextral shear located south of the former thrust front (Fig. 5). This strike-slip zone might be defined as a transform boundary which connected areas of synchronous crustal shortening in the Western Alps and southern Dinarides and Hellenides. By analogy, the previously convergent boundary in the outer Carpathians north and west of the Vienna basin, was, at about Karpatian time, replaced by a left-slip boundary localized along a fault or faults in the outer Carpathians. This left-slip fault system might also be defined as a transform boundary connecting a zone of compression in the northern Carpathians with a zone of synchronous extension in the Vienna basin, and probably connecting with the peri-Adriatic fault system.

Based on this interpretation of the Pannonian fragment as a system of semi-rigid blocks bounded by zones of greater deformation, we made a series of palinspastic reconstructions from the beginning of Karpatian time until present (Fig. 29). The method used was roughly analogous to that used for major plate reconstructions, and fragment boundaries were identified as: (1) extensional (basins), (2) convergent (thrusts and

folds in the outer Carpathians), or (3) transform boundaries (strike-slip faults and more diffuse shear zones). The main difficulties encountered in attempting to make "tectonic" reconstructions at this scale were: (1) The division between a "block" and a zone of deformation was often ambiguous because all blocks may have been subject to some internal deformation and (2) the direction of crustal extension was not always clearly defined.

This palinspastic reconstruction concerns only relative motions of upper crustal rocks, so that the behavior of the lithosphere at depth is irrelevant except in so far as it effects our estimates of crustal extension. Total crustal extension for most of the areas examined above was between about 50% (β = 1.5) and 200% (β = 3). For simplicity, we assumed that each basin (except the Transylvanian basin) extended by 100% (β = 2). The uncertainty in surface area occupied by each basin prior to extension is less than about ±30% due to this approximation. A more rigorous approach is probably unwarranted because uncertainties in estimating the present size of the extended areas and the direction of extension are also fairly large.

Because there was a major shift in the locus of extensional activity and subsidence from Ottnangian-Karpatian time (19.0-16.5 Ma) to Pannonian time (10.5-8.0 Ma), palinspastic reconstructions were made for three different times: The beginning of Karpatian time (17.5 Ma), the beginning of Badenian time (16.5 Ma), and the beginning of Sarmatian time (13.0 Ma). The age of extension for some basins was estimated from the ages of extension given above. For those basins not treated explicitly in this paper, (Sava, Drava, Transcarpathian and westernmost Zala basins), ages of extension were estimated by comparing

sediment thicknesses and structures with those of the other basins (see below for details).

During each time section, extension was accomodated by strike-slip motion along the major fault zones shown in Fig. 7, and ultimately by compression and shortening across the outer Carpathian flysch belt. The magnitudes of displacement are those required to close the relevant basins during the appropriate time intervals. The direction of displacement was determined by the trend of the strike-slip faults which connect the basins to one another and to the outer Carpathian thrust belt. Reconstructions for each phase of extension were developed by working backwards from the present. Although presented in chronologic order from oldest to youngest, reconstructions at each time are dependent upon those of each younger phase. Only those areas of extension, compression, and transcurrent faulting which have been identified or inferred from field studies are shown in Fig. 29. We realize that other structures not shown in Fig. 29(a-c) are needed to complete fragment boundaries (see below).

1) Beginning of Karpatian Time (17.5 Ma)

Karpatian extension occurred primarily in the northern Vienna and Transcarpathian basins (Fig. 29a). Because accurate ages for the oldest Miocene sedimentary rocks in the Sava and Drava troughs were not available, it is possible that Karpatian extension also occurred in these basins. During Karpatian time extension was accommodated by left-slip along a northeast trending fault system north of the Vienna basin, and probably also by right-slip along a northwest trending fault system in the vicinity of the Transcarpathian basin (along the Pienniny Klippen belt). Reconstruction of the basins shows Karpatian shortening

in the outer Carpathians (shaded area) from just east of the Vienna basin eastwards through the northern part of the East Carpathians. This reconstruction also shows the outer flysch belt to have been about 300 km wide in the East Carpathians.

2) Beginning of Badenian Time (16.5 Ma)

During Badenian time the locus of extension moved southward to the southern Vienna and Transcarpathian basins, the west Danube lowland, the Zala basin, the central (and now deepest) part of the Pannonian basin, and also occurred along the Sava and Drava troughs (Fig. 29b). According to this reconstruction, Badenian age shortening occurred from the central part of the West Carpathians eastward to the East Carpathian bend. Thus the area of active thrusting appears to have migrated to the east relative to Karpatian time (see also Fig. 6). Relative fragment motions required by basin extension and the orientation of the major fault zones seem to be associated with an east-west trending zone of dextral shear located south of the Pannonian (and Transylvanian) area and north of the Moesian platform. However, if a major fault zone existed here, it is now buried by the thick Upper Miocene and Pliocene molassic deposits of the South Carpathian foredeep.

3) Beginning of Sarmatian Time (13.0 Ma)

By Sarmatian time, the areas of major extension had moved still farther south into the main part of the Danube lowland, the Zala basin, and the Pannonian basin. The Sava and Drava troughs, along the continuation of the peri-Adriatic line, appear to have been still active during the Sarmatian (Fig. 29c). At this time shortening appears to have been confined almost exclusively to the East Carpathians (Fig. 5) with an assumed zone of dextral shear active between Moesian and the intra-Carpathian area.

This palinspastic reconstruction, based on closing up the intra-Carpathian basins, shows a west to east migration of crustal shortening in the outer Carpathians. This is consistent with the west to east migration of thrusting determined directly from geologic study of the thrust belt (see, for example, Mahel et al., 1968; Jiříček, 1979; Săndulescu et al., 1981; and others) and also with related west to east migration of arc volcanism (Fig. 2).

West to east migration of thrusting around the Carpathians is also consistent with the paleogeographic evolution and paleontologic evidence for environments of deposition in the outer belt of the Carpathians (Steininger and Rögl, 1979 and Steininger, 1980, pers. comm.). Emergence of the belt occurred first in Karpatian and early Badenian time in the central West Carpathians. The emergent area gradually extended to the east, so that by Sarmatian and Pannonian time the East Carpathians were also emergent. At the same time as these areas became emergent, they began to shed sediments into the subsiding intra-Carpathian basins. It seems likely that the uplift of the outer flysch Carpathians resulted from crustal thickening by the emplacement of the thrust complex onto the continental crust of the European plate. Thus the pattern of uplift probably also reflects eastward migration of thrusting along the Carpathian chain.

Figure 29d shows the displacements of different parts of the intra-Carpathian area relative to stable Europe from the beginning of the Karpatian until present. Arrow heads indicate present position, and tails the estimated pre-Karpatian position. A subjective estimate of the uncertainties in the displacement vectors is about ±50% in length and perhaps ±20° in direction. The magnitude of displacement,

shown by the length of the arrows, increases from west to east, reflecting extension across the intra-Carpathian area. Some eastward translation of crustal fragments west of the Sava and Drava troughs was found in these reconstructions, but this might be a consequence of using rigid plate tectonics on non-rigid blocks. Estimates of displacement for areas west of the Sava trough do not include the large amounts of dextral shear inferred between Apulia and the Pannonian fragment, because this motion is totally unconstrained by movements within the Pannonian region.

The calculated eastward displacements in Fig. 28d indicate 120 ($\pm$60) km of Badenian-Sarmatian convergence across the Eastern Carpathians. Direct reconstruction of shortening in the Eastern Carpathians from geologic cross-sections yields a minimum estimate for total Miocene shortening of 116 km (Fig. 30, Burchfiel, 1976). More recent work in Romania now suggests Badenian and Sarmatian ages for the major overthrusting of the three outer nappes within the East Carpathians (Tarcau, Marginal Folds and Sub-Carpathian nappes; Sǎndulescu et al., 1981). From the cross section shown in Fig. 30, it seems that emplacement of these nappes must involve a minimum of 50 km shortening, but it is difficult to estimate the accuracy of this cross section in the subsurface. The amount of material lost by erosion and hidden in the subsurface between nappes and digitations, could easily bring the amount of shortening in the thrust belt into agreement with the amount of shortening estimated from closing up the basins. These estimates of shortening are also consistent with the inferred presence of a steeply dipping slab to 140 km depth beneath the southern East Carpathians (Roman, 1970).

In each of the three reconstructions in Fig. 29, we found that in the central part of the outer West Carpathians significant extension (locally 50%?) parallel to the strike of the mountain belt was necessary to complete fragment boundaries in a consistent fashion. This part of the belt has the smallest radius of curvature in the West and East Carpathians. Thus, as units were thrust from a more internal to more external position, the total length of the belt increased, so that rocks within the nappes must have extended along strike to accommodate this increase. However, such extensional features have not been documented from field studies, and so have not been shown in Fig. 29.

In summary, the generally north to south and west to east migration of areas of extension within the intra-Carpathian region in the late Miocene is consistent with the west to east migration of thrusting around the outer Carpathian belt. Even over the short time intervals examined here, areas of extension seem to have moved in connection with areas of synchronous crustal shortening. Extension of at least one basin (Vienna basin) may have involved only thin-skinned extension above a detachment horizon. Extension of other basins seems to have involved the entire lithosphere. However, in all cases, extension was the result of differential motion between crustal blocks related to diachronous shortening around the irregularly shaped outer Carpathian belt.

The magnitude of east-west extension across the intra-Carpathian areas from the beginning of Karpatian time until present (120±60 km) seems to be roughly comparable to the amount of synchronous east-west crustal shortening across the East Carpathians. This suggests a source-sink relationship for tectonic deformation within the Pannonian fragment in late Miocene time.

DISCUSSION AND SPECULATIONS

The spatial and timing relations between crustal shortening in the outer Carpathians and extension within the intra-Carpathian basins suggest that the two phenomena are related and that they are probably the result of a single dynamic system. This source-sink relationship between areas of extension and areas of crustal shortening is consistent with the interpretation that during late Miocene time the Carpathian-intra-Carpathian area functioned as a "closed" system (see below). To the west, in the Eastern Alps and westernmost West Carpathians, and to the south, in the South Carpathians, convergence had ceased by late Miocene time. To the southwest, the intra-Carpathian area was bounded by the transcurrent peri-Adriatic-Vardar fault system. Although hundreds of kilometers of late Miocene dextral shear probably took place on this fault system, the general location of the fault system probably remained mostly unchanged with respect to Europe and Moesia (Fig. 5). To the north and east, the Carpathian area is bounded by the European foreland itself. Thus it is possible to encircle the Carpathian-intra-Carpathian system by a boundary accross which there was little movement of crustal material in late Miocene time (Fig. 5). This implies that late Miocene crustal shortening within the Carpathians must have been mostly compensated by crustal extension within the intra-Carpathian area, and vice versa.

One mechanism which has been suggested to link thrusting with synchronous extension is gravitational collapse of a central dome in the Pannonian area. However, the average elevation of the Pannonian area was probably no more than a few hundred meters above sea level in Miocene time, so that the amount of gravitational potential energy

available to drive this system was minimal. Many parts of the
Carpathian mountains became emergent during thrusting, at the same time
as the basement under extending basin areas subsided to depths of
several km. This implies that the system was gaining, rather than
losing, potential energy. Furthermore, initiation of thrusting preceeded
initiation of extension by about 10 my, which suggests that thrusting is
not the result of extension.

Another possibility, and the one we favor, is that both thrusting
and extension were the result of continued subduction of the European
plate, probably driven by negative buoyancy of the subducted slab.
Because the position of the peri-Adriatic-Vardar fault system was roughly
fixed with respect to Europe, subduction of European crust and lower
lithosphere required corresponding extension of the crust and lower
lithosphere of the Pannonian fragment (Fig. 31). Thus extension of the
intra-Carpathian basins occurred as Pannonian lithosphere moved eastward
to fill the space originally occupied by the European plate, while the
western edge of the Pannonian fragment remained fixed with respect to the
peri-Adriatic-Vardar fault system and the European foreland (Fig. 31).
This geometry implies migration of the subduction zone towards the
European foreland, possibly accompanied by steepening of the subducted
slab, as seismic data suggest that it is now in a nearly vertical
position (Fuchs et al., 1979).

We suggest that late Miocene subduction in the Carpathian region
resulted in widespread extension, and that thrusting occurred as light
sedimentary rocks, originally deposited on the European plate, were
involved in simple shear at the subduction boundary (Fig. 31). Shear
appears to have been localized along west dipping thrust planes located

within the sedimentary cover of the European plate, so that sedimentary rocks above the detachment surface were accreted to the over-riding Pannonian fragment. During subduction, new detachment planes were created external to the old detachment planes, and sedimentary rocks were stacked into a series of imbricate thrust slices in the outer Carpathians. We suggest that late Miocene thrusting in the outer Carpathians was only a thin-skinned, superficial phenomenon that occurred as buoyant sedimentary rocks were scraped off the European plate during subduction, rather than a direct response to large scale crustal shortening that extended far beyond the fragment boundary.

Thus, extension of the Pannonian fragment may have been a widespread response to continued subduction of the European plate and migration of the subduction zone towards the European platform, while the western and southern boundaries of the Pannonian fragment remained fixed with respect to Europe (Fig. 31). In contrast, thrusting may have been a local response to simple shear between the overriding and subducted plates near the subduction boundary. In this way, both thrusting and extension can be explained as the result of a single dynamic system operating at depth.

We suggest that the (temporary?) subsidence of the Transylvanian basin during Badenian to Pannonian time may be the result of dynamic loading from below during subduction (Fig. 31). Loading may have occurred in response to sinking of the European plate into the asthenosphere beneath the basin, or possibly to thickening of the lithosphere beneath the basin (because of eastward flow from beneath the Pannonian basin) (Fig. 31). Recent uplift of the Transylvanian basin and adjacent mountains may be the result of unloading as the subducted slab

(and possibly thickened lithosphere beneath the basin) became detached from the overlying plate. Seismic data also suggests that the subducted slab beneath the Eastern Carpathians may be discontinuous (Fuchs et al., 1979). Perhaps this scenario can explain why the age of early basin subsidence within the Pannonian and Transylvanian basins are similar, although the mechanisms are very different.

Our study suggests that the outer fold and thrust belts in the Eastern European Alpine system may have two fundamentally different tectonic settings. In one, the thrusting is a response to overall plate convergence that can create shortening and compression through much of the lithosphere for considerable distances from the plate boundary. In the second, the thrusting is primarily a result of simple shear at the plate boundary with very restricted compression; the overriding plate may be extending only a short distance from the thrust belt. The Eastern Alps might be an example of the first type, where convergence between Apulia and Europe generated shortening and elevation of the northern margin of Apulia across a broad zone from the northern border of the Austrian Alps to the northern border of the Po Basin. The outer Carpathian thrust belt is an example of the second case where shortening and thickening of the crust occurred along a narrow belt in the Carpathians contemporaneously with extension and subsidence of the intra-Carpathian region.

The earliest Miocene thrusting along the outer Carpathians was probably also of the first type, because it seems likely that subduction was initiated by regional compression accross the outer Carpathians. At some time after the initiation of thrusting in the outer Carpathians, deformation of the Pannonian fragment changed from mainly compressional

to mainly extensional. The appropriate question is: What controlled the shift from regional compression to regional extension within the Pannonian fragment?

We believe that the controlling factor was the relative movement between the larger Apulian fragment and stable Europe. In late Oligocene-earliest Miocene time, north-south convergent motion between Apulia and Europe probably resulted in the formation of the Pannonian fragment boundaries and in eastward and northeastward displacement of the Pannonian fragment relative to Europe, thus causing shortening across the Eastern Carpathians (Fig. 5). Later, the relative motion between Europe and Apulia was taken up by dextral shear along a large transcurrent fault zone extending through the Eastern Alps to the Hellenides (Fig. 5). This change in boundary activity roughly coincided in time with the initiation of extension in the intra-Carpathian area. We suggest that this change in fragment boundary activity coupled with continued subduction of the European plate was directly responsible for the shift from regional compression to regional extension within the Pannonian fragment, and that the initiation of extension within the Pannonian fragment was a direct response to the changing motion between Europe and Apulia.

The two types of thrust belts postulated here, which are probably only end-members of a broad spectrum of thrust belt types, are so similar at the surface that they have not been distinguished on the basis of their surface characteristics. At present, the only obvious criterion would be the presence of extensional or compressional features across a broad area internal to the thrust belt. We offer two speculations about the nature of these belts. First, that most thrust

belts and subduction zones begin as a response to overall plate

convergence. Second, that during collision of continental crust, thrust

belts associated primarily with compressional tectonic features often

imbricate and deform rocks at deep crustal levels (for example, the

Western to Eastern Alps, the southern Dinarides and northern Hellenides,

the thrust belts in eastern Turkey, and possibly the Betic Cordillera).

In contrast, those belts associated with back-arc extensional features

seem to involve imbrication and thrusting of sedimentary cover only (for

example, the outer Carpathians, the central and southern Apennines, the

Aegean arc, and the Cenozoic thrust belt of north Africa).

Finally, we believe that this study gives some insight into the

difficulties in reconstructing older Mesozoic events in the Eastern

European Alpine system. Mesozoic events in this region involved more

continental fragments and considerably more intense deformation than did

late Cenozoic events (Burchfiel, 1980). Yet Mesozoic events involved the

same type of repeated disruption and suturing of fragments, and at any

given time fragments displayed an intricate system of active faults in a

continuously deforming continental crust. Thus the complexity of

Mesozoic events in this region was probably much greater than that of

recent events, and many of the details of Mesozoic deformation have been

lost or obscured by the passage of time and by subsequent deformation.

It seems likely that some aspects of the early evolution of the Eastern

European Alpine system can never be fully reconstructed, and many other

aspects may have to be inferred from analogy with younger, better

understood, and more tightly constrained tectonic systems of a similar

type.

Conclusions

Surficially the intra-Carpathian area is a broad low-lying region, but structurally it is comprised of small distinct basins filled with Neogene and Quaternary sedimentary rocks. These basins were regions of late Miocene extension and are connected to one another and to areas of coeval shortening in the outer Carpathians by a system of strike-slip faults or fault zones. In general, sinistral northeast trending and dextral northwest trending sets of conjugate shears reflect overall east-west extension of the intra-Carpathian region during the late Miocene.

Quantitative analysis of sedimentation and thermal data indicates that crustal extension beneath most parts of the Pannonian basin was probably 85% to 170% (β = 1.85 to 2.70), although in the deepest parts of the basin (deeper than 4 km) crustal extension may have been much more. Our analysis indicates that, at about the same time as extension occurred, large amounts of heat were introduced into the uppermost mantle, and that this heat cannot reasonably be accounted for by assuming that extension occurred uniformly throughout the lithosphere. We believe that this extra heat was supplied to the uppermost mantle during, and is related to, extension and that this phenomenon can explain the apparent periods of basement uplift during extension. The processes by which heat was added are unknown.

We interpret the Vienna basin, which is superimposed partly on the flysch nappes of the outer West Carpathians, as the result of thin-skinned extensional tectonics above a shallow detachment surface within the upper crust. Extension of upper crustal rocks above this detachment was probably compensated by thrusting of the outermost nappes

of the West Carpathians over the European platform. Subsidence and
themal data from the Vienna basin support this interpretation.

Extension within the Danube and Zala basins seems to have involved
the entire lithosphere, possibly with the introduction of extre heat into
the upper mantle. The Transylvanian basin does not appear to be
extensional in origin and may be the result of temporary loading from
below during subduction. Heat flow data from the Transylvanian basin are
consistent with this interpretation.

Extension within the intra-Carpathian basins was not synchronous and
may be divided into three primary periods: Karpatian (17.5-16.5 Ma),
Badenian (16.5-13 Ma) and Sarmatian (13-10.5 Ma), probably extending into
early Pannonian time. Karpatian extension affected the north Vienna and
north Transcarpathian basins, and the locus of extension migrated
generally southward and eastward with time. Badenian extension was
dominant in the south Vienna and Transcarpathian basins, and affected the
Danube basin, and parts of the Zala, Sava, Drava and Pannonian basins.
Sarmatian and Pannonian age extension was responsible for most of the
subsidence of the east Danube and Pannonian basins.

Palinspastic reconstruction of the basins prior to each of these
periods of extension predicts eastward migration of the zone of thrusting
and shortening within the Carpathian mountains to accomodate eastward and
southward migration of areas of extension. This is consistent with the
eastward and southward migration of the last major thrusting and folding
event as determined directly from rocks within the thrust belt. From
these reconstructions we estimate about 120 (±60) km of east-west
shortening across the outer East Carpathians from the beginning of
Karpatian time until the present. This figure is consistent with

estimates of shortening based on direct reconstruction of nappes in the thrust belt. From this we infer a source-sink relationship for late Miocene extension of the intra-Carpathian region and late Miocene crustal shortening within the outer Carpathians.

We conclude that during late Micene time, deformation of the Pannonian fragment was dominated by extensional tectonics, except along a narrow zone in the outer Carpathian thrust belt. Late Miocene thrusting in the Carpathians is interpreted as the result of simple shear caused by relative motion between Europe and the overriding Pannonian fragment at the subduction boundary, rather than of regional compression of lithospheric rocks at depth. In this way, buoyant sedimentary rocks originally deposited on the European plate could have been stripped from the downgoing European basement and stacked into a series of imbricate slices without widespread compression and crustal shortening extending far beyond the fragment boundaries. Overall compression of lithospheric rocks at depth would not have been necessary to cause imbrication of sedimentary cover, and thus the proximity of an active thrust belt to areas of coeval extension can be easily explained. The initation of extensional tectonics within the intra-Carpathian region was probably the direct result of reorganization of major fragment boundaries of the Eastern European Alpine system in late Oligocene-early Miocene time.

Three fundamental conclusions suggested by our work may be relevant to studies of other sedimentary basins. First, a fundamental difference does, or at least can, exist between the behavior of upper crustal and lower lithospheric rocks during extension. A one-to-one correspondence should not necessarily be expected between the magnitude, style, and spatial distribution of crustal and sub-crustal deformation. Second,

sedimentary basins can be created by a variety of mechanisms. Even within the small intra-Carpathian area there appear to be at least three distinctly different types of basins, with similar ages and depths. An understanding of the mechanisms of basin formation is critical to incorporation of any basin within its regional tectonic setting. Third, Miocene shortening in the outer Carpathians and development of several different types of basins can probably be tied together within a simple mechanical framework. In this paper we have tried to reconcile several different types of coeval tectonic activity within a simple dynamic system. It seems likely that similar studies may be equally useful for the understanding of other young tectonic systems.

APPENDIX

I) Temperature Calculation (one dimensional)

Under thermal equilibrium conditions, the temperature profile within the lithosphere may be written:

$$T(x) = T_a(x/\ell) + T^R(x) \qquad \text{1a}$$

where x is measured downwards from the surface and T^R is the contribution from radiogenic heat sources. If the radiogenic sources are assumed to be concentrated at a plane source with magnitude Q_R and depth d, then:

$$T^R(x) = (Q_R/K) ((1-d/\ell)x - (x-d) H(x-d)) \qquad \text{2a}$$

where:

$$H(x) = \begin{cases} 0 & x < 0 \\ 1 & x > 0 \end{cases}$$

(See Table III for symbols not explained in appendix). In this study d was assumed to be 8 km. If all radiogenic sources are located within the upper crust (shallower than 20 km), then the maximum error in surface heat flow due to assuming that all heat sources are concentrated at 8 km depth is about 10% of the total heat flow from radiogenic sources. Because uncertainties in the total contribution of radiogenic sources to surface heat flux are much larger, a plane source should be a sufficient approximation to a more realistic distribution of heat sources.

The temperature structure within an extending lithosphere can be approximated as follows. Suppose that over a fixed time, t, the crust extends at a constant rate by a percentage β^c, and the subcrustal

lithosphere by β^a. Dividing the total time, t, into small increments, Δt, extension may be assumed to take place instantaneously at the beginning of each time increment. The percent extension which occurs during the ith time increment is:

$$\beta_i = \frac{\Delta t \cdot (\beta-1)}{t + (i-1) \cdot \Delta t \cdot (B-1)} + 1 \qquad 3a$$

Immediately before the ith episode of extension, let the temperature profile be given by $T_{i-1}(x, \Delta t)$ and the crustal thickness by y_{i-1}. Then the crustal thickness after extension is:

$$y_i = y_{i-1} / (\beta^c)_i$$

The temperature immediately after extension is:

$$T_i(x,0) = \begin{cases} T_{i-1}(x \cdot (\beta^c)_i , \Delta t) & x \leqslant y_i \\ T_{i-1}(x \cdot (\beta^a)_i + y_i \cdot ((\beta^c)_i - (\beta^a)_i), \Delta t) & x \geqslant y_i \end{cases} \qquad 4a$$

If, in addition, an amount of sediment s_i is added during the ith time interval, we readjust the temperatures by:

$$T_i(x,0) = \begin{cases} 0 & x \leqslant s_i \\ T_i(x-s_i, 0) & x \geqslant s_i \end{cases} \qquad 5a$$

Because a plane source was used to approximate an arbitrary distribution of radioactive elements within the crust, the depth and magnitude of the plane source must decrease proportionally to the decrease in total thickness:

$$(Q_R)_i = (Q_R)_{i-1} / (\beta^c)_i$$

$$d_i = d_{i-1} / (\beta^c)_i$$

6a

The temperature at the end of the ith time interval in given by:

$$T_i(x, \Delta t) = T^R_i(x) + \sum_{n=1}^{\infty} c_n \sin(n\pi x/\ell) \, e^{-n^2 \pi^2 \kappa \Delta t/\ell^2}$$

7a

where:

$$T^R_i(x) = ((Q_R)_i/K) \, (1-d_i/\ell)x - (x-d_i) \, H(x-d_i))$$

8a

$$c_n = (2/\ell) \int_0^a \sin(n\pi x/\ell) \, (T_i(x,0) - T^R_i(x)) \, dx$$

(For further details, see Carslaw and Jaeger, 1959, p. 93-94). The coefficients in equation 8a can be determined by numerical integration. If these steps are repeated iteratively beginning with equation 4a then the accuracy of this method depends mainly upon the size of the time step chosen. In this study Δt was chosen to be 0.5 my.

One complication is that the thermal condictivity within the sediments, K_{sed}, is not generally equal to the conductivity of crustal rocks, K, and usually varies with depth. This difficulty may be circumvented by using an effective sediment thickness, s_e, which is related to the true sediment thickness, s, by:

$$s_e = K \int_0^s \frac{dx}{K_{sed}(x)}$$

9a

where $K_{sed}(x)$ is the themal conductivity of sediments as a function of depth. If the conductivity in the sediments can be written as:

$$K_{sed} = K_o + bx$$

Then:

$$s_e = K \ln (1 + sb/K_o) / b$$

10a

It should be noted that this substitution gives only an approximation to exact temperature structure because the time constant of the sedimentary layer is increased by (s_e/s) by the substitution in Eq. 10a. However, for sediment thicknesses less than about 8 km, with thermal conductivities as shown in Fig. 18, the temperature differences are undetectable after 1 to 2 million years.

REFERENCES

Ádám, A., Horváth, F. and Stegena, L., 1977. Geodynamics of the Pannonian basin: geothermal and electromagnetic aspects: Acta Geol. Acad. Sci. Hung., v. 21, p. 13-17.

Ádám, A. and Wallner, Á., 1981. Information from electromagnetic induction data on Carpatho-Pannonian geodynamics: Earth Evolution Sci., v. 1, no. 3, in press.

Anderson, R.E., 1971. Thin skin distension in Tertiary rocks of southeastern Nevada: Geol. Soc. Am. Bull., v. 82, p. 43-58.

Andrusov, D., 1965. Aperçu général sur la géologie des Carpathes occidentales: Bull. Geol. Soc. Fr., v. 7, p. 1029-1062.

Andrusov, D., 1968. Grundriss der Tektonik der Nordlichen Karpaten: Acad. Slov. Edit., Bratislave, 187 p.

Aubouin, J., 1973. Des tectoniques superposées et de leur signification par rapport aux modèles géophysiques: l'exemple des Dinarides; paléotectonique, tectonique, tarditectonique: Bull. Geol. Soc. Fr., v. 15, p. 426-460.

Aubouin, J., Blanchet, R., Cadet, J.P., Celte, P., Charvet, J., Chorowicz, J., Cousin, M. and Rampnoux, J.P., 1970. Essai sur la géologie des Dinarides: Bull. Geol. Soc. Fr., v. 12, p. 1060-1093.

Báldi, T., 1969. On the Oligocene/Miocene stages of the Middle Paratethys area and the Egerian formations in Hungary: Ann. Univ. Sci. Rol. Eötvös, Budapest, sect. geol., v. 12, p. 19-28.

Báldi, T., 1982. On the age and history of the Oligocene-lower Miocene formations of Hungary: Akad. Kiadó, Budapest, in press.

Balla, Z., 1981. Neogene volcanism of the Carpatho-Pannonian region: Earth Evolution Sci., v. 1, no. 3, in press.

Bleahu, M. Bombliţă, G. and Kräutner, H., 1968. Explanation to the geologic map of Romania: Sheet 4, Viseu: Geol. Inst. Roumânia, scale 1:200,000, 54 p.

Boccaletti, M., Manetti, P., and Peltz, S., 1973. Evolution of the Upper Cretaceous and Cenozoic magmatism in the Carpathian arc: Geodynamic Significance, Mem. Geol. Soc. Italy, v. 12, p. 252-276.

Boccaletti, M., Horvath, F., Loddo, M., Mongelli, F. and Stegena, L., 1976. The Tyrrhenian and Pannonian basins: a comparison of two Mediterranean interarc basins: Tectonophys., v. 35, p. 45-69.

Brix, F. and Schultz, O. (eds), 1980. Erdöl und Erdgas in Österreich: Verlag: Naturhistorisches Museum Wien und F. Berger, Horn, Wien, 312 p.

Burchfiel, B.C., 1976. Geology of Romania, Geol. Soc. Am. Spec. Paper 158, 82 p.

Burchfiel, B.C., 1980. Eastern Alpine system and the Carpathian orocline as an example of collision tectonics, Tectonophys., v. 63, p. 31-62.

Carslaw, H.S. and Jaeger, J.C., 1959. Conduction of heat in solids: Clarendon Press, Oxford, 496 p.

Čermák. V., 1979. Review of heat flow measurements in Czechoslovakia, in: Čermák, V. and Rybach, L. (eds.), Terrestrial heat flow in Europe, Springer-Verlag, Berlin, p. 152-160.

Čermák, V. and Rybach, L. (eds.), 1979. Terrestrial heat flow in Europe: Springer-Verlag, Berlin, 328 p.

Channell, J.E.T., D'Argenio, B. and Horváth, F., 1979. Adria, the African promontory in Mesozoic time: Earth Sci. Rev., v. 15, p. 213-292.

Ciupagea, D., Paucǎ, M., and Ichem, Tr., 1970. Geolgia Depresiunii Transilvaniei: Edit. Acad. Rep. Social. Romania, Bucureşti, 256 p.

Cooke, H.B.S., Hall, J.M. and Rónai, A., 1979. Paleomagnetic, sedimentary and climatic records from boreholes at Dévaványa and Vésztő, Hungary: Paper prepared for IGCP Project 128, 28 p.

Crowell, J.C., 1974. Origin of late Cenozoic basins in southern California: in Dickinson, W.R. (ed.), Tectonics and Sedimentation, Soc. Econ. Paleo. Miner. Spec. Pub. 22, p. 190-204.

Davis, G.A., and Burchfiel, B.C., 1973. Garlock fault: an intra-continental transform structure, southern California: Geol. Soc. Am. Bull., v. 84, p. 1407-1422.

Dank, D.R., 1962. Sketch of the deep geological structure of the south Zala basin: Föld. Közl., v. 92, p.150-159. (in Hungarian with English summary)

Demetrescu, C., 1977. The thermal conductivity of some sedimentary rocks from the Transylvania Depression -Romania: Rev. Roum. Géol. Géophys. Géogr. Ser. Géophys., v. 21, p. 301-307.

Demetrescu, C., 1978. On the geothermal regime of some tectonic units in Romania: Pure Appl. Geophys., v. 117, p. 124-134.

Fuchs, K., Bonjer, P., Bock, G., Cornea, D., Radu, C., Enescu, D., Jiame, D., Nouescu, G., Merkler, G., Moldoveanu, T. and Tudorache, G., 1979. The Romanian earthquake of March 4, 1977: aftershocks and migration of seismic activity: Tectonophys., v. 53, p. 225-247.

Geological map series of Hungary, scale 1:200,000, map sheets no. II, III, IV, V, VIII, IX, X, XIV, XV, XVI and XXXV, 1965-1975. Hungarian Geol. Surv., Budapest. (in Hungarian)

Grill, R., Kapounek, J., Küpper, H., Papp, A., Plöchinger, B., Prey, S. and Tollmann, A., 1968. Neogene basins and sedimentary units of the Eastern Alps near Vienna, Guide to Excursion 3c, 23rd Intl. Geol. Congr., Prague, 1968.

Grubić, A., 1980. An outline of the geology of Yugoslavia -Excursions 201 A -202 C: 26th Intl. Geol. Congr., Paris, 92 p.

Gutdeutsch, R. and Aric, K., 1976. Erdbeben im ostalpin Raum: Arbeiten aus der Zentralanstalt für Meteorologie und geodynamic, v. 19, no. 210, 23 p.

Hörnes, M., 1856. Die fossilen mollusken des Tertiar-beckens von Wien: Wien, 736 p.

Horváth, F., Bodri, L. and Ottlik, P., 1979. Geothermics of Hungary and tectonophysics of the Pannonian basin "red spot", in: Cermak, V. and Rybach, L. (eds.), Terrestrial heat flow in Europe, Springer-Verlag, Berlin, p. 206-217.

Horváth, F., Dövényi, P. and Liebe, P., 1981. Geothermics of the Pannonian basin: Earth Evolution Sci., v. 1., no. 3, in press.

Horváth, F., and Royden, L.,1981. Mechanism for the formation of the intra-Carpathian basins: a review: Earth Evolution Sci., v. 1, no. 3, in press.

Horváth, F. and Stegena, L., 1977. The Pannonian basin: a Mediterranean interarc basin: in Biju-Duval, B. and Montadert, L. (eds.), Intl. Symp. on the structural history of the Mediterranean basins, Split, Yugoslavia, Oct. 25-29, 1976, Editions technip, Paris, p. 133-142.

Jiříček, R., 1979. Tectogenetic development of the Carpathian arc in the Oligocene and Neogene, in Mahel, M. (ed.), Tectonic profiles through the West Carpathians, Geol. Úst. Dion. Štúra, Bratislava, p. 205-214.

Jiříček, R. and Tomek, Č., 1981. Sedimentary and structural evolution of the Vienna basin, Earth Evolution Sci., v. 1, no. 3, in press.

Juhász, P., 1977. Processing of temperature logs from oil wells: Magyar Geofizika, v. 18, no. 6, p. 201-210. (in Hungarian with English summary)

Kober, L., 1912. Uber bau und Entstehung der Ostalpen: Mitt. Geol. Ges. Wien, v. 5, p. 368-481.

Körössy, L., 1968. Entwicklungsgeschichte und palaogeographische grundzuge des Ungarischen unterpannons: Acta Geol. Acad. Hung., v. 12, no. 1-4, p. 199-217.

Körössy, L., 1970. Entwicklungsgeschichte der Neogenen becken in Ungarn, Acta Geol. Acad. Sci. Hung., v. 14, p. 421-429.

Körössy, L., 1977. Flysch formations of Hungary: structural positions and connections: Fold. Kozl., v. 107, no. 3-4, p. 398-405.

Körössy, L., 1981. Regional geological profiles in the Pannonian basin: Earth Evolution Sci., v. 1, no. 3, in press.

Kröll, A., Schimunek, K. and Wessely, G., 1981. Ergebnisse und erfahrungen bei der exploration in der kalkalpenzone in Ostösterreich: Erdoel, Erdgas, Zeitschrift, v. 97, no. 4, p. 134-148.

Krs, M. and Roth, Z., 1977. A hypothesis of the development of the insubric-Carpathian Tertiary block system: Acta Geol. Acad. Sci. Hung., v. 21, no. 4, p. 237-249.

Krs, M. and Roth, Z., 1979. The insubric-Carpathian Tertiary block aystem: its origin and disintegration: Geol. Zborn. Geol. Carpat., v. 30, no. 1, p. 3-17.

Ksiazkiewicz, M., Oberc, J. and Pozaryski, W., 1977. Geology of Poland v. IV, Tectonics: Geological Institute, Warsaw, 718 p.

Lachenbruch, A.H. and Sass, S.H., 1978. Models of an extending lithosphere and heat flow in the Basin and Range province, in: Smith, R.B. and Eaton, G.P. (eds.), Cenozoic tectonics and regional geophysics the western Cordillera, Geol. Soc. Am. Mem. 152, p. 209-250.

Laskerev, V., 1924. Sur les équivalents du Sarmatien supérieur en Serbie: Zbornik Cvijic, 1-5, Beograd.

Laubscher, H. 1971, Das Alpen-Dinariden problem und die palinspastik der südlichen Tethys: Geol. Rundschau, v. 60, p. 813-833.

Lexa, J. and Konečný, V., 1974. The Carpathian Volcanic Arc: A Discussion: Acta Geol. Acad. Sci. Hung., v. 18, no 3-4, p. 279-293.

Mahel, M., Buday, T. and others, 1968. Regional geology of Czechoslovakia, part II, the west Carpathians: E. Schweizerbart'sche Verlagsbuchhandlung, Stuttgart, 723 p.

McKenzie, D., 1972. Active tectonics of the Mediterranean region: Geophys. Jour. R. Astr. Soc., v. 30, p. 109-185.

McKenzie, D., 1978. Some remarks on the development of sedimentary basins, Earth Planet. Sci. Lett., v. 40, p. 25-32.

McKenzie, D., 1981. The variation of temperature with time and hydrocarbon maturation in sedimentary basins formed by extension: Earth Planet. Sci. Lett., v. 55, p. 87-98.

Morelli, C., Belleno, S. and De Visintini, G., 1968. Non-directional travel-time anomalies for European stations: Boll. Geofis. Teor. Appl., v. 10, no1 38, p. 164-180.

Metwalli, M.H., 1971. Stratigraphic setting of the subsurface Miocene sediments in Transdanubia (Hungary) I: Acta Geol. Acad. Sci. Hung., v. 15, p. 155-172.

Nagymarosy, A., 1981. Chrono- and biostratigraphy of the Pannonian basin: a review based mainly on data from Hungary: Earth Evolution Sci., v. 1, no. 3, in press.

Nagymarosy, A., 1981. Subsidence profiles of the deep Neogene basins in Hungary, Earth Evolution Sci., v. 1, no. 3, in press.

Oberhauser, R. (ed.), 1980. Der geologische aufbau Österreichs: Springer-Verlag, Vienna, 699 p.

Oxburgh, E.R., 1968. An outline of the geology of the central Eastern Alps: Proc. Geol. Assoc., v. 79, p. 1-46.

Oxburgh, E.R., 1974. Eastern Alps: in Spencer, A.M. (ed.), Mesozoic-Cenozoic orogenic belts, Scoittish Acad. Press, Edinburgh, p. 100-126.

Papp, A., 1968. Nomenclature of the Neogene of Austria: Vehr. Geol. Budansanst, Jg. 1968, p. 9-27.

Parsons, B. and Sclater, J.G., 1977. An analysis of the variation of ocean floor bathymetry and heat flow with age: Jour. Geophys. Res., v. 82, p. 802 -825.

Posgay, K., 1975. Mit reflexionsmessungen bestimmte Horizonte und Geschwindigkeitsverteilung in der Erdkruste und im Erdmantel: Geofiz. Kozl. (Budapest), v. 23, P. 13-17.

Posgay, K., Albu, I, Petrovics, I. and Ráner, G., 1981. Character of the Earth's crust and upper mantle on the basis of seismic reflection measurements in Hungary: Earth Evolution Sci., v. 1, no. 3, in press.

Radócz, Gy., 1968. Preliminary report on the results of the reference drillings in the Cserehát: Annual Report of the Hungarian Geological Survey from the year 1967, p. 281-286. (in Hungarian)

Republique Socialiste de Roumanie, 1967, Carte geologique 1:200,000, map sheets no. 5, 13, 20, 21, 28, 29, 35, 36.

Roman, C., 1970. Seismicity in Romania - evidence for the sinking lithosphere: Nature, v. 228, p. 1176-1178.

Roman, C., 1973. Travel time residuals in the Carpathians and plate tectonics : Rev. Roum. Géol. Géophys. et Géogr., Ser. Géphys., v. 17, no. 1, p. 77-83.

Rónai, A., 1981. Magnetostratigraphy of Pliocene-Quaternary sediments in the Great Hungarian Plain: Earth Evolution Sci., v. 1, no. 3, in press.

Royden, L., Horváth, F. and Burchfiel, B.C., 1982. Transform faulting, extension and subduction in the Carpathian Pannonian region, Geol. Soc. Am. Bull., in press.

Royden, L. and Keen, C.E., 1980. Rifting process and thermal evolution of the continental margin of eastern Canada determined from subsidence curves: Earth Planet. Sci. Lett., v. 51, p. 343-361.

Royden, L., Sclater, J.G. and Von Herzen, R.P., 1980. Continental margin subsidence and heat flow: important parameters in formation of petroleum hydrocarbons: Am. Assoc. Petr. Geol. Bull., v. 64, p. 173-187.

Rudinec, R., 1978. Paleogeographical, lithofacial and tectogenetic development of the Neogene in eastern Slovakia and its relation to volcanism and deep tectonics: Geol. Zborn., Geol. Carpat., v. 29, p. 225-240.

Rudinec, R., Tomek, Č. and Jiříček, R., 1981. Sedimentary and structural evolution of the Transcarpathian depression: Earth Evolution Sci., v. 1, no. 3, in press.

Sãndulescu, M., 1975. Essai de synthèse structurale des Carpathes, Bull. Geol. Soc. France, v. XVII, p. 299-358.

Sãndulescu, M., 1980. Analyse géotectonique des chaînes alpines situées au tour de la mer noire occidentale, Ann. Inst. Geol. Geophys., v. LVI, p. 5-54.

Sãndulescu, M., Stefanescu, M., Butac, A., Pãtruţ, I. and Zaharescu, P., p., 1981. Genetical and structural relations between flysch and molasse (the East Carpathians model), Guide to Excursion A5: XII Congr. of the Carpatho-Balkan Geol. Assoc., Bucharest, 95 p.

Schönlaub, H.P., 1980. Die gailtallinie: in Oberhauser, R. (ed.), Der Geologische aufbau Osterreichs, Springer-Verlag, Wien, p. 422-425.

Sclater, J.G. and Christie, P.A.F., 1980. Continental stretching: an explanation of the post-mid-Cretaceous subsidence of the central North Sea basin: Jour. Geophys. Res., v. 85, no. B7, p. 3711-3739.

Sclater, J.G., Royden L., Horváth, F., Burchfiel, B.C., Semken, S. and Stegena, L., 1980. The formation of the intra-Carpathian basins as determined from subsidence data: Earth Planet. Sci. Lett., v. 51, p. 139-162.

Smith, A. G. and Moores, E.M., 1974. Hellenides: in Spencer, A. M. (ed.), Mesozoic-Cenozoic Orogenic belts, Scottish Acad. Press, Edinburgh, p. 159-185.

Sollogub, V.B. et al. (eds.), 1980. Structure of the Earth's crust in Central and Eastern Europe based on geophysical investigations: Naukova Dumka, Kiev, 206 p.

Steckler, M.S. and Watts, A.B., 1978. Subsidence of the Atlantic-type continental margin off New York, Earth Planet. Sci. Lett.,v. 41, p. 1-13.

Steckler, M.S. and Watts, A.B., 1980. The Gulf of Lion: subsidence of a young continental margin: Nature, v. 287,p. 425-429.

Stegena, L., 1964. The structure of the Earth's crust in Hungary: Acta Geol. Acad. Sci. Hung., v. 8, p. 413-431.

Stegena, L., Géczy, B. and Horváth F., 1975. Late Cenozoic evolution of the Pannonian basin, Tectonophys., v. 26, p. 71-90.

Steininger, F., Papp, A., Cicha, I., Senes, J., and Vass, D., 1975. Excursion "A", marine Neogene in Austria and Czechoslovakia: VIth Congr. Reg. Comm. Med. Neogene Strat., 96 p.

Steininger, F.F. and Rögl,F., 1979. The Paratethys history - a contribution towards the Neogene geodynamics of the Alpine orogen (an abstract): Ann. Geol. Pays Hellèn., Tome hors serie, 1979, v. III, p. 1153-1165. VIIth Int. Congr. Med. Neogene, Athens.

Szalay, A. and Koncz, I., 1980. Hydrocarbon genesis and migration processes in the southeastern Plain and Drava depression: Köolaj es Földgáz, v. 13, no. 6, p. 177-187. (in Hungarian)

Szepesházy, K., 1973. Tiszantúl északnugati részenek felsőkreta es paleogén koru képződményei (Rocks of upper Cretaceous and Paleogene age of the northwestern part of the Tiszantul): Akad. Kiado, Budapest, 1973, 96 p. (in Hungarian).

Tollmann, A., 1963. Ostalpensynthese: Franz Deuticke, Vienna, 256 p.

Tollmann, A., 1968. Die alpidischen Gebirgbildung-Phasen in den Ostalpen und Westkarpaten: Geotekt. Forsch., v. 21, 156 p.

Varga, I. and Pogácsás, Gy., 1981. Reflection seismic investigations in the Hungarian part of the Pannonian basin: Earth Evolution Sci., v. 1, no. 3, in press.

Vass, D., 1978. World Neogene radiometric time-scale (estate to the beginning of 1976): Geologicke prace, Geol. Ust. D. Stura, v. 70, p. 197-236.

Vass D., and Bagdasarian, G.P., 1978. A radiometric time scale for the Neogene of the Paratethys region: Am. Assoc. Petr. Geol., Stud. in Geol. 6, p. 179-204.

Vass, D., Slavik, J. and Bagdasarjan, G.P., 1975. Radiometric time scale for Neogene of Paratethys (to August 1, 1974): 6th Cong. Reg. Comm. Mediterranean Neogene Stratigraphy Proc., p. 259-297.

Veliciu, S., Cristian, M., Paraschiv, D. and Visarion, M., 1977. Preliminary data of heat flow distribution in Romania. Geothermics, v. 6, no. 1, p. 95-98.

Wachtel, G. and Wessely, G., 1981. Die Tiefbohrung Berndorf 1 in der östlichen Kalkalpen und ihr geologischer rahmen: Mitt. Österr. Geol. Ges., v. 74/75, p. 137-165,

Wernicke, B., 1981. Low-angle normal faults in the Basin and Range province: nappe tectonics in an extending orogen: Nature, v. 291, no. 5817, p. 645-648.

Zoback, M.L., Anderson, R.E., and Thompson, G.A., 1981. Cainozoic evolution of the state of stress and style of tectonism of the Basin and Range province of the western United States: Phil. Trans. R. Soc. Lond., A 300, p. 407-434.

FIGURE CAPTIONS

Fig. 1.   Major structural divisions of the Carpathians into inner
           and outer units. EA, Eastern Alps; SA, South Alps; pA,
           peri-Adriatic line; WC, West Carpathians; E, Europe; EC,
           East Carpathians; SC, South Carpathians; HmM; Hungarian mid-
           Mountains; A, Apuseni Mountains; M, Moesia; V, Vardar zone;
           DA, Dinaric Alps; Ap, Apulia. Dashed line shows
           continuation of peri-Adriatic line in subsurface. Inner and
           outer boundaries of the Carpathian flysch belt are given as
           reference lines in later figures.

Fig. 2.   Isopach map showing depth to base Miocene. Approximate
           ages of igneous rocks are also shown (T. Poka, 1981, pers.
           comm.). Fold axis symbols show location and trend of some
           of the Sava folds. Basins: S-Sava, Dr-Drava, Z-Zala,
           G-Graz, D-Danube, V-Vienna, P-Pannonian, Tc-Transcarpathian,
           Ts-Transylvanian. Dashed lines show regions of pre-Neogene
           outcrop. (Modified after Horvath and Royden, 1981).

Fig. 3.   Correlation and absolute age determinations for
           Mediterranean and Central and East Paratethyan
           biostratigraphic stages. Modified after Steininger and Rögl
           (1979).

Fig. 4a.   Schematic reconstruction of the outer Carpathian-East
           Alpine system during (late) Paleocene time. Width of the
           flysch belt is not well constrained, but probably was
           several hundred km.

Fig. 4b.   Reconstruction of the outer Carpathian-East Alpine system
           during Late Oligocene time. Continental collision had
           already occurred in the Eastern Alps and South Carpathians,
           but the West and East Carpathian flysch belt is roughly
           several hundred km wide. Little or no shortening of East
           Carpathian flysch had occurred since Paleocene time.

Fig. 5.   Plate tectonic sketch showing present position of boundaries
           of continental fragments for Eocene, early Miocene and late
           Miocene time. The boundaries between continental fragments
           are shown in single heavy line, but in reality are broad
           zones of differential motion. Big arrows indicate inferred
           direction of fragment motion relative to Europe. Shaded
           region shows approximate area of late Miocene crustal
           extension.

Fig. 6.   Age of last major thrusting and folding event versus
            horizontal distance along the Carpathian chain (see Fig. 2
            for locations). Vertical bars show upper and lower time
            limits for this final event. Where a minimum age could not
            be determined, the vertical bars were extended downward with
            arrows. Dashed arrows indicate probable, but not certain,
            determination of the last thrusting or folding event.
            Shaded region represents the Badenian stage. Data from
            Steininger et al., 1975; Ksiazkiewicz et al., 1977; Mahel et
            al., 1968; and Republique Socialiste de Roumania, 1967,
            Carte Geologique, 1:200,000.

Fig. 7.   Generalized map of Neogene faults in the intra-Carpathian
            region. Shaded pattern covers areas that have undergone
            significant extension. Arrows indicate sense of shear on
            zones of strike-slip displacement. Some basins are
            interpreted as "pull-apart" basins, whereas others are
            regions of extension bounded by zones of differential
            shear.

Fig. 8.   Approximate extent of marine and brackish water sedimentary
            rocks in Eocene time and late Oligocene-early Miocene time.
            Data from: Grubić (1980); Steininger and Rögl (1979);
            Nagymarosy (1981); and Steininger (1980, pers. comm.)

Fig. 9a.   Migrated reflection profile accross the Drava trough,
            location shown in Fig. 10. Flat-lying Pannonian age and
            younger rocks unconformably overlie older Miocene and
            basement rocks. Middle Miocene rocks occur in tilted fault
            blocks (central part of profile); bedding planes are rotated
            down along a large normal fault which separates Middle
            Miocene rocks from basement. From Varga and Pogacsas,
            1981.

Fig. 9b.   Migrated reflection profile accross part of the Pannonian
            basin, location shown in Fig. 10. I and II indicate
            pre-Miocene rocks; III indicates Pannonian age rocks which
            show a prograding deltaic structure in their middle part.
            From Varga and Pogácsás, 1981.

Fig. 10.   Location of boreholes used to analyze subsidence history of
            different intra-Carpathian basins (see text and Table I).
            Subsidence histories from wells a-d in the Transylvanian
            basin (from Ciupagea et al.,1970) were averaged to obtain
            overall subsidence history for the Transylvanian basin. D
            and V indicate wells with sedimentary rocks dated
            paleomagnetically (see text). Dark lines labeled A, B and
            30' indicate location of profiles and cross-section in Figs.
            9a, 9b and 30, respectively. Shaded area shows basement
            deeper than 2 km.

Fig. 11.   Uncorrected basement depth through time (or uncorrected sediment thickness versus time) determined for 23 boreholes, grouped by location, and for the Vienna basin (see Fig. 10 for locations).

Fig. 12a.   Heat flow map of the Carpathian-Pannonian region; heat flow contoured in 10 mW/m^2 intervals. Dark lines show location of outer Carpathian flysch belt. After Čermák and Rybach (1979), Horváth et al. (1979), Čermák (1979) and Veliciu and Demetrescu (1979).

Fig. 12b.   Location of heat flow measurements used in this study (solid dots) and values in mW/m^2. Triangles show location of wells in which bottom hole temperatures were used for comparison to predicted temperatures calculated from extension parameters. Diamond indicates location of heat flow measurement in the Transylvanian basin that was not used in this study (see text). Data from papers in Čermák and Rybach (eds.) (1979) and from Horváth et al. (1981). Shaded area shows basement depth greater than 2 km.

Fig. 12c.   Location of heat flow measurements in Vienna basin and adjacent flysch nappes and foredeep. Values in mW/m^2. Data from Čermák (1979). Shading shows areas where basement is deeper than 2 km.

Fig. 13.   Map of depth to Moho determined from seismic refraction data. 1 - foreland (lines) and foredeep molasse (circles). 2 - Miocene (dots) and older (shaded) thrust nappes. 3 - Miocene basin sediments. 4 - depth to Moho in km (lighter lines) and location of seismic refraction profiles (darker lines). Data from Sollogub et al., (1980) and Posgay et al., (1981).

Fig. 14a.   Schematic diagram of continental crust (crosses) and sub-crustal lithosphere (shaded) at equilibrium thermal conditions prior to extension. Initial crustal thickness is assumed to be 35 km and the base of the lithosphere is assumed to be maintained at a constant temperature throughout. Initial surface elevation (light line above diagram) is at sea level.

Fig. 14b.   Uniform lithospheric extension by β = 1.5. Immediately after extension, thermal gradient is elevated by about 50% and initial basin subsidence is about 1 km (water loaded).

Fig. 14c.   Modified lithospheric extension (crust is extended by β = 2.25 within the basin and unextended in uplifted blocks; subcrustal lithosphere is attenuated by about a factor of 10 everywhere). Immediately after extension, near surface temperatures are much higher than in (b), even though basement elevation within the basin (water loaded) is identical. Outside the basin, basement is uplifted.

Fig. 14d.   After cooling, temperature reflects thermal equilibrium
             conditions. Within the basin depth (water loaded) is
             roughly 2 km.

Fig. 14e.   As for Fig. 11d except that basement depth within the basin
             (water loaded) is roughly 3.5 km, so that even though
             initial subsidence was identical to that for uniform
             extension by β = 1.5, thermal subsidence is about 2.5
             times greater. If no erosion has occurred, regions flanking
             the deep basin will return to sea level.

Fig. 15.   Initial subsidence as a function of crustal and sub-crustal
             extension assuming an initial crustal thickness of 35 km.
             Subsidence is water loaded but uplift (shown by shaded
             region) is unloaded. A fixed initial subsidence may be the
             result of varying amounts of crustal extension, depending
             upon the degree of attenuation of the underlying
             lithosphere.

Fig. 16.   Measured porosity vs. depth values for sandstone (triangles)
             and claystone (dots). Lighter lines show theoretical
             porosity relationship assumed for sandstone and claystone.
             Darker line is intermediate porosity-depth relationship
             assumed. Shaded area shows assumed uncertainty in porosity
             range. Numbers refer to porosity as a function of depth
             (x). Data from Szalay and Koncz (1980).

Fig. 17.   Subsidence determined from sedimentation data for wells
             1-23, corrected for effects of sediment compaction and
             sediment loading. Darker lines and solid symbols show
             corrected subsidence determined from intermediate porosity
             and density values. Lighter lines and open symbols for
             wells 1-6 show corrected subsidence for extreme values of
             porosity and density (Table III and text). Shaded area
             shows uncertainty range for corrected subsidence.

Fig. 18.   Thermal conductivity vs. depth for six wells in the
             Pannonian and Danube basins. Solid dots are measured values
             for claystone and shale, open dots for sandstone. Darker
             line shows intermediate conductivity depth relationship
             assumed, lighter lines show exteme conductivity depth
             relationships. Numbers refer to conductivity (W/m°K) as a
             function of depth (x). Shaded area shows assumed
             uncertainty range.

Fig. 19.   Discrete symbols show corrected subsidence determined from
            sedimentation data for wells 1-12 (as in Fig. 17). Solid
            lines show predicted subsidence determined from theoretical
            extension parameters assuming uniform extension (see text
            and Tables IV and V). Dark lines show intermediate
            predicted subsidence histories that correspond to
            intermediate values of corrected subsidence for each well
            group (solid symbols). Lighter lines (for wells 1-6) show
            maximum and minimum predicted subsidence histories that
            correspond to maximum and minimum values of corrected
            subsidence (open symbols). Shaded area shows uncertainty
            range in predicted subsidence curves.

Fig. 20.   Observed and predicted temperatures in the Pannonian basin
            assuming uniform extension. Diamonds show temperatures
            determined from formation tests near the bottom of wells 1
            and 6. Open circles indicate bottom hole temperatures for
            wells 7,8,10 and 12. Dots are bottom hole temperatures for
            some other wells in the Pannonian basin (see text and Fig.
            12b). Solid lines show predicted temperatures. Black area
            shows uncertainty in predicted temperatures for wells 2-4;
            shaded area shows uncertainty range for well 5; dots show
            uncertainty ranges for wells 1 and 6.

Fig. 21.   Present depth below surface (uncorrected) vs. age for
            sediments dated magnetostratigraphically at Dévaványa
            (triangles) and Vésztő (dots). Dark lines show predicted
            depth-age relationship assuming uniform extension and
            present basement depths of 3 and 7.5 km. Lighter lines and
            shaded areas show uncertainty ranges in predicted depths.

Fig. 22.   Schematic diagram showing assumed pattern of extension
            through time for the modified extension model proposed.
            Crosses represent continental crust, shaded area represents
            sub-crustal lithosphere. a -equilibrium thermal conditions
            and 35 km crust prior to Badenian extension; b -during
            Badenian extension, lithosphere extends uniformly; c
            -Sarmatian extension results in crustal thinning (by about a
            factor of 1.6), and in severe attenuation of sub-crustal
            lithosphere, which may result in uplift (see text and Fig.
            15), d -Pannonian age extension is assumed to be uniform,
            but lower lithosphere is already highly attenuated.

Fig. 23.   Discrete symbols show corrected subsidence determined from
            sedimentation data for wells 1-12 (as in Fig. 17). Solid
            lines show predicted subsidence determined from theoretical
            extension parameters assuming modified extension as described
            in text (see also Tables IV and V). Dark lines show
            intermediate predicted subsidence histories that correspond
            to intermediate values of corrected subsidence for each well
            group (solid symbols). Lighter lines (for wells 1-6) show
            maximum and minimum predicted subsidence histories that
            correspond to maximum and minimum values of corrected
            subsidence (open symbols). Shaded area shows uncertainty
            range in predicted subsidence curves.

Fig. 24.   Observed and predicted temperatures in the Pannonian basin
            assuming modified extension as descibed in text. Diamonds
            show temperatures determined from formation tests near the
            bottom of wells 1 and 6. Open circles indicate bottom hole
            temperatures for wells 7,8,10 and 12. Dots are bottom hole
            temperatures for some other wells in the Pannonian basin (see
            text and Fig. 12b). Solid lines show predicted temperatures.
            Black area shows uncertainty range in predicted temperatures
            for wells 2-4, shaded area shows uncertainty range for well
            5; dots show uncertainty ranges for wells 1 and 6.

Fig. 25.   Present depth below surface (uncorrected) vs. age for
            sediments dated magnetostratigraphically at Dévaványa
            (triangles) and Vésztő (dots). Dark lines show predicted
            depth-age relationship assuming modified extension as
            described in text and present basement depths of 3 km.
            Lighter lines and shaded area show uncertainty range.

Fig. 26.   Predicted (lines) and observed (symbols) subsidence for wells
            13-23 in the Danube and Zala basins for (a) uniform extension
            and (b) modified extension, corrected for compaction and
            sediment loading.

Fig. 27.   Block diagram to illustrate proposed style of extension
            within the Vienna basin. Shaded area shows European
            platform and inactive nappes of the West Carpathians, which
            may be considered a part of Europe at this time. Unshaded
            area shows active nappes east and north of the Vienna basin
            which are being transported northwestward. Active and
            inactive nappes are separated by transcurrent faults which
            flatten into a shallow dipping detachment. Vienna basin
            pulls apart by surficial extension above the detachment
            surface.

Fig. 28.   Predicted (lines) and observed (symbols) subsidence for the
            north Vienna basin for (a) uniform extension and (b)
            modified extension. Dark lines and solid symbols show
            intermediate values of subsidence; lighter lines and open
            symbols show maximum and minimum subsidence profiles.
            Shaded area shows region of uncertainty.

Fig. 29.   Palinspastic reconstruction of the Carpathian-Pannonian
            region at (a) beginning of Karpatian time, (b) beginning of
            Badenian time, (c) beginning of Sarmatian time, and (d)
            present. Solid line shows present external limit of
            Carpathian flysch, and is fixed with respect to Europe.
            Shaded areas show regions of active extension during each
            timestage (Karpatian, Badenian, and Sarmatian); vertical
            lines indicate areas of shortening; small arrows indicate
            direction of motion inferred along strike-slip fault zones.
            We show only the areas of extension, compression and
            transcurrent faulting which have been identified and are
            known to belong to the time periods indicated. We realize
            that other structures are required to complete fragment
            boundaries, but such structures have not yet been identified
            from field studies. Large arrows in (d) show motions of
            various crustal fragments from the beginning of Karpatian
            time until present. Arrow heads indicate present position;
            arrow tails indicate pre-Karpatian location.

Fig. 30.   Palinspastic reconstruction of flysch nappes in the outer
            East Carpathians (from Burchfiel, 1976), showing:
            top-present configuration of nappes and, bottom-nappes
            restored to pre-Miocene configuration. Main overthrusting
            of Tarcau, Marginal Folds and Sub-Carpathian nappes are
            intra-Badenian and intra-Sarmatian, giving minimum
            shortening from Badenian to present as about 50 km.
            Location of cross-section shown in Fig. 10.

Fig. 31.   Schematic east-west section across the Pannonian fragment
            showing how continued subduction of the European plate could
            have resulted in extension of the Pannonian fragment. The
            European foreland and the peri-Adriatic-Vardar fault system
            are considered fixed relative to one another. During
            subduction, eastward movement is induced in the overriding
            plate to fill the space formerly occupied by the subducted
            plate. Note that subduction also implies migration of the
            subduction zone towards the European foreland. Some
            steepening of the subducted slab has also been shown. Big
            arrows show sense of shear between European plate and
            Pannonian fragment. Subsidence of the Transylvanian basin
            may have resulted from thickening of lithospheric material
            beneath the basin, or from other transient forces associated
            with subduction. Subsequent uplift of the
            Transylvanian-East Carpathian area might be the result of
            unloading as the subducted slab (and possibly thickened
            lithosphere?) became detached from the overlying plate. E
            -Europe; EC -East Carpathians; Ts -Transylvanian basin; A
            -Apuseni Mountains; P -Pannonian basin. Shaded area
            represents crustal material, dots represent subcrustal
            lithosphere and black represents sedimentary cover within
            the Neogene basins and in the outer flysch Carpathians.

Table 1

SEDIMENTATION DATA FOR 23 WELLS IN THE INTRA-CARPATHIAN REGION

Well	Name	Depth (m) to Base of:					
		Badenian (16.5 Ma)	Sarmatian (13.0 Ma)	Pannonian (10.5 Ma)	Pontian (8.0 Ma)	Dacian (5.0 Ma)	Quaternary (2.0 Ma)
1	Derecske 1	5000	4500	4500	2050	400	100
2	Kismarja 2	1630	1630	1630	1000	580	280
3	Turta 3	2240	2190	2190	1250	870	540
4	Biharnagybajom 2	1440	1440	1440	900	680	290
5	Békés 1	3450	3300	3230	1950	1000	350
6	Hómenzovásárhely 1	7500	5350	5350	2450	1200	650
7	Makó 2	4900	4600	4600	2100	1100	550
8	Algyő K-1	3560	3560	3560	2460	960	260
9	Maroslele 1	3180	3180	3180	2280	1880	260
10	Szank 2	2000	1950	1950	1300	700	300
11	Harka 1	1770	1770	1770	1070	650	170
12	Üllés-ÉNy 1	2320	2220	2220	1320	780	400
13	Senec 1	2900	1940	1280	–	–	–
14	Ivanka pri Dunaji 1	1900	1480	1100	–	–	–
15	Diakovce 1	3360	3060	2410	–	–	–
16	Mihaly 28	2900	2760	2500	1450	–	–
17	Györszemerc 2	2180	1680	1680	950	–	–
18	Bősárkány 1	4500	4200	3600	1950	–	500
19	Csapod 1	3950	3110	2710	2200	–	100
20	Nagylengyel 108	2300	2200	2100	1200	–	–
21	Csersztreg 1	2800	2540	2350	1000	–	–
22	Szentgyörgyvölgye 1	2700	2650	2370	1400	–	–
23	Resznek 1	3500	3300	3150	1700	–	–

Table II

Key Geomagnetic Markers and Depth - Age Relationship
for Sediments at Devavanya and Veszto

Epoch or Event	Age (Ma)	Depth (m)	
		Devavanya	Veszto
Brunhes-Matuyama	0.72	115	152
Jaramillo			
Phase A	0.89	152	197
Phase B	0.94	172	224
Olduvai			
Top	1.76	275	323
Base	1.91	316	368
Matuyama-Gauss	2.47	416	482
Gauss-Gilbert	3.41	542	615
Cochiti and Nunivak			
Top	3.82	617	683
Base	4.25	678	752
Epoch 5-Epoch 6	5.77	926	1011
Basement	13.0(assumed)	3000	3000

Table III

Definitions and Values Used [+]

symbol	value	definition
x		depth
ϕ	$= \phi_0 \, e^{-ax}$	porosity
a	.6 km^{-1} (.45–1.0)[*]	porosity decay constant
ϕ_0	40 % (35–45)[*]	surface porosity
ρ_a	3.20 ± .05 g cm^{-3}	density of asthenosphere
ρ_{crust}		density of crust
ρ_w	1.0 g cm^{-3}	density of water
$\dfrac{\rho_a - \rho_{crust}}{\rho_a - \rho_w}$	0.180	
ρ_{matrix}	2.68 ± .03 g cm^{-3}	matrix density of sedimentary rocks
$\bar{\rho}_{sed}$		average density of sedimentary rocks
K_{sed}	$= K_0 + bx$	thermal conductivity of sediment
K_0	1.28 ± .17 W m^{-1} °K^{-1}	surface conductivity
b	.49 ± .15 mW m^{-2} °K^{-1}	conductivity gradient
κ	8·10^{-7} m^2 s^{-1}	thermal diffusivity of lithosphere
ℓ	125 km	thickness of lithosphere
α	3.1·10^{-5} °C^{-1}	coefficient of thermal expansion
T_a	1333 °C	temperature of asthenosphere
T_0	5 °C	surface temperature
$\dfrac{\alpha(T_a-T_0)\ell\rho_a}{\rho_a-\rho_w}$	7500 m	
Q_R	16 mW m^{-2}	initial heat generation from plane source at depth d
d	8 km	initial depth of radiogenic plane source

[+] The values in this table give the following depths: cold continental lithosphere with 35 km crust – 0 m; mid-ocean ridge – 2630 m; and cold ocean floor – 6380 m.

[*] Figures in parentheses give uncertainty range; see text and Fig. 16 for details.

Table IV

SUBSIDENCE AND HEAT FLOW FOR WELLS 1-5 IN THE PANNONIAN BASIN: OBSERVED AND PREDICTED[1]

Wells	Age Timestage	Age at Base (Ma)	Basement Subsidence (Observed)(m)			Observed Heatflow (mW/m²)[5]	Uniform Extension (Predicted Values)			Modified Extension (Predicted Values)		
			Uncorrected[2]	Decompacted[3]	Corrected[4]		Extension (β)	Depth (M)	Heatflow (mW/m²)	Extension (β)	Depth (m)	Heatflow (mW/m²)
	Badenian	16.5	0	0	0		1.14	0		1.14	0	
	Sarmatian	13.0	500	725	350		1.00	353		1.66*	353	
	Pannonian	10.5	500	725	350		1.92	373		1.66	350	
1	Pontian	8.0	2950	3365	1235		-	1495		-	1342	
	Dac/Rom	5.0	4600	4735	1600		-	1550		-	1474	
	Quaternary	2.0	4900	4935	1650		-	1606		-	1594	
	Present	0.0	5000	5000	1665 (1370-1855)	102±11	total 2.19 (1.81-2.62)	1644	62 (51-74)	total 3.14 (2.63-3.63)	1669	111 (106-122)
	Badenian	16.5	0	0	0		1.00	0		1.00	0	
	Sarmatian	13.0	15	20	10		1.00	0		1.66*	0	
	Pannonian	10.5	15	20	10		1.32	0		1.17	36	
2-4	Pontian	8.0	720	870	410		-	672		-	485	
	Dac/Rom	5.0	1060	1200	540		-	711		-	592	
	Quaternary	2.0	1400	1490	650		-	745		-	697	
	Present	0.0	1770	1770	750 (650-790)	102±11	total 1.32 (1.26-1.35)	764	50 (46-51)	total 1.94 (1.86-1.98)	763	103 (95-103)
	Badenian	16.5	0	0	0		1.04	0		1.04	0	
	Sarmatian	13.0	150	230	120		1.00	116		1.66*	108	
	Pannonian	10.5	220	330	170		1.65	122		1.44	130	
5	Pontian	8.0	1500	1820	770		-	1148		-	963	
	Dac/Rom	5.0	2450	2700	1045		-	1200		-	1071	
	Quaternary	2.0	3100	3210	1195		-	1248		-	1176	
	Present	0.0	3450	3450	1260 (1045-1380)	102±11	total 1.72 (1.51-1.85)	1278	55 (48-63)	total 2.49 (2.24-2.71)	1243	103 (98-104)

[1]Values shown are for median values of parameters (Table III). Values in parentheses show extreme range using end-member values of each parameter (Table III).
[2]Uncorrected basement depth = sediment thickness above basement at beginning of each timestage.
[3]Basement subsidence corrected for effects of sediment compaction at beginning of each timestage.
[4]Equivalent basement subsidence if basin were filled with water at beginning of each timestage.
[5]Average of 8 measurements.

*Crustal extension = β; subcrustal lithospheric extension = 10β.

Table V

SUBSIDENCE AND HEAT FLOW FOR WELLS 6-12 IN THE PANNONIAN BASIN: OBSERVED AND PREDICTED[1]

Wells	Timestage	Age at Base (Ma)	Basement Subsidence (Observed)(m) Uncorrected[2]	Decompacted[3]	Corrected[4]	Observed Heatflow (mW/m^2)[5]	Uniform Extension (Predicted Values) Extension (β)	Depth (m)	Heatflow (mW/m^2)	Modified Extension (Predicted Values) Extension (β)	Depth (m)	Heatflow (mW/m^2)
	Badenian	16.5	0	0	0		1.60	0		1.60*	0	
	Sarmatian	13.0	2150	2660	1035		1.00	1026		1.68*	1026	
	Pannonian	10.5	2150	2660	1035		2.50	1061		1.90	1027	
6	Pontian	8.0	5050	5550	1800		-	2056		-	1898	
	Dac/Rom	5.0	6300	6640	2070		-	2146		-	2056	
	Quaternary	2.0	6850	7060	2170		-	2234		-	2189	
	Present	0.0	7500	7500	2275 (1880-2570)	102±11	total 4.00 (2.61-5.88)	2292	79 (59-99)	total 5.11 (3.63-7.10)	2269	109 (102-122)
	Badenian	16.5	0	0	0		1.08	0		1.08	0	
	Sarmatian	13.0	300	450	230		1.00	217		1.66*	217	
	Pannonian	10.5	300	450	230		2.05	229		1.70	229	
7	Pontian	8.0	2800	3255	1225		-	1501		-	1303	
	Dac/Rom	5.0	3800	4100	1435		-	1558		-	1434	
	Quaternary	2.0	4350	4530	1545		-	1615		-	1553	
	Present	0.0	4900	4900	1640	102±11	total 2.21	1654	64	total 3.05	1628	112
	Badenian	16.5	0	0	0		1.00	0		1.00	0	
	Sarmatian	13.0	0	0	0		1.00	0		1.65*	0	
	Pannonian	10.5	0	20	0		1.70	0		1.48	20	
8-9	Pontian	8.0	1000	1290	580		-	1121		-	942	
	Dac/Rom	5.0	2450	2730	1070		-	1168		-	1061	
	Quaternary	2.0	3110	3200	1190		-	1214		-	1173	
	Present	0.0	3370	3370	1240	102±11	total 1.70	1245	56	total 2.44	1244	108
	Badenian	16.5	0	0	0		1.01	0		1.01	0	
	Sarmatian	13.0	50	75	40		1.00	31		1.66*	31	
	Pannonian	10.5	50	75	40		1.35	34		1.20	62	
10-12	Pontian	8.0	800	970	455		-	742		-	564	
	Pac/Rom	5.0	1320	1470	645		-	785		-	678	
	Quaternary	2.0	1740	1820	770		-	823		-	788	
	Present	0.0	2030	2030	840	102±11	total 1.36	843	49	total 2.01	853	99

[1]Values shown are for median values of parameters (Table III). Values in parentheses show range using end-member values of each parameter (Table III).
[2]Uncorrected basement depth = sediment thickness above basement at beginning of each timestage.
[3]Basement subsidence corrected for effects of sediment compaction at beginning of each timestage.
[4]Equivalent basement subsidence if basin were filled with water at beginning of each timestage.
[5]Average of 8 measurements.

*Crustal extension = β; subcrustal lithospheric extension = 10β.

Table VI

SUBSIDENCE AND HEAT FLOW FOR THE DANUBE AND ZALA BASINS: OBSERVED AND PREDICTED[1]

Wells	Timestage	Age at Base (Ma)	Basement Subsidence (Observed)(m) Uncorrected[2]	Decompacted[3]	Corrected[4]	Observed Heatflow (mW/m²)[5]		Uniform Extension (Predicted Values) Extension (β)	Depth (m)	Heatflow (mW/m²)		Modified Extension (Predicted Values) Extension (β)	Depth (m)	Heatflow (mW/m²)
	Badenian	16.5	0	0	0			1.14	0			1.14	0	
13-15	Sarmatian	13.0	560	750	360			1.11	353			1.86*	353	
	Pannonian	10.5	1120	1370	610			1.18	606			1.03	598	
	Pontian	8.0	–	–	–			–	949			–	739	
	Present	0.0	2720	2720	1050	73±8	total	1.49	1057	52 total		2.18	1035	102
	Badenian	16.5	0	0	0			1.09	0			1.09	0	
16-17	Sarmatian	13.0	320	445	225			1.02	241			1.69*	241	
	Pannonian	10.5	450	610	300			1.32	307			1.18	294	
	Pontian	8.0	1340	1570	680			–	904			–	726	
	Present	0.0	2540	2540	1000	73±8	total	1.47	1010	53 total		2.17	1017	108
	Badenian	16.5	0	0	0			1.15	0			1.15	0	
18-19	Sarmatian	13.0	570	800	385			1.11	374			1.88*	374	
	Pannonian	10.5	1070	1400	620			1.49	626			1.28	636	
	Pontian	8.0	2150	2530	995			–	1322			–	1158	
	Quaternary	2.0	3920	4020	1415			–	1425			–	1404	
	Present	0.0	4220	4220	1465	73±8	total	1.90	1459	58 total		2.77	1478	109
	Badenian	16.5	0	0	0			1.04	0			1.04	0	
20-23	Sarmatian	13.0	150	225	115			1.05	116			1.72*	116	
	Pannonian	10.5	330	465	235			1.40	253			1.25	223	
	Pontian	8.0	1500	1760	745			–	967			–	778	
	Present	0.0	2820	2820	1080	88±6	total	1.53	1076	53 total		2.24	1066	106

[1]Values shown are for median values of parameters (Table III). Values in parentheses show extreme range using end-member values of each parameter (Table III).
[2]Uncorrected basement depth = sediment thickness above basement at beginning of each timestage.
[3]Basement subsidence corrected for effects of sediment compaction at beginning of each timestage.
[4]Equivalent basement subsidence if basin were filled with water at beginning of each timestage.
[5]Average of 12 measurements for Wells 13-19, average of 2 measurements for Wells 20-23.

*Crustal extension = β; subcrustal lithosphere extension = 10β.

TABLE VII

SUBSIDENCE AND HEAT FLOW FOR THE NORTH VIENNA AND TRANSYLVANIAN BASINS

Location	Timestage	Age at Base (Ma)	Basement Subsidence (Observed)(m)			Observed Heatflow (mW/m²)[5]	Uniform Extension				Modified Extension		
			Uncorrected[2]	Decompacted[3]	Corrected[4]		Extension (β)	Depth (m)	Heatflow (mW/m²)		Extension (β)	Depth (m)	Heatflow (mW/n²)
North Vienna Basin	Ottnangian	19.0	0	0	0		2.24	-684			1.70*	-684	
	Badenian	16.5	3000	3180	1185		-	1019			-	1245	
	Present	0.0	3600	3600	1300 (1075-1425)	50±7	total 2.24 (1.98-2.40)	1319	64 (56-67)	total	1.70 (1.60-1.75)	1302	46 (44-47)
Transylvanian Basin	Badenian	16.5	0	0	0		1.35	0			1.0	-	
	Sarmatian	13.0	1400	1700	725		1.17	720			1.0	-	
	Pannonian-Present	10.5	2900	3000	1135		-	902			-	-	
	Present	0	3200	3200	1190 (990-1300)	42±10	total 1.58 (1.46-1.71)	1172	56 (51-60)	total	1.0 -		43 (42-43)

[1]Values shown are for median values of parameters (Table III). Values in parentheses show extreme range using end-member values of each parameter (Table III).
[2]Uncorrected basement depth = sediment thickness above basement at beginning of each timestage.
[3]Basement subsidence corrected for effects of sediment compaction at beginning of each timestage.
[4]Equivalent basement subsidence if basin were filled with water at beginning of each timestage.
[5]Average of 9 measurements for North Vienna basin, average of 5 measurements for Transylvanian basin.

*Crustal extension only, upper mantle assumed to be unextended.
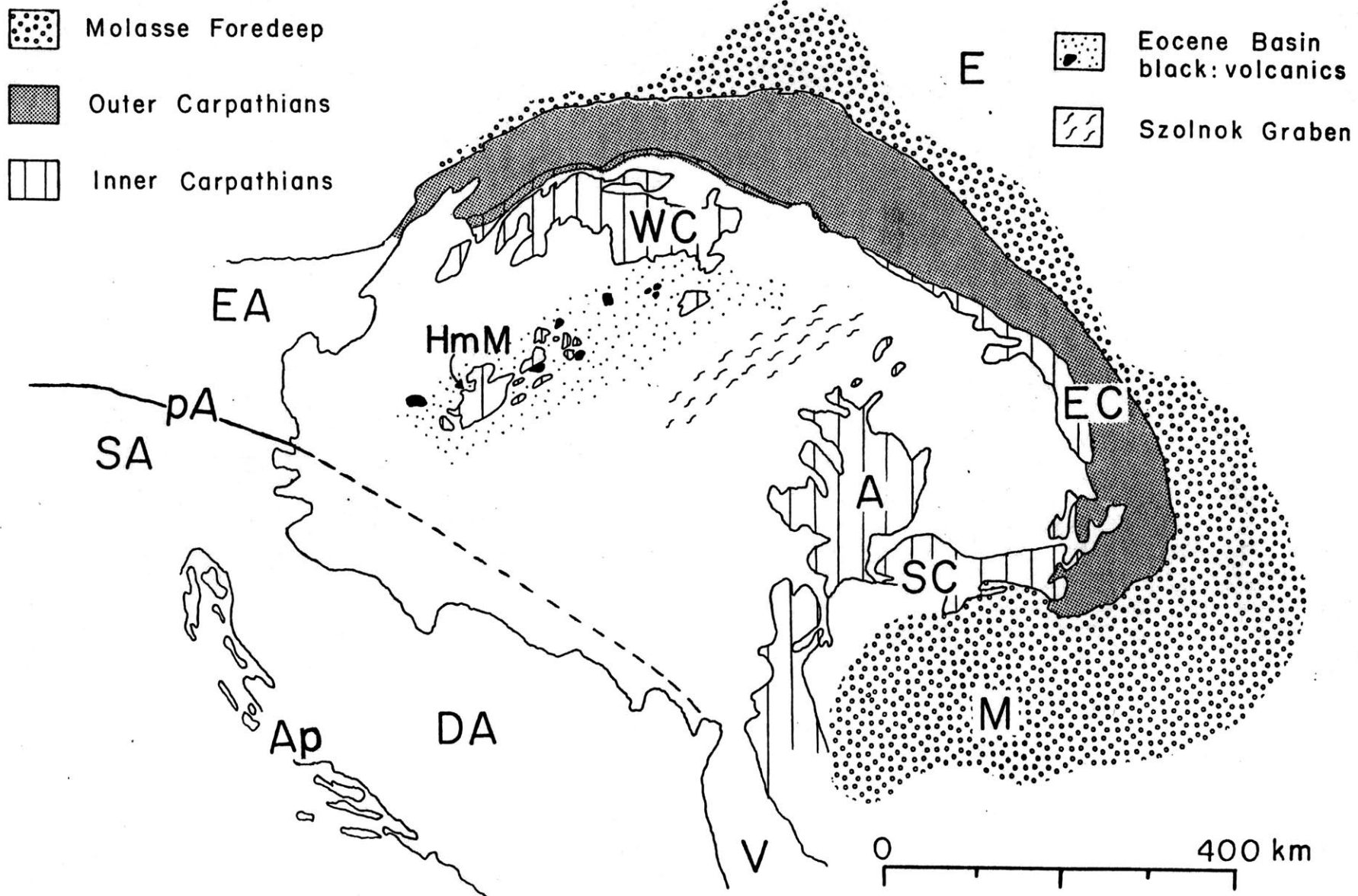
Figure 1
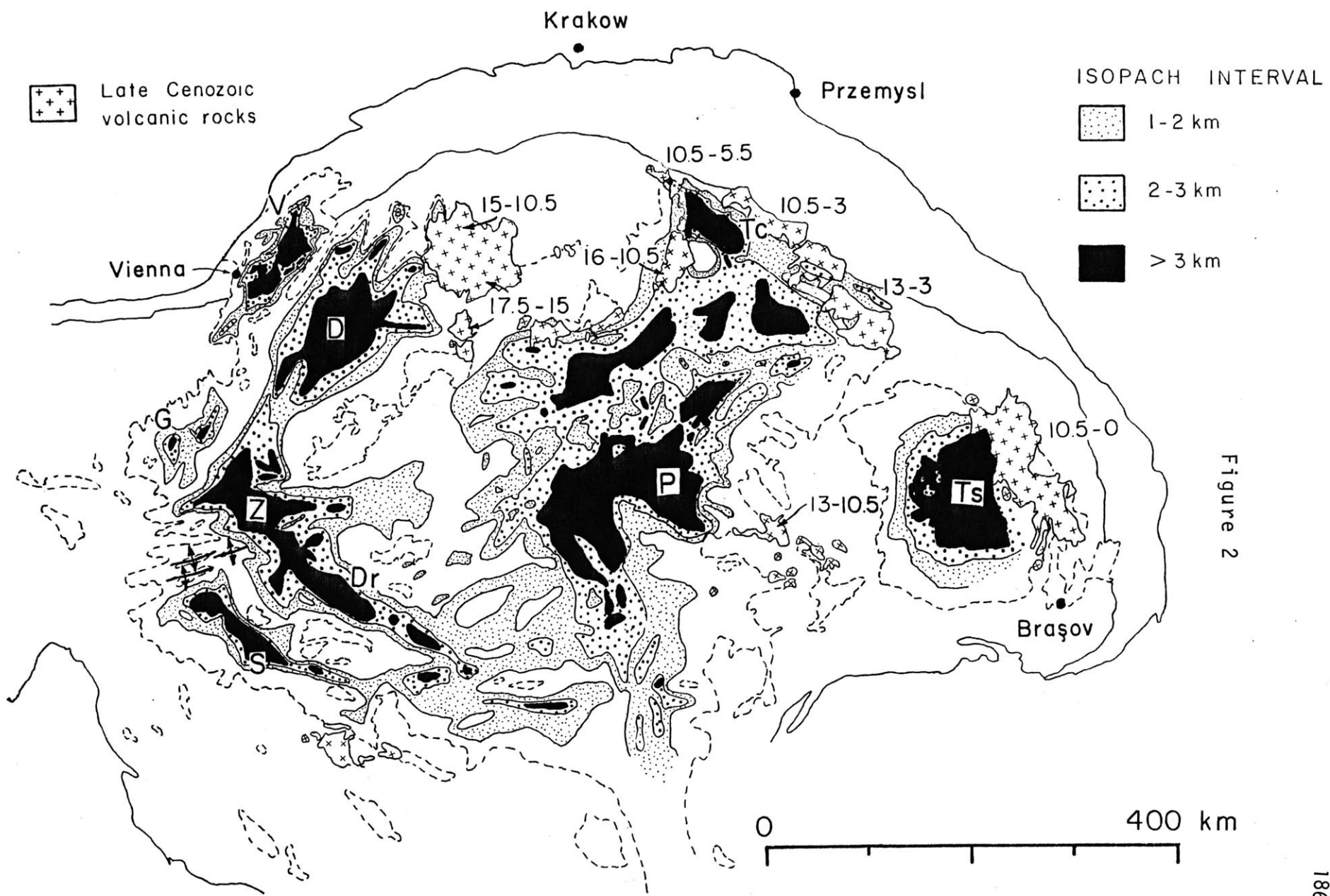
Figure 2

BIOSTRATIGRAPHIC STAGES

Figure 3

Ma	EPOCH	MEDITERRANEAN	PARATETHYS CENTRAL	PARATETHYS EAST	FORMER STAGES
	QUAT.				
	PLIOCENE L		ROMANIAN	AKTSCHAGYLIAN	LEVANTIN
	PLIOCENE E		DACIAN	KIMMERIAN	LEVANTIN
5	MIOCENE LATE	MESSINIAN			PANNONIAN s.l.
	MIOCENE LATE	TORTONIAN	PONTIAN	PONTIAN	PANNONIAN s.l.
	MIOCENE LATE	TORTONIAN	PANNONIAN	MAEOTIAN	PANNONIAN s.l.
10	MIOCENE LATE	TORTONIAN	PANNONIAN	CHERSONIAN	PANNONIAN s.l.
	MIOCENE MIDDLE		SARMATIAN	BESSARABIAN	SARM. s.SUESS / SARMAT.s.l.
	MIOCENE MIDDLE		SARMATIAN	VOLHYNIAN	SARM. s.SUESS / SARMAT.s.l.
	MIOCENE MIDDLE	SERRAVALLIAN	BADENIAN	KONKIAN	TORTON. / VINDOBON.
15	MIOCENE MIDDLE	SERRAVALLIAN	BADENIAN	KARAGANIAN	TORTON. / VINDOBON.
	MIOCENE MIDDLE	SERRAVALLIAN	BADENIAN	TSHOKRAKIAN	TORTON. / VINDOBON.
	MIOCENE MIDDLE	LANGHIAN	BADENIAN	TARKHANIAN	TORTON. / VINDOBON.
	MIOCENE EARLY	BURDIGALIAN	KARPATIAN	KOZACHURIAN	HELV. / VINDOBON.
	MIOCENE EARLY	BURDIGALIAN	OTTNANGIAN	KOZACHURIAN	HELV. / VINDOBON.
20	MIOCENE EARLY	BURDIGALIAN	EGGENBURGIAN	SAKARAULIAN	BURDIGAL. / VINDOBON.
	MIOCENE EARLY	AQUITANIAN	EGERIAN ↓	CAUCASIAN	AQUITAN.
	MIOCENE EARLY	AQUITANIAN	EGERIAN ↓	CAUCASIAN	CHATT.

A

Present boundaries of flysch belt

flysch

EASTERN ALPS

INNER CARPATHIANS

Southern boundary
– Paleocene

DINARIDES

0   400 km

FLYSCH BELT - PALEOCENE

B

Present boundaries of flysch belt

molasse

EASTERN ALPS

flysch

INNER CARPATHIANS

Southern boundary
– end Oligocene

DINARIDES

molasse

0   400 km

FLYSCH BELT – LATE OLIGOCENE

Figure 4

EOCENE

LATE MIOCENE

EARLY MIOCENE

Figure 5

Figure 6

Figure 7

0   400 km

AREAL DISTRIBUTION OF MARINE AND BRACKISH WATER SEDIMENTARY ROCKS

EUROPE

WC

EC

SC

DINARIDES

MOESIA

0   200 km

EOCENE

EUROPE

WC

EC

SC

DINARIDES

MOESIA

0   200 km
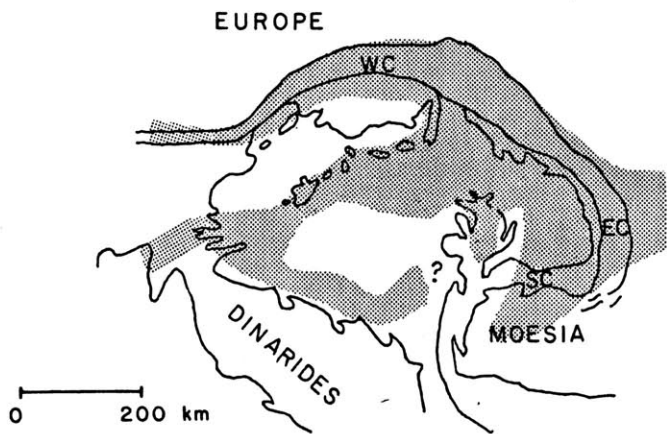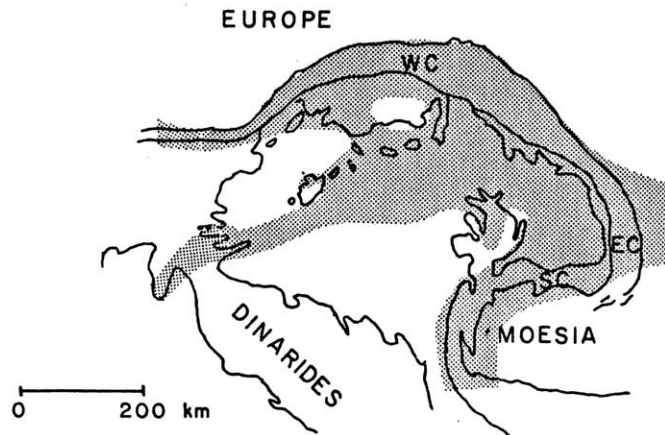
LATE   OLIGOCENE-
EARLY   MIOCENE
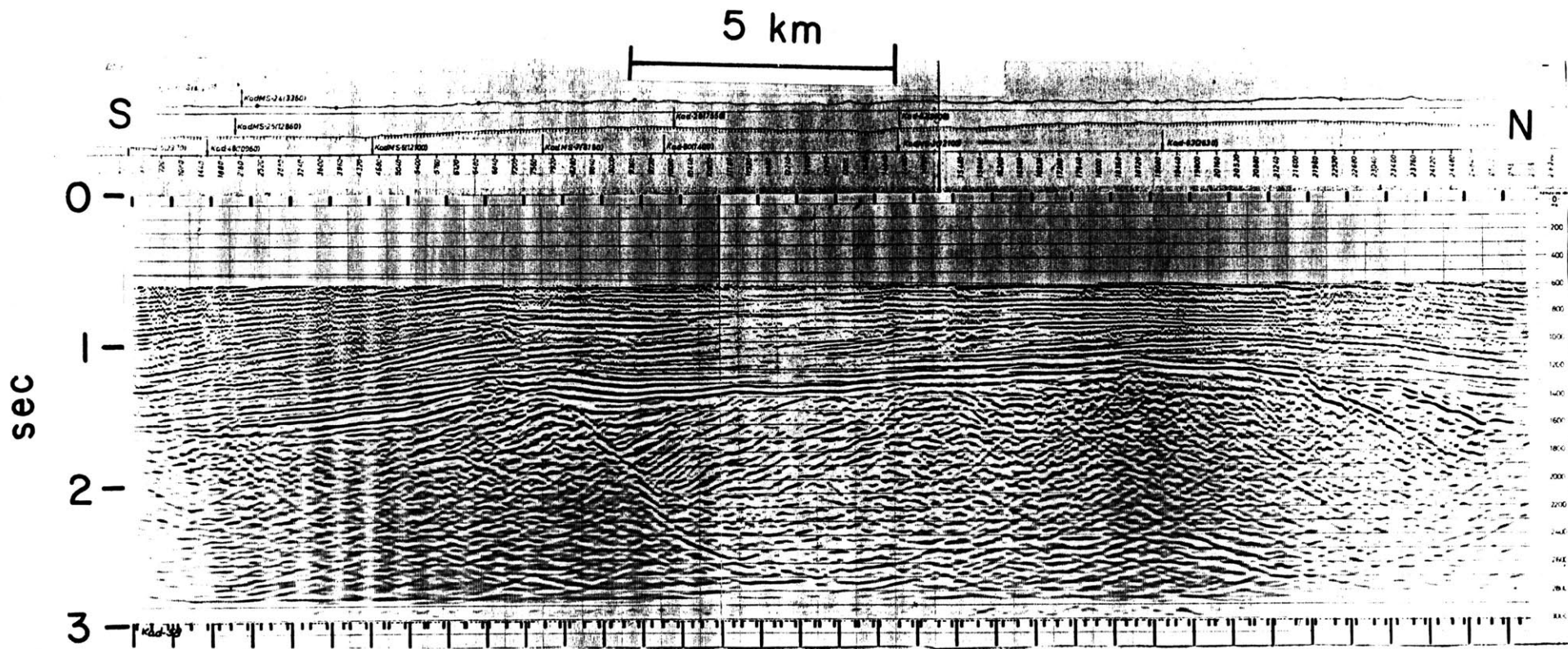
Figure 8

Figure 9a
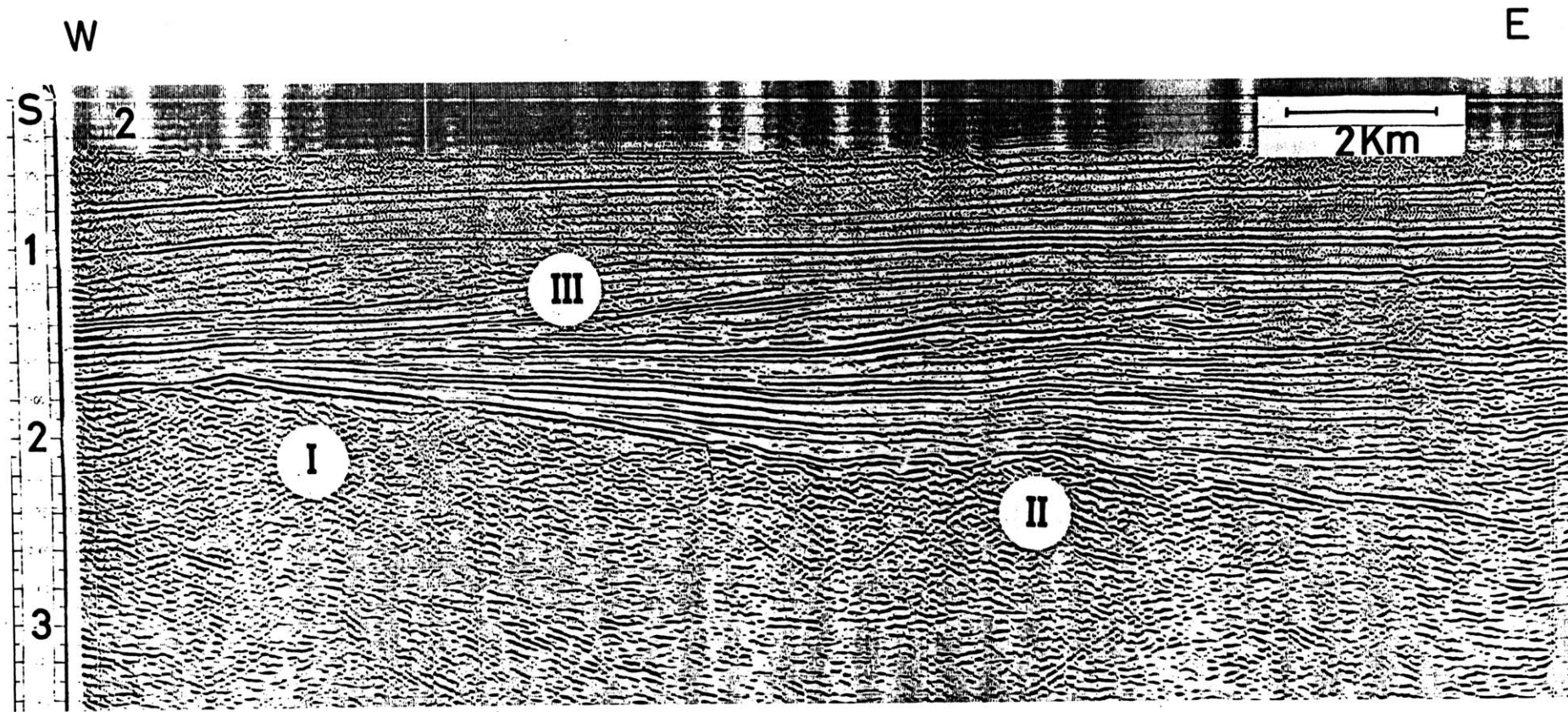
Figure 9b
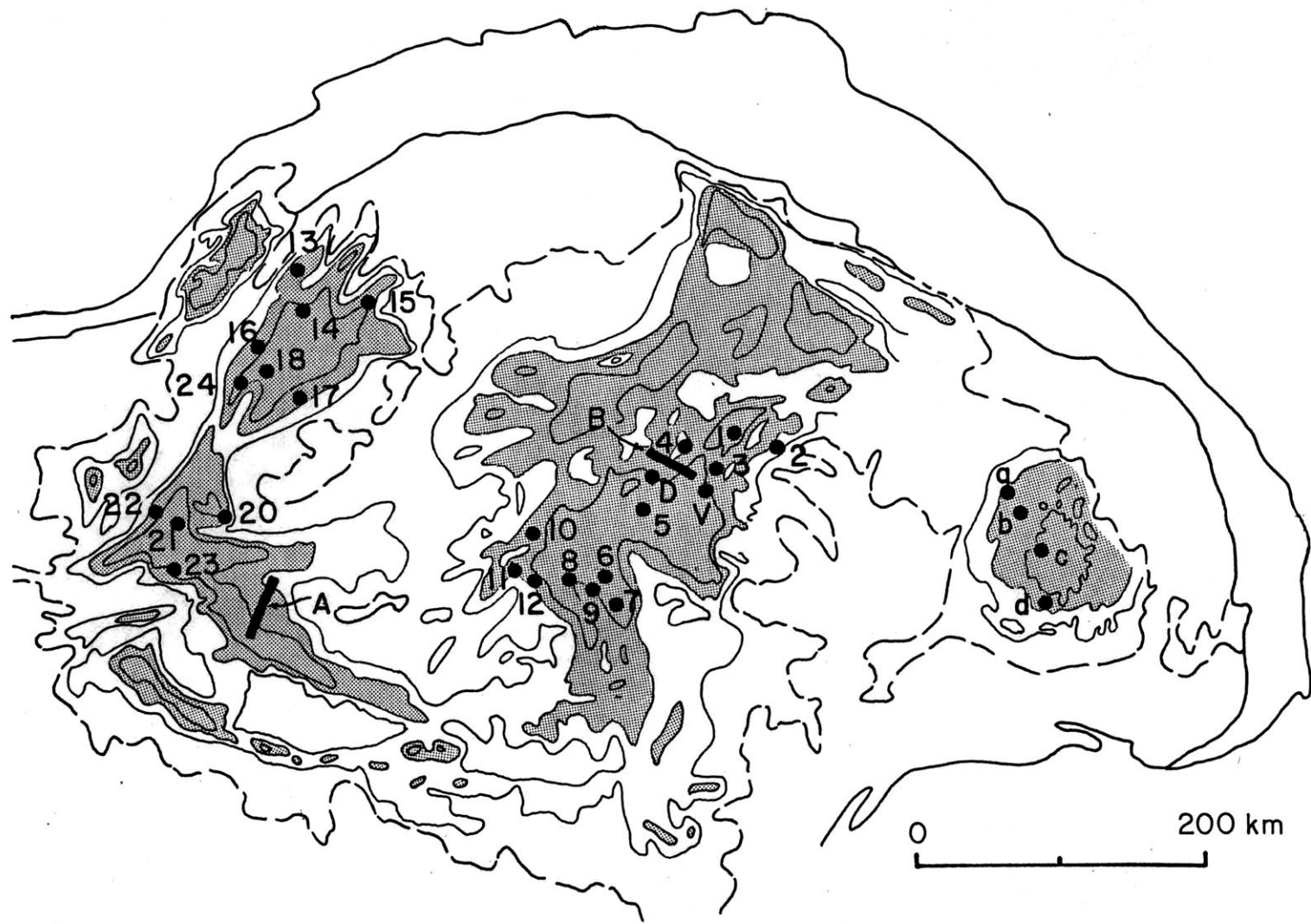
LOCATIONS OF WELLS

Figure 10

UNCORRECTED DEPTH
TO BASEMENT
VERSUS TIME

Figure 11

Figure 12a

■ >100 mW/m²	▨ 60-80 mW/m²	□ <40 mW/m²
▨ 80-100 mW/m²	░ 40-60 mW/m²	▲ ▲ HEAT FLOW STATIONS
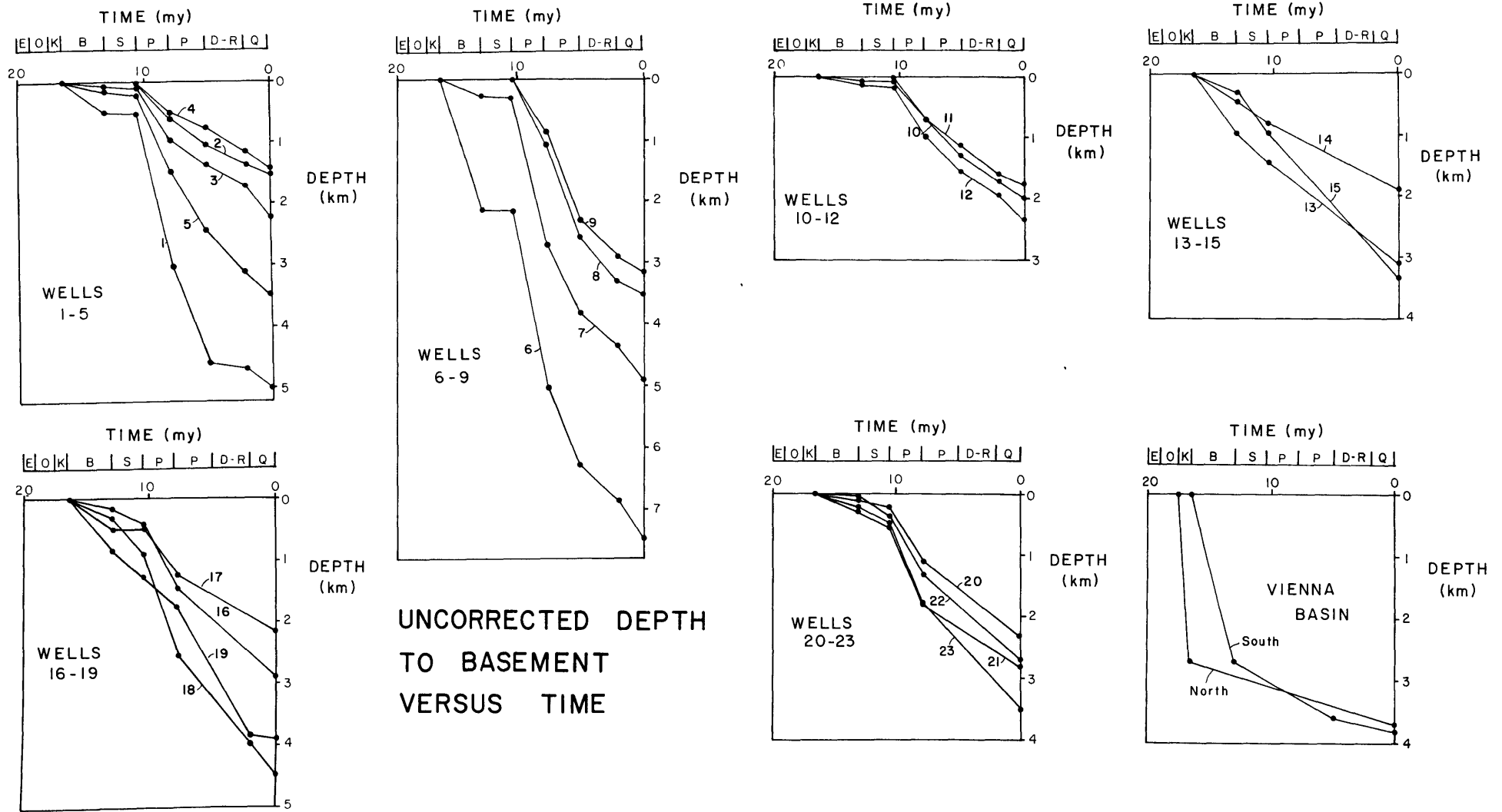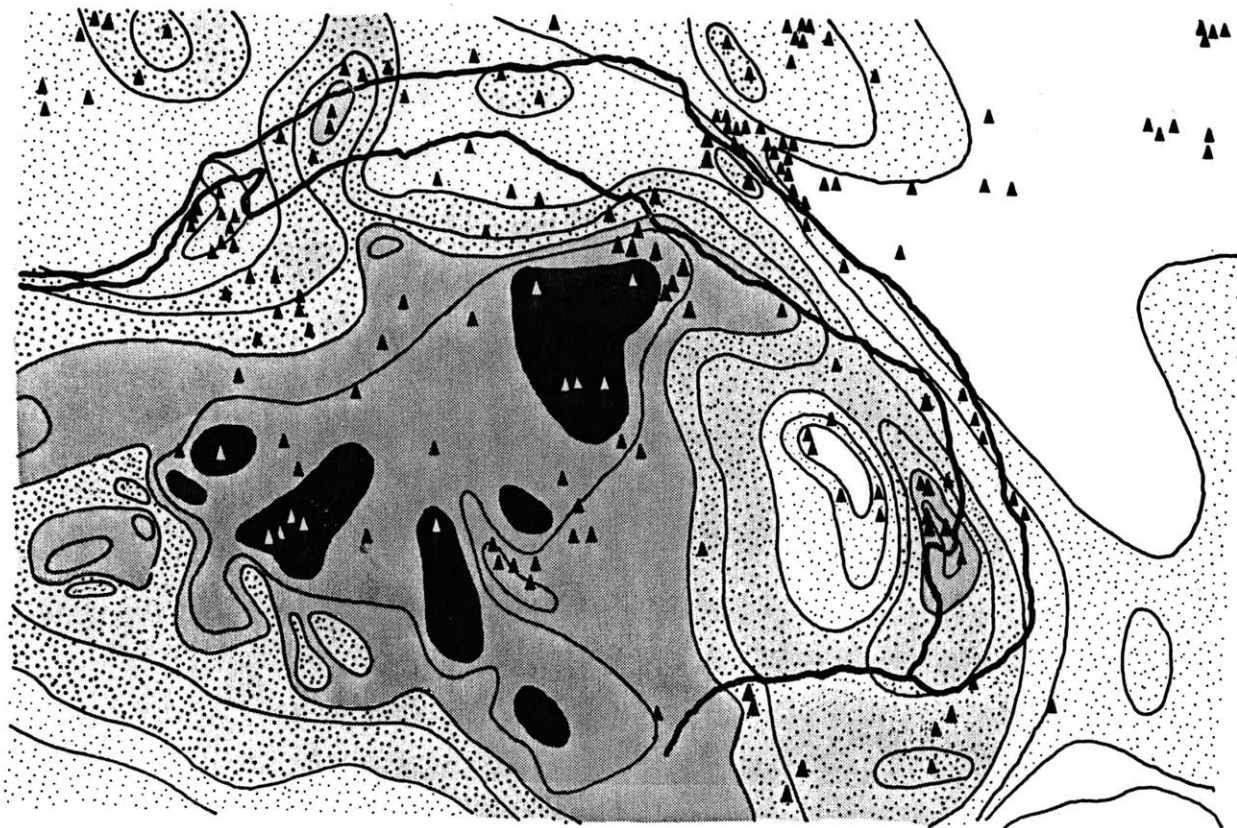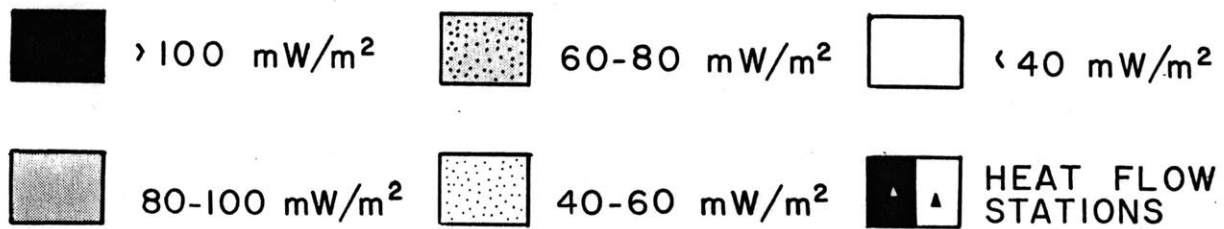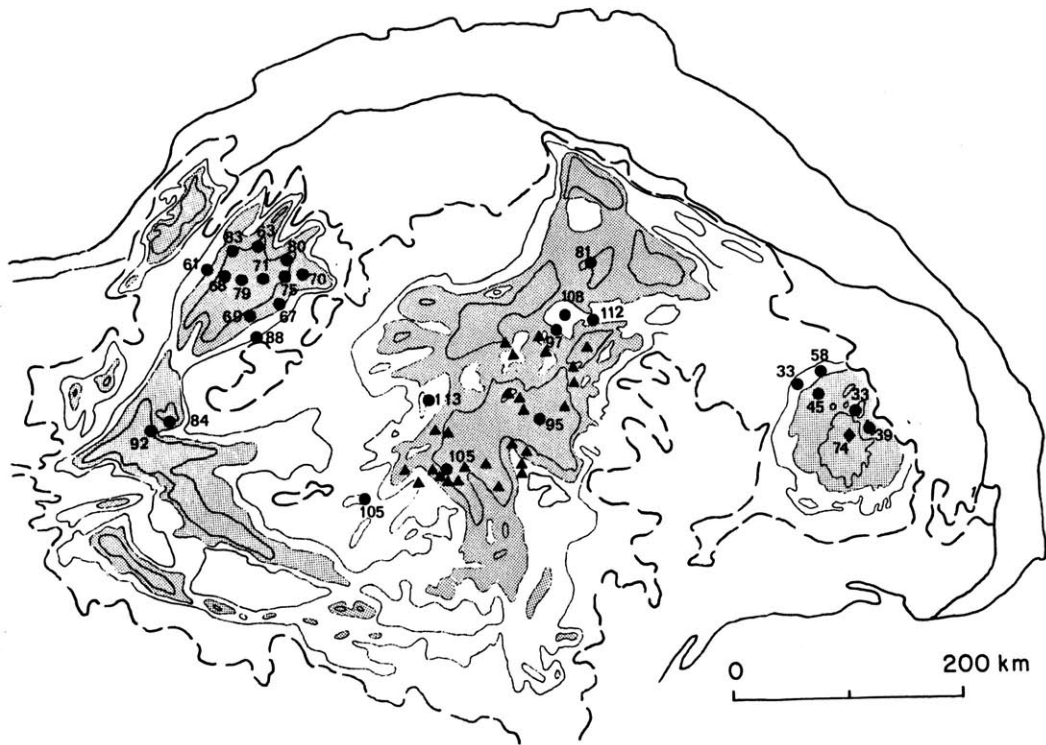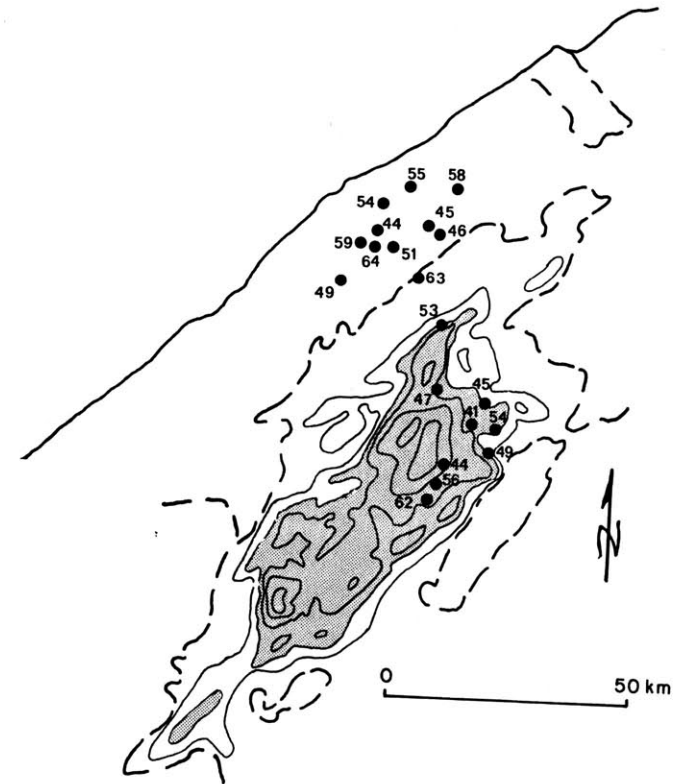
LOCATIONS OF TEMPERATURE AND HEAT FLOW MEASUREMENTS

Figure 12b

Figure 12c

198

Figure 13

DEPTH TO MOHO (in kms)

1   2   3   4 — 25

0 20 40 60 80 100   200 km

b) UNIFORM EXTENSION

β = 1.50

d) AFTER COOLING

a) INITIAL CONDITIONS

c) MODIFIED EXTENSION

β = 2.25

e) AFTER COOLING

Figure 14

INITIAL SUBSIDENCE
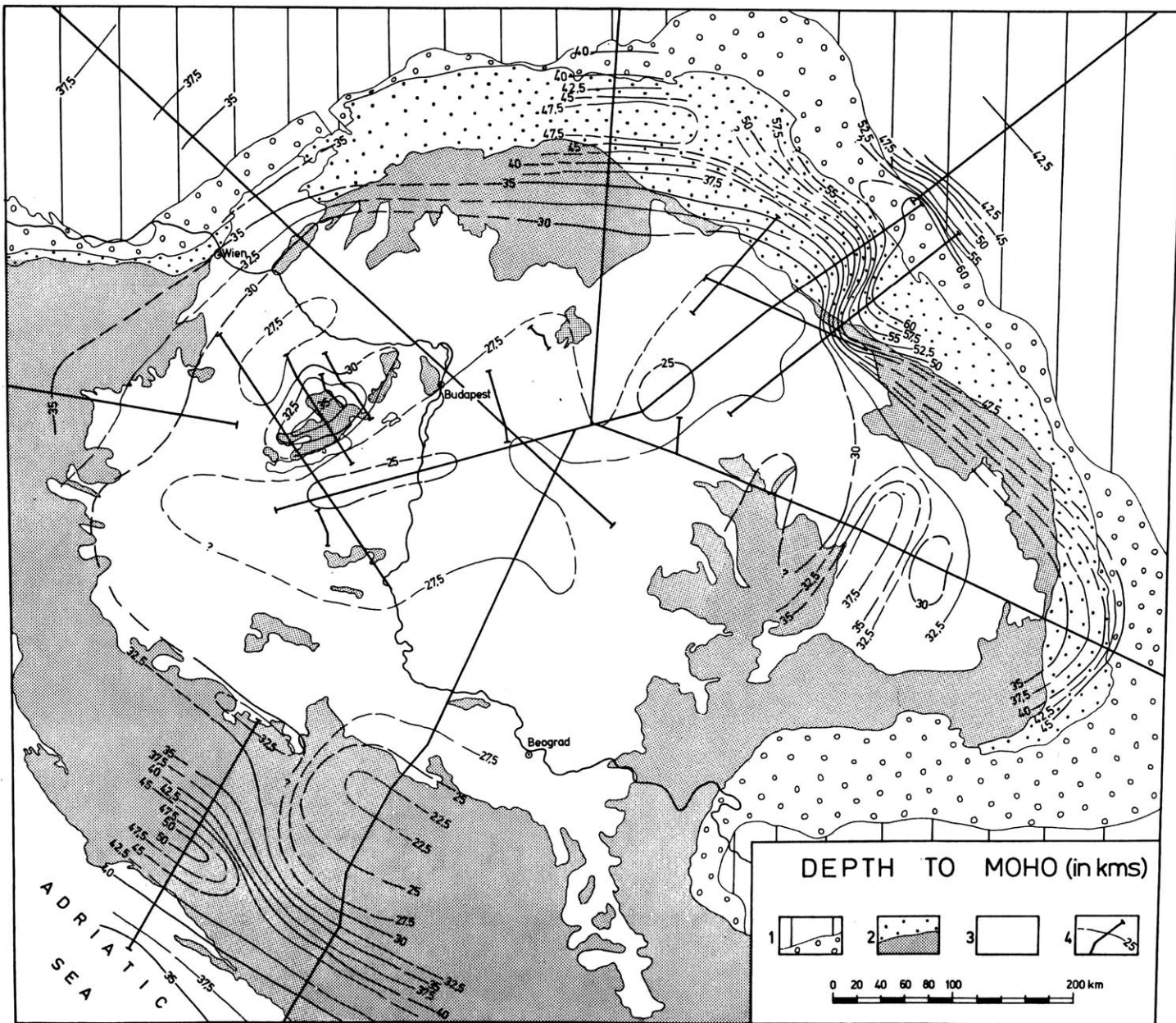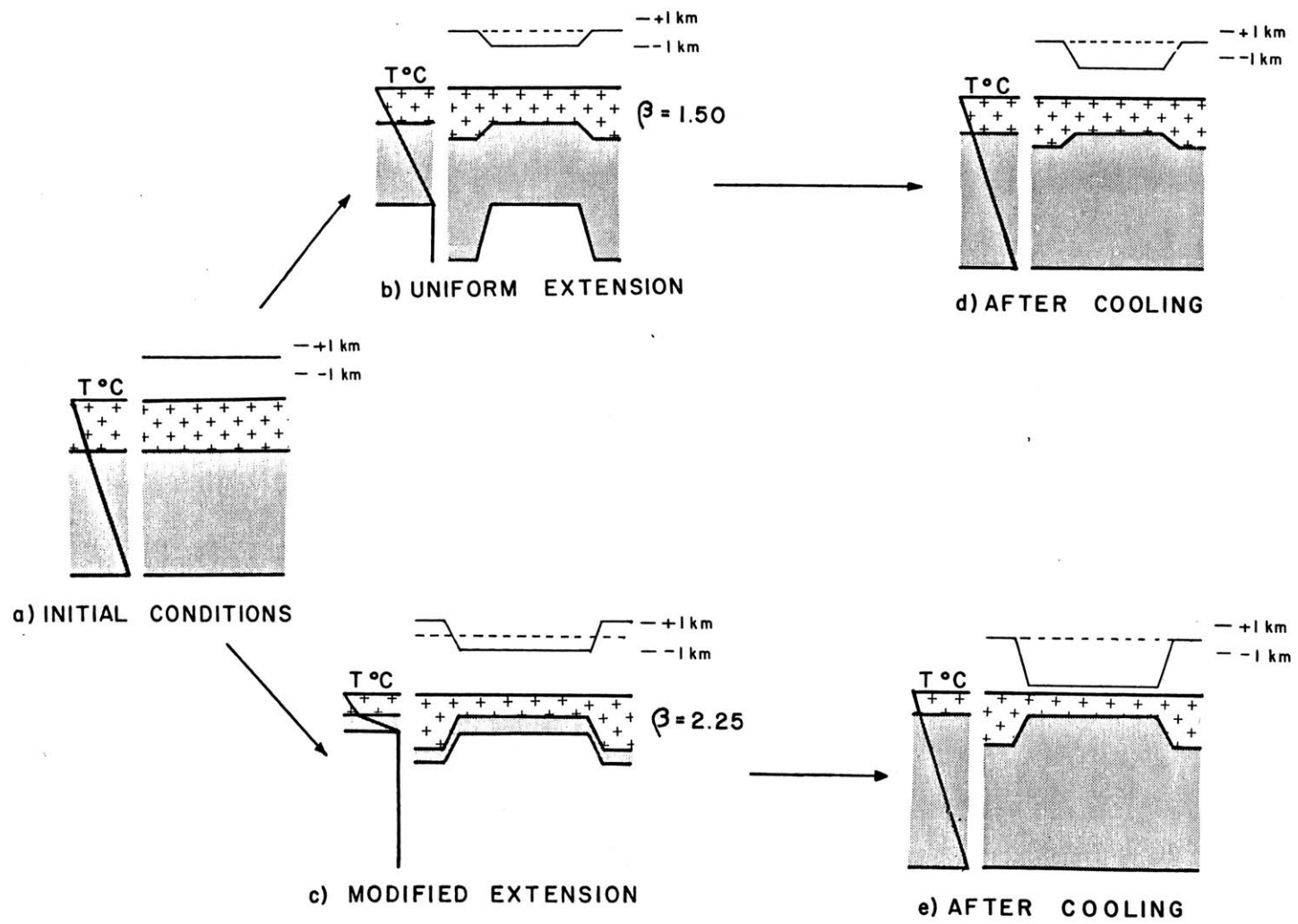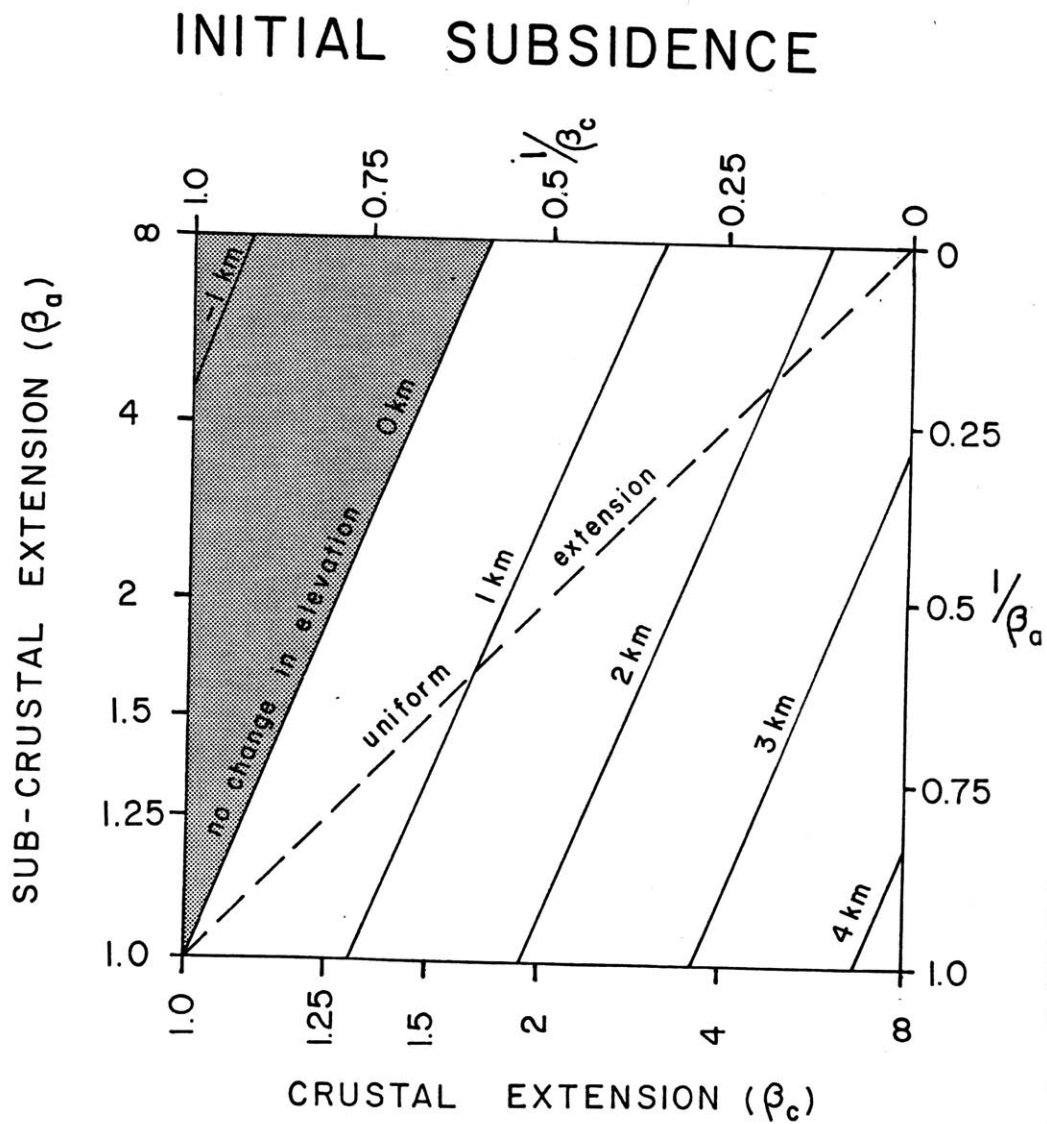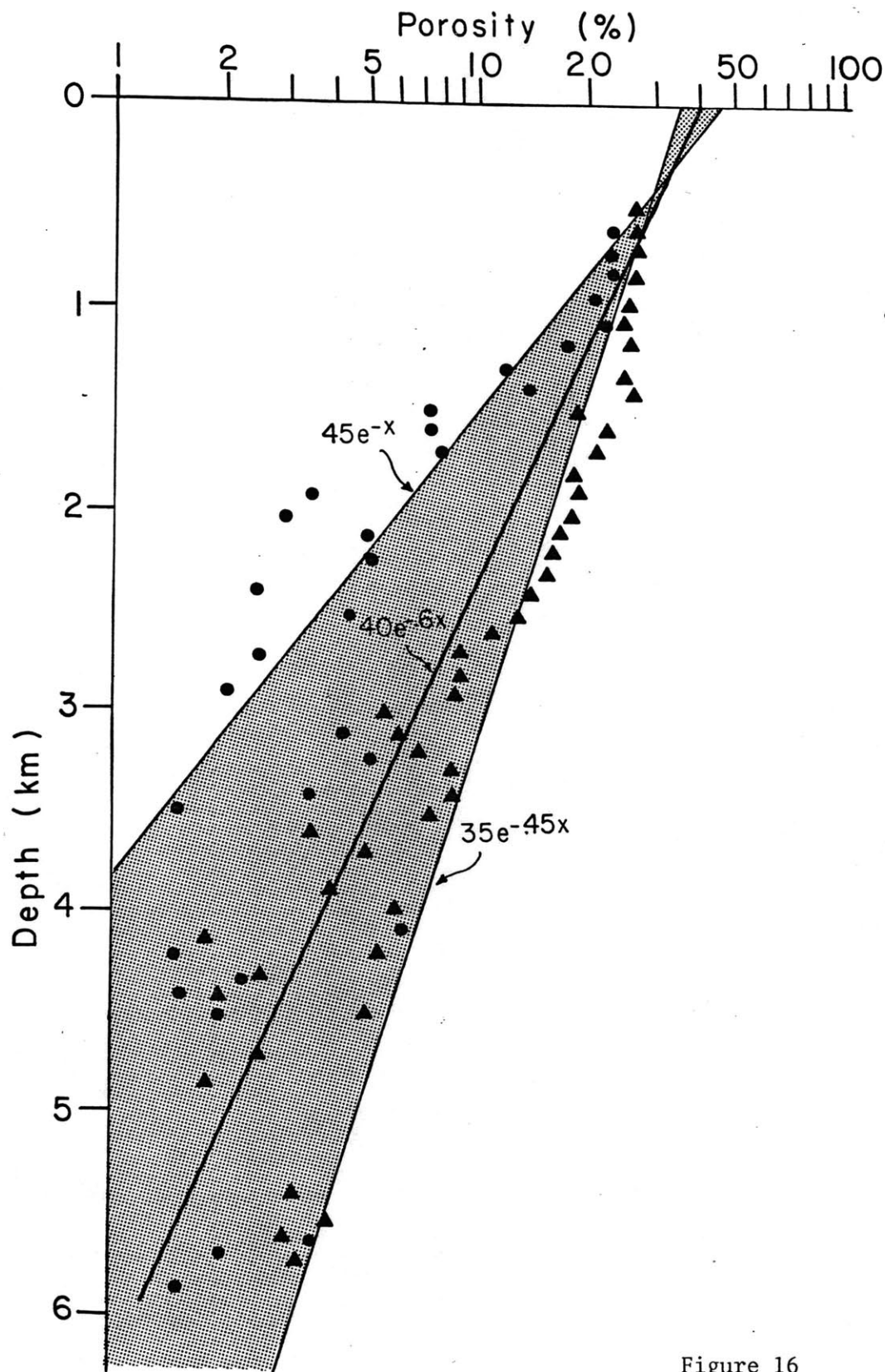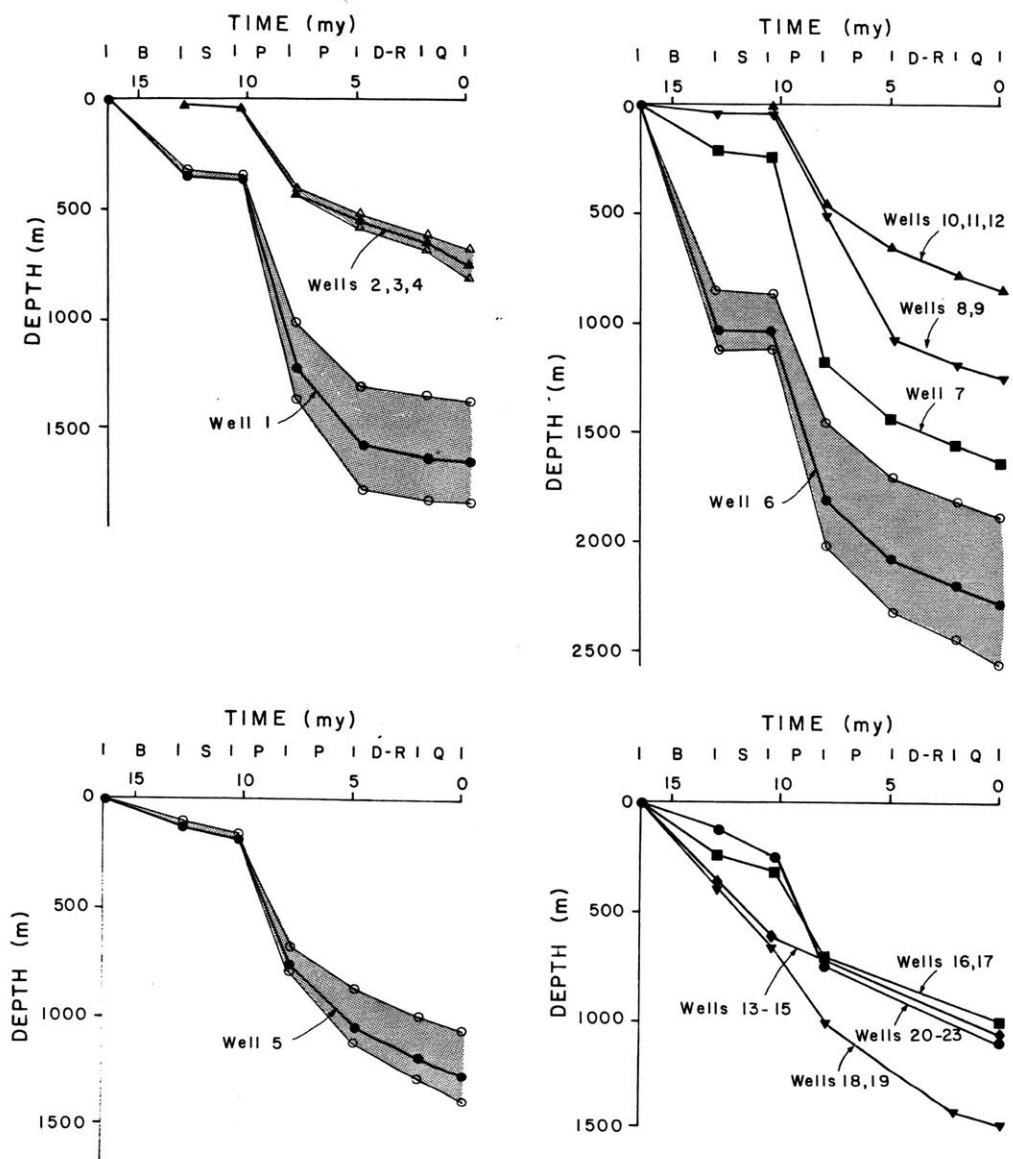
Figure 15

Figure 16

CORRECTED SUBSIDENCE DETERMINED FROM SEDIMENTATION DATA

Figure 17

Figure 18

THERMAL CONDUCTIVITY (W/m°K)
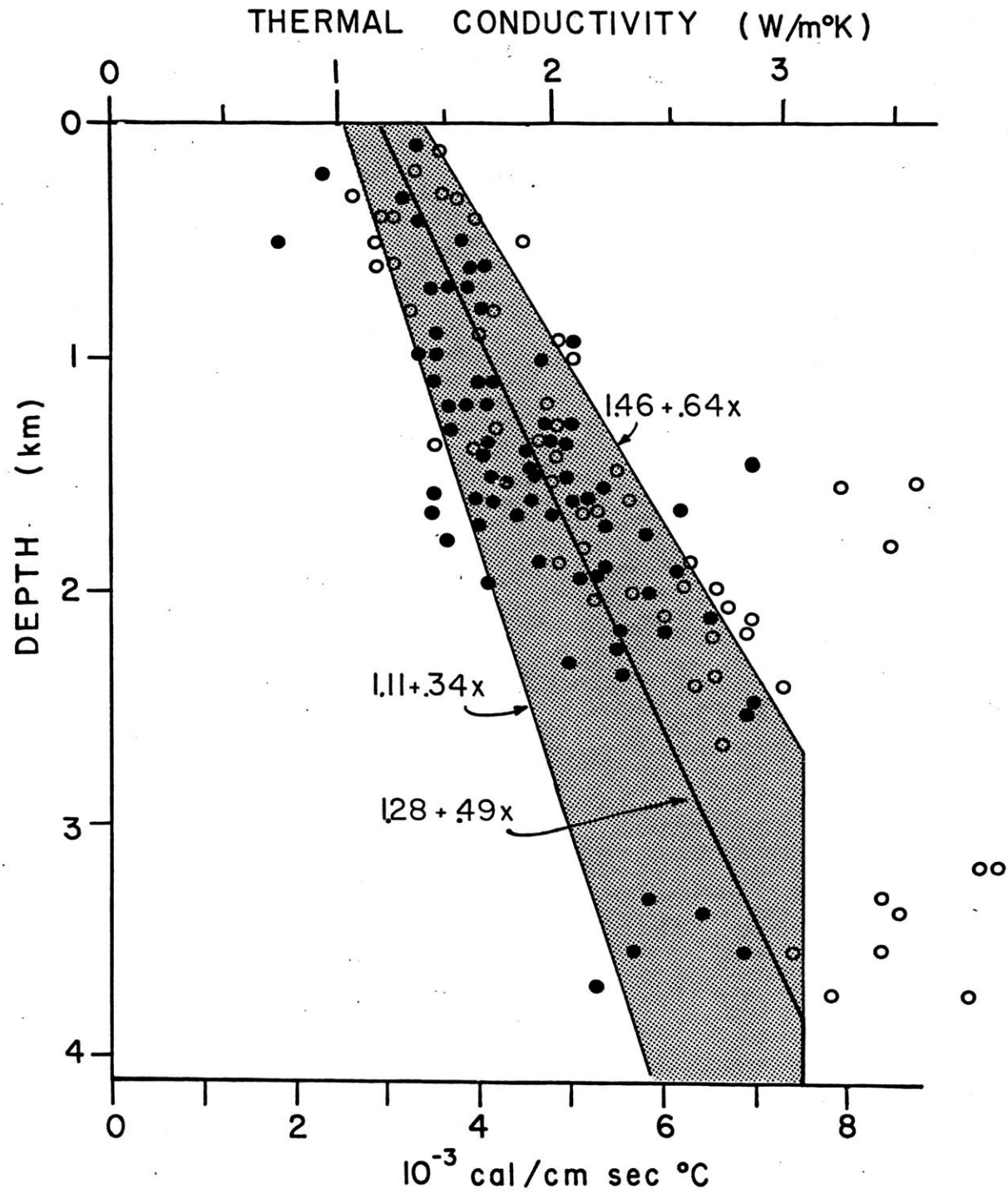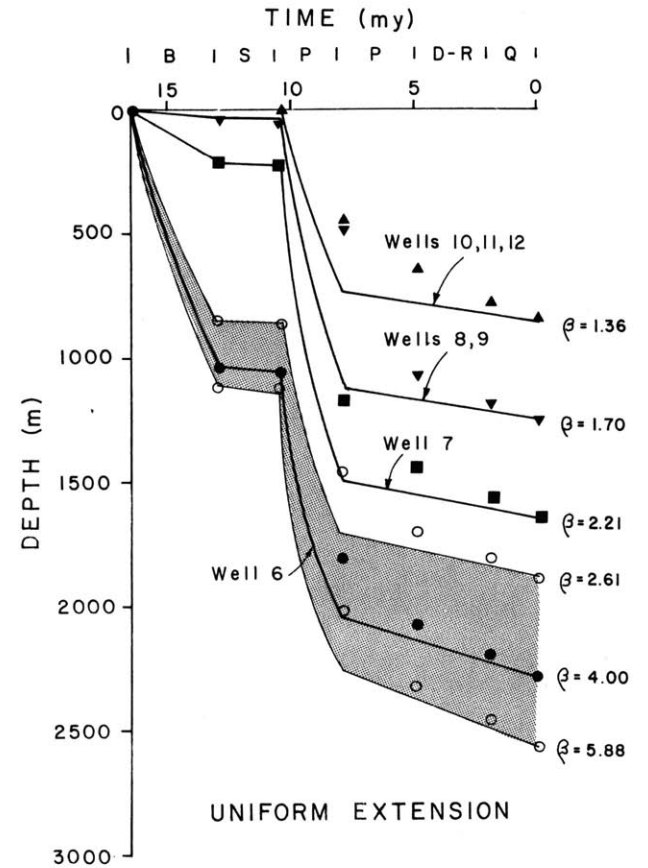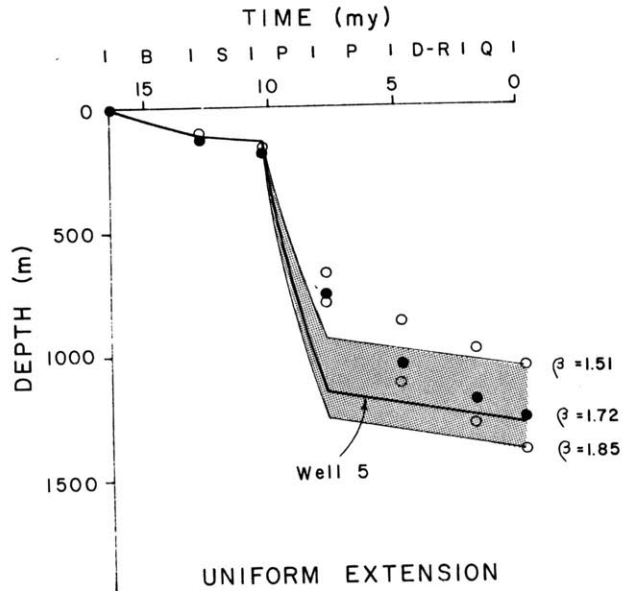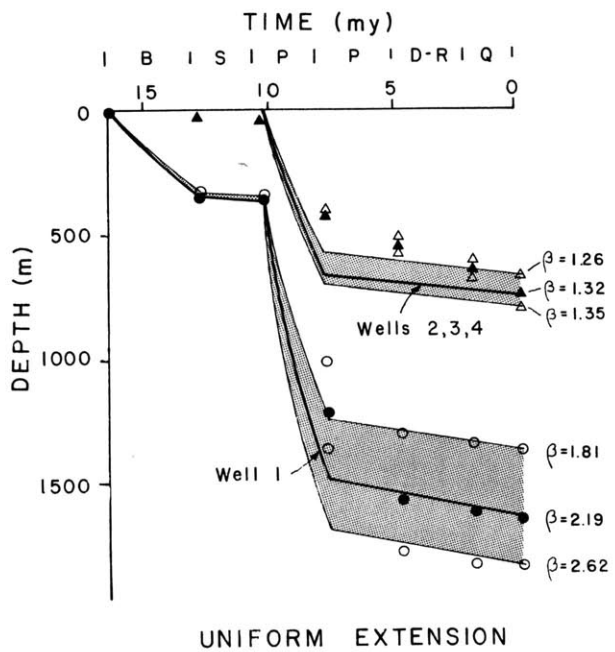
CORRECTED SUBSIDENCE (PREDICTED): WELLS 1-12
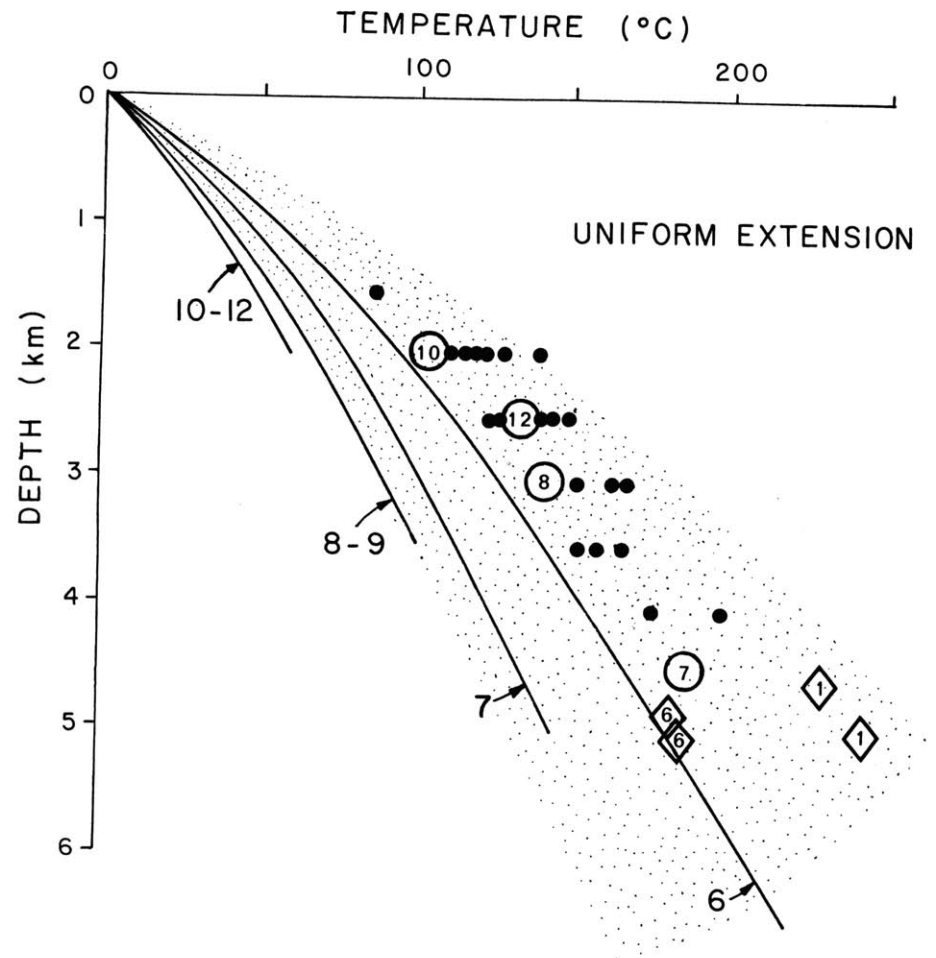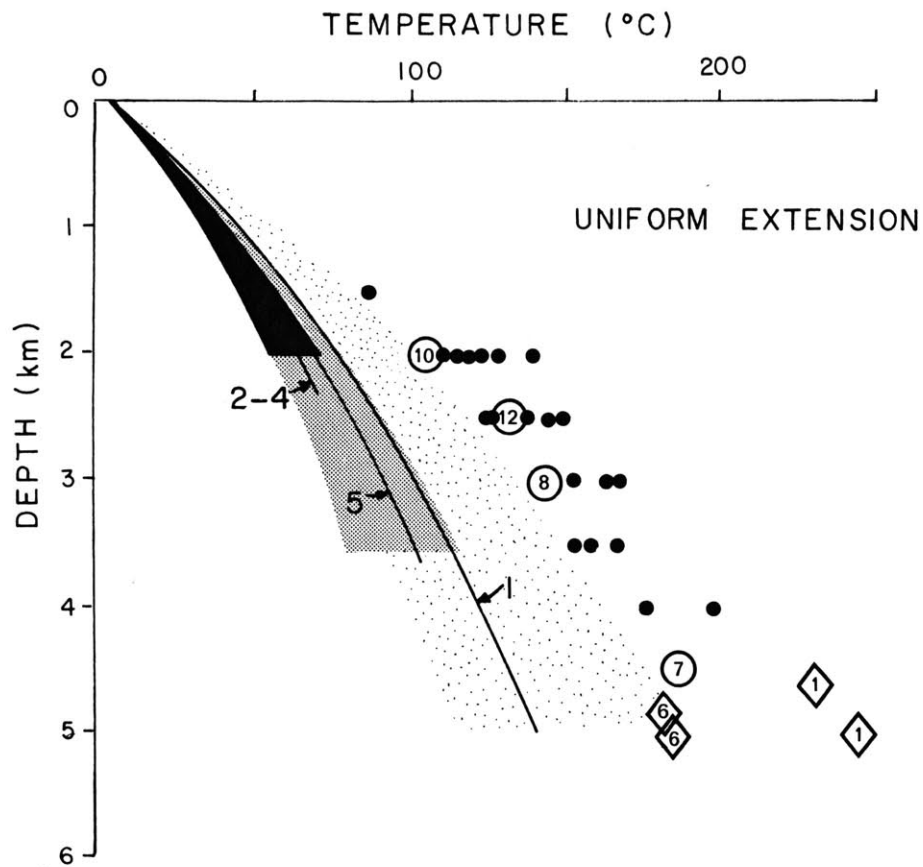
Figure 19

COMPARISON OF OBSERVED AND PREDICTED TEMPERATURES

Figure 20

Figure 21

a   b   c   d

BADENIAN   SARMATIAN   PANNONIAN

16.5 Ma   13.0 Ma   10.5 Ma   8.0 Ma

Figure 22

208
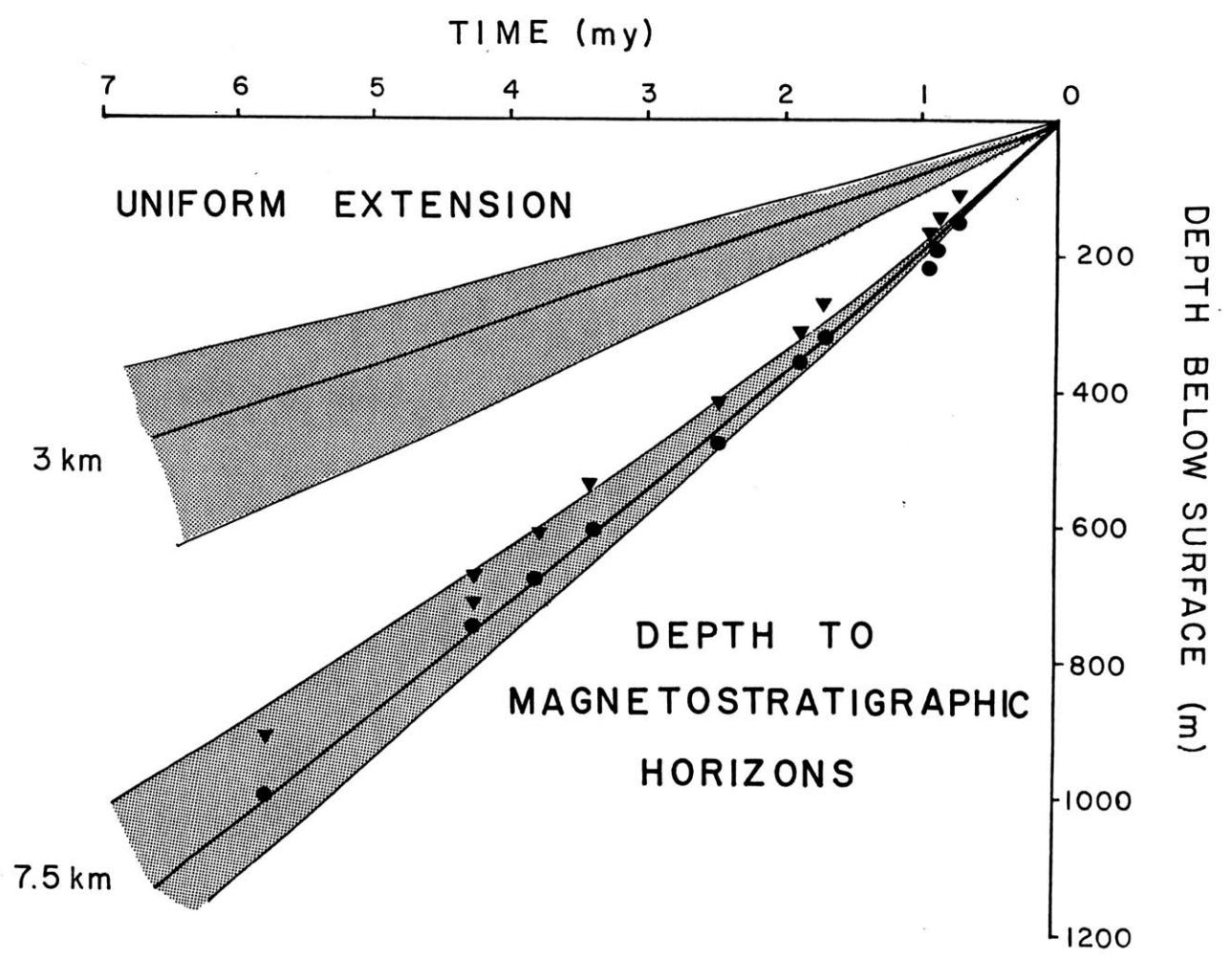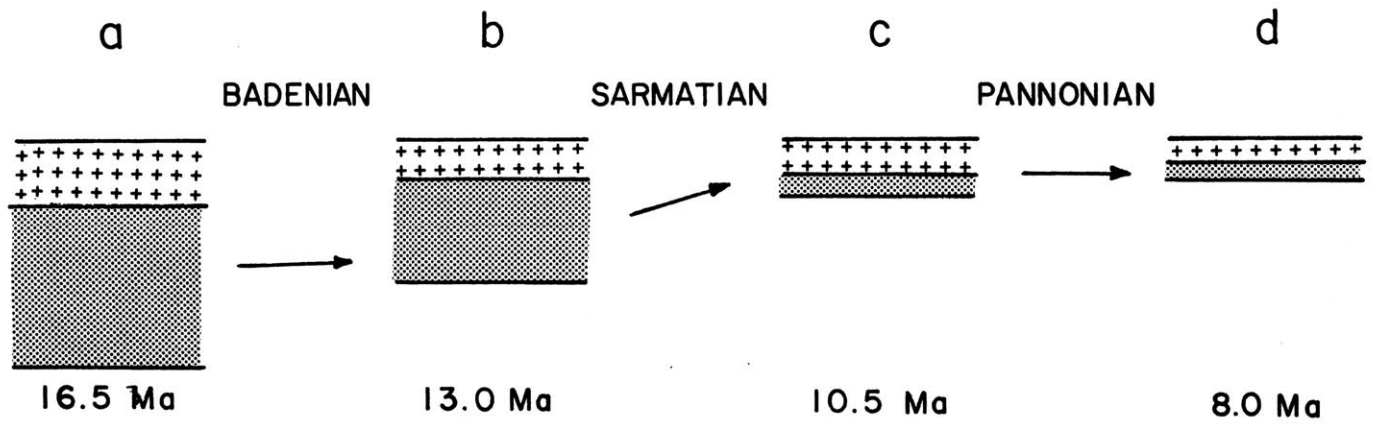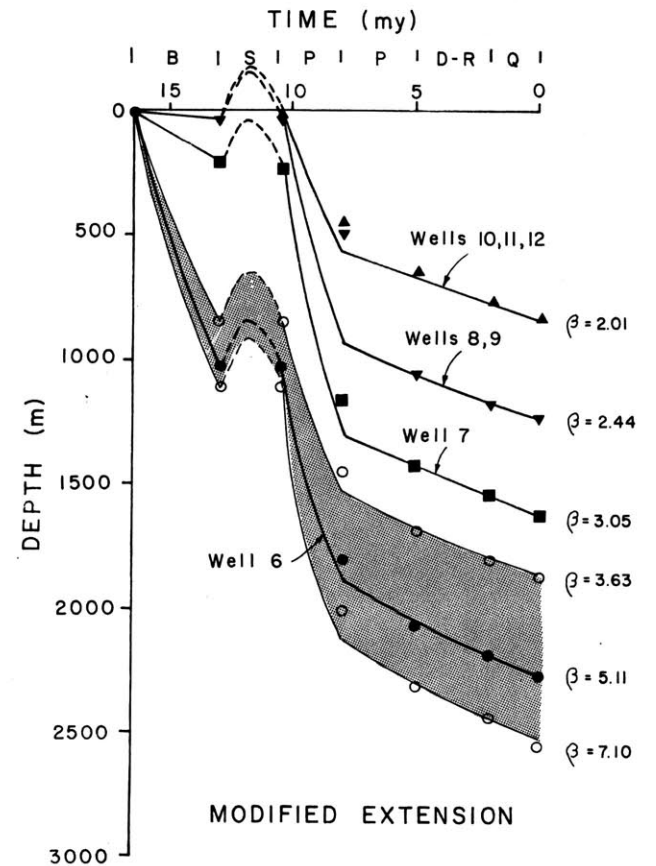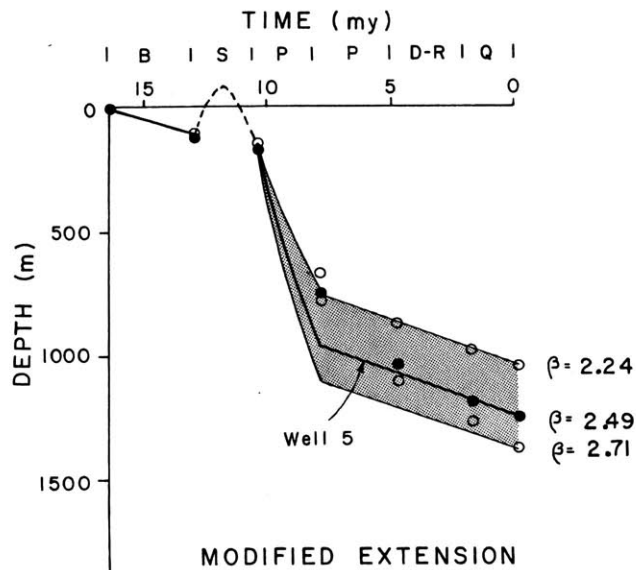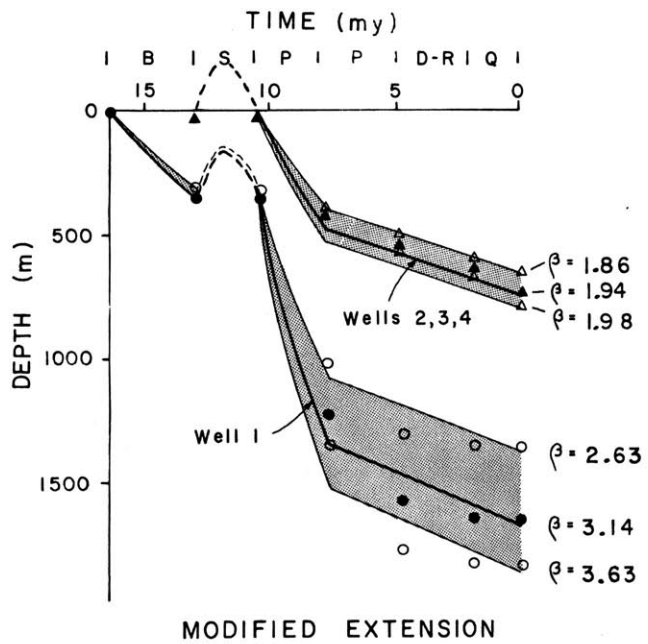
CORRECTED SUBSIDENCE (PREDICTED): WELLS 1-12
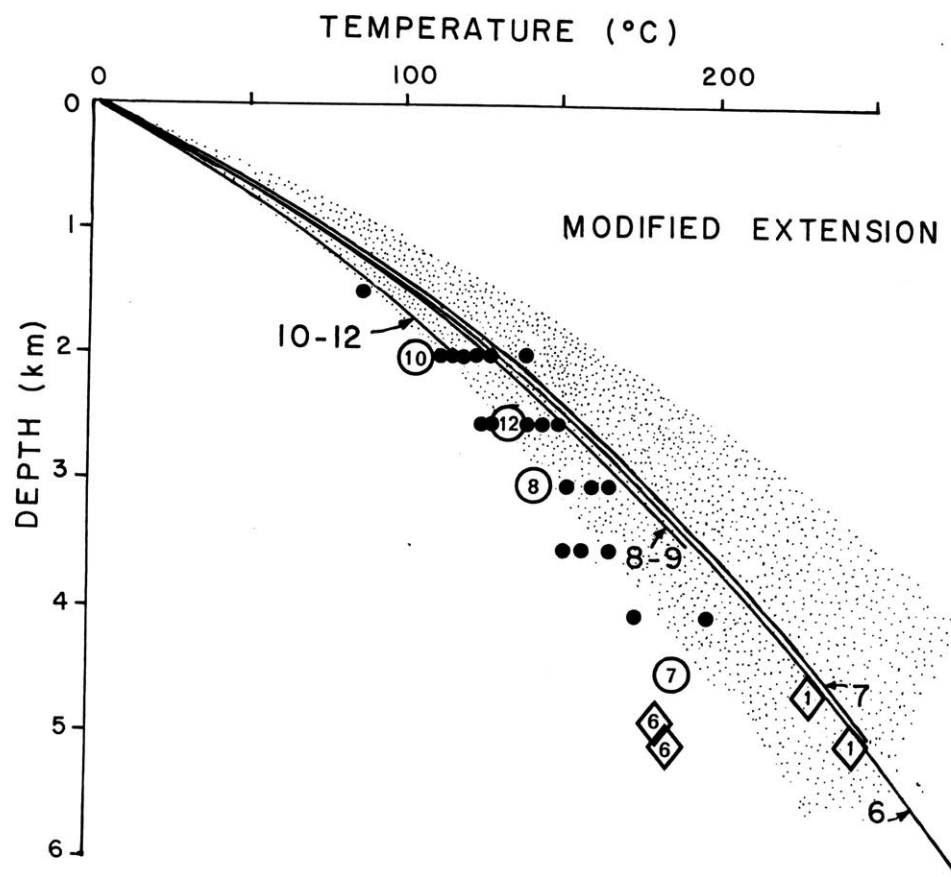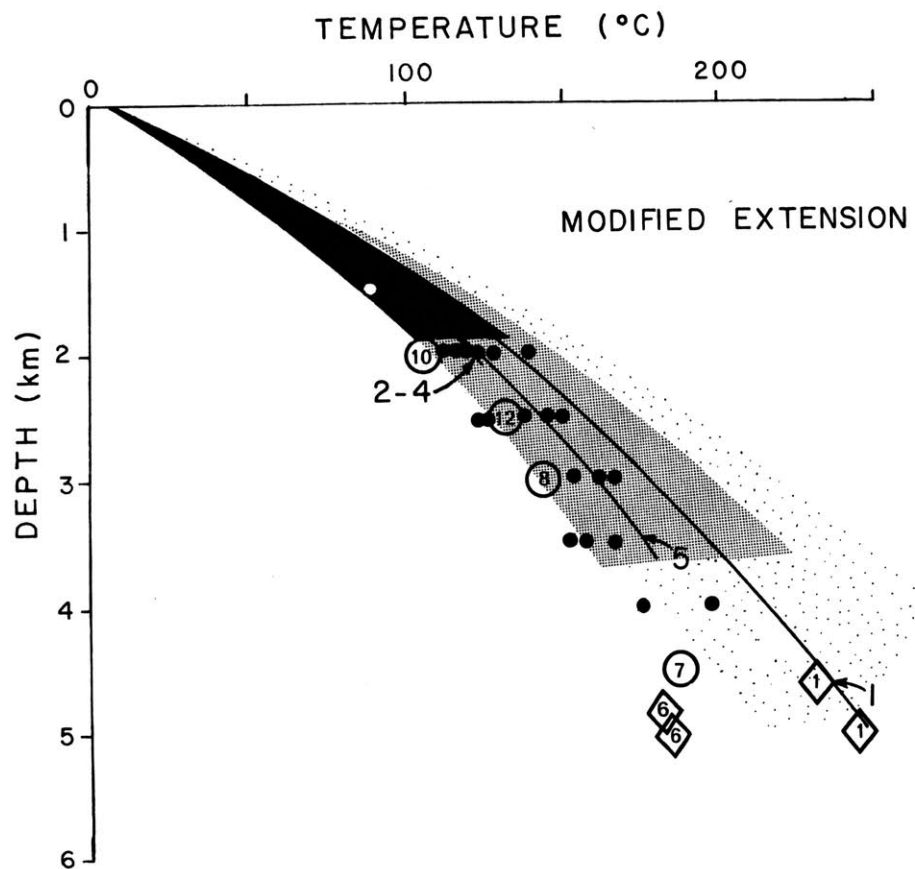
Figure 23

COMPARISON OF OBSERVED AND PREDICTED TEMPERATURES

Figure 24
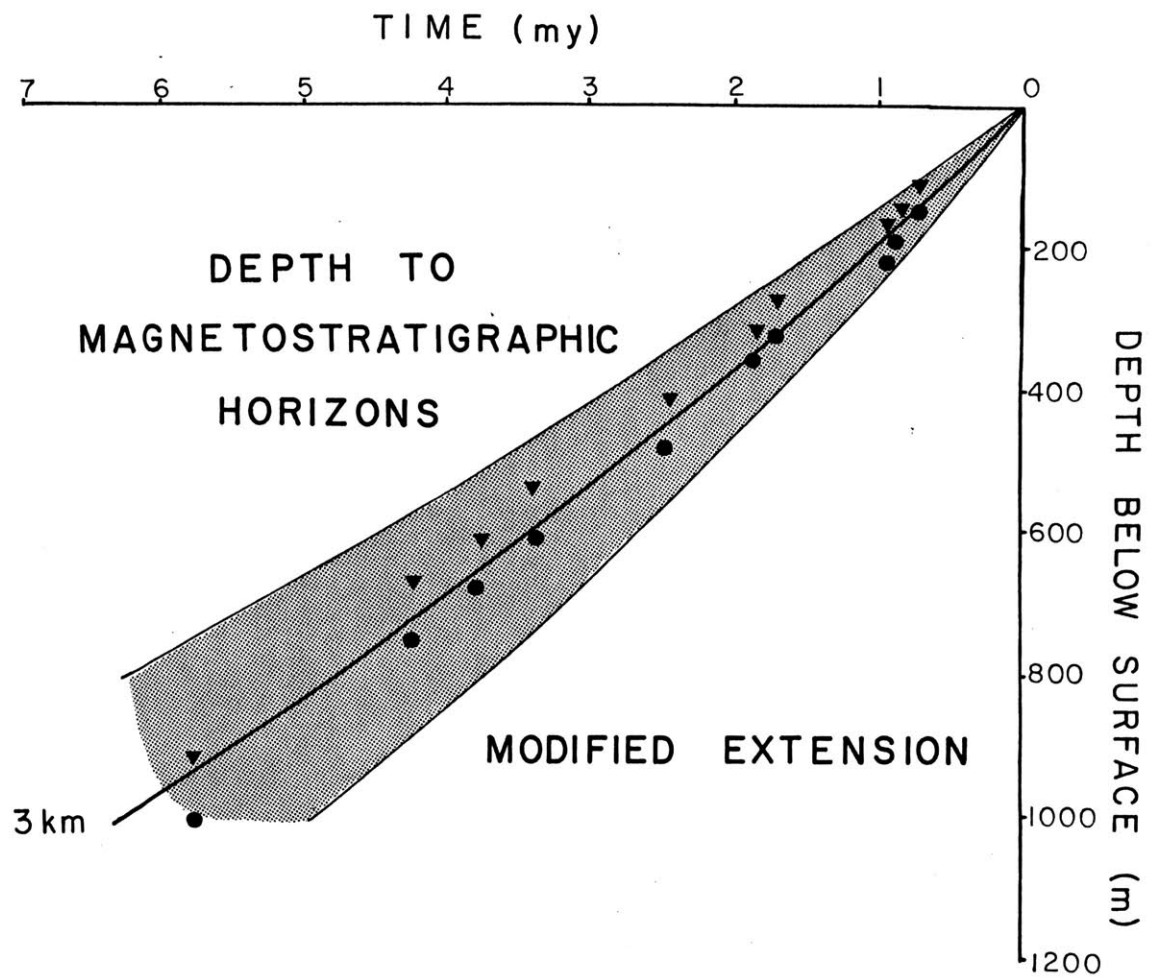
Figure 25
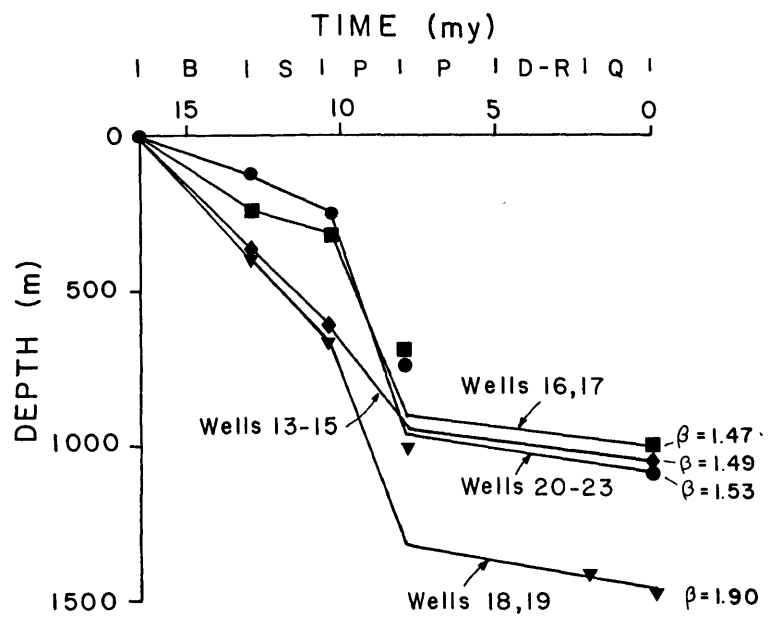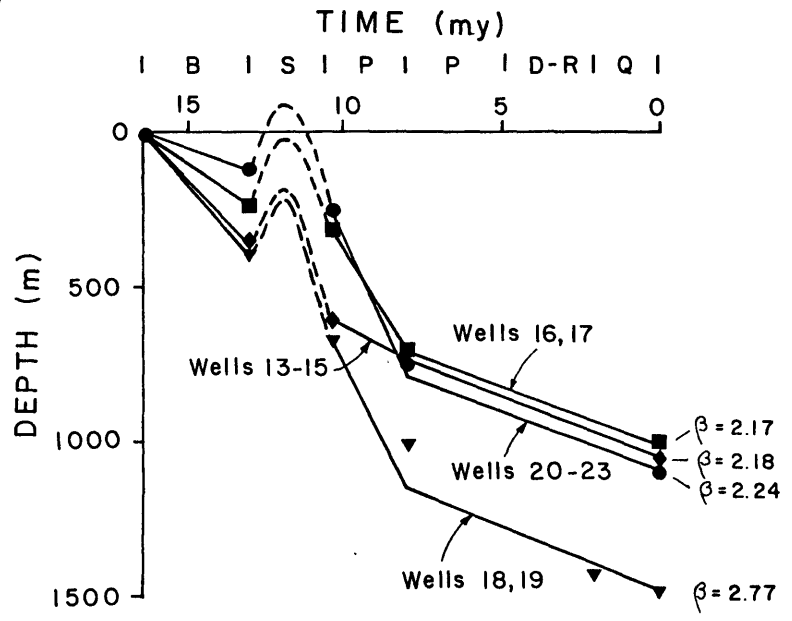
CORRECTED SUBSIDENCE (PREDICTED): WELLS 13-23

Figure 26
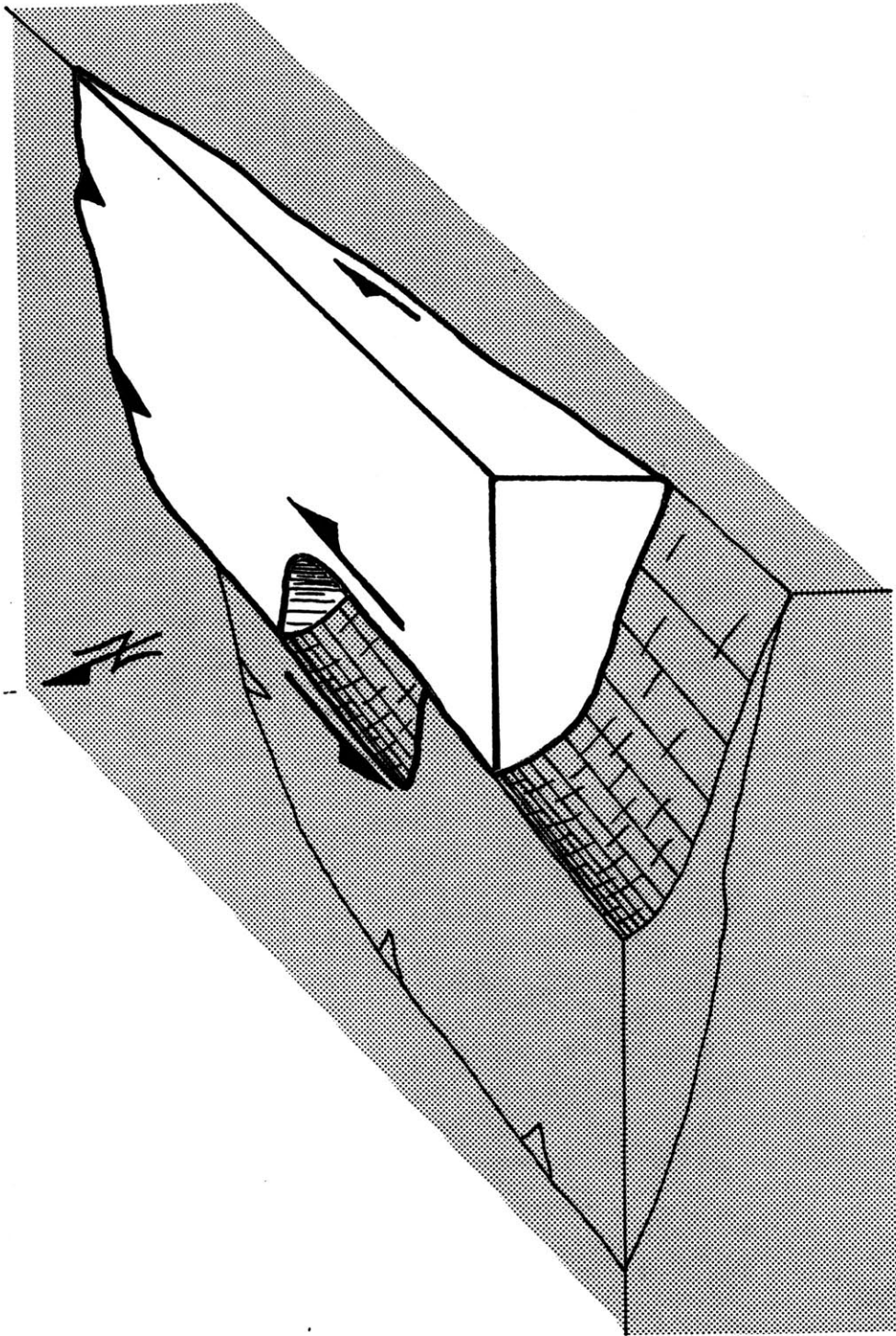
Figure 27
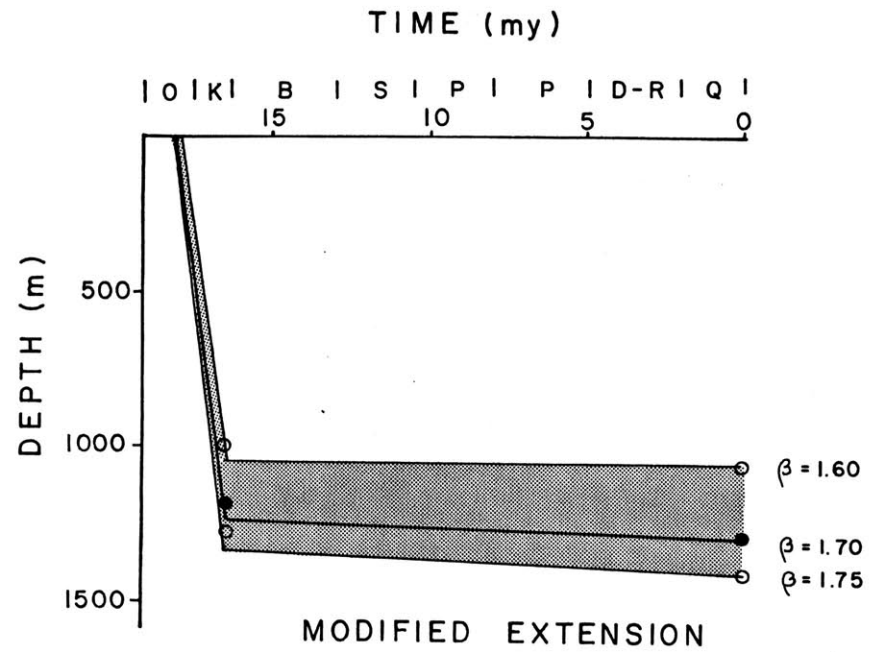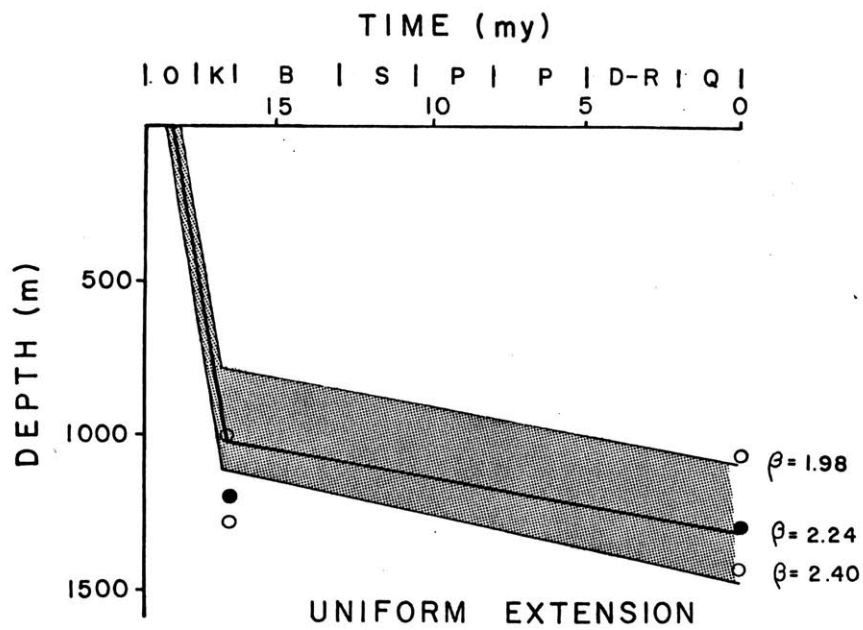
CORRECTED SUBSIDENCE (PREDICTED): VIENNA BASIN

Figure 28

BEGINNING OF KARPATIAN (17.5 Ma)

Figure 29a

BEGINNING OF BADENIAN (16.5 Ma)
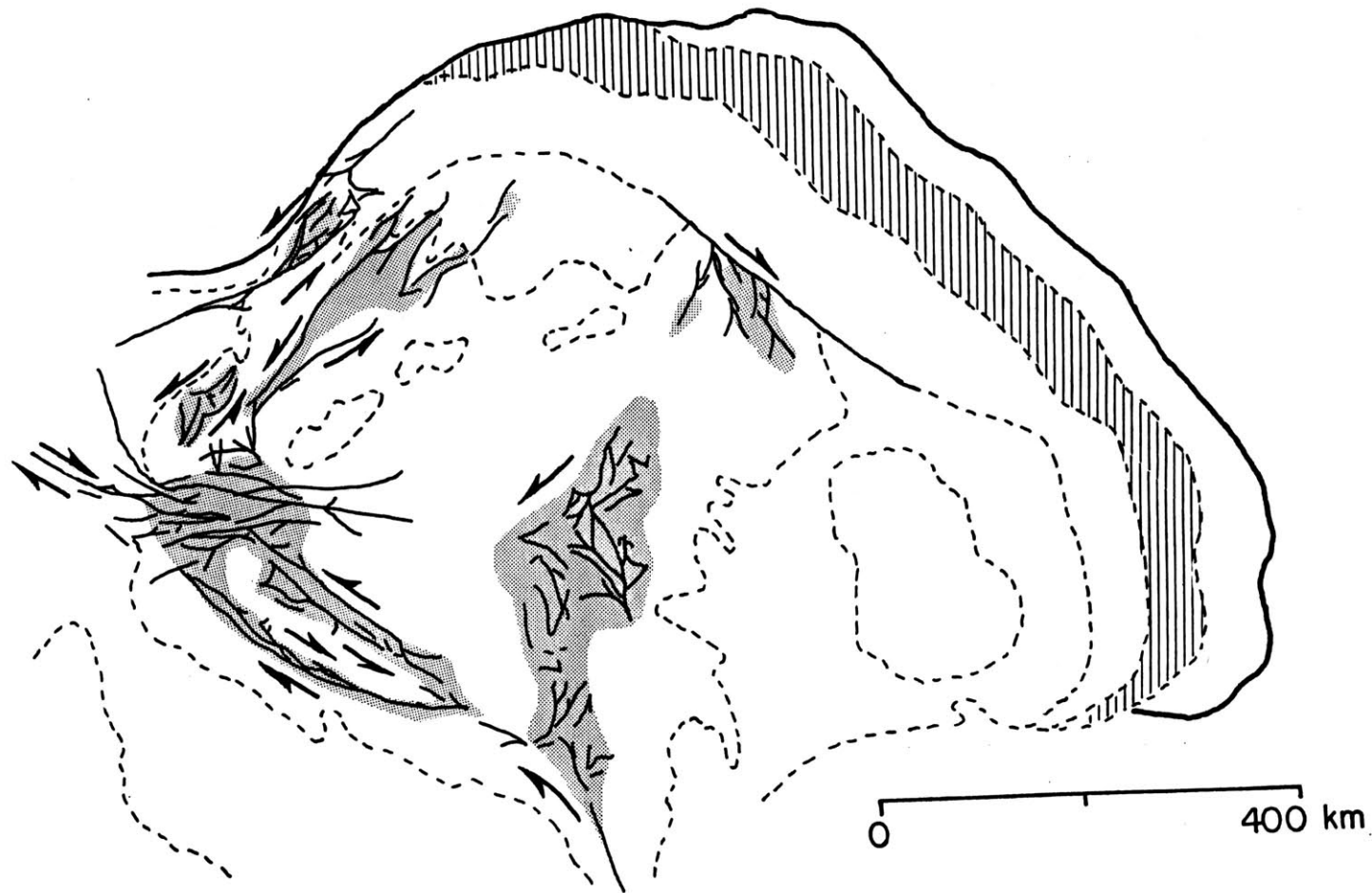
Figure 29b

BEGINNING OF SARMATIAN (13.0 Ma)

0 — 400 km

Figure 29c

PRESENT

400 km

W   E

E

Marginal Folds
nappe

Sub Carpathian
nappe

W   Ceahleau
nappe

Curbicortical Flysch
nappe

Audia
nappe

Tarcau nappe

0   5   30km

Horizontal and vertical scale.
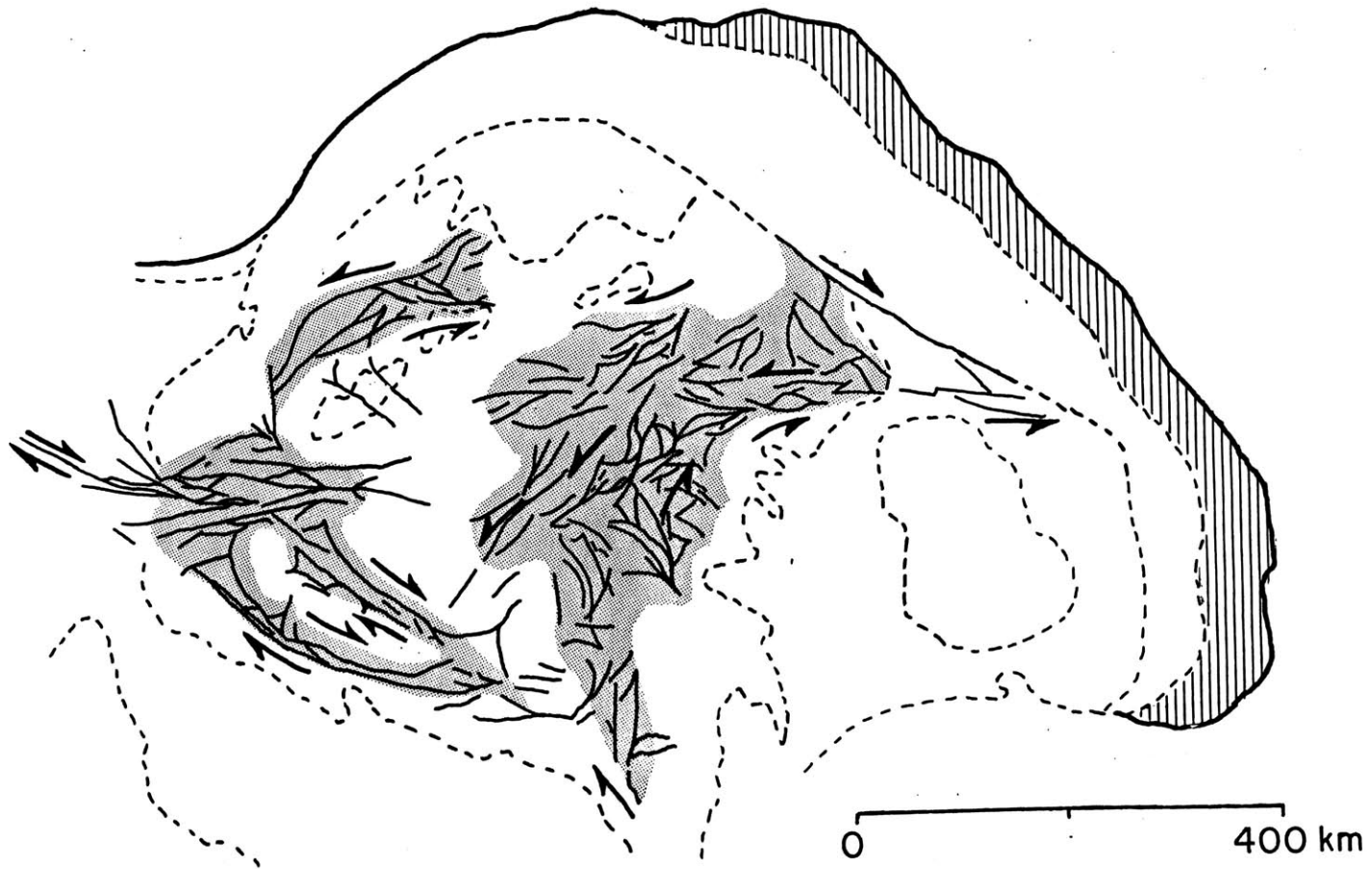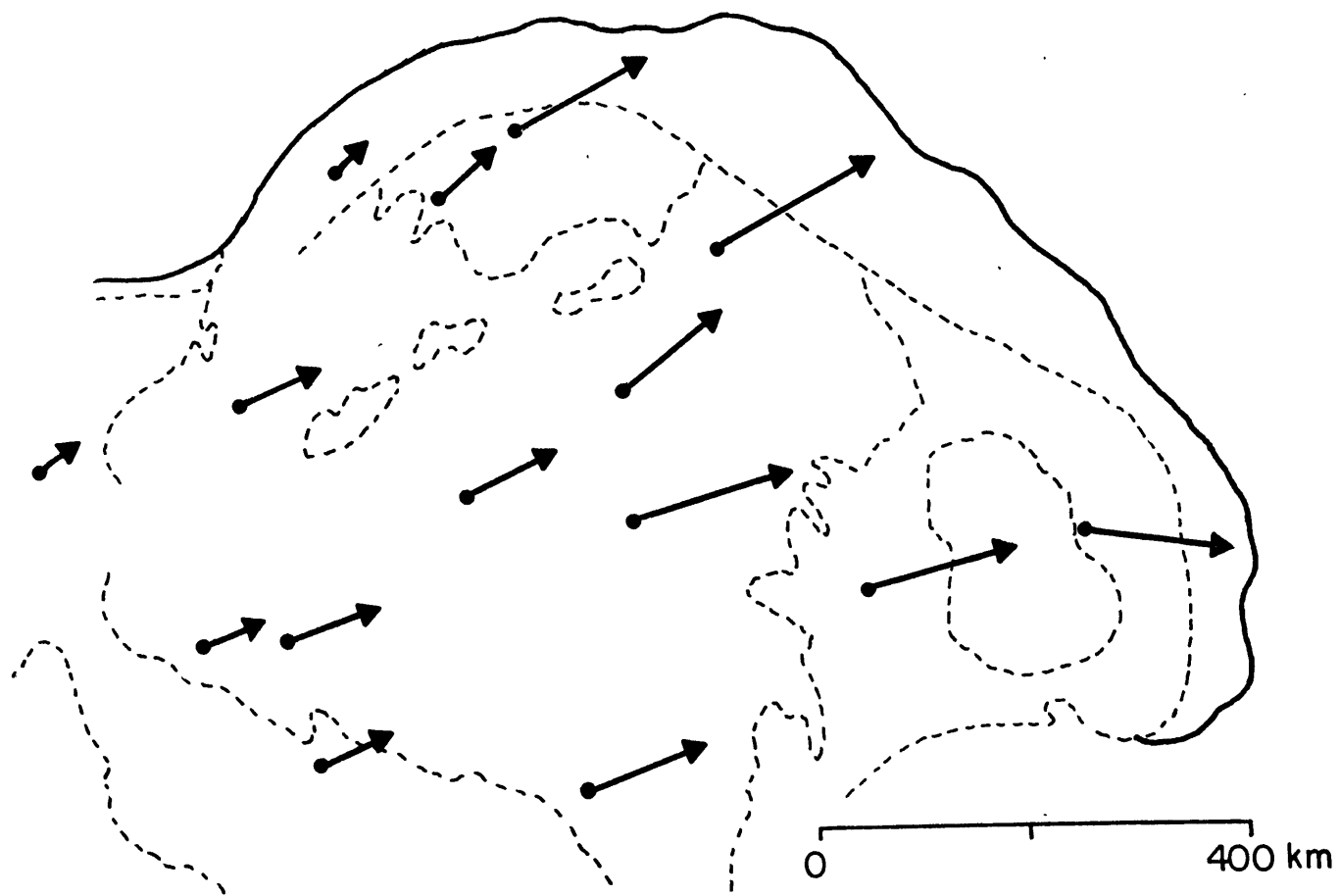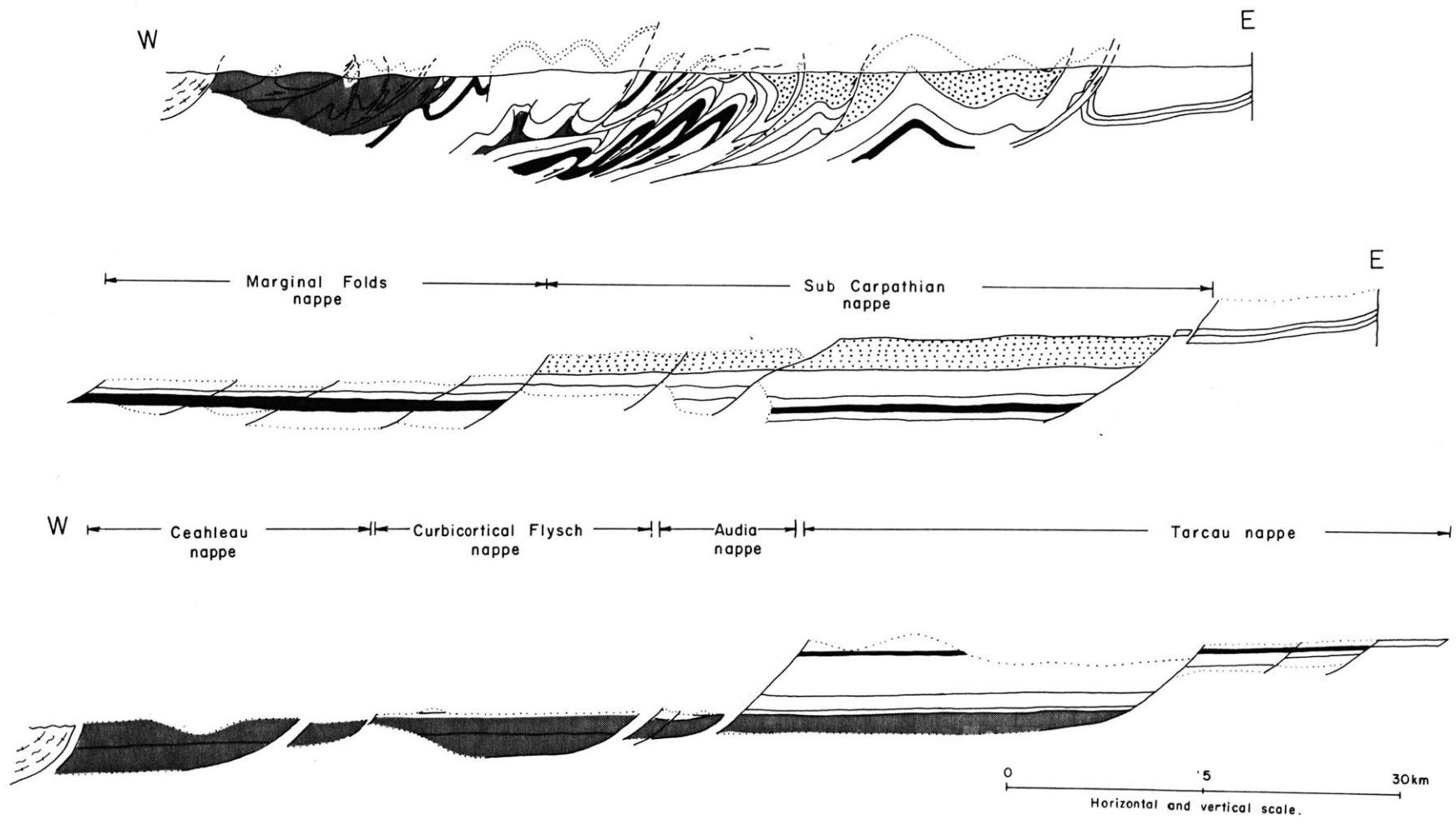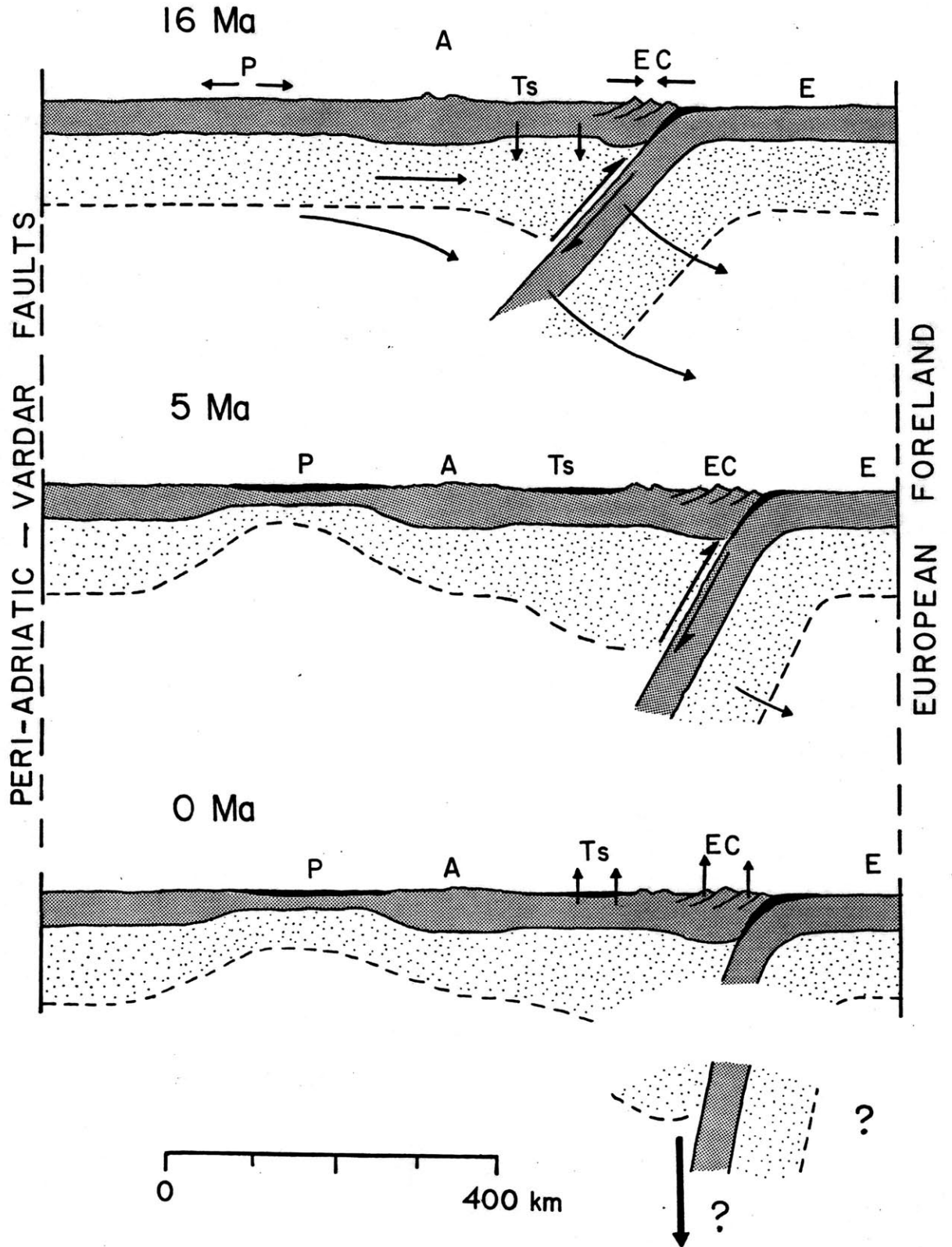
Figure 30

Figure 31

APPENDIX 1

CONTINENTAL MARGIN SUBSIDENCE

AND HEATFLOW

PREFACE

L. Royden did almost all of the work on this paper, and wrote all of the text. J. Sclater provided the initiative for this study and helped with the organizaton of the text. R. Von Herzen contributed his expertise on thermal problems and provided helpful suggestions.

Continental Margin Subsidence and Heat Flow: Important Parameters in Formation of Petroleum Hydrocarbons[1]

LEIGH ROYDEN,[2] J. G. SCLATER,[3] and R. P. VON HERZEN[4]

Abstract Passive continental margins have been shown to subside with a 50-m.y. exponentially decaying rate which cannot be explained by isostatic compensation for sediment loading. This suggests that the subsidence is dominated by geodynamic processes similar to those in the deep ocean. Two simple geologic models for continental breakup are developed: (1) attenuation of continental lithosphere and (2) intrusion of mantle diapirs.

These models for rifting give a direct relation between subsidence of passive margins and their surface heat flow through time. On this basis we develop a method of reconstructing the thermal history of sedimentary strata from regional subsidence and sedimentation history. Because generation of petroleum hydrocarbons depends on the integrated time/temperature history of buried organic material, this reconstruction technique can be used to determine the depth to the oil range of the "hydrocarbon generation window" in advance of drilling. By way of example, we reconstruct time/temperature/depth plots and estimate hydrocarbon maturity for one site in the Falkland Plateau and three sites in the North Atlantic near Cape Hatteras. In addition to providing a method for evaluating hydrocarbon potential in frontier regions where there is little or no well control, this approach suggests that there may be significant potential for oil and gas generation on the outer part of the continental rise and in deep-sea sedimentary basins.

INTRODUCTION

Variations of heat flow and topography in the ocean floor can be adequately explained as the thermal contraction of a cooling lithosphere (Langseth et al, 1966; Parker and Oldenburg, 1973; Parsons and Sclater, 1977). Parsons and Sclater (1977) considered a simple plate model in which the lithosphere is assumed to be a slab of uniform thickness. Material is intruded at constant temperature along mid-ocean ridges and subsequently spreads away from the ridge axis. The lithosphere is allowed to cool conductively while the lower slab boundary is maintained at the temperature of intrusion, and the ocean floor subsides owing to thermal contraction. Initially, depth increases as the square root of time ($\sqrt{t}$; symbols used in text are defined in Table 1) but for older ocean floor ($t \geqslant 80$ m.y.) appears to increase at an exponentially decaying rate toward a constant asymptotic value. From observation of seafloor bathymetry Parsons and Sclater (1977) concluded that between 0 and 70 m.y. after intrusion, depth is given by $d(t) = 2,500 + 350 \ t^{1/2}$m. For older lithosphere the relation becomes $d(t) = 6,400 - 3,200 \exp(-t/62.8)$. An analogous age relation holds for surface heat flow. Surface

measurements in impermeable sedimentary basins, where the heat transfer is entirely by conduction, give average values in agreement with this theoretical model. For oceanic crust younger than about 120 m.y., the heat flow (Q) may be expressed as $Q(t) = 11.3 \ t^{1/2}$ cal cm^{-2}sec^{-1}, and for older crust $Q(t) = 0.9 + 1.6 \exp(-t/62.8)$ cal cm^{-2}sec^{-1}.

There is considerable evidence in the sedimentary record from passive continental margins that a significant fraction of margin subsidence cannot be explained entirely by isostatic compensation for sediment loading. Sleep (1971) has shown that subsidence follows an exponential decay with time constant ∼50 m.y. across large regions of the continental shelf (Fig. 1). Similar results were obtained by Watts and Ryan (1976) for the Hatteras region and the Gulf of Lyon. The similarity between these subsidence histories and the

Leigh Royden et al

Table 1. Symbols and Values Used

Symbol	Value	Definition
a	$3.3 \times 10^{-5}\,°C^{-1}$	Coefficient of thermal expansion
d		Depth below sea level
γ_d		Fraction (by volume) of lithosphere composed of dikes and intrusive bodies
γ_s		Fraction of lithosphere replaced from below by aesthenosphere
γ		Oceanization or thermal parameter; $\gamma=0$ is continental lithosphere, $\gamma=1$ is oceanic lithosphere.
κ	$8 \times 10^{-3}\,cm^2\,sec^{-1}$	Thermal diffusivity of lithosphere
K	$7.5 \times 10^{-3}\,cal\,cm^{-1}\,sec^{-1}\,°\,C^{-1}$	Thermal conductivity of lithosphere
K_{sed}	$4 \times 10^{-3}\,cal\,cm^{-1}\,sec^{-1}\,°C^{-1}$	Thermal conductivity of sediment
l	$125\ km$	Equilibrium thickness of lithosphere
$l^2\,\kappa/\pi^2$	$62.8\ m.y.$	Time constant of thermal decay
Q		Heat flow
ρ_m	$3.33\ gm\ cm^{-3}$	Density of mantle
ρ_w	$1.0\ gm\ cm^{-3}$	Density of water
ρ_c	$2.8\ gm\ cm^{-3}$	Density of crustal rock
S_i		Initial subsidence due to stretching
t		Time measured in millions of years
t_c		Crustal thickness
T		Temperature
T_m	$1,350°\ C$	Temperature of upper mantle
U		Height above equilibrium elevation

depth-age relation for older ocean floor strongly suggests that the subsidence of passive continental margins results from thermal contraction of
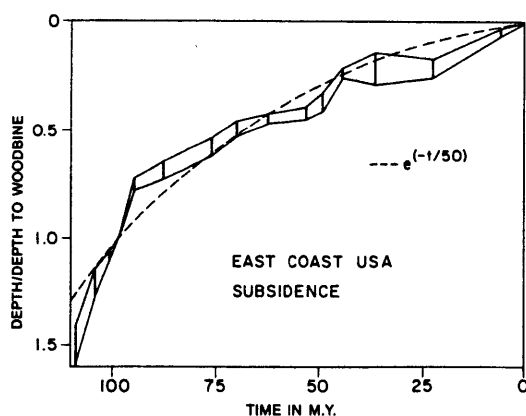
FIG. 1—Depth normalized to base of Woodbine is plotted as function of age for wells on East Coast of United States. Dashed smooth curve is 50-m.y. exponential constrained to fit data at base of Woodbine and at present (after Sleep, 1971).

the lithosphere, and that there may be a simple thermal model to explain the geologic history of some margins. Most recently, Steckler and Watts (1978) have used a thermal model to explain the subsidence observed at the COST B-2 well.

Early attempts to model passive continental margins (Sleep, 1971) simply considered the continental lithosphere to be heated from below. This produced doming of the lithosphere along the plane of incipient rifting (Fig. 2A), and adequately described the subsidence history of the margin. Two more sophisticated models have been suggested: the first entails rapid stretching and attenuation of the continental lithosphere at the time of continental breakup (Fig. 2B; McKenzie, 1978); the second, a modification of Burke's aulacogen theory (Burke and Whiteman, 1973), involves cracking of the continental lithosphere and large-scale intrusion of diapirs across the incipient margin (Fig. 2C). At present it is not clear which of these mechanisms dominates margin formation; both produce the same subsidence history, but differ radically in estimates of initial heat flow. It seems probable that both mechanisms may be active during continental breakup.

If marginal evolution can be explained by a combination of these mechanisms, the paleoheat

Continental Margin Subsidence and Heat Flow

flow must lie within a range bounded by the two extreme models. Thus by correlating subsidence with thermal evolution of sedimentary basins, we can predict a range for paleoheat flow. To reconstruct paleoheat flow for individual basins, the following parameters must be known: regional subsidence, depth to basement, sedimentation history, and sediment density. In addition, if thermal conductivities are known or if they can be estimated from sediment lithology, the thermal

history of any sedimentary unit can be traced from the time of its deposition.

SIMPLE RIFTING MODELS

Passive margins may be subdivided into two distinct regions: that part of the margin underlain by oceanic basement, and the region landward from there. For normal ocean floor, the subsidence and heat flow are well determined as a function of age (Fig. 3; Parsons and Sclater,

CRUST
CONTINENTAL LITHOSPHERE
ASTHENOSPHERE
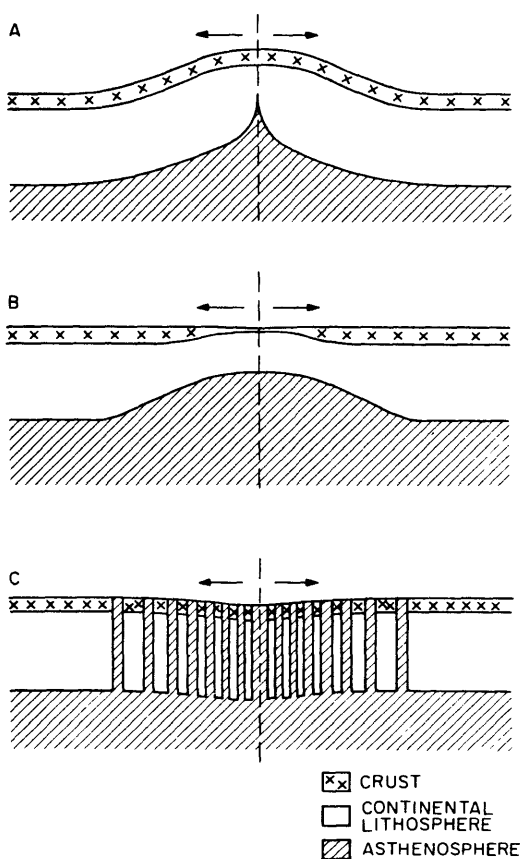
FIG. 2—A, In simple rifting model, continental lithosphere is heated along plane of incipient rifting, producing thermal expansion of lithosphere, and doming of surrounding region. B, More sophisticated extension model stretches lithosphere across plane of rifting. Hot material rises from asthenosphere to replace thinned continental lithosphere. There is initial subsidence in continental crust as isostatic equilibrium is maintained. C, Continental margin is formed by series of ultrabasic dikes intruded across incipient margin. Percentage of dike material increases seaward across margin, with 100% dike material corresponding to pure oceanic lithosphere.
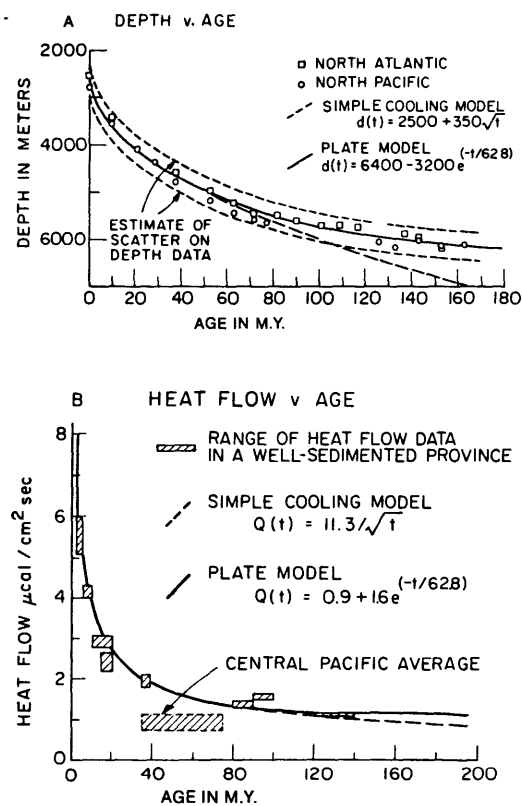
FIG. 3—A, Diagram presenting relation between mean depth and age for North Atlantic and North Pacific. Area between short dashed lines represents estimate of scatter in original points used to determine mean data. Solid line beyond 60 m.y. is theoretical elevation from plate model where $d(t) = 6,400 - 3,200 \, e^{-(t/62.8)}$. Line of longer dashes is elevation calculated assuming that lithosphere is simple boundary layer and continues to thicken with time. B, Plot of mean heat flow against age. Only values in areas covered by thick layer of sediments are shown. Except for one point in central Pacific there is strong correlation between heat flow and age. Dashed line represents relation between heat flow and age predicted by simple thermal boundary layer model. Heavy continuous line represents relation $Q(t) = 0.9 + 1.6e^{(-t/62.8)}$ predicted by plate model.

Leigh Royden et al

1977). Landward of oceanic basement, the situation becomes more complex. We have assumed that margin subsidence can be explained by simple thermal contraction of the lithosphere rather than phase changes in the earth, a process about which little is known. Subsidence and heat flow can then be expressed as the decay of initial thermal conditions toward an equilibrium state, and may be determined by the specific dynamics of margin formation.

Sleep (1971) assumed that the "transitional"[?] part of the margin was continental lithosphere, heated at the time of rifting, and subsequently allowed to cool conductively in the vertical direction, producing subsidence:

$$U(t) = U_o(x)\exp(-at)$$

where $U_o(x)$ is initial uplift and $1/a$ ~50 m.y. This approach was successful in explaining the general subsidence observed on the East Coast of the United States but encounters substantial quantitative difficulties in some regions. Any region which is uplifted by thermal expansion of the lithosphere will subside to its initial elevation as the lithosphere cools. Consequently, to transform a surface initially at or above sea level into a sedimentary basin (or sedimented margin), the average density of the lithosphere must be increased, either by subaerial erosion, subcrustal thinning, or some other mechanism. Sleep estimated that for an initial uplift of 1.5 km (from sea level), 3.0 km of crust is removed by subaerial erosion and 2.0 km of sediment accumulates in the resulting basin. This result has difficulty in accounting for regions of the East Coast of the United States where thick sediment accumulations of up to 10 km or more overlie continental basement. Sleep's calculations imply removal of ~15 km of crust and an initial uplift of ~7.5 km. There are two problems. (1) Thermal expansion of the lithosphere by 7.5 km is equivalent to raising the temperature to 2,000°C throughout; this is an unlikely supposition, for the base of the lithosphere is generally accepted to remain at about 1,300°C. (2) This model generates huge volumes of terrigenous sediment fairly soon after rifting, but it is difficult to determine where such a large volume of sediment could have been deposited. There is no evidence that it was deposited inland and there does not seem to be enough early sediment accumulation on the continental rise and farther out in the deep ocean to account for an erosional event of this magnitude (E. Uchupi, personal commun.).

Another objection to this simple thermal expansion/contraction mechanism for producing marginal basins is the existence of subsiding sedimentary basins which appear to have had neither uplift nor erosion. Sleep (1971) has shown that several of these basins in North America are subsiding with an exponential decay rate similar to that observed along the East Coast margin. If the mechanism of subsidence in these basins is similar to that along passive margins, uplift and erosion apparently are not an integral part of their evolution. Yet despite these difficulties with this simple thermal model, its success in producing the general subsidence on the East Coast margin strongly indicates that the subsidence for this region is primarily a cooling effect in the lithosphere.

The general problem of excessive uplift can be avoided if there is crustal extension and thinning at the time of rifting (Fig. 4). Such a model was
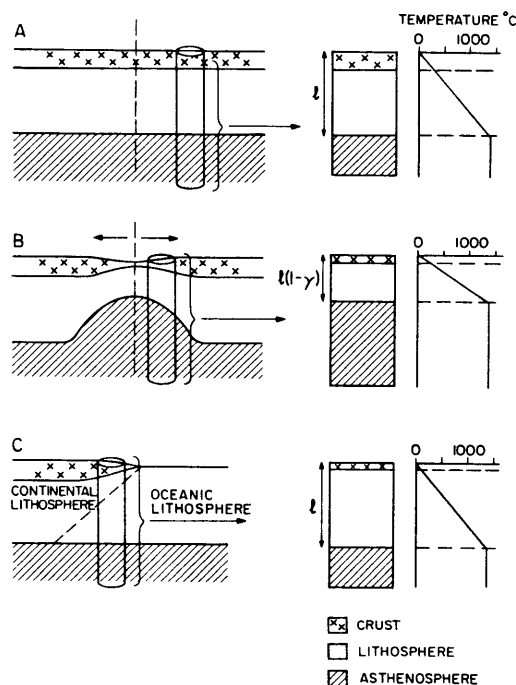
FIG. 4—A, Schematic diagram of continental lithosphere prior to initiation of rifting. Temperature profile at right shows lithospheric slab to be at thermal equilibrium with $T_m = 1,300°C$ at base of lithosphere. B, As rifting proceeds, continental lithosphere stretches across plane of rifting, thinning both lithosphere and continental crust. Temperature remains fixed at base of lithosphere, thus steepening thermal gradient. C, Long after margin formation, temperature has cooled to equilibrium (Fig. 5A). Margin itself consists of wedge of formerly continental lithosphere which thins seaward (shown by dashed line). Ocean-continent boundary in lithosphere is descriptive only, having no structural significance in old (i.e., cool) margin.

Continental Margin Subsidence and Heat Flow

first proposed by Artemyev and Artyushkov (1969) to explain seismic and gravimetric data from Baikal basin. Shallow-angle listric normal faults observed in the Great Basin provide a possible mechanism for stretching and thinning of rigid crustal material (Wright, 1976). These faults, which dip at angles of less than 45°, are associated with steeply tilted blocks. Palinspastic restoration of southern Death Valley indicates that the faulted rock units have been extended by 30 to 50% (Wright and Troxel, 1967). Thinned crust has also been observed under other sedimentary basins (Stegena, 1964; Artemyev and Artyushkov, 1969).

The thermal effects of stretching the lithosphere during margin and basin formation have been explored in detail by McKenzie (1978), where attenuated lithosphere is replaced by passive upwelling of hot asthenosphere. For regions with initial crustal thickness greater than ~20 km, crustal attenuation results in immediate subsidence to maintain isostatic equilibrium. Although there is evidence for some uplift and erosion along passive continental margins, this phenomenon may be due to the introduction of additional heat into the lithosphere which is not directly associated with the thermal effects of lithospheric attenuation. This model is compatible with the observational work done by Sleep and others on margin subsidence. For time greater than ~30 m.y., the subsidence rate is approximately an exponential decay, similar to the exponential subsidence in the deep ocean. The total amount of subsidence is determined by the degree of lithospheric attenuation.

Another model which provides an exponential subsidence compatible with observational data consists of cracking of the continental lithosphere and intrusion of dikes or diapirs from the mantle (Fig. 5). Replacement of light crustal rocks by denser ultrabasic or basaltic material results in initial subsidence and avoids the general problem of uplift. The primary evidence for intrusional activity during margin formation is the extensive dike swarms in east Greenland (Wager, 1947). Other evidence of intrusional activity associated with continental breakup is present in the Lebombo monocline (Cox, 1972) and the Panvel flexure, south of Bombay (Auden, 1972). Whether this intrusional activity is a primary mechanism of margin formation or only an incidental by-product of some other process is unclear. It seems unlikely that this mechanism can be operant at depths where the lithosphere may behave as a viscous fluid rather than a rigid, brittle slab. Nevertheless, the lithosphere possibly extends by ductile flow near its lower boundary and by extensional cracking and dike intrusion in its upper part.
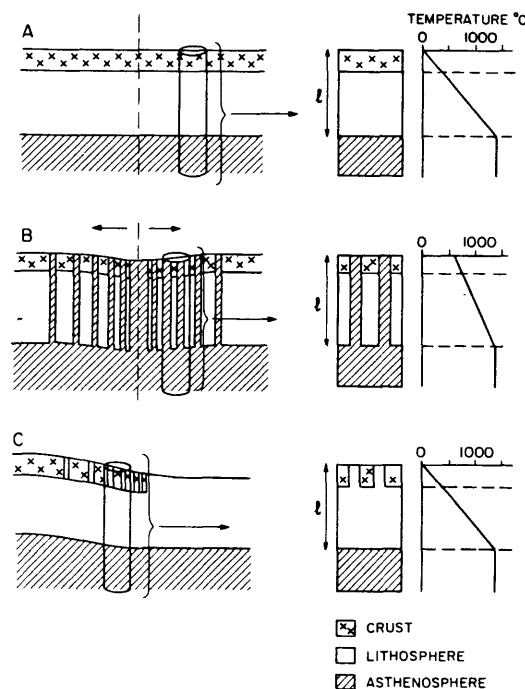
FIG. 5—A, Continental lithosphere prior to rifting, as in Figure 4A. B, As rifting proceeds, lithosphere cracks and ultrabasic dikes are intruded along plane of rifting. Dikes increase in volume and/or frequency toward axis of rifting. Transition to pure oceanic crust occurs when intruded ultrabasic material becomes 100% of total. Temperature gradient through lithosphere becomes less steep, but surface temperature is raised considerably. C, Long after rifting, temperature gradient has returned to equilibrium. Margin consists of continental crust interrupted by series of dikes which may not all reach surface.

DISCUSSION

The theoretical subsidence and heat flow resulting from these models have been calculated mathematically (Appendix) and the results are plotted in Figure 6. The degree of "oceanization" is indicated by a thermal parameter, γ. For both models of rifting, $\gamma = 1$ represents pure oceanic crust and $\gamma = 0$ represents undisturbed continent. Corresponding values of γ reflect the addition of equal amounts of heat to the continental lithosphere at time $t = 0$. Because the system returns to equilibrium at $t \to \infty$, the total subsidence and net heat loss from the lithosphere are a function only of γ, and independent of the model. For equal values of γ, there are slight differences in subsidence versus time for the two models but they do not appear large enough to be distin-

guished from observational data. Likewise, for equal values of γ, the heat flow curves are virtually identical after about 20 m.y., but for γ < 0.6 there are significant differences in heat flow at times <20 m.y. This is to be expected considering the different initial temperature distribution, particularly in the near-surface region (Figs. 4B, 5B).

Because initial elevation was taken to be at or below sea level, Figures 6A and 6C show both the effect of thermal contraction of the lithosphere and the related effect of isostatic compensation. for water loading. Most subsiding sedimentary

basins and margins contain large thicknesses of sediment, and regional subsidence must be determined indirectly by examining the time stratigraphy in the sediments and compensating for the effect of sediment loading.

This gives a simple method for calculating a range of paleoheat flow along margins and in basins where the sedimentation history is known. Because theoretical subsidence depends primarily on γ and not on the specific thermal model (Fig. 6A, C), calculation of empirical subsidence yields a unique value for γ. Because we do not know the
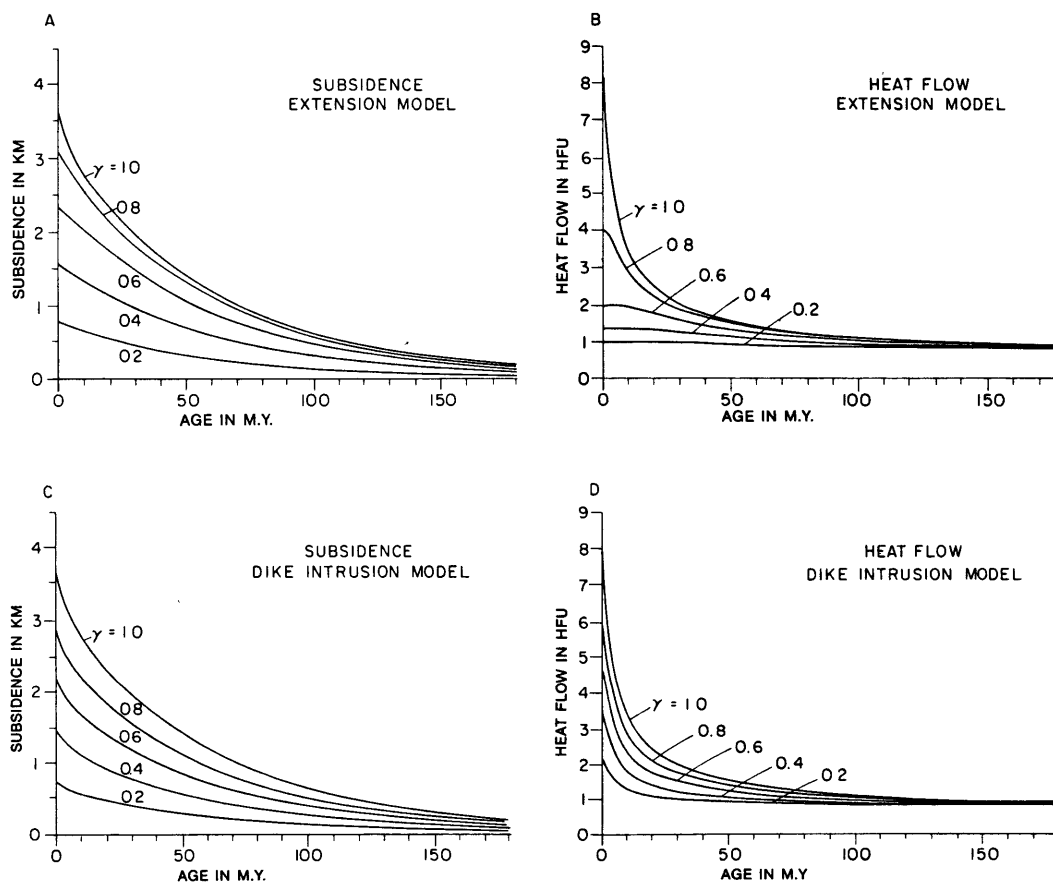
FIG. 6—A, Theoretical surface elevation calculated from equation 7a for extensional margin. Curve given by γ = 1 corresponds to pure oceanic lithosphere and is identical to Figure 4A. For all values of γ, depth approaches constant value. B, Theoretical heat flow calculated from equation 6a. Again, γ = 1 corresponds to pure ocean floor. After about 100 m.y., heat flow becomes 1.0 heat flow unit (HFU) for all values of γ. For γ < 0.6, initial heat flow is quite low, which results from great depth at which heat is added to lithosphere; the greater the depth, the longer the time until effects are felt at surface. C, Theoretical surface elevation calculated from equation 11a; γ = 1 corresponds to pure oceanic lithosphere, and is identical to curve for γ = 1 in A. For all values of γ in this figure, rate of subsidence is equal to that in deep ocean multiplied by factor of γ, that is $U(t) = \gamma{:}\Delta E(t)$ where $E(t)$ is surface elevation of oceanic lithosphere. D, Theoretical heat flow calculated from equation 10a. High values of initial heat flow reflect addition of heat close to surface.

Continental Margin Subsidence and Heat Flow

specific mechanism for margin formation, we cannot reconstruct the heat flow exactly. However, the two models developed previously may be taken as limiting examples and hence we can reasonably expect the paleoheat flow to lie within the bounds set by these two extremes. Because temperature at depth is directly related to heat flow, our thermal models may be used to determine paleotemperatures in specific sedimentary strata and to estimate the thermal potential for petroleum genesis. In near-surface regions heat flux can be considered invariant with depth, and within the sedimentary layer temperature at z_0 is given by:

$$T = T_{surface} + \int_0^{z_0} \frac{Q(t)dz}{K(z)}. \qquad (1)$$

Equation 1 is a good approximation provided that an equilibrium situation prevails throughout the sedimentary layer, that no heat is derived from radioactive isotopes in the sediment or underlying crust, and that convection of interstitial water provides a negligible contribution to total heat transport. The sedimentary layer should be in thermal equilibrium when the sedimentation rate does not exceed 1 km in a million years. In general, the contribution from radiogenic heat sources is not negligible, and for precise temperature calculations this equation should contain a third term for this. We expect that the two models will produce similar thermal histories for $\gamma = 1.0$ and $\gamma = 0$ but for intermediate values of γ we expect higher temperatures in the dike intrusion model for very early times, and hence more mature hydrocarbons in the early sedimentary series.

Paleoheat flow cannot be measured directly, but there are at least two other tests of these models. We can compare calculated values for heat flux with present-day heat flux in very young sedimentary basins ($\leq$ 10 m.y.), or we can compare them with the extent of thermal alteration of organic material in older sediments as an indication of prior thermal gradients. It would be more straightforward to measure heat flow directly in a young basin, but the subsidence history in such a basin may not be well enough defined to calculate any meaningful value of γ. In the second test, most passive margins are older than about 70 m.y. and may be buried by up to 15 km of sediment. Thermal alteration in the sediments deposited shortly after rifting and during the period of variable heat flow ($<$30 m.y. after rifting) is generally obliterated by the subsequent burial and high-temperature environment. Exceptions are present in regions where considerable thicknesses of pre- and syn-rift sediments have gone through the peak thermal event and been highly altered

during the high heat flow phase. Thermal alteration in sediment deposited after this period of variable heat flow is less conclusive, for the heat flow curves become very flat and often indistinguishable. Nevertheless, it is possible to make some gross generalizations about temperature history in older, well-sedimented basins and continental shelves.

For a sedimentary basin filling to sea level, the temperature at the sediment-basement interface is a function of two variables: sedimentary thickness and heat flow. Because the basin fills to sea level, the sedimentation rate is effectively determined by thermal contraction of the lithosphere and hence is directly related to heat flow. It can be shown from the equations derived in the appendix that the temperature at the sediment-basement interface remains relatively constant after about 70 m.y. The temperature variations which may occur after 70 m.y. are primarily determined by regional geologic processes and, to a lesser extent, by the elevation of basement immediately after rifting. These regional processes include development of horst and graben structures, nonuniform sedimentation, and progradation of the margin.

In basins younger than 70 m.y. it is difficult to make a similar generalization about the temperature at the sediment-basement interface because the basement temperature is also more strongly dependent on initial elevation, sediment supply, and other variables. Likewise, in basins which are sediment starved and do not fill to sea level, the sedimentary thickness and the heat flow are not directly related, and the temperature at basement must be calculated formally. In these regions with a more complex thermal environment, this temperature reconstruction technique is particularly useful.

We have applied the technique to (1) the Falkland Plateau, a subsiding sediment-starved basin; (2) the North American continental shelf near Cape Hatteras, an older sediment-filled basin; and (3) a sedimented region well off the continental rise in North America. Using these results in conjunction with a simple model describing the effects of temperature on metamorphism of organic material, we can estimate the depth of the "hydrocarbon window" for these regions. We do not intend to make a realistic assessment of potential for generation of petroleum hydrocarbons but only to illustrate the possible use of this reconstruction technique. The potential for useful hydrocarbons depends on the presence of source rocks and the possibilities for migration and accumulation, factors which are outside of this discussion. One major source of error lies in our assumption of an arbitrary, uniform thermal

Leigh Royden et al

conductivity in the sediment. Because temperature at depth varies inversely with conductivity, accurate determination of thermal conductivity is essential to a rigorous application of this method. Furthermore, this method is clearly inappropriate for regions where there is significant transfer of heat by horizontal or vertical migration of fluids.

THERMAL METAMORPHISM OF ORGANIC SEDIMENTS

Petroleum hydrocarbons are formed by thermal alteration of organic-rich sediments during burial. Although many factors contribute to organic metamorphism, the process is primarily dependent on the integrated time/temperature history of the buried organic material (Tissot et al, 1974). Generally, first-order organic reaction rates approximately double for every 10 to 15°C rise in temperature. In particular, Lopatin (1971) and others have concluded experimentally that the reaction rate for thermal alteration of organic sediments doubles for each 10°C increase in temperature. Hood et al (1975) have shown that this elementary approach gives results in excellent agreement with a more theoretical model which assumes that the reaction is first order in temperature and obeys the Arrhenius equation.

On the basis of these observations, we shall use the following relation for calculating the state of thermal alteration where the parameter C increases as the level of thermal alteration increases.

$$C = \ln \int_o^t 2^{T(t)°C/10} dt \qquad (2)$$

where t = time measured in millions of years and T = temperature in degrees Centigrade. Figure 7 shows how C is related to the level of organic metamorphism (LOM; Hood et al, 1975) and to vitrinite reflectance R_o, which is the most universally accepted measure of the level of thermal alteration of organic matter. As noted on this figure, the oil generation process has barely started at C ≅ 10, and is essentially complete at C ≅ 16. The gas generation process is essentially complete at C ≅ 20. The initiation of gas generation is strongly dependent on the type of organic matter and thus has not been shown on the figure.

APPLICATION

Four major steps in calculating degree of thermal alteration from regional subsidence are: (1) compensation for subsidence due to sediment loading; (2) calculation of γ from thermal subsidence of the region, that is, subsidence not due to sediment loading; (3) from γ, determination of heat flux versus time and thus temperature versus time for specific sedimentary strata; and (4) sub-

stitution of T(t) into equation 2 yields thermal potential for hydrocarbon maturation.

As mentioned, it is necessary to subtract the component of subsidence due to sediment loading from the total subsidence so that the remaining or "thermal" subsidence can be compared to theoretical subsidence curves (Fig. 6A, C). In this paper we have chosen to consider only the Airy model for regional isostasy partly because the numerical calculations for this model are less complex than those entailed in a flexural model. It may also be argued that the Airy model gives a better approximation of the loading effect for sediments deposited shortly after rifting (less than about 50 m.y.) when the lithosphere is thinner, hotter, and less rigid than older lithosphere which is near thermal equilibrium. Thus we assume that the subsidence of a sediment-loaded plate (U_s) is related to the subsidence of a water-loaded plate (U_w) by:

$$\frac{\rho_m - \rho_s}{\rho_m - \rho_w} U_s = U_w . \qquad (3)$$

Once a thermal subsidence curve has been plotted, an appropriate value of γ can be chosen by
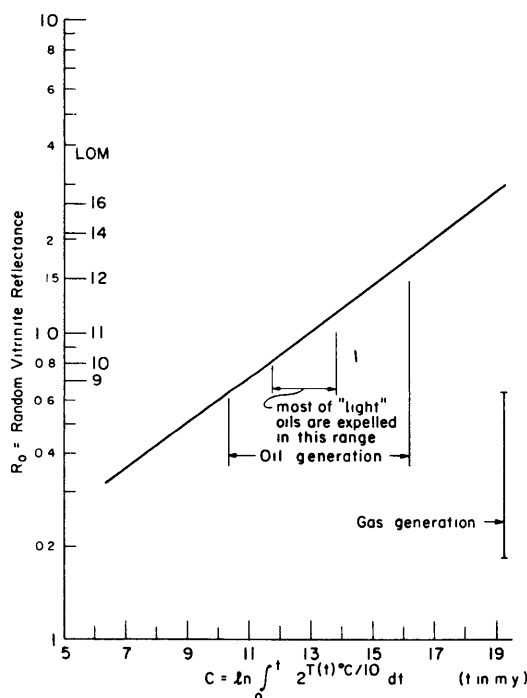
FIG. 7—Plot showing relation of random vitrinite reflectance, LOM, and C. LOM is from Hood et al (1975). Major zones of oil and gas generation are indicated. Start of gas generation is strongly dependent on type of organic material and thus is not shown.

Continental Margin Subsidence and Heat Flow

comparison with Figures 6A and 6C. This value of γ can be used to calculate heat flow mathematically, or heat flow may be read directly from Figure 6. This correlation between subsidence history and heat flow is the fundamental step in this reconstruction procedure. Although the mathematical derivation of this may be somewhat complex, the concept is straightforward. This reconstruction technique shows that once heat flow and subsidence have been plotted for a sufficient range of γ, it is unnecessary to recalculate each time the technique is used.

Together with equation 1, this correlation procedure enables us to trace the temperature history

of any sedimentary unit where z_o is the depth below the sediment/water interface at any time. Thermal conductivity (K) can be estimated for each lithologic unit in the overlying sediment. Major factors which affect thermal conductivity include sediment composition, porosity, type of interstitial fluid (or gas), and temperature. To avoid the more complex situation of K increasing with compaction and depth of burial, we chose an average value of K and assumed that K remains constant through time. However, it should be strongly emphasized that temperature at depth is directly related to variations in thermal conductivity, and that accurate assessments of conduc-
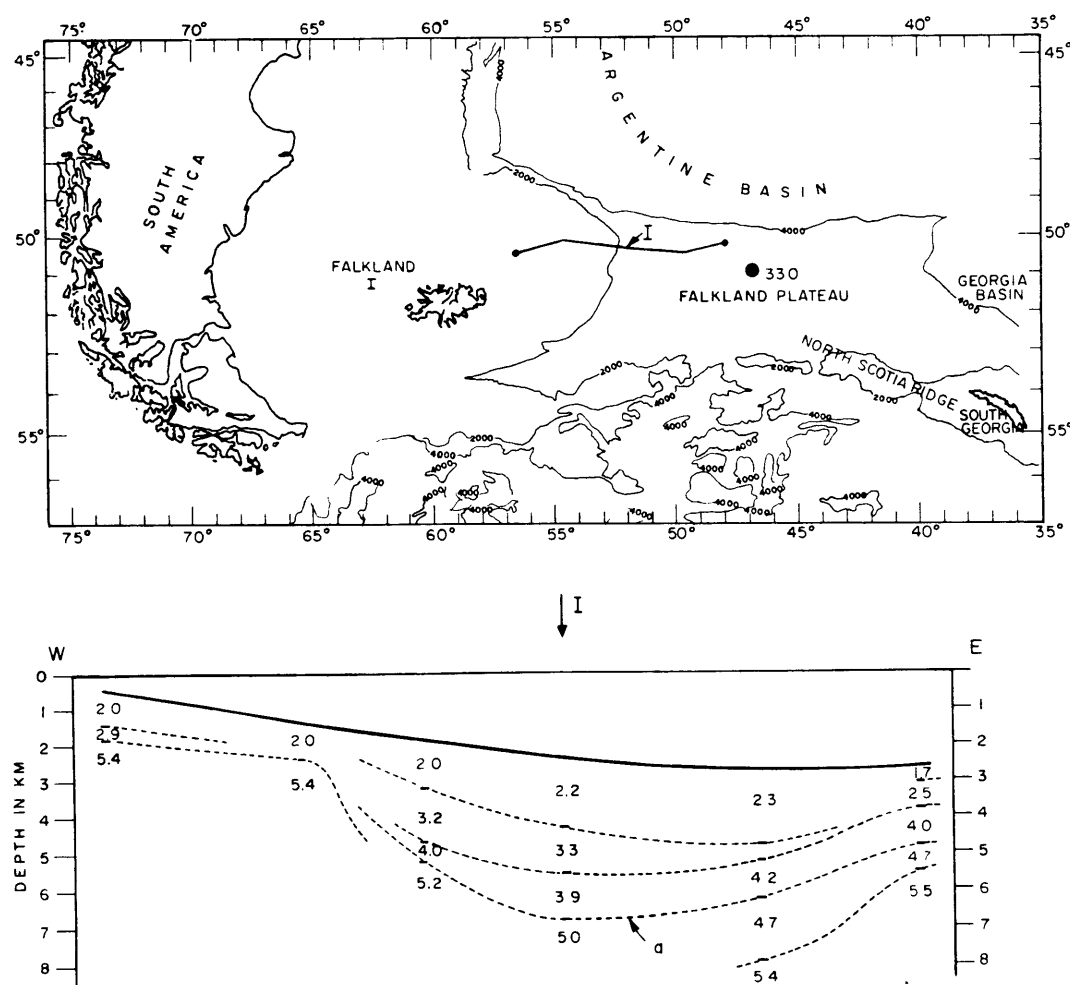
FIG. 8—Location of site I on Falkland Plateau (contours show water depth in meters) and seismic reflection/ refraction line (after Ludwig et al, 1979). Reflector a is interpreted as pre-Albian depositional hiatus. Figures between dotted lines on section are interval velocities in kilometers/second.

Leigh Royden et al

tivity throughout the evolution of the basin are crucial in the application of this technique.

After the temperature history has been calculated for an individual sedimentary package, the stage of thermal alteration (C) can be determined from equation 2 or by any other method which estimates thermal alteration from temperature history. Following are examples in the use of this technique for estimating hydrocarbon potential.

Falkland Plateau

The Falkland Plateau is a sediment-filled basin containing 4 to 5 km of south-dipping sediment. DSDP drilling in the eastern end of the Falkland Plateau has revealed a fairly detailed reconstruction of the post-Paleozoic geologic history, and seismic reflectors can be traced downslope into the major part of the basin (Barker, 1976). Sedimentary records from DSDP Site 330 indicate a marine transgression or minor subsidence event during the Oxfordian. Following this was a depositional hiatus and period of restricted circulation until the end of the Aptian when rapid subsidence established open-marine conditions by early Albian time (Barker et al, 1976). Rapid subsidence during the early Albian can be correlated with the rifting of South America from Africa (van Andel et al, 1977), which strongly suggests that subsidence of the Falkland Plateau is due to thermal effects resulting from continental breakup about 125 m.y. ago. If this is the reason, paleoheat flow and paloetemperature can be reconstructed from the subsidence history of the region.

Figure 8 shows a seismic profile from the central part of the Falkland basin. We have interpreted reflector a as the pre-Albian depositional hiatus and have calculated subsidence history from this horizon. Using density estimates from seismic velocity (Nafe and Drake, 1963), a water-loaded subsidence of 3.5 km (i.e., 3.5 km of subsidence would have occurred without sediment loading) was calculated for basement at site I, roughly corresponding to subsidence of oceanic lithosphere, and suggesting that site I overlies either oceanic basement or transitional basement which is primarily oceanic in character. Assuming a thermal conductivity of $K = 4.0 \times 10^{-3}$ cal cm^{-1} sec $^{-1}$°C^{-1} thoughout the sedimentary layer (King and Simmons, 1972), paleotemperature can be calculated from equation 1. Present-day conductivity for this region is probably closer to 5 $\times$ 10^{-3}, but conductivities in the past must have been considerably lower, for the deeper sediments were initially less compact than at present. Paleotemperature has been superimposed on the sedimentation history of the region and the results are plotted in Figure 9.

Figure 9 shows that the temperature at reflector a has remained relatively constant for the past 80 m.y., whereas temperatures in the overlying sediments have increased somewhat during this time. At no time in the past did these sediments experience temperatures significantly higher than their present temperature. Substitution of temperature versus time into equation 2 for Site I yields the results shown in Table 2. Calculated values of C
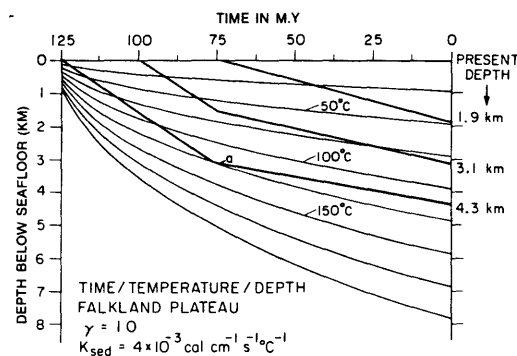
FIG. 9—Time/temperature/depth (TTD) reconstruction for Falkland Plateau at site I. Depth = 0 represents sediment-water interface at all times, and depth is defined as kilometers subbottom. Temperature isotherms, shown by smooth curves, move downward through time, indicating that thermal gradient is becoming less steep. Dark lines represent depositional isochrons, and temperature of specific sedimentary layer can be traced by following appropriate isochron. For example, sedimentary unit deposited at t = 125 m.y. increased rapidly in temperature to 125°C at t = 80 m.y., by which time it had subsided to about 3 km subbottom. At present, that sedimentary unit lies about 4.3 km subbottom and has a temperature of 115°C.

Table 2. Predicted Vitrinite Reflectance

Location (Figs. 8, 10)	Present Depth (km)	Thermal Alteration (C)	Vitrinite Reflectance (Predicted R$_o$)
Site I	1.9	5.9	x (immature)
	3.1	9.2	0.5
	4.35	12.3	0.9
Site IIa	3.9	9.1	0.5
	5.4	11.9	0.8
	6.9	19.3	x (overly mature)
Site IIb	3.8	7.5 - 9.4	0.4 - 0.5
	6.1	11.8 - 13.0	0,9 - 1.0
Site IIc	3.5	8.2 - 9.4	0.4 - 0.5
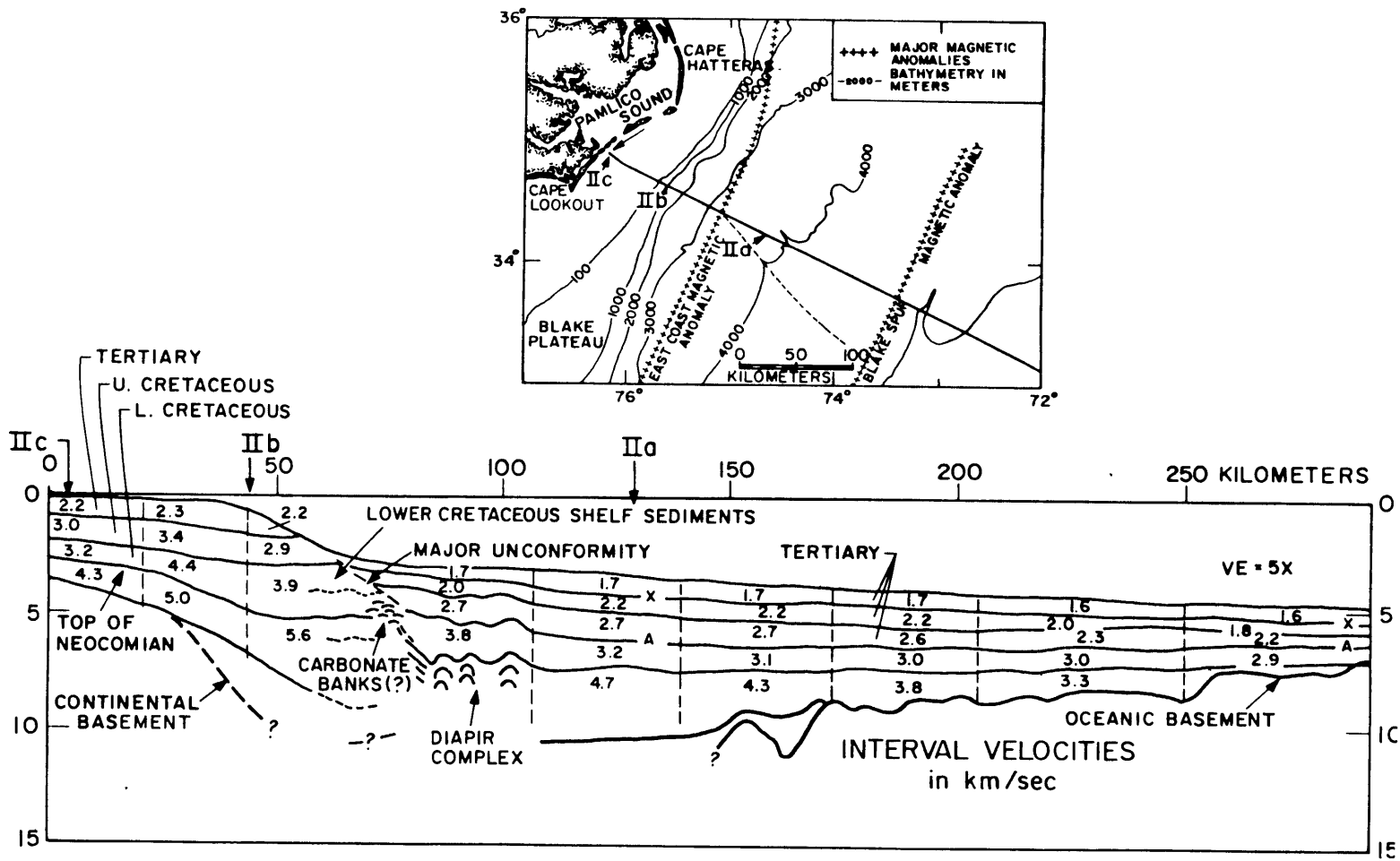
FIG. 10—Seismic refraction line from East Coast continental shelf across Hatteras Abyssal Plain, and location of sites IIa, IIb, and IIc (after Grow and Markl, 1977).

Leigh Royden et al

indicate a thermal history compatible with oil generation and possibly gas condensate at depths between 3 and 4.3 km in this part of the Falkland Plateau. However, the presence of oil or gas in this region depends not only upon the thermal history of the area, but also upon sediment composition and structures.

Cape Hatteras: Shelf Region and Abyssal Plain

Figure 10 shows a cross section of the continental shelf near Cape Hatteras and extending across the Hatteras Abyssal Plain. We have chosen three sites, one in the deep ocean (IIa) and two on the shelf (IIb, IIc). Site IIa is almost certainly normal oceanic floor despite the thick sedimentary layer; a significant fraction of this section (layer with interval velocity of 4.7 km/sec) was deposited with 10 m.y. of rifting (Klitgord and Grow, in prep.).

The temperature history of site IIa can be determined by superimposing depositional isochrons onto isotherms calculated from oceanic heat flow. Conductivity of the sedimentary layer has been taken as 4×10^{-3} cal cm^{-1}sec^{-1}°C^{-1}, and creation of oceanic basement estimated at 185 m.y. ago.

Figure 11 shows a time/temperature/depth (TTD) plot for site IIa. Early sedimentation caused the temperature at the sediment basement interface to rise to about 250°C. This sediment then cooled to 100°C at 50 m.y.B.P., when an increase in the sedimentation rate again caused a rise in the temperature to its present value of 160°C. Substitution of this temperature history into equation 2 yields the results shown in Table 2 for site IIa. Thermal conditions suitable for oil generation occur at ~4 km depth. This example

suggests that there may be oil and gas in other sedimentary basins in the deep sea as well as on the continental rise. On the rise, sediments which were once deeply buried may lie at shallow depth as the result of large-scale erosion coupled with landward retreat of the shelf edge (Grow and Markl, 1977).

Sites IIb and IIc lie on the shelf. Relatively thin initial sediment accumulation suggests that basement was above sea level for a short time after rifting. Estimates of total subsidence from the sedimentation history may be slightly low and hence affect early thermal gradients. Inspection of Figures 12 and 13 shows that this has little effect on the integrated time-temperature history, as early temperatures and sediment accumulation were extremely low.

Subsidence for sites IIb and IIc was corrected to 2.6 and 1.7 km of water-loaded subsidence, corresponding to $\gamma = 0.8$ and $\gamma = 0.5$, respectively. Figures 12 and 13 show TTD plots for both rifting models discussed previously; there is little difference in thermal history produced by each model. Calculation of C and of vitrinite reflectance gives the results shown in Table 2.

FIG. 11—Time/temperature/depth plot for site IIa on Hatteras Abyssal Plain. Isotherms are calculated from oceanic heat-flow curves and formulae indicated on figure.
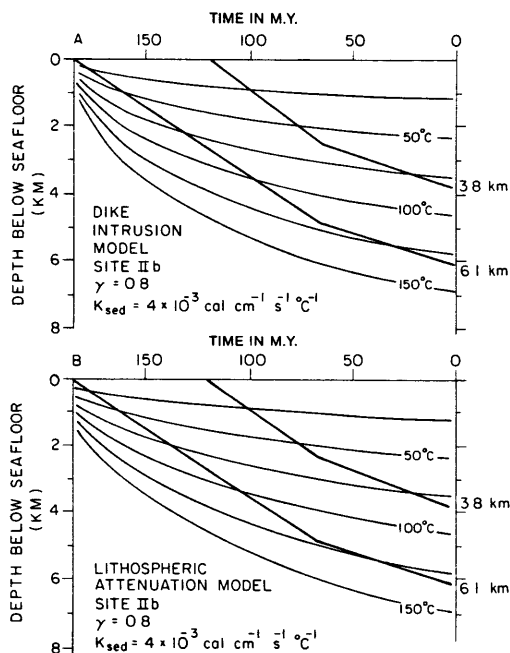
FIG. 12—Time/temperature/depth plot for site IIb on continental rise near Cape Hatteras showing isotherms calculated for two models.

Continental Margin Subsidence and Heat Flow
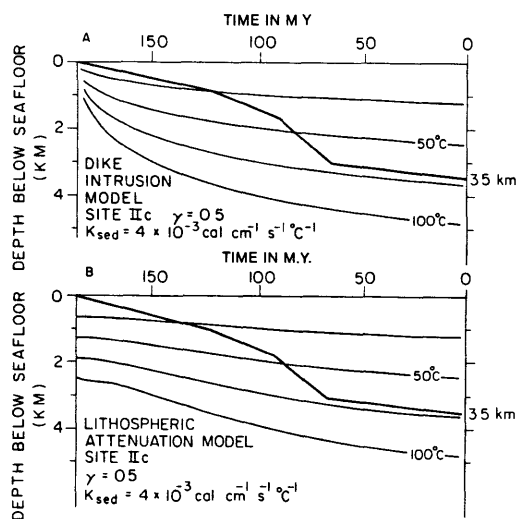
FIG. 13—Time/temperature/depth plot for site IIc showing isotherms calculated for two rifting models.

Higher values of C and R_o are given in each case by the dike intrusion model. Thermal conditions for oil generation begin at about 4 to 5 km depth in site IIb, whereas in site IIc the integrated time/temperature does not appear sufficient for petroleum formation, even at basement.

IMPLICATIONS

The thermal reconstruction technique developed previously is applicable to most passive margins and sedimentary basins formed by thermal contraction and subsidence of the lithosphere, and is a "bare bones" approach to calculating the thermal history of sedimentary sections from their subsidence history. This promises to have immediate application to the evaluation of hydrocarbon potential in frontier areas because, under favorable conditions, the depth of the oil window may be determinable in advance of drilling, or with only sparse well control. More accurate estimates of thermal conductivities in the sediment and of heat supply from radiogenic sources are crucial.

Results from sites IIb and IIc suggest that specific geologic models for rifting may show little difference in temperature history of the sediments unless the sedimentation rate was extremely high just after rifting. Even so, there is little difference in temperature gradient at early times for large values of γ, corresponding to basement which is primarily oceanic in character. This implies that the exact nature of continental breakup may not

be determinable from heat flow and subsidence alone because many geologic mechanisms for rifting may yield the observed subsidence and heat flow. Conversely, in most regions hydrocarbon potential may be determined with a fair degree of confidence despite uncertainties about rifting processes.

Perhaps the most interesting application of this model is to starved sedimentary basins where sediment supply was cut off shortly after the peak thermal event. In these regions, sediments which have undergone high thermal gradients associated with basin formation have not been deeply buried by later sedimentation. Consequently, favorable conditions for oil generation are predicted to lie much higher in the sedimentary column than in basins which have filled continuously since initiation of subsidence. In some places, sedimentary sequences on the outer continental rise and just off the rise coincide with this thermal and deposition history.

Prior to 50 m.y. ago, site IIa was a sediment-starved basin comprised of postrifting Jurassic sediments with little or no subsequent accumulation (Fig. 11). This presents a favorable environment for oil generation at shallow depth below the seafloor. If this is a typical deposition pattern for deep-sea basins adjacent to continental margins, many of these basins may also be excellent candidates for oil generation. Although a large pulse of Tertiary sedimentation in the region of site IIa has greatly increased the depth to the hydrocarbon window, this later phase of sedimentation may be missing in other areas. DSDP drilling in the North Atlantic has shown the presence of black shales with organic content in the range conducive to hydrocarbon generation (Lancelot et al, 1972) and sediments containing crude oil have been found in the Caribbean in 3,500 m of water (Davis and Bray, 1969). It seems likely that oil fields in the deep sea may be the next frontier in petroleum exploration.

CONCLUSIONS

1. Two geologic models for rifting, attenuation of continental lithosphere, and injection of mantle material into a series of vertical dikes produce thermal subsidence compatible with observational data for North America. For margins older than 60 m.y., subsidence rate is approximately an exponential decay with time constant ~60 m.y.

2. Heat flux versus time is directly linked with thermal subsidence, that is, subsidence not due to sediment loading. If subsidence and sedimentation history are well known, and estimates of thermal conductivity can be made throughout the section, temperature versus time for individual

sedimentary units can be calculated directly from the regional subsidence history.

3. Most time/temperature reconstructions are not strongly dependent on the exact mechanism of continental breakup, providing that the thermal regime is dominated by simple thermal expansion/contraction of the lithosphere. Exceptions may occur when there are considerable thicknesses of pre- and syn-rifting sediments.

4. Both heat-flow and subsidence curves are fairly flat for margins older than about 70 m.y., and, in basins which fill continuously to sea level, the sediment-basement interface tends toward a constant temperature. However, for very young margins and young sedimentary basins, temperature may vary rapidly with time and cannot be assumed to have remained constant.

5. Used in conjunction with a model which relates level of organic metamorphism to temperature history of organic material, time/temperature/depth reconstructions can determine the thermal potential for organic metamorphism in individual sedimentary units. These reconstructions have immediate application to petroleum exploration because frontier regions could be evaluated for hydrocarbon potential in advance of drilling.

6. This approach suggests that sediment-starved basins, where sediment supply was cut off shortly after the peak thermal event, are a particularly favorable environment for oil and gas generation. In particular, there may be significant potential for petroleum formation in deep-sea sedimentary basins adjacent to the continental rise.

APPENDIX

Thermal Models

1. *Crustal attenuation and stretching of continental lithosphere* — This model, discussed in detail by McKenzie (1978), is illustrated in Figure 4. At t = 0, the time of rifting, the continental lithosphere is stretched rapidly in the horizontal direction, causing effective thinning of the lithosphere from thickness l to $l(1 - \gamma_s)$. Isostatic compensation is maintained by upwelling of the hot asthenosphere, which then cools conductively, causing subsidence until thermal equilibrium is reached.

We have assumed throughout that the lithosphere is a slab of thickness l with constant temperature T_m at the base and that the system at all times remains in isostatic equilibrium. The surface of the continent is taken to be at or below sea level so that water occupies the entire volume created by subsidence. We have ignored contributions from radioactivity of crustal rocks, and have neglected two-dimensional effects for the sake of clarity and simplicity. The contribution of sediment loading to overall subsidence has been discussed. Physical parameters are shown in Table 1.

There is an initial change in elevation associated with stretching (McKenzie, 1978, equation 1).

$$S_i = \frac{-l\gamma_s[(\rho_m - \rho_c)(t_c/l)(1 - \alpha T_m t_c/l) - \alpha T_m \rho_m/2]}{\rho_m(1 - \alpha T_m) - \rho_w} , \quad (1a)$$

where t_c is the initial crustal thickness, α is the coefficient of thermal expansion, and ρ_m, ρ_c, and ρ_w are the densities of the mantle, the continental crust, and seawater, respectively. For the parameters in Table 1, S_i will be negative for regions with $t_c \geqslant 18$ km, and these areas will show an initial decrease in surface elevation due to stretching.

At time t = 0, the temperature distribution is:

$$T = T_m, \quad 0 < z/l < \gamma_s,$$
$$T = T_m \left(\frac{1}{1 - \gamma_s}\right)(1 - z/l), \quad \gamma_s < z/l < 1 . \quad (2a)$$

where z is measured upward from the original lithosphere/asthenosphere boundary.

Maintaining boundary conditions:

$$T = 0, \quad z = l,$$
$$T = T_m, \quad z = 0, \quad (3a)$$

we must solve the one-dimensional heat conduction equation:

$$\frac{\partial^2 T}{\partial z^2} = \frac{1}{\varkappa}\frac{\partial T}{\partial t} , \quad (4a)$$

where $\varkappa$ is the thermal diffusivity of the lithosphere. The solution for T is (Carslaw and Jaeger, 1959, p. 94):

$$\frac{T}{T_m} = 1 - z/l + \frac{2}{\pi}\sum_{n=1}^{\infty}\frac{(-1)^{n+1}}{n}\frac{\sin n\pi(1 - \gamma_s)\sin\frac{n\pi z}{l}}{n\pi(1 - \gamma_s)} \quad (5a)$$

$$\exp(-n^2\pi^2\varkappa t/l^2)$$

Solving for the surface heat flux we find

$$Q(t) = -K[\frac{\partial T(z,t)}{\partial z}]|_{z=0}$$

$$= \frac{KT_m}{l}(1 + 2\sum_{n=1}^{\infty}\frac{\sin n\pi(1 - \gamma_s)}{n(1 - \gamma_s)}\exp(-n^2\pi^2\varkappa t/l^2), \quad (6a)$$

where K is the thermal conductivity. The surface elevation is given by:

$$U(t) = \frac{\alpha\rho_m}{\rho_m - \rho_w}[\int_0^l Tdz|_{t=t} - \int_0^l Tdz|_{t\to\infty}]$$

$$= \frac{\alpha l\rho_m T_m}{\rho_m - \rho_w}(\frac{4}{\pi^2} - \sum_{m=0}^{\infty}\frac{1}{(2m+1)^2}[\frac{\sin[(2m+1)\pi(1 - \gamma_s)]}{(2m+1)\pi(1 - \gamma_s)}]$$

$$\exp(-(2m+1)^2\pi^2\varkappa t/l^2) , \quad (7a)$$

where U(t) is height above final depth as $t\to\infty$. Subsidence and heat flow results are summarized in Figure 6.

2. *Large-scale dike intrusion* — This model is illustrated in Figure 5. At time t = 0, hot material from the asthenosphere is intruded into the continental lithosphere through a series of vertical dikes. Exposed dike swarms in east Greenland (Wager, 1947) indicate that the density of the intrusions ranges from 5 to 10 per km to 50+ per km. Even if dikes were present only at a spacing of 5 km, the thermal effects of intrusion are averaged horizontally within 1 m.y., which allows us to neglect the horizontal component of heat conduction and consider only a simple one-dimensional problem.

Continental Margin Subsidence and Heat Flow

Letting γ_d be the fraction of the lithosphere which is composed of dike material intruded from the asthenosphere, the initial temperature distribution is:

$$T = (1 - \gamma_d)(1 - z/l) T_m + \gamma_d T_m \quad 0 < z/l < 1 \ , \qquad (8a)$$

where z is measured as before. As in the previous model

$$\begin{aligned} T &= 0, & z &= l, \\ T &= T_m, & z &= 0, \end{aligned} \qquad (3a)$$

and

$$\frac{\partial^2 T}{\partial z^2} = \frac{1}{\varkappa} \frac{\partial T}{\partial t}, \qquad (4a)$$

the solution for T is given by

$$\frac{T}{T_m} = 1 - z/l + \frac{2\gamma_d}{\pi} \sum_{n=1}^{\infty} \frac{(-1)^{n+1}}{n} \sin \frac{n\pi z}{l} \exp(-n^2 \pi \varkappa t/l^2). \quad (9a)$$

Likewise the heat flow and surface elevation are respectively:

$$Q(t) = \frac{T_m K}{l} \left(1 + 2\gamma_d \sum_{n=1}^{\infty} \exp(-n^2 \pi^2 \varkappa t/l^2)\right), \qquad (10a)$$

$$U(t) = \frac{\alpha l \rho_m T_m}{\rho_w - \rho_w} \frac{4\gamma_d}{\pi^2} \sum_{m=0}^{\infty} \frac{1}{(2m+1)^2} \exp(-(2m+1)^2 \pi^2 \varkappa t/l^2) \ . \qquad (11a)$$

Results are plotted in Figure 6.

REFERENCES CITED

Artemyev, M., and Ye. Artyushkov, 1969, Origin of rift basins: Internat. Geol. Rev., English Trans., v. 11, p. 582-593.

Auden, J. B., 1972, in discussion of K. G. Cox, The Karoo volcanic cycle: Geol. Soc. London Jour., v. 128, p. 334-335.

Barker, P. F., 1976, Underway geophysical observations: Initial Repts. Deep Sea Drilling Project, v. 36, p. 945-970.

———— et al, 1976, Initial reports of the Deep Sea Drilling Project, v. 36: Washington, D.C., U.S. Govt. Printing Office, 1080 p.

Burke, K., and A. J. Whiteman, 1973, Uplift, rifting and the breakup of Africa, in Implications of continental drift to the earth sciences, v. 12, pt. 7, Rifts and oceans: London, Academic Press, p. 735-755.

Carslaw, H. S., and J. C. Jaeger, 1959, Conduction of heat in solids: Oxford, Clarendon Press, 496 p.

Cox, K. G., 1972, The Karoo volcanic cycle: Geol. Soc. London Jour., v. 128, p. 311-333.

Davis, J. B., and E. E. Bray, 1969, Analysis of oil and cap rock from Challenger (Sigsbee) Knoll: Initial Repts. Deep Sea Drilling Project, v. 1, p. 415-500.

Grow, J. A., and R. G. Markl, 1977, IPOD-USGS multichannel seismic reflection profile from Cape Hatteras to the mid-Altantic Ridge: Geology, v. 5, p. 625-630.

Hood, A., C. C. M. Gutjahr, and R. L. Heacock, 1975, Organic metamorphism and the generation of petroleum: AAPG Bull., v. 59, p. 986-996.

King, W., and G. Simmons, 1972, Heat flow near Orlando, Florida, and Uvalde, Texas, determined from well cuttings: Geothermics, v. 1, p. 133-139.

Klitgord, K. D., and J. A. Grow, in prep., Jurassic stratigraphy and basement structure of the western Atlantic magnetic quiet zone.

Lancelot, Y., J. C. Hathaway, and C. D. Hollister, 1972, Lithology of sediments from the western North Atlantic, Leg II: Initial Repts. Deep Sea Drilling Project, v. 2, p. 901-949.

Langseth, M. G., X. Le Pichon, and M. Ewing, 1966, Crustal structure of mid-ocean ridges: Jour. Geophys. Research, v. 71, p. 5321-5355.

Lopatin, N. V., 1971, Temperatur a i geologicheskoye uremya kak faktory uglefikatsii: Akad. Nauk SSSR Izv. Ser. Geol., no. 3, p. 95-106.

Ludwig, W. J., et al, 1979, Structure of Falkland Plateau and offshore Tierra del Fuego, Argentina, in Geological and geophysical investigations of continental margins: AAPG Mem. 29, p. 125-137.

McKenzie, D., 1978, Some remarks on the development of sedimentary basins: Earth and Planetary Sci. Letters, v. 40, p. 25-32.

Nafe, J. E., and C. L. Drake, 1963, Physical properties of marine sediments, in M. N. Hill, ed. The sea, v. 3: New York, Interscience Pub., p. 784-815.

Parker, R. L., and D. W. Oldenburg, 1973, Thermal model of ocean ridges: Nature, Phys. Sci., v. 242, p. 137-139.

Parsons, B., and J. G. Sclater, 1977, An analysis of the variation of ocean floor bathymetry and heat flow with age: Jour. Geophys. Research, v. 82, p. 802-825.

Sleep, N. H., 1971, Thermal effects of the formation of Atlantic continental margins by continental breakup: Royal Astron. Soc. Geophys. Jour., v. 24, p. 325-350.

Steckler, M. S., and A. B. Watts, 1978, Subsidence of the Atlantic-type continental margin off New York: Earth and Planetary Sci. Letters, v. 41, p. 1-13.

Stegena, L., 1964, The structure of the earth's crust in Hungary: Acta Geol. Hungary, v. 8, p. 413-431.

Tissot, B., et al, 1974, Influence of nature and diagenesis of organic matter in formation of petroleum: AAPG Bull., v. 58, p. 499-506.

van Andel, T. H., et al, 1977, Depositional history of the South Atlantic Ocean during the last 125 million years: Jour. Geology, v. 85, p. 651-698.

Wager, L. R., 1947, Geological investigations in East Greenland, pt. IV: Medd. om Grønland, v. 134, p. 1-64.

Watts, A. B., and W. B. F. Ryan, 1976, Flexure of the lithosphere and continental margin basins: Tectonophysics, v. 36, p. 25-44.

Wright, L. A., 1976, Late Cenozoic fault patterns and stress fields in the Great Basin and westward displacement of the Sierra Nevada block: Geology, v. 4, p. 489-494.

———— and B. W. Troxel, 1967, Limitations on right-lateral strike-slip displacement, Death Valley and Furnace Creek fault zones, California: Geol. Soc. America Bull., v. 78, p. 933-958.

APPENDIX 2

COMPUTER PROGRAMS

WITH

SAMPLE INPUT AND OUTPUT

FILE: FIX   FORTRAN A   VM/SP CONVERSATIONAL MONITOR SYSTEM

```
C                                                                FIX00010
C      THIS PROGRAM DOES EVERYTHING YOU EVER WANTED TO DO TO      FIX00020
C      WELL DATA TO CALCULATE CORRECTED SUBSIDENCE AND            FIX00030
C      CONDUCTIVITIES                                             FIX00040
C                                                                FIX00050
C                  SET 1 WELL NAME                                FIX00060
C                                                                FIX00070
C                  SET 2 RHOM,RHOS                                FIX00080
C                   ARE ASTHENOSPHERIC AND SEDIMENT              FIX00090
C                     MATRIX DENSITIES,RESP. IN GM/CM**3          FIX00100
C                                                                FIX00110
C      INPUT       SET 3   TIME(I),I=1,NT                        FIX00120
C                   ARE TIMES AT WHICH COMPUTATIONS REQUIRED      FIX00130
C                    IN MY                                        FIX00140
C                                                                FIX00150
C                   SET 4                                         FIX00160
C                   ZL(I),A(I),FO(I),V1(I),V2(I),K1(I),K2(I)      FIX00170
C                    I=1,NL                                       FIX00180
C                   WHERE NL= NO. OF LITHOLOGIES                  FIX00190
C                   A(I) IS SLOPE OF LOG POROSITY VS DEPTH        FIX00200
C                    FO(I) IS SURFACE POROSITY IN %              FIX00210
C                    V1(I),V2(I) ARE % OF TWO MATRIX COMPOINENTS  FIX00220
C                     V1+V2=100%                                  FIX00230
C                   K1(I),K2(I) ARE THERMAL CONDUCTIVITIES        FIX00240
C                    IN MCAL/CMS OF TWO MATRIX COMPONENTS         FIX00250
C                                                                FIX00260
C                   SET 5 BT(I),BZ(I),I=1,NB                      FIX00270
C                    ARE BIOSTATIGRAPHIC AGE(MY) AND DEPTH(KM)    FIX00280
C                                                                FIX00290
C                                                                FIX00300
       DIMENSION ZL(10),A(10),FO(10),V1(10),V2(10)               FIX00310
       DIMENSION R(20)                                           FIX00320
       DIMENSION BT(30),BZ(30),TIME(20),Z1(20)                   FIX00330
       REAL K(30),K1(30),K2(30)                                  FIX00340
       DIMENSION MATRIX(2),MATT(2),WELNAM(2)                     FIX00350
C                                                                FIX00360
C      READ WELL NAME                                            FIX00370
       READ(5,987) WELNAM                                        FIX00380
C      READ MANTLE DENSITY,SED DENSITY                           FIX00390
       READ(5,102)RHOM,RHOS                                      FIX00400
C                                                                FIX00410
C      READ NO TIMES,BIOSTRAT UNITS,LITH UNITS                   FIX00420
       READ(5,100) NT,NB,NL                                      FIX00430
       WRITE(6,100) NT,NB,NL                                     FIX00440
C                                                                FIX00450
C      READ IN TIMES IN MY                                       FIX00460
       READ(5,101) (TIME(I),I=1,NT)                              FIX00470
C                                                                FIX00480
C      READ LITH DATA                                            FIX00490
       READ(5,102) (ZL(I),A(I),FO(I),V1(I),V2(I),K1(I),K2(I),I=1,NL)  FIX00500
C                                                                FIX00510
C      READ BIOSTRAT DATA                                        FIX00520
C      NOTE OPTION ***IF NT SET EG ZERO THEN TIME(I) SET         FIX00530
C      EQUAL TO BIOSTRAT TIMES***FOR SUBSIDENCE***               FIX00540
C      TIME(I) MUST ALWAYS BE PART OF INPUT                      FIX00550
```

```
         READ(5,103) (BT(I),BZ(I),I=1,NB)                        FIX00560
         IF (NT.NE.0) GO TO 11                                   FIX00570
         NT=NB+1                                                 FIX00580
         TIME(1)=0.                                              FIX00590
         DO 12 I=1,NB                                            FIX00600
   12    TIME(I+1)=BT(I)                                         FIX00610
   11    CONTINUE                                                FIX00620
C        READ NAMES OF LITH UNITS EG SANDSTONE AND SHALE         FIX00630
C                                                                FIX00640
C        MAXIMUM OF EIGHT LETTERS ALLOWED PER UNIT               FIX00650
         WRITE(2,988) WELNAM                                     FIX00660
         WRITE(2,207)                                            FIX00670
         DO 23 I=1,NL                                            FIX00680
         READ(5,104) MATRIX,MATT                                 FIX00690
         WRITE (2,204) I,MATRIX,MATT                             FIX00700
   23    CONTINUE                                                FIX00710
C                                                                FIX00720
C        WRITE OUT INPUT DATA                                    FIX00730
C                                                                FIX00740
         WRITE (2,300)                                           FIX00750
         WRITE (2,202) (ZL(I),A(I),FO(I),V1(I),V2(I),K1(I),K2(I),FIX00760
        1I=1,NL)                                                 FIX00770
         WRITE(2,303)RHOM,RHOS                                   FIX00780
         WRITE(2,301)                                            FIX00790
         WRITE(2,203) (BT(I),BZ(I),I=1,NB)                       FIX00800
         WRITE(2,205)                                            FIX00810
         WRITE(3,404) NT                                         FIX00820
         DO 5 I=1,NT                                             FIX00830
C                                                                FIX00840
         CALL INTERP(TIME(I),BT,BZ,NB,ZL,A,FO,V1,V2,K1,K2,Z1,NS,K,NL,R  FIX00850
        1,SCOMP,RHOM,RHOS)                                       FIX00860
C                                                                FIX00870
         DO 6 J=NS,NL                                            FIX00880
         WRITE(2,206) TIME(I),J,Z1(J),R(J),K(J)                  FIX00890
   6     CONTINUE                                                FIX00900
C                                                                FIX00910
C        WRITE PLOT TAPE                                         FIX00920
         WRITE(3,403) (Z1(NL),SCOMP,TIME(I))                     FIX00930
         SSCC=SCOMP*3.2/2.2                                      FIX00940
         WRITE(2,401) SCOMP,SSCC                                 FIX00950
   5     CONTINUE                                                FIX00960
  987    FORMAT(5A4,5A4)                                         FIX00970
  988    FORMAT (///20X,' SUPERWELL OUTPUT FOR ',5A4)            FIX00980
  100    FORMAT (3I5)                                            FIX00990
  101    FORMAT (10F7.0)                                         FIX01000
  102    FORMAT (7F7.0)                                          FIX01010
  103    FORMAT (2F7.0)                                          FIX01020
  104    FORMAT (5A4,5A4)                                        FIX01030
  207    FORMAT ('LITHOLOGICAL DATA'//'LITH UNIT   MATRIX1   MATRIX2')  FIX01040
  204    FORMAT (I5,5X,5A4,5A4)                                  FIX01050
  300    FORMAT ('  DEPTH KM SLOPE POR  SURF POR  %MATRIX1  %MATRIX2    FIX01060
        1COND1     COND2')                                       FIX01070
  401    FORMAT ('UNLOADED SUBS=',F8.4,3X,'WATER LOAD SUBS=',F8.4///)   FIX01080
  404    FORMAT (1X,I2)                                          FIX01090
  403    FORMAT (3E14.6)                                         FIX01100
```

```
 1403 FORMAT(2E14.6)                                              FIXO1110
  202 FORMAT (7F10.5)                                             FIXO1120
  301 FORMAT ('BIOSTRATIGRAPHIC DATA'//'   TIME MY   DEPTH')      FIXO1130
  203 FORMAT (2F10.5)                                             FIXO1140
  205 FORMAT ('DECOMPACTED DEPTHS AND COMPUTED CONDUCTIVITIES'/'  FIXO1150
     1TIME   LITH UNIT  DEPTH KM    RATIO   CONDUCT')             FIXO1160
  206 FORMAT (7X,F10.5,I4,3F10.5)                                 FIXO1170
  303 FORMAT('MANTLE DENSITY (HOT)=',F7.4,5X,'MATRIX=',           FIXO1180
     1F7.4)                                                       FIXO1190
      STOP                                                        FIXO1200
      END                                                         FIXO1210
C                                                                 FIXO1220
C                                                                 FIXO1230
      SUBROUTINE INTERP(TIME,BT,BZ,NB,ZL,A,FO,V1,V2,K1,K2,Z1,NS,K,NL,R, FIXO1240
     1SCOMP,RHOM,RHOS)                                            FIXO1250
C     FINDS DEPTH ZI IN PRESENT SECTION WHICH WAS AT SURFACE AT TIME FIXO1260
C     BY LINEAR INTERPLATION OF BIOSTAT DATA                      FIXO1270
C                                                                 FIXO1280
C                                                                 FIXO1290
C     THEN CALLS SUBROUTINE DECOMP WHICH DECOMPACTS THE SEDIMENTS FIXO1300
C     USING SLOPES OF LOG POROSITY VS DEPTH. THESE ARE A(I).      FIXO1310
C     ALSO USES SURFACE INTERCEPTS OF POROSITY,FO(I).             FIXO1320
C     ONE VALUE OF A(I)AND FO(I) PER LITH UNIT                    FIXO1330
C     LITH UNIT LOWER BOUNDARIES AT ZL(I)                         FIXO1340
C     V1,V2,K1,K2 DESCRIBED IN MAIN PROGRAM                       FIXO1350
C     DECOMPACTION METHOD ASSUMES THAT POROSITY-DEPTH CURVES      FIXO1360
C     ARE EXPONENTIAL AND THAT THE SHAPE OF THE EXPONENTIAL       FIXO1370
C     DPENDS ON LITHOLOGY,GIVING DIFFERENT A(I),FO(I) FOR EACH    FIXO1380
C     LITH UNIT. EACH UNIT IS MOVED UP THE CURVE CORRESPONDING    FIXO1390
C     TO ITS LITHOLOGY ON DECOMPACTION. AT TIMES SOMES LITH       FIXO1400
C     UNITS NOT YET DEPOSITED SO THAT START AT LITH UNIT NS       FIXO1410
C                                                                 FIXO1420
C                                                                 FIXO1430
C     THEN CALLS SEDCMP WHICH GIVES SUBSIDENCE CORRECTED FOR      FIXO1440
C       SEDIMENT LOADING.                                         FIXO1450
C                                                                 FIXO1460
C                                                                 FIXO1470
C     THEN CALLS CONDCT WHICH CALCULATES THE THERMAL CONDUCTIVITIES FIXO1480
C     TAKING INTO ACCOUNT THE LITHOLOGY AND NEW POROSITIES,GIVEN  FIXO1490
C     MATRIX CONDUCTIVITIES ,K1 AND K2 MATRIX K(I) CONTAINS NEW   FIXO1500
C     CONDUCTIVITIES AND MATRIX Z1(I) CONTAINS NEW DEPTHS         FIXO1510
C     TO BASE OF DECOMPACTED LITH UNITS                           FIXO1520
C      K AND Z1  VALUES ARE OUTPUT IN MAIN PROGRAM                FIXO1530
C     FOR EACH TIME                                               FIXO1540
C                                                                 FIXO1550
C                                                                 FIXO1560
      DIMENSION BT(1),BZ(1),ZL(1),A(1),FO(1),V1(1),V2(1)          FIXO1570
      DIMENSION Z1(1),Z11(20)                                     FIXO1580
      REAL K1(1),K2(1),K(1)                                       FIXO1590
      DIMENSION R(1)                                              FIXO1600
C                                                                 FIXO1610
C     FIND ZI                                                     FIXO1620
      N=NB-1                                                      FIXO1630
      DO 2 I=1,N                                                  FIXO1640
      IF(TIME.LE.BT(I+1).AND.TIME.GE.BT(I)) GO TO 3               FIXO1650
```

```
        GO TO 2                                             FIX01660
     3  ZI=BZ(I)+((BZ(I+1)-BZ(I))/(BT(I+1)-                 FIX01670
       1BT(I)))*(TIME-BT(I))                                FIX01680
        GO TO 4                                             FIX01690
     2  CONTINUE                                            FIX01700
        ZI=(BZ(1)/BT(1))*TIME                               FIX01710
     4  CONTINUE                                            FIX01720
C                                       .                   FIX01730
C       FIND LITH UNIT IN WHICH ZI FALLS                    FIX01740
C       NS IS THE INDEX OF THE UPPER RELEVANT LITH UNIT     FIX01750
        NS=1                                                FIX01760
        DO 5 I=1,NL                                         FIX01770
        IF(ZI.GE.ZL(I)) NS=NS+1                             FIX01780
   346  FORMAT(F12.5,I5,I5)                                 FIX01790
     5  CONTINUE                                            FIX01800
C                                                           FIX01810
C       DECOMPACT                                           FIX01820
   345  FORMAT(I4)                                          FIX01830
C                                                           FIX01840
        CALL DECOMP(A,FO,ZL,NL,NS,Z1,ZI,J)                  FIX01850
C                                                           FIX01860
C       CHANGE INDECES OF Z1(I) SO SAME AS THOSE OF A(I) ETC FIX01870
        JJ=J+1                                              FIX01880
        DO 20 I=1,JJ                                        FIX01890
        Z11(I)=Z1(I)                                        FIX01900
    20  CONTINUE                                            FIX01910
        DO 21 I=2,JJ                                        FIX01920
        Z1(NS+I-2)=Z11(I)                                   FIX01930
   775  FORMAT(I4,F10.5)                                    FIX01940
    21  CONTINUE                                            FIX01950
C                                                           FIX01960
C       CALCULATE RATIO R OF INITIAL THICK TO FINAL THICK   FIX01970
        DO 22 I=NS,NL                                       FIX01980
        IF(I.EQ.NS) GO TO 23                                FIX01990
        R(I)=Z1(I)-Z1(I-1)                                  FIX02000
        GO TO 22                                            FIX02010
    23  R(I)=Z1(NS)                                         FIX02020
    22  CONTINUE                                            FIX02030
C                                                           FIX02040
C        NOW Z1(NS) CORRESPONDS TO BOTTOM OF DECOMPACTED    FIX02050
C        LITH UNIT WITH PARAMETERS A(NS) ETC                FIX02060
C                                                           FIX02070
C                                                           FIX02080
        CALL SEDCMP(Z1,A,FO,NS,NL,SCOMP,RHOM,RHOS)          FIX02090
C                                                           FIX02100
C        COMPUTE THE CONDUCTIVITY OF EACH DECOMPACTED LITH UNIT FIX02110
C        USING SUBROUTINE CONDCT                            FIX02120
C                                                           FIX02130
C                                                           FIX02140
        CALL CONDCT(A,FO,V1,V2,K1,K2,Z1,NS                  FIX02150
       1,NL,K)                                              FIX02160
C                                                           FIX02170
C        K MATRIX CONTAINS THE COMPUTED CONDUCTIVITIES      FIX02180
        DO 24 I=NS,NL                                       FIX02190
        IF (I.EQ.NS) GO TO 123                              FIX02200
```

```
FILE: FIX      FORTRAN  A              VM/SP CONVERSATIONAL MONITOR SYSTEM


       R(I)=R(I)/K(I)+R(I-1)                              FIX02210
       GO TO 24                                           FIX02220
  123  R(I)=R(NS)/K(NS)                                   FIX02230
   24  CONTINUE                                           FIX02240
C                                                         FIX02250
       RETURN                                             FIX02260
       END                                                FIX02270
C                                          .              FIX02280
       SUBROUTINE DECOMP(A,FO,ZL,NL,NS,Z1,ZI,J)           FIX02290
C                                                         FIX02300
C      TO DECOMPACT SEDIMENT COLUMN WITH MATERIAL NOW AT LEVEL ZI   FIX02310
C      THEN AT SEA FLOOR. NS IS THE FIRST(UPPER) RELEVANT LITH UNIT FIX02320
C      ASSUMES EXPONENTIAL POROSITY DEPTH CURVES WITH DIFFERENT     FIX02330
C      SHAPES FOR DIFFERENT LITHOLOGIES. THE PARAMETERS OF THESE    FIX02340
C      EXPONENTIAL CURVES DETERMINED FROM WELL LOG DATA AND         FIX02350
C      OBTAINING SLOPE OF LOG(POROSITY) VS DEPTH AND SURFACE        FIX02360
C      POROSITY BY EXTRAPOLATION FOR EACH LITH UNIT                 FIX02370
C                                                         FIX02380
C                                                         FIX02390
C      CALLS NEWTON TO SOLVE EQUATION F(Z)=O. NUMERICALLY FIX02400
C      WHERE Z IS DECOMPACTED DEPTH                       FIX02410
C                                                         FIX02420
C      FUNCTION ROUTINES FX ABD FPRM USED BY NEWTON       FIX02430
C                                                         FIX02440
C      RETURNS Z1(I) WHICH CONTAINS THE DECPMPACTED DEPTH TO  FIX02450
C      LITH UNITS                                         FIX02460
       DIMENSION A(1),FO(1),ZL(10),Z1(1)                  FIX02470
C                                                         FIX02480
C      START DECOMPACTING FROM THE SURFACE DOWN           FIX02490
C                                                         FIX02500
       Z1(1)=0.0                                          FIX02510
       J=0                                                FIX02520
       DO 2 I=NS,NL                                       FIX02530
       J=J+1                                              FIX02540
       IF (J.EQ.1) ZU=ZI                                  FIX02550
       C=-(ZL(I)-ZU)-Z1(J)+FO(I)*(EXP(-A(I)*ZU)-EXP(-A(I)*  FIX02560
      1ZL(I)))/(A(I)*100.)-FO(I)*EXP(-A(I)*Z1(J))/(A(I)*100  FIX02570
      2.)                                                 FIX02580
       ZO=Z1(J)+(ZL(I)-ZU)                                FIX02590
C                                                         FIX02600
C      ZO IS FIRST ESTIMATE OF ROOT FOR NEWTON            FIX02610
C                                                         FIX02620
       PO=FO(I)/100.                                      FIX02630
       CALL NEWTON(50,.001,A(I),PO,C,ZO)                  FIX02640
       Z1(J+1)=ZO                                         FIX02650
       ZU=ZL(I)                                           FIX02660
    2  CONTINUE                                           FIX02670
       RETURN                                             FIX02680
       END                                                FIX02690
C                                                         FIX02700
       SUBROUTINE NEWTON(N,TOL,A,PO,C,ROOT)               FIX02710
C      SOLVES FOR ROOT OF EQUATION F(X)=0                 FIX02720
C      USING NEWTONS METHOD. DOES N ITERATIONS            FIX02730
C      TO FIND ROOT TO TOLERANCE TOL.                     FIX02740
C      CALLS FUNCTION SUBPROGS FX AND FPRM                FIX02750
```

```
C      TO FIND VALUES OF F(X) AND DF/DX                      FIX02760
C                                                            FIX02770
       DO 1 I=1,N                                            FIX02780
       FO=FX(A,PO,ROOT,C)                                    FIX02790
       IF (ABS(FO).LT.TOL) GO TO 2                           FIX02800
       FPO=FPRM(A,PO,ROOT)                                   FIX02810
       CORREC=FO/FPO                                         FIX02820
     1 ROOT=ROOT-CORREC                                      FIX02830
       PRINT 200, ROOT,FO,N,TOL                              FIX02840
   200 FORMAT ('MAX ITER REACHED'/2E14.5,I5,E14.5)           FIX02850
     2 RETURN                                                FIX02860
       END                                                   FIX02870
C                                                            FIX02880
       FUNCTION FX(A,FO,ZO,C)                                FIX02890
C                                                            FIX02900
C      CALCULATES F(ZO)                                      FIX02910
C      USED BY NEWTON                                        FIX02920
       FX=ZO+FO*EXP(-A*ZO)/A+C                               FIX02930
       RETURN                                                FIX02940
       END                                                   FIX02950
C                                                            FIX02960
C                                                            FIX02970
       FUNCTION FPRM(A,FO,ZO)                                FIX02980
C      CALCULATES DF(ZO)/DZ                                  FIX02990
C      USED BY NEWTON                                        FIX03000
       FPRM=1.-FO*EXP(-A*ZO)                                 FIX03010
       RETURN                                                FIX03020
       END                                                   FIX03030
C                                                            FIX03040
       SUBROUTINE SEDCMP(Z1,A,FO,NS,NL,SCOMP,RHOM,RHOS)      FIX03050
       DIMENSION Z1(1),A(1),FO(1)                            FIX03060
C                                                            FIX03070
C      THIS SUBROUTINE GIVES SUBSIDENCE CORRECTED FPR SED. LOADING  FIX03080
C      USING AN AIRY ISOSTATIC MODEL.Z1 IS DEPT TO EACH LITH UNIT   FIX03090
C      (LOWER BOUNDARY),FO AND A ARE POROSITY PARAMETERS.SCOMP       FIX03100
C      IS CORRECTED DEPTH TO BASEMENT.                       FIX03110
C      PARAMETERS ASSUMED; DENSITY OF LITH=3.2, DENSITY OF CRUST=2.8 FIX03120
C      DENSITY OF SED AT 0 POROSITY =2.85                    FIX03130
C      DENSITY OF WATER IS 1.0                               FIX03140
C                                                            FIX03150
C                                                            FIX03160
       WT=0.0                                                FIX03170
       DO 6 I=NS,NL                                          FIX03180
       IF(I.EQ.NS) GO TO 5                                   FIX03190
       WT=RHOS*(Z1(I)-Z1(I-1))-(RHOS-1.)*FO(I)*(EXP(-A(I)*Z1(I-1))-EXP  FIX03200
      1(-A(I)*Z1(I)))/(A(I)*100.)+WT                         FIX03210
       GO TO 6                                               FIX03220
     5 WT=Z1(NS)*RHOS-(RHOS-1.)*FO(NS)*(1.-EXP(-A(NS)*Z1(NS)))/(A(NS)   FIX03230
      1*100.)                                                FIX03240
     6 CONTINUE                                              FIX03250
       SLOAD=(Z1(NL)*RHOM-WT)/RHOM                           FIX03260
       SCOMP=SLOAD                                           FIX03270
       RETURN                                                FIX03280
       END                                                   FIX03290
C                                                            FIX03300
```

FILE: FIX   FORTRAN A   VM/SP CONVERSATIONAL MONITOR SYSTEM

```
        SUBROUTINE CONDCT(A,FO,V1,V2,K1,K2,Z1,NS,NL,K)          FIX03310
        REAL KAV,KPART,KTOT,K1(1),K2(1)                         FIX03320
        REAL K(1)                                               FIX03330
        DIMENSION A(1),FO(1),V1(1),V2(1),Z1(1)                  FIX03340
    349 FORMAT('NS,NL',4X,I5,I5)                                FIX03350
    340 FORMAT('K1,K2',F8.4,4X,F8.4)                            FIX03360
C                                                               FIX03370
C       THIS SUBROUTINE CALCULATES THE THERMAL CONDUCTIVITY     FIX03380
C       OF A SEDIMENTARY SEQUENCE                               FIX03390
C       V1,V2ARE THE PERCENT(WITHOUT WATER OF THE PRIMARY AND SEC- FIX03400
C       CONDARY ROCK TYPES.K1,K2 ARE THE RESPEDTIVE CONDUCTIVITIES. FIX03410
C       POROSITY= FO*EXP(-Z*A),Z1(I)IS LOWER BOUNDARY OF EACH   FIX03420
C       LITHOLOGIC UNIT.                                        FIX03430
C                                                               FIX03440
        DO 100 I=NS,NL                                          FIX03450
C                                                               FIX03460
C       DIVIDE EACH UNIT INTO 4 SUBSECTIONS AND COMPUTE MIDPOINT FIX03470
C       OF EACH                                                 FIX03480
        KAV=0.0                                                 FIX03490
        IEND=4                                                  FIX03500
        DO 95 INC=1,IEND                                        FIX03510
        IF (I.EQ.NS) GO TO 5                                    FIX03520
        ZZ=Z1(I-1)+((Z1(I)-Z1(I-1))/IEND)*(INC-0.5)            FIX03530
        GO TO 6                                                 FIX03540
      5 ZZ=(Z1(NS)/IEND)*(INC-.5)                               FIX03550
C       NOW COMPUTE POROSITY AT Z=ZZ                            FIX03560
      6 F=FO(I)*EXP(-ZZ*A(I))                                   FIX03570
C                                                               FIX03580
C       NOW COMPUTE THERMAL CONDUCTIVITY OF EACH POINT          FIX03590
C       ZZ USING A MAXWELL MODEL                                FIX03600
        R1=K1(I)/1.4                                            FIX03610
        S1=F/(F+V1(I)*(100.-F)/100.)                            FIX03620
        KPART=K1(I)*((2.0*R1+1.0)-2.0*S1*(R1-1.0))             FIX03630
       1/((2.0*R1+1.0)+(R1-1.0)*S1)                             FIX03640
        R2=KPART/K2(I)                                          FIX03650
        S2=V2(I)*(100.-F)/100.                                  FIX03660
        S2=S2/100.                                              FIX03670
        KTOT=KPART*((2.0*R2+1.0)-2.0*S2*(R2-1.0))             FIX03680
       1/((2.0*R2+1.0)+(R2-1.0)*S2)                             FIX03690
    200 FORMAT(2E14.5)                                          FIX03700
C                                                               FIX03710
C       COMPUTE THE WEIGHTED HARMONIC MEAN OF EACH              FIX03720
C       LITHOLOGIC UNIT,K(I),                                   FIX03730
     95 KAV=KAV+1.0/KTOT                                        FIX03740
    351 FORMAT('KAV',F8.4)                                      FIX03750
    100 K(I)=IEND/KAV                                           FIX03760
     80 FORMAT(F12.5,8X,I5)                                     FIX03770
        RETURN                                                  FIX03780
        END                                                     FIX03790
```

FILE: FIX   DATA   A   VM/SP CONVERSATIONAL MONITOR SYSTEM

```
   FIX
  3.2     2.65
    6      6     2
  O.      2.      4.      7.     13.     16.5
   2.50   .6     40.     80.    20.      6.0    7.5
  4.35    .5     60.     50.    50.      6.0    5.0
  O.      O.
   2.      .5
   5.     1.26
  10.5    3.89
   13.    3.90
  16.5    4.35
  SHALE      SS
  SHALE      LS
```

```
FILE: FIX      OUTPUT   A              VM/SP CONVERSATIONAL MONITOR SYSTEM



                    SUPERWELL OUTPUT FOR      FIX
LITHOLOGICAL DATA

LITH UNIT    MATRIX1    MATRIX2
    1        SHALE      SS
    2        SHALE      LS
  DEPTH KM SLOPE POR   SURF POR   %MATRIX1   %MATRIX2      COND1     COND2
  2.50000   0.60000   40.00000   80.00000  ·20.00000    6.00000   7.50000
  4.35000   0.50000   60.00000   50.00000   50.00000    6.00000   5.00000
MANTLE DENSITY (HOT)= 3.2000      MATRIX= 2.6500
BIOSTRATIGRAPHIC DATA

   TIME MY    DEPTH
   0.0        0.0
   2.00000    0.50000
   5.00000    1.26000
  10.50000    3.89000
  13.00000    3.90000
  16.50000    4.35000
DECOMPACTED DEPTHS AND COMPUTED CONDUCTIVITIES
        TIME    LITH UNIT   DEPTH KM    RATIO    CONDUCT
        0.0         1       2.50000   0.50416   4.95872
        0.0         2       4.35000   0.88128   4.90557
UNLOADED SUBS=  1.1217   WATER LOAD SUBS=  1.6315



        2.00000     1       2.13728   0.44015   4.85578
        2.00000     2       4.03221   0.83495   4.79980
UNLOADED SUBS=  1.0716   WATER LOAD SUBS=  1.5586



        4.00000     1       1.70461   0.36137   4.71705
        4.00000     2       3.66738   0.78340   4.65077
UNLOADED SUBS=  1.0154   WATER LOAD SUBS=  1.4770



        7.00000     1       0.39750   0.09564   4.15600
        7.00000     2       2.71496   0.67281   4.01526
UNLOADED SUBS=  0.8876   WATER LOAD SUBS=  1.2910



       13.00000     2       0.81885   0.26011   3.14805
UNLOADED SUBS=  0.3486   WATER LOAD SUBS=  0.5071



       16.50000     2       0.00000   0.00000   2.72472
UNLOADED SUBS=  0.0000   WATER LOAD SUBS=  0.0000
```

FILE: CLEAN   FORTRAN A   VM/SP CONVERSATIONAL MONITOR SYSTEM

```
C     THIS PROGRAM CALCULATES SUBSIDENCE AND TEMPERATURE            CLE00010
C     (1 DIMENSIONAL) FOR AN EXTENDING REGION BY DIVIDING           CLE00020
C     THE TOTAL TIME INTO SMALL INCREMENTS. THE PROGRAM             CLE00030
C     THEN CALCULATES THE AMOUNT OF EXTENSION WHICH                 CLE00040
C     SHOULD HAVE OCCURRED OVER EACH INCREMENT AND                  CLE00050
C     ASSUMES THAT IT OCCURS INSTANTANEOUSLY AT THE BEGINNING       CLE00060
C     OF THAT INCREMENT. IF THE TIME INCREMENTS ARE CHOSEN          CLE00070
C     SUFFICIENTLY SMALL, THIS APPROXIMATION CAN BE MADE            CLE00080
C     AS ACCURATE AS DESIRED.  THIS PROGRAM ALSO TAKES INTO         CLE00090
C     CONSIDERATION THE EFFECTS OF SEDIMENT COOLING, RADIOGENIC     CLE00100
C     SOURCES IN THE CRUST (BUT NOT IN THE SEDIMENTS), AND          CLE00110
C     VARIATION OF CONDUCTIVITY OF THE SEDIMENTS WITH DEPTH.        CLE00120
C     ASSUMES SURFACE AT O DEG C.                                   CLE00130
C                                                                   CLE00140
C     THIS PROGRAM WAS DESIGNED TO BE USED ON VERY YOUNG BASINS.    CLE00150
C                                                                   CLE00160
C     ALL PARAMETERS ARE FROM PARSONS AND SCLATER, 1977,           CLE00170
C     EXCEPT FOR ASTHENOSPHERE DENSITY (3.2) AND CRUSTAL DENSITY    CLE00180
C     (2.8).                                                        CLE00190
C     TEMPERATURE IS NORMALIZED TO BE 1 AT BASE OF                  CLE00200
C     LITHOSPHERE AND FOR CALCULTIONS DEPTH IS ALSO CONVERTED       CLE00210
C     TO BE ONE AT BASE OF THE LITHOSPHERE (125 KM).                CLE00220
C                                                                   CLE00230
C                                                                   CLE00240
C                                                                   CLE00250
      DIMENSION B(10),D(10),X(10),TTIM(10),T(1000),TOUT(50,50)      CLE00260
     1,TEND(10),TST(10),XR(10)                                      CLE00270
C                                                                   CLE00280
      WRITE(2,1003)                                                 CLE00290
C     READ DEPTH INCREMENT (KM), TIME INCREMENT (MY), TIME          CLE00300
C     INCREMENT FOR WRITING TEMPERATURE OUTPUT (MY)                 CLE00310
      READ(5,1000) DELX,DELT,TWRI                                   CLE00320
C                                                                   CLE00330
C     READ INITIAL CRUSTAL THICKNESS (KM),  SURFACE CONDUCTIVITY    CLE00340
C     AND CONDUCTIVITY GRADIENT (PER KM)                            CLE00350
C     IN 10**-3 CAL/CM SEC DEG. C                                   CLE00360
      READ(5,1000) CRUST,AK,BK                                      CLE00370
      CCR=CRUST                                                     CLE00380
C                                                                   CLE00390
C     READ NUMBER OF EXTENSIONAL PERIODS INCLUDING TIMES           CLE00400
C     OF NO EXTENSION AS DISTINCT EXTENSIONAL EPISODES.            CLE00410
      READ(5,1001) KNO                                              CLE00420
C                                                                   CLE00430
C     READ AMOUNT EXTENSION; D=AMOUNT CRUSTAL EXTENSION             CLE00440
C     D*B=AMOUNT SUBCRUSTAL EXTENSION                               CLE00450
C     (SEE ROYDEN AND KEEN,1980)                                    CLE00460
      READ(5,1002)(B(K),D(K),K=1,KNO)                               CLE00470
C                                                                   CLE00480
C     READ TIME (MA) FOR BEGINNING AND END OF EACH EXTENSION        CLE00490
C     PERIOD                                                        CLE00500
      READ(5,1002)(TST(K),TEND(K),K=1,KNO)                          CLE00510
C                                                                   CLE00520
C     READ NUMBER OF POINTS FOR WHICH SEDIMENT THICKNESS            CLE00530
C     WILL BE READ IN.                                              CLE00540
      READ(5,1001) NXPTS                                            CLE00550
```

```
C                                                                  CLE00560
C       READ SEDIMENT THICKNESS (KM) AND TIME (MA)                 CLE00570
        READ(5,1002) (XR(I),TTIM(I),I=1,NXPTS)                     CLE00580
C                                                                  CLE00590
C       CHANGE SEDIMENT THICKNESS TO EFFECTIVE THICKNESS TO        CLE00600
C       COMPENSATE FOR DIFFERENT CONDUCTIVITIES. LITHOSPHERE       CLE00610
C       CONDUCTIVITY ASSUMED IS 7.5, SEDIMENT CONUCTIVITY          CLE00620
C       IS AK+BK*DEPTH(KM), WITH A MAXIMUM VALUE OF 7.5.           CLE00630
        XK=(7.5-AK)/BK                                             CLE00640
        ADDK=7.5*ALOG(1.+BK*XK/AK)/BK                             CLE00650
        DO 02 I=1,NXPTS                                            CLE00660
        IF (XR(I).GT.XK) X(I)=XR(I)-XK+ADDK                        CLE00670
        IF (XR(I).EQ.XK) X(I)=ADDK                                 CLE00680
        IF (XR(I).LT.XK) X(I)=7.5*ALOG(1.+BK*XR(I)/AK)/BK         CLE00690
    02  CONTINUE                                                   CLE00700
        JWR=0                                                      CLE00710
C                                                                  CLE00720
C       SET SEDIMENT THICKNESS TO 0.                              CLE00730
C       SEDIMENT THICKNESS=(NSED-1)*DELX                          CLE00740
        NSED=1                                                     CLE00750
C                                                                  CLE00760
C       INITIALIZE TIME (TIM)                                     CLE00770
        TIM=TST(1)                                                 CLE00780
C                                                                  CLE00790
C       SET NUMBER OF DEPTH POINTS FOR LITHOSPHERE                 CLE00800
        JSTOP=IFIX(125./DELX+.0001)+1                             CLE00810
C                                                                  CLE00820
C       SET DEPTH AND MAGNITUDE OF RADIOGENIC POINT SOURCES        CLE00830
C       AR IS HEAT PRODUCTION IN 10 EXP(-6) CAL/CM*CM*SEC          CLE00840
C       AO IS TEMPERATURE GRADIENT NEAR SURFACE DUE TO             CLE00850
C       RADIOGENIC SOURCE, (WITH TEMPERATURE=1 AT BASE             CLE00860
C       OF LITHOSPHERE)                                            CLE00870
        RDEP=8.                                                    CLE00880
        AR=.375                                                    CLE00890
        AO=AR/(.0075*1333.)*.1                                     CLE00900
C                                                                  CLE00910
C       CALCULATE TEMPERATURE CONTRIBUTION FROM POINT SOURCE       CLE00920
        JR=IFIX(RDEP/DELX+.001)+1                                  CLE00930
        DO 10 J=1,JSTOP                                            CLE00940
        IF (J.LT.JR.OR.J.EQ.JR) T(J)=AO*FLOAT(J-1)*DELX            CLE00950
        IF (J.GT.JR) T(J)=AO*FLOAT(JR-1)*FLOAT(JSTOP-J)/FLOAT(JSTOP-JR)  CLE00960
       1*DELX                                                      CLE00970
C                                                                  CLE00980
C       ADD ON EQUILIBRIUM THERMAL CONDITIONS TO GIVE              CLE00990
C       TOTAL TEMPERATURE PROFILE BEFORE STRETCHING.               CLE01000
    10  T(J)=FLOAT(J-1)*DELX/125.+T(J)                             CLE01010
        DO 30 K=1,KNO                                              CLE01020
C                                                                  CLE01030
C       SET NUMBER OF TIME INCREMENTS FOR EACH PHASE OF EXTENSION. CLE01040
        ISTOP=IFIX((TST(K)+.0001-TEND(K))/DELT)                    CLE01050
        DO 20 I=1,ISTOP                                            CLE01060
C                                                                  CLE01070
C       SET AMOUNT OF EXTENSION (DELB,DELD) FOR EACH TIME INCREMENT, DELT CLE01080
        TIM=TIM-DELT                                               CLE01090
C       WRITE(2,1000)TIM                                           CLE01100
```

```
        QI=FLOAT(I)                                              CLE01110
        Q=FLOAT(ISTOP)                                           CLE01120
        DELB=(1.+QI*(B(K)-1.)/Q)/(1.+(QI-1.)*(B(K)-1.)/Q)        CLE01130
        DELD=(1.+QI*(D(K)-1.)/Q)/(1.+(QI-1.)*(D(K)-1.)/Q)        CLE01140
C                                                                CLE01150
C       CALCULATE TEMPERATURE FOR NEXT TIMESTEP                  CLE01160
C       BY STRETCHING INSTANTANEOULSY AT BEGINNING OF EACH TIME  CLE01170
C       STEP, THEN CALCULATING RESULTING TEMPERATURES AT         CLE01180
C       END OF TIME STEP.                                        CLE01190
        CALL TSTEP(NXPTS,TTIM,TIM,X,DELX,NSED,MSED,JSTOP,T,DELT,  CLE01200
       1DELD,DELB,CRUST,RDEP,AO)                                 CLE01210
C                                                                CLE01220
C       CALCULATE AMOUNT OF SUBSIDENCE                           CLE01230
        CALL SUBSID(JSTOP,NSED,SUBS,T,CRUST,JWR,TIM,DELX)        CLE01240
C                                                                CLE01250
C       SET UP TEMPERATURE OUTPUT GRID                           CLE01260
        CALL SETPT(TIM,TWRI,NSED,JWR,T,TOUT)                     CLE01270
   20   CONTINUE                                                 CLE01280
   30   CONTINUE                                                 CLE01290
C                                                                CLE01300
C       WRITE OUTPUT                                             CLE01310
        CALL OUTPUT(TST,TEND,B,D,CCR,TWRI,DELX,NSED,TOUT         CLE01320
       1,KNO,JWR,AK,BK,XK,ADDK)                                  CLE01330
 1000   FORMAT(3F7.4)                                            CLE01340
 1001   FORMAT(I3)                                               CLE01350
 1002   FORMAT(2F7.4)                                            CLE01360
 1003   FORMAT('     TIME        UNLOAD SUBS (KM)   WATER LOAD SUBS')  CLE01370
        STOP                                                     CLE01380
        END                                                      CLE01390
C                                                                CLE01400
C                                                                CLE01410
        SUBROUTINE TSTEP(NXPTS,TTIM,TIM,X,DELX,NSED,MSED,JSTOP,  CLE01420
       1T,DELT,DELD,DELB,CRUST,RDEP,AO)                          CLE01430
C                                                                CLE01440
C       THIS SUBROUTINE CALCULATES NEW TEMPERATURES, ETC. FOR    CLE01450
C       EACH INSTANTANEOUS EPISODE OF EXTENSION.                 CLE01460
        DIMENSION TTIM(10),X(10),T(1000),PT(1000)                CLE01470
 1000   FORMAT(F7.4)                                             CLE01480
C                                                                CLE01490
C       SET SEDIMENT THICKNESS                                   CLE01500
        CALL DSED(NXPTS,TTIM,TIM,X,DELX,NSED,MSED)               CLE01510
C                                                                CLE01520
C       ADD ON SEDIMENT AT O DEGREES C                           CLE01530
C       AND READJUST TEMPERATURES                                CLE01540
        DO 15 J=1,JSTOP                                          CLE01550
   15   PT(J+MSED-1)=T(J)                                        CLE01560
        DO 20 J=1,MSED                                           CLE01570
   20   PT(J)=O.                                                 CLE01580
        DO 22 J=1,JSTOP                                          CLE01590
   22   T(J)=PT(J)                                               CLE01600
C                                                                CLE01610
C       STRETCH WHOLE LITHOSPHERE BY DELD, COMPUTE NEW TEMPERATURES  CLE01620
        DO 25 J=NSED,JSTOP                                       CLE01630
        A=DELD*FLOAT(J-NSED)+FLOAT(NSED)                         CLE01640
        JOLD=IFIX(A)                                             CLE01650
```

FILE: CLEAN   FORTRAN A   VM/SP CONVERSATIONAL MONITOR SYSTEM

```
      PT(J)=T(JOLD)+(A-FLOAT(JOLD))*(T(JOLD+1)-T(JOLD))        CLE01660
      IF (FLOAT(JOLD).GT.FLOAT(JSTOP-1)) PT(J)=1.              CLE01670
   25 CONTINUE                                                 CLE01680
      DO 30 J=NSED,JSTOP                                       CLE01690
   30 T(J)=PT(J)                                               CLE01700
C                                                              CLE01710
C     ADJUST CRUSTAL THICKNESS AND DEPTH, MAGNITUE OF RADIOGENIC  CLE01720
C     POINT SOURCE                                             CLE01730
      CRUST=CRUST/DELD                                         CLE01740
      RDEP=RDEP/DELD                                           CLE01750
      AO=AO/DELD                          .                    CLE01760
C                                                              CLE01770
C     STRETCH SUB-CRUSTAL LITHOSPHERE BY DELB, COMPUTE NEW     CLE01780
C     TEMPERATURES                                             CLE01790
      JSTART=IFIX(CRUST/DELX+.0001)+NSED                       CLE01800
      DO 35 J=JSTART,JSTOP                                     CLE01810
      B=DELB*FLOAT(J-JSTART)+FLOAT(JSTART)                     CLE01820
      JJOL=IFIX(B)                                             CLE01830
      T(J)=PT(JJOL)+(B-FLOAT(JJOL))*(PT(JJOL+1)-PT(JJOL))      CLE01840
      IF ( FLOAT(JJOL).GT.FLOAT(JSTOP-1)) T(J)=1.              CLE01850
   35 CONTINUE                                                 CLE01860
C                                                              CLE01870
C     COMPUTE TEMPERATURE AT END OF TIME INCREMENT             CLE01880
      DO 45 J=NSED,JSTOP                                       CLE01890
   45 IF (T(J).GT.1.) T(J)=1.                                  CLE01900
      CALL INTEG(JSTOP,T,DELX,DELT,AO,RDEP,NSED)               CLE01910
      RETURN                                                   CLE01920
      END                                                      CLE01930
C                                                              CLE01940
C                                                              CLE01950
      SUBROUTINE DSED(NXPTS,TTIM,TIM,X,DELX,NSED,MSED)         CLE01960
C                                                              CLE01970
C     THIS SUBROUTINE SETS THE SEDIMENT THICKNESS FOR EACH     CLE01980
C     TIME INCREMENT                                           CLE01990
C     TOTAL SEDIMENT THICHNESS=(NSED-1)*DELX                   CLE02000
C     NEW SEDIMENT ADDED=(MSED-1)*DELX                         CLE02010
      DIMENSION X(10),TTIM(10)                                 CLE02020
      DO 10 I=1,NXPTS                                          CLE02030
      IF (TTIM(I).LT.TIM) GO TO 20                             CLE02040
   10 CONTINUE                                                 CLE02050
   20 SED=((X(I)-X(I-1))/(TTIM(I-1)-TTIM(I)))*(-TIM+TTIM(I-1)) CLE02060
     1+X(I-1)                                                  CLE02070
      MSED=IFIX(SED/DELX+.0001)+2-NSED                         CLE02080
      NSED=NSED+MSED-1                                         CLE02090
      RETURN                                                   CLE02100
      END                                                      CLE02110
C                                                              CLE02120
C     '                                                        CLE02130
      SUBROUTINE INTEG(JSTOP,T,DELX,DELT,AO,RDEP,NSED)         CLE02140
C                                                              CLE02150
C     THIS SUBROUTINE FINDS TEMPERATURE AFTER TIME DELT        CLE02160
C     SEE CARSLAW AND JAEGER FOR ANALYTICAL SOLUTION FOR       CLE02170
C     COOLING SLAB          .                                  CLE02180
      DIMENSION T(1000),TT(1000),CN(50),X(1000)               CLE02190
 1000 FORMAT(F7.4)                                             CLE02200
```

```
       JR=NSED+IFIX(RDEP/DELX)                                      CLE02210
       PI=3.14159265                                                CLE02220
C                                                                   CLE02230
C       SUBTRACT EQUILIBRIUM TEMPERATURE FROM TOTAL TEMPERATURE     CLE02240
       DO 40 J=1,JSTOP                                              CLE02250
       X(J)=DELX*(J-1)/125.                                         CLE02260
    40 TT(J)=T(J)-X(J)                                              CLE02270
C                                                                   CLE02280
C       SUBTRACT RADIOGENIC CONTRUIBUTION TO TEMPERATURE PROFILE    CLE02290
       DO 45 J=1,JR                                                 CLE02300
    45 TT(J)=TT(J)-AO*FLOAT(J-1)*DELX            .                  CLE02310
       JJR=JR+1                                                     CLE02320
       DO 50 J=JJR,JSTOP                                            CLE02330
    50 TT(J)=TT(J)-AO*FLOAT(JR-1)*FLOAT(JSTOP-J)/FLOAT(JSTOP-JR)    CLE02340
      1*DELX                                                        CLE02350
C                                                                   CLE02360
C       FIND FOURIER COEFFICIENT                                    CLE02370
       DO 65 N=1,20                                                 CLE02380
       AN=FLOAT(N)                                                  CLE02390
       CN(N)=0.                                                     CLE02400
       DO 55 J=2,JSTOP                                              CLE02410
    55 CN(N)=CN(N)+(TT(J)*SIN(AN*PI*X(J))+TT(J-1)*SIN(AN*PI*X(J-1)))CLE02420
      1*DELX/125.                                                   CLE02430
C      WRITE(2,1000)CN(N)                                           CLE02440
    65 CONTINUE                                                     CLE02450
       DO 85 J=1,JSTOP                                              CLE02460
       TT(J)=0.                                                     CLE02470
C                                                                   CLE02480
C       RECONSTRUCT TEMPERATURE AT END OF TIME INCREMENT            CLE02490
C       WITHOUT RADIOGENIC CONTRIBUTON                              CLE02500
       DO 75 N=1,20                                                 CLE02510
       AN=FLOAT(N)                                                  CLE02520
    75 TT(J)=TT(J)+CN(N)*SIN(AN*PI*X(J))*EXP(-DELT*AN*AN/62.8)      CLE02530
       T(J)=TT(J)+X(J)                                              CLE02540
    85 CONTINUE                                                     CLE02550
C                                                                   CLE02560
C       ADD ON RADIOGENIC CONTRIBUTION                              CLE02570
       DO 90 J=1,JR                                                 CLE02580
    90 T(J)=T(J)+AO*FLOAT(J-1)*DELX                                 CLE02590
       DO 95 J=JJR,JSTOP                                            CLE02600
    95 T(J)=T(J)+AO*FLOAT(JR-1)*FLOAT(JSTOP-J)/FLOAT(JSTOP-JR)      CLE02610
      1*DELX                                                        CLE02620
       RETURN                                                       CLE02630
       END                                                          CLE02640
C                                                                   CLE02650
C                                                                   CLE02660
       SUBROUTINE SETPT(TIM,TWRI,NSED,JWR,T,TOUT)                   CLE02670
C                                                                   CLE02680
C       THIS SUBROUTINE CHECKS TO SEE IF THE TEMPERATURES SHOULD    CLE02690
C       BE READ INTO OUTPUT FILE.  IF SO, STORES TEMPERATURE        CLE02700
C       UNDER TOUT(JWR,J)                                           CLE02710
       DIMENSION T(1000),TOUT(50,50)                                CLE02720
       ITEST=IFIX(TIM/TWRI+.0001)                                   CLE02730
       TEST=TIM/TWRI-ITEST                                          CLE02740
       IF (TEST.GT..0001) GO TO 100                                 CLE02750
```

FILE: CLEAN   FORTRAN   A   VM/SP CONVERSATIONAL MONITOR SYSTEM

```
          JWR=JWR+1                                          CLE02760
          NSNS=20                                            CLE02770
          DO 10 J=1,NSNS                                     CLE02780
    10    TOUT(JWR,J)=T(J)                                   CLE02790
   100    CONTINUE                                           CLE02800
  1000    FORMAT(F7.4)                                       CLE02810
          RETURN                                             CLE02820
          END                                                CLE02830
C                                                            CLE02840
C                                                            CLE02850
          SUBROUTINE OUTPUT(TST,TEND,B,D,CRUST,TWRI,DELX,NSED,   CLE02860
         1TOUT,KNO,JWR,AK,BK,XK,ADDK)                        CLE02870
C                                                            CLE02880
C         THIS SUBROUTINE WRITES THE OUTPUT FILE             CLE02890
          DIMENSION TST(10),TEND(10),B(10),D(10),TOUT(50,50)  CLE02900
         1,TTOUT(50,50)                                      CLE02910
C                                                            CLE02920
C         CHANGE EFFECTIVE SEDIMENT THICHNESS BACK TO REAL   CLE02930
C         SEDIMENT THICKNESS.                                CLE02940
C         AND COMPUTE TEMPERATURE GRID FOR REAL SEDIMENTS    CLE02950
          JJEND=14                                           CLE02960
          DO 20 JJ=2,JJEND                                   CLE02970
          Y=FLOAT(JJ-1)*DELX                                 CLE02980
          IF (Y.LT.XK) AJ=(7.5*ALOG(1.+BK*Y/AK)/BK)/DELX+1.  CLE02990
          IF (Y.EQ.XK) AJ=(ADDK-XK+Y)/DELX+1.                CLE03000
          IF (Y.GT.XK) AJ=(ADDK-XK+Y)/DELX+1.                CLE03010
          J=IFIX(AJ)                                         CLE03020
          XXX=AJ-FLOAT(J)                                    CLE03030
          IF (XXX.EQ.0.) XXX=1000.                           CLE03040
          DO 10 I=1,JWR                                      CLE03050
          TTOUT(I,1)=0.                                      CLE03060
          TTOUT(I,JJ)=(TOUT(I,J+1)-TOUT(I,J))*XXX+TOUT(I,J)  CLE03070
    10    CONTINUE                                           CLE03080
    20    CONTINUE                                           CLE03090
    33    CONTINUE                                           CLE03100
          WRITE(2,1000)                                      CLE03110
          WRITE(2,1001)                                      CLE03120
C                                                            CLE03130
C         COMPUTE TOTAL EXTENSION                            CLE03140
C                                                            CLE03150
          BB=1.                                              CLE03160
          DD=1.                                              CLE03170
          DO 999 K=1,KNO                                     CLE03180
          BB=BB*B(K)                                         CLE03190
          DD=D(K)*DD                                         CLE03200
          WRITE(2,1002)(TST(K),TEND(K),D(K),B(K))            CLE03210
   999    CONTINUE                                           CLE03220
          WRITE(2,1010) DD,BB                                CLE03230
          WRITE(2,1003)CRUST,TWRI,DELX                       CLE03240
          WRITE(2,1006)TWRI                                  CLE03250
C                                                            CLE03260
          WRITE (2,1011) AK,BK                               CLE03270
          WRITE(2,1012)                                      CLE03280
C                                                            CLE03290
C         CHANGE TEMPERATURE SO THAT TEMPERATURE IS 1333 DEG C   CLE03300
```

FILE: CLEAN   FORTRAN A   VM/SP CONVERSATIONAL MONITOR SYSTEM

```
C       AT BASE OF LITHOSPHERE                                          CLE03310
        DO 100 J=1,JJEND                                                CLE03320
        DO 90 I=1,JWR                                                   CLE03330
   90   TTOUT(I,J)=1333.*TTOUT(I,J)                                     CLE03340
        WRITE(2,1004)(TTOUT(I,J),I=1,JWR)                              CLE03350
  100   CONTINUE                                                        CLE03360
 1000 FORMAT(//'EXTENSION PARAMETERS FOR UPPER AND LOWER LITHOSHHERE'/) CLE03370
 1001 FORMAT(3X,'TIME',7X,'STR U',5X,'STR L')                          CLE03380
 1002 FORMAT(2(F5.2,1X),2(1X,F7.4))                                    CLE03390
 1003 FORMAT(/,'CRUST=',F5.0,3X,'TIME INT=',F5.2,3X                    CLE03400
      1,'DELX=',F7.4)                                                  CLE03410
 1004 FORMAT(20(F5.0,1X))                                              CLE03420
 1005 FORMAT(3I3,1X)                                                   CLE03430
 1006 FORMAT('TEMPERATURES EVERY ',F7.4,'.MY'/)                       CLE03440
 1010 FORMAT('    TOTAL     ',2(1X,F7.4))                             CLE03450
 1011 FORMAT('SEDIMENT CONDUCTIVITY=',2X,F6.3,2X,'+',2X,F6.3,' * DEPTH(KCLE03460
      1M)'/)                                                          CLE03470
 1012 FORMAT('                  TEMPERATURES')                        CLE03480
        RETURN                                                          CLE03490
        END                                                            CLE03500
C                                                                       CLE03510
C                                                                       CLE03520
        SUBROUTINE SUBSID (JSTOP,NSED,SUBS,T,CRUST,JWR,TIM,DELX)        CLE03530
C                                                                       CLE03540
C       THIS SUBROUTINE CALCULATES SUBSIDENCE (WATER LOADED AND UNLOADED) CLE03550
C       (SSU AND SUBS RESPECTIVELY)                                     CLE03560
        DIMENSION T(1000)                                              CLE03570
C       JWR=JWR+1                                                       CLE03580
        JJSTOP=JSTOP-1                                                  CLE03590
        SUBS=0.                                                         CLE03600
C                                                                       CLE03610
C       CALCULATE CONTRIBUTION FROM THERMAL EXPANSION                   CLE03620
        DO 10 J=NSED,JJSTOP                                             CLE03630
   10   SUBS=SUBS+T(J)*DELX/125.                                        CLE03640
        SUBS=SUBS+FLOAT(NSED-1)*DELX/125.                              CLE03650
        SUBS=(SUBS-.513)*5.16                                           CLE03660
C                                                                       CLE03670
C       CALCULATE CONTRIBUTION FROM CRUSTAL THINNING                    CLE03680
        SUBS=SUBS-(35.-CRUST)*4.32/35.                                 CLE03690
        SSU=SUBS*3.2/2.2                                                CLE03700
        WRITE(2,1000)TIM,SUBS,SSU                                       CLE03710
        WRITE(6,1000)TIM,SUBS,SSU                                       CLE03720
 1000 FORMAT(3X,F6.2,8X,F7.3,14X,F7.3)                                 CLE03730
        RETURN                                                          CLE03740
        END                                                            CLE03750
```

```
FILE: CLEAN    DATA     A                    VM/SP CONVERSATIONAL MONITOR SYSTEM

    .5      .5     2.
    35.     2.60   0.80
    4
    1.00    1.04
    1.      1.00
    1.      1.78
    1.      1.
    16.5    13.0
    13.     10.5
    10.5    8.
    8.      0.
     6
    0.      16.5
    .24     13.
    .35     10.5
    1.83    5.
    2.72    2.
    3.45    0.
```

FILE: CLEAN   OUTPUT   A   VM/SP CONVERSATIONAL MONITOR SYSTEM

TIME	UNLOAD SUBS (KM)	WATER LOAD SUBS
16.00	-0.011	-0.016
15.50	-0.023	-0.033
15.00	-0.034	-0.050
14.50	-0.046	-0.067
14.00	-0.058	-0.084
13.50	-0.068	-0.099
13.00	-0.079	-0.115
12.50	-0.080	-0.116
12.00	-0.081	-0.118
11.50	-0.082	-0.119
11.00	-0.083	-0.120
10.50	-0.084	-0.122
10.00	-0.322	-0.468
9.50	-0.504	-0.734
9.00	-0.650	-0.945
8.50	-0.768	-1.117
8.00	-0.866	-1.260
7.50	-0.873	-1.269
7.00	-0.879	-1.278
6.50	-0.885	-1.287
6.00	-0.891	-1.296
5.50	-0.897	-1.305
5.00	-0.903	-1.313
4.50	-0.909	-1.322
4.00	-0.915	-1.330
3.50	-0.920	-1.339
3.00	-0.926	-1.347
2.50	-0.932	-1.355
2.00	-0.937	-1.363
1.50	-0.943	-1.371
1.00	-0.948	-1.379
0.50	-0.953	-1.387
0.0	-0.959	-1.394

EXTENSION PARAMETERS FOR UPPER AND LOWER LITHOSHHERE

TIME		STR U	STR L
16.50	13.00	1.0400	1.0000
13.00	10.50	1.0000	1.0000
10.50	8.00	1.7800	1.0000
8.00	0.0	1.0000	1.0000
TOTAL		1.8512	1.0000

CRUST= 35.   TIME INT= 2.00   DELX= 0.5000
TEMPERATURES EVERY   2.0000 MY

SEDIMENT CONDUCTIVITY=   2.600 +   0.800 * DEPTH(KM)

TEMPERATURES

0.	0.	0.	0.	0.	0.	0.	0.	0.
21.	22.	21.	22.	27.	24.	23.	22.	21.
40.	40.	39.	41.	51.	45.	43.	41.	40.
56.	57.	55.	58.	73.	64.	61.	58.	57.
71.	72.	70.	73.	92.	81.	77.	74.	72.
85.	86.	83.	88.	110.	97.	92.	89.	86.
97.	98.	95.	101.	126.	112.	107.	102.	99.
109.	110.	106.	113.	139.	125.	120.	115.	112.
119.	121.	117.	124.	151.	138.	132.	127.	123.
126.	127.	126.	132.	163.	149.	144.	138.	134.
132.	134.	132.	139.	174.	158.	154.	148.	144.
138.	140.	138.	146.	184.	168.	163.	158.	153.